DYNAMIC ABRASION RESISTANCE OF ADVANCED COATING SYSTEMS

by

DAVID M. KENNEDY, *B.Sc., M.A.I., C.Eng.*

SUPERVISOR: Professor M.S.J. Hashmi.

This Thesis is submitted to Dublin City
University as the fulfilment of the
requirement for the award of the Degree of

Doctor of Philosophy

School of Mechanical and Manufacturing Engineering

Dublin City University

September, 1995

DECLARATION

I hereby certify that this material which I now
submit for assessment on the programme of study
leading to the award of Doctor of Philosophy
is entirely my own work and has not been taken
from the work of others save and to the extent
that such work has been cited and acknowledged
within the text of my work.

Signed _David Ikeanyichukwu_   I.D. No.: 91701279
Candidate

Date: _Sep / 1995._

i

ACKNOWLEDGEMENTS

TABLE OF CONTENTS

DYNAMIC ABRASION RESISTANCE OF ADVANCED COATING SYSTEMS

ABSTRACT

A novel test rig was designed and developed for testing the dynamic abrasion resistance of advanced coating systems used in engineering applications. Testing undertaken included abrasion, impact and combined impact-abrasion on uncoated and coated systems. Different coating thicknesses applied to a number of different substrates were tested during the experimental stage. Substrate materials consisted of aluminium, mild steel, and tool steels in annealed and heat treated conditions.

Thick and thin coatings of TiN, Ti$_x$C, WC-Co and Ni-Cr were applied to the substrates which were then subjected to dynamic wear tests. Coatings were applied using High Velocity Oxy Fuel (HVOF) thermal spray and Physical Vapour Deposition (PVD) processes.

An on-line data acquisition system was adapted by writing an appropriate computer programme for measuring and recording the applied load during the testing process.

A comparison is made between existing wear test equipment and the one used for this research. Suggestions for further work are discussed.

Surfaces subjected to the dynamic wear conditions were examined using optical and scanning electron microscopes. Comparisons are made between the coated and uncoated substrates for wear resistance. Comparisons are also made between the experimental results and mathematical models for determining the wear coefficients of materials tested.

The main wear characteristics associated with surfaces in sliding and impact conditions and the effects of rebound on impact of materials are discussed. The application of advanced coating systems to reduce wear are also mentioned.

The main findings drawn from this research are based on the effects of dynamic abrasion tests on coated and uncoated samples and the effect of different substrates and coating combinations on wear resistance. The main differences between the sliding and impact test conditions, the coating type and the effects of coating thickness on wear resistance are reported.

This information may assist tool designers to specify and recommend suitable coating systems, thicknesses and processes to suit conditions associated with dynamic abrasion.

x

NOMENCLATURE

A	= Cross sectional area (mm2)
a	= Crater radius (mm)
L	= Normal load (N)
S, S1	= Sliding distance (mm)
α, β	= Included angles (Degrees)
θ	= Angular displacement (Degrees)
m	= Mass (kg)
n	= Ratio of con-rod length to crank radius
W, W1	= Width of wear scar (mm)
h	= Depth of wear scar (mm)
H	= Material Hardness (N/m^2)
V	= Wear volume (mm^3)
r	= Radius (mm)
l	= Connecting-rod length
r_2	= Radius of curved surface (mm)
h_c	= Crater depth (mm)
K	= Wear coefficient
k	= Wear constant
k_c	= Wear constant for coating
k_s	= wear constant for substrate
k_1	= wear constant for variable velocity

v	=	Linear velocity (m/s)
w	=	Angular velocity (radians/sec)
t	=	time (seconds)
F, R	=	Impulse force (N)
e	=	coefficient of restitution
P	=	Applied pressure (N/m^2)
W_3	=	Work done (N-m)
V_r	=	Volume of permanent indentation (mm^3)
E, E_1, E_2	=	Young Modulus of elasticity (N/m^2)
E_e	=	Elastic energy
E_r	=	Rebound energy
ν	=	Poissons ratio
x	=	Displacement (mm)
σ_f	=	Flow stress (N/m2)
ρ	=	Density (kg/m^3)
Q	=	Plastic zone size
u	=	Velocity during restitution (m/s)
v1	=	Velocity after restitution (m/s)
rf	=	Radio frequency
dc	=	Direct current
C	=	Spring constant (N/m)

LIST OF FIGURES

xv

APPENDIX A

LIST OF TABLES

LIST OF PHOTOGRAPHS

CHAPTER 1

INTRODUCTION AND JUSTIFICATION

1.1 SURFACE ENGINEERING

Surface engineering involves design of systems to deal with situations where components are subjected to complex external loading [1.1]. The role of surface engineering in preventing wear is well recognised and has evolved over the last few decades through the growing commercial maturity of a wide range of cost-effective surface technologies. Surface modification or surface engineering includes heat treatment, surface coatings, mechanical work-hardening processes, implantation processes and surface shape design [1.1].

Most of the functional requirements of products relate to the surface properties and by modifying the surface conditions, operating characteristics can be improved. In most surface engineering systems, both coatings and substrate will contribute to the overall tribological performance of the system.

1.2 WEAR OF ENGINEERING MATERIALS

Wear of engineering components such as cutting tools, machine parts and dies is a significant problem in industrial applications. Wear, fatigue and corrosion are the three most commonly encountered industrial problems leading to the replacement of components and assemblies in engineering [1.2,1.3]. High temperatures and humidity

can speed up the wear and destruction of materials [1.4-1.6]. Low friction will result in low wear generally but some parts may need to be replaced after a small amount of material has been removed or if surfaces are roughened while in operation.

For some applications, removal of 0.1 to 0.2 mm of material from a surface through wear may render it unserviceable, however, if this can be replaced by applying a coating, the component may become useful again. There are many types of wear that are of concern to the user of coatings, including sliding wear and friction, low and high stress abrasion, dry particle erosion, and slurry erosion [1.7]. Lubricity reduces the likelihood of built up edges (B.U.E.) forming on machining tools, and cratering, as well as tearing and galling of workpieces. Reducing the coefficient of friction has many advantages in machining processes but it may also require a change in the tool design [1.8]. Investigation of the wear resistant properties of advanced coating systems are carried out in this thesis. The corrosion and wear of a given metal depends on the environmental conditions (temperature, pressure, chemical, velocity, agitation etc), to which it will be subjected to in service. Many pure metals have a good resistance to atmospheric corrosion but they are usually too expensive and many are mechanically weak [1.9]. Reducing wear is important both for the life of the component and the efficiency of the machine or process that it is part off and surface coatings are becoming more extensively used for a wide range of modern applications.

1.3 ADVANCED SURFACE COATINGS

Designing the surface of components to match operating conditions is important especially if more expensive bulk material can be replaced by cheaper materials. Coatings perform functions which differ from the bulk material and are used under conditions which would normally lead to the failure of the bulk material. Such examples include cutting tools, jet engines and processes involving high temperatures and wear. In some applications, it may be economical to make the whole component from a particular material rather than apply a coating. Cutting tools of polycrystalline cubic boron nitride (PCBN) for machining hardened cast iron is such an example [1.10]. Surface coatings can offer a hard surface with a ductile core. In tribological applications where conventional lubricants fail under certain conditions, coatings may be used to replace them [1.11]. Coatings can be soft or hard, thick or thin, porous or dense, single or multi-layer, amorphous or crystalline. The choice of a coating material depends on the application and the substrate used.

Even though most materials can be coated, not every one can be protected with wear resistant coatings. In some coating processes, high temperatures are required. This limits the range of substrate materials for coating purposes to special tool steels and carbides for wear-resistant conditions [1.11].

In practice it is possible for a coating to wear and the substrate to be unaffected. Also the substrate may deform without any noticeable wear of the coating. This second form of wear may cause the coating to fail by spalling or breaking due to the collapse of the supporting substrate. A suitably designed coating system is then required for optimum conditions. A working coating system design involves two

3

critical interfaces, interface 1, between the coating and the environment or work material, and interface 2, between the coating and the substrate [1.12]. The generalised features of a working coating system are shown in Figure 1.1 [1.13]. The designer of components is now in a stronger position to optimise surface properties which can be independent of those of the bulk material.

1.4 JUSTIFICATION FOR PRESENT WORK

With the development of surface engineering design, the need to evaluate the properties of new raw materials and substrate-coating combinations is important. Numerous tests, coating processes and investigations have shown that the quality of the substrate reflects the quality and life of the combined system of substrate, interface, and coating. Tests on identical coating materials will ascribe different properties to the coating for different substrates and even for different coating thicknesses [1.14]. In many research works to date, authors have investigated the effects of contact abrasion, erosion and impact on uncoated components, mainly as separate problems [1.15]. More recently, experiments and testing on coated materials have occurred and some standardised, and experimental test equipment has been produced to meet specifications on wear resistance. Standard test methods such as pin-on-disc are used extensively to simulate rubbing action in which plastic yielding occurs at the tip of individual asperities. This testing is mainly carried out on a microscopic scale and contact pressures are less than 1 MN/m^2 [1.16]. In thin films technology, scratch testing has emerged as a widely practiced technique for assessing adhesion of coatings to substrates [1.17].

4
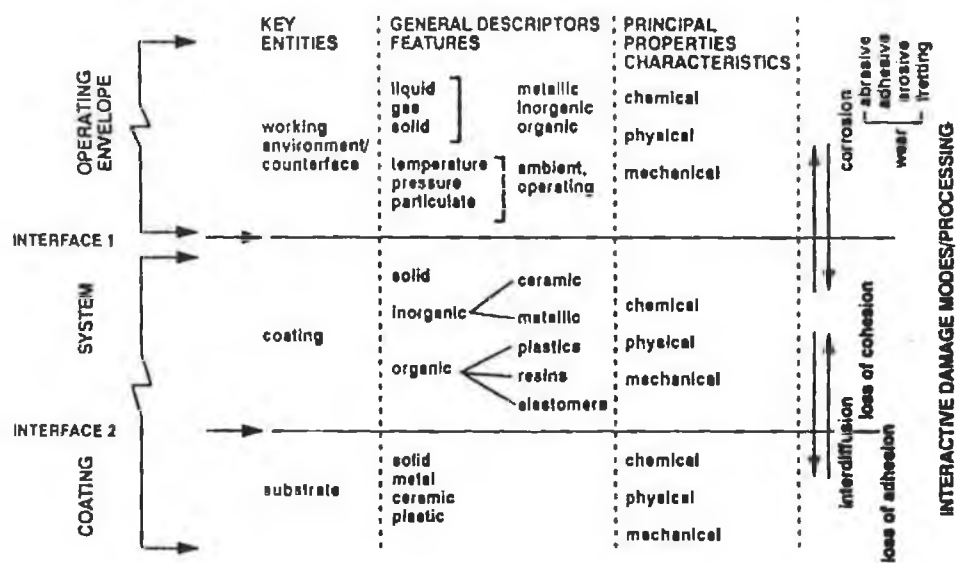
Figure 1.1 General features of a working coating system [1.13].

5

Unlike the pin-on-disc apparatus, the testing process for this research is done on a larger scale, abrading a wider surface area and, therefore, attempting to simulate industrial applications more closely. Thick coatings such as those produced in thermal spraying and weld facing seldom experience penetration during some standard wear tests available today. As yet, it is unclear whether behavioural models developed for thin, hard coatings necessarily apply to thicker coatings [1.18]. Using the test rig developed for this research, impact abrasion resulted in penetration of both thick and thin coatings. Pure impact testing on coatings have been conducted by some researchers, applying impact forces until the coating/substrate combination reaches its yield point [1.19]. The type of wear occuring under combined impact and sliding wear has hardly been studied according to Swick et al [1.20], and forms the main basis of this work. As most engineering components experience a more complicated situation than just pure rubbing or impact, a means of testing their combined effects seems a logical and necessary process at this time. Combined impact and abrasion occur in punching and cutting operations [1.21-1.23] as well as compression and metal forging operations, impact extrusion [1.24], and interrupt cutting operations. Other applications include the compression and extrusion of peat fuel, animal feeds, plastic granulating, machining operations such as milling, cutting, and turning, and earth moving equipment. Components subjected to impact-compression apply dynamic wear combinations to the forming tools producing them. In mining processes involving excavation, drilling, crushing and grinding of ore for example, wear is a combination of impact and abrasion [1.3]. Under the actions of continuous and intermittent cutting processes, the different wear parameters are shown in Figures 1.2. and 1.3 respectively.

6
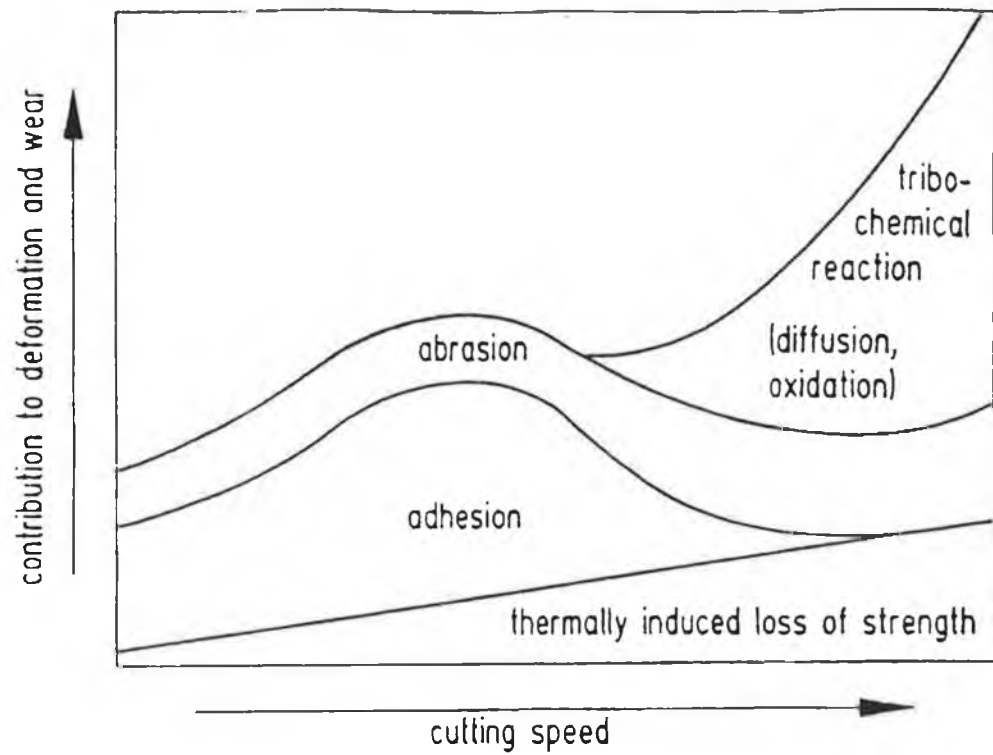
Figure 1.2 Wear mechanisms for continuous machining [1.26].
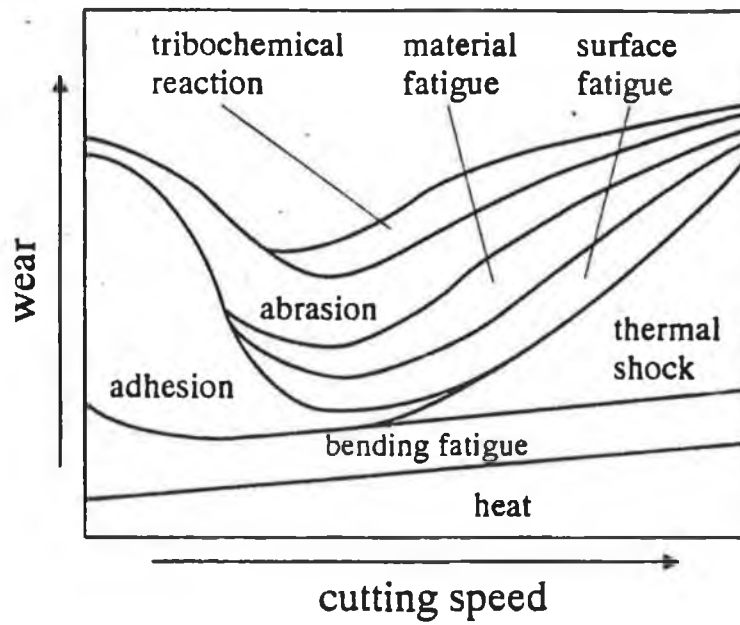
Figure 1.3 Wear mechanisms in interrupt cutting operations [1.27].

7

1.5 AUTHORS MAIN INTEREST IN RESEARCH AREA

A research project investigating the accelerated wear of tool steels used in briquette manufacturing for fuel purposes discovered that tool materials were been worn away at almost eight times their normal rate encountered over a period of twenty years. Initially, a number of suggestions were put forward as possible causes including:

(i)   Wrong material specifications and incorrect material supplied.

(ii)   Poor machining of tools leading to residual stresses on the surface which reduced wear resistance.

(iii)   Heat treatment and annealing of the tool in service leading to a weaker and less wear resistant component.

(iv)   Misalignment of machine parts, thus increasing wear of moving parts.

(v)   Increase in grit and abrasive particles in the peat due to deep cutting of the bog causing an increase in abrasive wear on the tools and dies.

Each component of the die set was machined and ground four times before it was scrapped, resulting in a large wastage of tool steel. The effects of tool failure due to wear increased down-time of the production machines, increased machining costs, increased maintenance costs, led to loss of production, increased costs in tool steel requirements, and led to incorrect briquette sizes in the production process. Although the briquette dies, shown in Figure 1.4 were subjected to the combined effect of impact and abrasion, other problems such as thermal, and chemical corrosion of the tools were encountered. An investigation found that the tool material specification had not changed with time, that the loads applied to the tools were consistent with previous values, and that the main source of tool wear was a combination of dynamic

abrasion and plastic deformation. Investigations suggested the following possible solutions to the problem:

(i)   New and better materials for the tools. An AISI D7 [1.25], tool steel which is recommended for briquette production was sought but was not readily available.

(ii)   Heat treatment of the tools was investigated using vacuum heat treatment processes, however wear through abrasion and deformation continued.

(iii)   Recommending changes to the shape of the tool profile to increase the load bearing contact area was not welcomed.

(iv)   The final suggestion to solving this problem centered on surface coating technology. However the Company did not see this as a possible solution at the time due to the costs involved.

Considering the case discussed above, the author has highlighted a number of typical approaches to addressing the problems of counteracting wear and its effects on machine components. The study also highlights the complex nature of wear on materials and indicates that it is a combination of a number of wear patterns which many standard wear tests fail to address. This investigation led to the design and development of a novel test rig for testing coated and uncoated materials under the effects of dynamic or combined impact-abrasion conditions which is more realistic of the real operating conditions.

1.6 AIMS OF THE STUDY

The main aims of this study were:

(i)   to design, develop, manufacture and commission equipment for testing coated and uncoated engineering materials under combined impact and abrasion.

(ii)   to compare the effects of coated with uncoated samples under dynamic abrasion test conditions and the influence of rebound following impact.

(iii)   to examine the performance of the coating-substrate combination and effects of different substrates on the overall wear resistance of the system.

(iv)   to assess the performance of different coating thicknesses on substrate under dynamic abrasion wear tests.

(v)   to describe the main wear parameters produced during the dynamic abrasion testing.

(vi)   to compare the separate effects of impact and abrasion with the combined effects of impact abrasion on coated and uncoated materials.
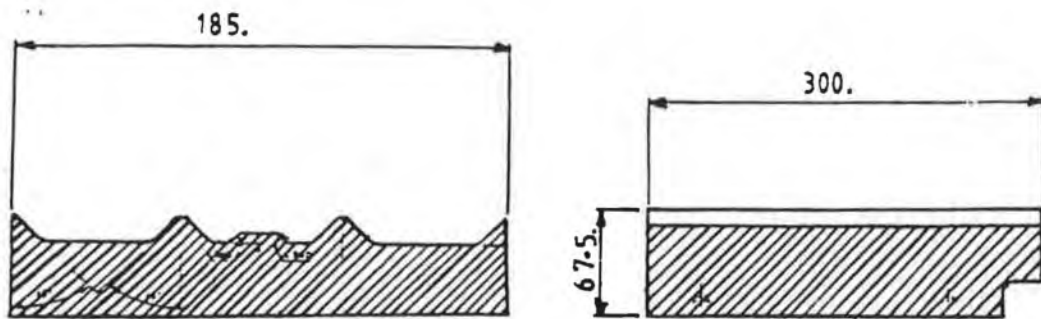
Figure 1.4   Briquette die profile.

1.7 METHOD OF APPROACH

The method of approach is outlined in Figure 1.5. The theoretical approach consists of the analysis of abrasion and impact models. The experimental approach consists of (i) the test rig development, (ii) coating processes and wear test performed, (iii) examination of the samples tested and (iv) analysis of the results.

11
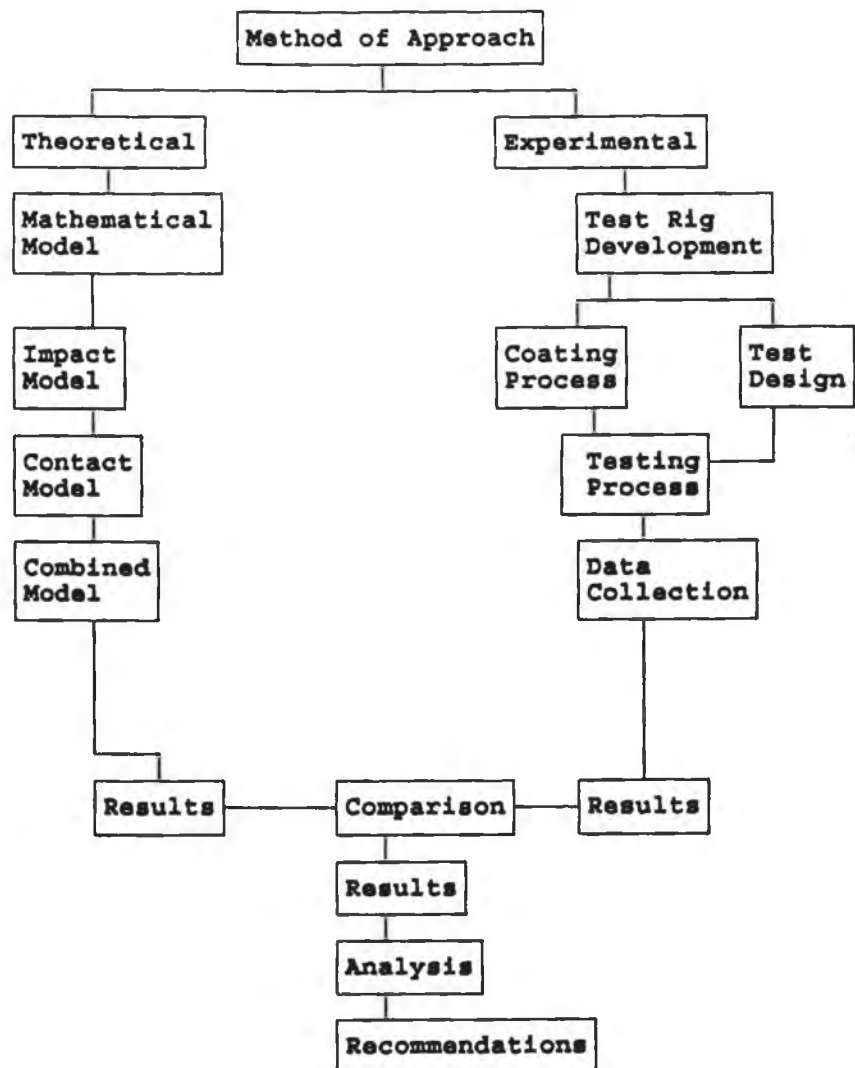
Figure 1.5 Method of Approach for the study.

12

1.8 PRESENTATION OF THESIS

The thesis is arranged into seven chapters. Following the introductory chapter, chapter two is a literature review of surface engineering and advanced coatings and processes. Chapter three covers the main area of wear and wear testing equipment used in examination of bulk materials and coating systems. It also identifies an approach to solving methods of wear testing. Chapter four is dedicated to the test rig developed for the experimental work and compares the features of the test rig used in this investigation to that of existing wear test equipment. Chapter five describes the theoretical approach for the dynamic system of combined impact and abrasion. Mathematical formulae of abrasion and impact wear are analysed and a wear coefficient model is developed for the operating conditions of the test rig. In chapter six, the experimental approach is explained and the main results of the thesis are presented, analysed and discussed. Chapter seven highlights the main conclusions from the work and comments on future recommendations.

CHAPTER 2

LITERATURE SURVEY

SURFACE ENGINEERING AND SURFACE COATINGS

2.1 INTRODUCTION

A large number of research papers and publications have been produced on surface engineering and coating processes by researchers working in different disciplines. Some processes are considered traditional such as electroplating and heat treatment applications.

Techniques such as Physical Vapour Deposition(PVD) and laser processing etc., are also well established. Various surface engineering processes are shown in Figure 2.1, and more specific processes, coating types, coating properties and applications for high wear resistance are shown in Figure 2.2. Coating applications are so advanced today that some processes are computer controlled [2.1].

2.2 COATINGS DEVELOPMENT

Coating of carbide inserts was introduced in the late 1960s and coating of High Speed Steels (HSS) in the late 1970s. In 1991, about 60% of all carbide tools used for cutting were coated, especially in the area of turning where the percentage was in the region of 80%. For milling, only 25% to 35% of the carbide inserts were coated as described by Konig et al [2.2]. The application of thin, hard, and

14

Figure 2.1 Surface coating processes [2.3].

COATING

MISCELLANEOUS TECHNIQUES

1. ATOMIZED LIQUID SPRAY
2. BRUSH, PAD & ROLLER
3. SCREENING & LITHOGRAPHY
4. ELECTROCHEMICAL DEPOSITION
5. CHEMICAL DEPOSITION
6. INTERMETALLIC COMPOUND
8. FLUIDIZED BED
9. SPARK HARDENING
10. SOL-GEL
11. SPIN-ON
12. DIP

VAPOUR DEPOSITION

CHEMICAL VAPOUR DEPOSITION (CVD)

1. CONVENTIONAL CVD
2. LOW PRESSURE CVD
3. LASER INDUCED CVD
4. ELECTRON-ASSISTED CVD

PHYSICAL VAPOUR DEPOSITION (PVD)

EVAPORATION
1. DIRECT
2. REACTIVE
3. ACTIVATED REACTIVE
4. ION-BEAM ASSISTED

ION PLATING

GLOW DISCHARGES
1. DC/RF DIODE
2. ALTERNATING
3. TRIODE
4. HOLLOW CATHODE DISCHARGE
5. CATHODIC ARC
6. SPUTTER PLATING

ION BEAM
1. DIRECT BEAM
2. ION BEAM
3. CLUSTER ION BEAM

SPUTTERING

GLOW DISCHARGE
1. DC/RF DIODE
2. TRIODE
3. MAGNETRON

ION BEAM
1. SINGLE ION BEAM
2. DUEL ION BEAM

PHYSICAL-CHEMICAL VAPOUR DEPOSITION

1. PLASMA ENHANCED CVD
2. REACTIVE PULSED PLASMA
3. CHEMICAL VAPOUR POLYMERIZATION

HARD/SOFT FACING

THERMAL SPRAYING

ELECTRIC ARC

SPRAY AND FUSE

PLASMA ARC

FLAME

CONTINUOUS COMBUSTION
1. JET KOTE
2. *DIAMOND JET*
3. TOP GUN

PULSED COMBUSTION
DETONATION GUN

WELDING

1. OXY-FUEL GAS FLAME
2. ELECTRIC ARC
3. PLASMA ARC

CLADING

1. WELD
2. BRAZE
3. LASER
4. EXPLOSIVE
5. MECHANICAL METHOD
6. DIFFUSION BONDING
7. ELECTROMAGNETIC IMPACT BONDING

Processes	Coating type	Properties	Applications
Chemical Vapour deposition.	Diamond film.	Hardness.	Cutting tools & dies.
Physical vapour deposition.	Diamond like carbon.	Wear resistance.	Drilling.
	Titanium nitride.	Shock resistance.	Punching.
	Titanium carbide.	Resist galling.	Tapping.
Ion plating.	Tungsten carbide.	High temperature resistance.	Reaming.
Ion implantation*	P.C.B.N.		Broaching.
Weld facing.	C.B.N.	Resist B.U.E.	Extruders.
Thermal spray.	Zirconium nitride.	Tribological characteristics.	Injection moulding.
Plasma spray.	Titanium carbo-nitride.	Toughness.	Ball bearings. Rolling mills.
Sputtering.	Aluminium oxide.	Impact resist-ance.	Mining equipment.
Laser surfacing.	Hafnium carbide.		Forging.
HVOF process.	Hafnium nitride.	Fatigue resist-ance.	Quarrying.
	Chromium carbide.		Turning.
	Zirconium carbide.	Corrosion resistance.	Milling.
	Titanium diboride.		
	Silicone carbide.	Surface finish.	
	Tungsten carbide-cobalt.	Improve tool life.	
	Chromium oxide.	Higher cutting speeds and feeds.	
	Silicon nitride.		

* Surface treatment process.

Figure 2.2 Processes, coating types, properties and applications of coatings applied to tools and dies.

16

wear resistant coatings of carbides, nitrides, and oxides to carbide and steel cutting tools is now common practice [2.4]. Thin coatings (1μm to 8μm), properly applied tend to flex with the substrate and if fixed to a tough substrate, can provide shock resistance during machining operations. It is claimed in [2.4] that hard coatings applied to cutting tools increase tool life (2 to 10 times that of uncoated tools), increased productivity (increase of cutting speeds by 25-29%), improved workpiece quality (smoother surface finish and closer tolerances), and reduced machining forces (reduced power requirements). Coated tools combine wear resistance in their coatings with toughness and strength in their substrate. Hard coatings also have some disadvantages which include porosity, insufficient bonding to the substrate and in some cases, limited thickness [2.5]. Coatings provide high hardness at high cutting temperatures, thus reducing abrasive wear. Coatings act as barriers to decrease diffusion or reaction between tools and workpieces. It is well established that micron thick coatings of either wear resistant or low friction ceramic materials, applied by heating an insert in the presence of chemical vapours, producing a chemical vapour deposition coating, can improve performance of machining inserts [2.6]. Titanium carbide, (TiC) was one of the earliest coatings applied in this way and it improved wear resistance and reduced flank wear of tools. The PVD process which makes TiN coatings on tools was patented in 1969 by Alvin Snapper [2.7]. Some of the first coatings on tools in this form became available in 1981 in the West following earlier developments by the Soviet Union at the Kharkov Institute. Titanium Nitride (TiN) has become the most common coating for HSS cutting tools requiring sharp edges. It is highly inert, with no tendency to form alloys with common metals. As a result, TiN and Titanium Carbide (TiC) coated tools resist abrasion, adhesion, galling,

17

welding, cratering and the formation of Built Up Edges (BUE) [2.4].

Multiple coating layers can be tougher than one thick layer as the grain structure may be more refined and they may possess better elastic behaviour over a single thick coating. Cemented carbide inserts are commonly coated with a combination of TiN, TiC and Aluminium oxide [2.8]. Most, if not all, coatings will be in a state of internal stress when applied. They experience shear, tensile and compressive stresses and in some cases, the interfacial shear stress may exceed the adhesion strength of the coating-substrate interface and lead to cracking and spalling of the coating [2.9]. Coatings tend to be less beneficial on high stress, short life parts where the substrate is likely to yield, chip or break [2.10]. In other applications such as dimpling punches, life may be extended three or four times using coatings.

2.3 COATING PROCESSES

In researching this work, many coatings and coating processes were investigated, however only those related to the experimental procedure are discussed in detail with a brief outline given on other coatings. Some emphasis has been placed on coatings suitable for wear resistance applications.

2.3.1 Selecting a coating

Before selecting a particular coating the following factors may be considered:

(i)   What are the objectives of the coating.

(ii)   Can the coating material be applied to the substrate.

18

(iii)   What effects will the coating have on the substrate.

(iv)   Can the coating be applied economically.

(v)   How will the coating be applied.

(vi)   Can the coating be renewed at a later date if necessary.

(vii)   Can the substrate material withstand the processing steps
required to deposit the coating.

(viii)   Will the coating impair the properties of the bulk material.

(ix)   Will the shape of the component restrict the application of a coating.

In practice, coatings may confer one or more of the following properties:

(i)   Corrosion protection.

(ii)   Build up of material due to restoration.

(iii)   Decorative purposes.

(iv)   Wear resistance.

(v)   Hardness.

(vi)   Optical or thermal reflectivity.

(vii)   Electrical conductivity.

(viii)   Oil retention.

(ix)   Solderability.

(x)   Thermal conductivity.

Some important requirements for protective coatings at high

temperatures [2.11] include:

(i)   High melting temperature.

(ii)   Hardness.

(iii)   Corrosion resistance.

(iv)   Low permeability and diffusion for oxygen to prevent internal substrate corrosion.

(v)   High density, to avoid gas flux through open pores to the substrate.

(vi)   Stress free or in a state of compressive stress at working temperature.

(vii)   Good adhesion.

At temperatures up to 540°C, coatings based on tungsten carbide and cobalt in varying proportions are commonly used. Temperatures up to 670° C call for tungsten carbide and nickel chromium. At temperatures up to 980° C, coatings based on chromium carbide and nickel chromium are used.

Oxide coatings can offer advantages over carbide-based coatings because of better corrosion and oxidation protection. Zirconium oxide coatings, for instance, are used for high temperature thermal barrier applications. However, oxide coatings are more easily damaged by mechanical and thermal shock compared with carbide coatings. For multi-coating systems, by optimising the thickness of individual layers, the hardness of the coatings can be maximised, as reported by Chu et al [2.12].

2.3.2 Coatings for cutting tools

The main coatings applied to cutting tools include:

(i)   Titanium carbide (TiC).

(ii)   Titanium nitride (TiN).

(iii)   Titanium carbonitride Ti(C,N).

(iv)   Aluminium oxide (Al_2O_3).

20

(v)   Hafnium nitride and Hafnium carbide (HfN & HfC).

(vi)   Chromium Carbide (Cr_7C_3).

(vii)   Tantulum carbide and nitride (TaC & TaN).

(viii) Zirconium carbide and nitride (ZrC & ZrN).

(ix)   Silicon carbide and nitride (SiC & S_3N_4).

(x)   Boron nitride and Cubic boron nitride (BN & CBN).

(xi)   Boron-carbon alloys and diamond like carbon (BC & DLC).

(xii)   Niobium nitride (Nb-N).

(xiii) Chromium nitride (CrN).

(xiv)   Aluminium nitride (AlN).

2.4 SURFACE TREATMENT PROCESSES

2.4.1 Shot peening

A mechanical solution to changing the surface properties of materials consists of shot peening, which work-hardens the surface but not to the extent of flame or induction hardening. The material at the surface yields, while the core material exerts an opposite reaction thereby inducing a hemispherical field of compressive residual stress in the surface [2.13]. This process improves fatigue resistance. Micro shot blasting of coated surfaces also improves wear resistance. If however the material is then heated above a certain temperature it may anneal which may reduce its overall strength.

21

2.4.2 Diffusion

Surface layers may be altered by diffusing elements such as nitrogen, silicone, sulphur and boron into the surface layer. This process can improve wear resistance of metal surfaces.

2.4.3 Carburization

This process is restricted to steels with low carbon content (0.2% C or less). It takes place at temperatures above 850°C. The rate of diffusion depends on the atmosphers, time and temperature and the steel composition. On quenching after carburizing, some distortion of the material may occur.

2.4.4 Nitriding

This process involves heating steels of certain compositions in an atmosphere of cracked ammonia around 550°C and it produces a fine, well dispersed precipitate of hard nitrides in the surface layers. Elements with a high affinity for nitrogen such as molybdenum, chromium, vanadium, aluminium and titanium are usually added to the steel to perform the nitriding process effectively.

2.4.5 Cyaniding and Carbo-nitriding

Cyaniding is used to describe a salt bath process. Carbo-nitriding refers to a gaseous

22

diffusion process. In these processes, carbon and nitrogen are diffused into the surface layers. The cyaniding process uses low temperatures (500 to 600°C) and higher temperature processes (800 to 900°C). The low temperature process gives thin, hard layers rich in nitrogen. No heat treatment is required following the process. The higher temperature process gives thicker layers high in carbon. These layers have to be hardened by quenching after the process. Diffusion borochromizing, as reported by Kolesnikov et al [2.14], produces a surface layer of chrome borides (in addition to iron borides), which provide high hardness and high crack resistance under dynamic impact loading.

2.4.6 Induction hardening

With this process, the core depth can be controlled, producing hardness values up to 600 to 700 VPN if the material is stress relieved and has the correct structure. Flame hardening on the other hand is not so precisely controlled and it is important to avoid long heating cycles at high temperatures as this can give rise to grain coarsening, embrittlement, cracking and distortion.

2.4.7 Ion Implantation Processes

This process involves the bombardment of surface layers of materials with other elements. It is a vacuum process and a line of sight method [2.15], although plasma ion implantation techniques have recently emerged as non-line-of-sight methods [2.16]. In conventional processes, ion penetration is about 0.2μm [2.17,2.18].

23

Components are placed into a vacuum chamber at a pressure of $2x10^{-6}$ torr and the ion source is activated to bombard the workpiece surfaces with projectile ions. These collide with atoms in the crystal lattice of the material, are slowed down and cause local dislocations and radiation damage. The ions lodge below the surface and lock into place. This offers wear resistance at depth. Due to impact, the ions are in a compressive state and tend to close up any microcracks on the surface [2.19]. The impact improves the tensile strength of the material and increases fatigue resistance. The closing of surface cracks by the ions blocks out other chemically abrasive materials thereby reducing corrosion effects. The main advantages of the process include:

(i)   No distortion of the material as the temperature of the process is carried out at around 200° C.

(ii)   No oxidation occurs due to the vacuum process.

(iii)   No adhesion problems because it is not a coating process.

(iv)   No dimensional changes.

(v)   No surface damage.

Applications of the Ion Implantation process include Tungsten carbide dies and drills, mould tools, extrusion and injection screws, slitting, cutting, punching and stamping tools, medical prostheses and ball bearings [2.15,2.20,2.21].

2.5 THERMAL AND MECHANICAL PROCESSES

Coatings may be applied mechanically by roll or extrusion bonding or by forging. These processes use pressure welding between the coating and substrate.

24

Contaminants (oxides) are difficult to eliminate in these processes. Such contaminants are normally broken down and diffused into the plastically deformed metals. Cladding and extrusion processes are well-practised processes and coatings produced in this way are free from pores or other coating discontinuities.

2.5.1 Sheradising

This is a cementation process where steel components are heated in a drum in the presence of zinc powders at about 370°C. A thin, uniform layer is applied to the component without affecting the tolerances to any great degree [2.22].

2.5.2 Cladding

In this process, a base metal is sandwiched between sheets of the coating metal and then rolled to the required thickness. The sheets are welded together in the process. Along with rolling and explosive bonding methods, overlay rolling, cast rolling, diffusion bonding, brazing and rolling, and the explosive rolling have been developed [2.23]. Laser cladding technology is also used for producing surface layers suitable for corrosion, wear and erosion resistance [2.24].

2.5.3 Anodising

This process is normally applicable to alloys of aluminium to improve the oxide layer of the material. The oxide film forms a hard wear, resistant coating, which

may be dyed for appearance.

2.5.4 Thermal sprayed deposited coatings

Thermal sprayed processes take a suitable powder or wire, heat it to its melting temperature and project the molten particles on to a correctly prepared substrate to form a bonded coating [2.25]. They are line of sight processes. The flattened, solidified globules adhere by mechanical means and there is no alloying action between the two metals. As successive globules strike and flatten on a surface, they become partially welded together and a cohesive coating is built up. The porous nature of such coatings allows some attack to take place within the coating thickness. Corrosion products may then be readily entrapped, plugging the pores and stifling further corrosion. These coatings may be applied by welding or thermal spraying, and plasma spray techniques. They are mainly applied for corrosion and abrasion wear resistance. Oxyfuel Flame-Powder(OFP), Oxyfuel Flame-Wire(OFW), Oxyfuel Flame-Rod or cord(OFR), Electric Arc-wire(EA), Plasma Arc-Powder(PAP), Hypersonic Oxyfuel Process(HOP), and Controlled athmosphere Plasma spray(CPA) are examples of such processes. Some of the thermal spray processes produce porous, thick coatings. Plasma spraying is performed in a low pressure, inert athmosphere and is capable of producing dense, oxide free coatings.

Grit blasting or chemical pre-treatment of the substrate can be performed, the former giving a roughness for adhesion of the coating. Post treatment is confined to machining components to size and some receive heat treatment. Thickness of coatings range from 0.1 to 1.0 mm [2.26].

26

2.5.5 High Velocity Oxy Fuel (HVOF) Process

This process was used for applying some of the coatings to the different substrates in the experimental work of this thesis and a schematic of the process is shown in Figure 2.3. A schematic of the diamond jet spraying gun used with the process is shown in Figure 2.4. A Tungsten Carbide-Cobalt coated aluminium sample, viewed by a scanning electron microscope and showing a cross section of the coating thickness and adhesion to the substrate is shown in Figure 2.5. The HVOF spray process uses an oxygen/propylene/air gas mixture and consists of a manually operated Diamond Jet Gun, a powder feed unit, a flow rate meter, air supply and control unit. A spray booth and extractor system are required to remove unused sprayed particles. The coating powder is carried by nitrogen and fed into the center of the flame. It is heated to its molten or semi molten state and is accelerated towards the surface [2.25,2.27]. Due to the high velocity and high impact, the coating is less porous than normal thermal spray processes, and has good bonding strength to the substrate.

The main advantages of this process and similar thermal processes are that they can be used for repair work on components without the use of a vacuum chamber. This permits applications of thick and thin coatings to large and small surface areas.
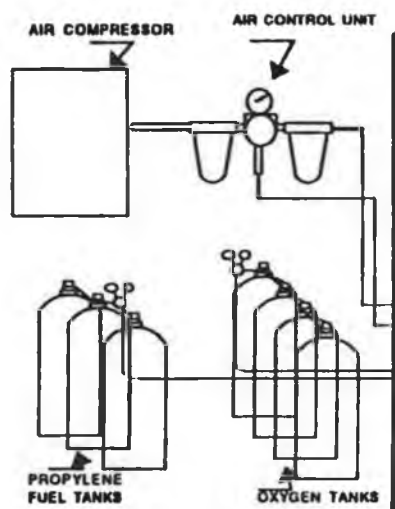
Figure 2.3   HVOF thermal spraying unit.

28

POWDER FEED UNIT

SPRAY
BOOTH

FLOW METER UINT

SOUND PROOF ROOM

GUN

NITROGEN
TANK

ELECTRIC
CONTROL BOX

EXTRACTOR
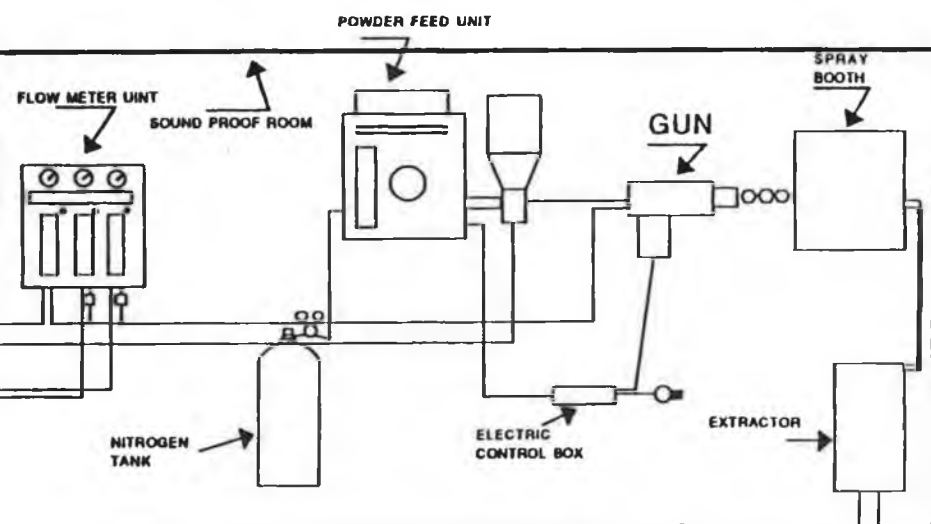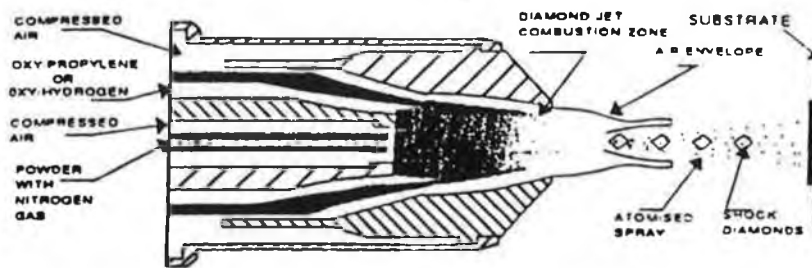
Figure 2.4 Schematic of cross section of diamond jet spray gun.
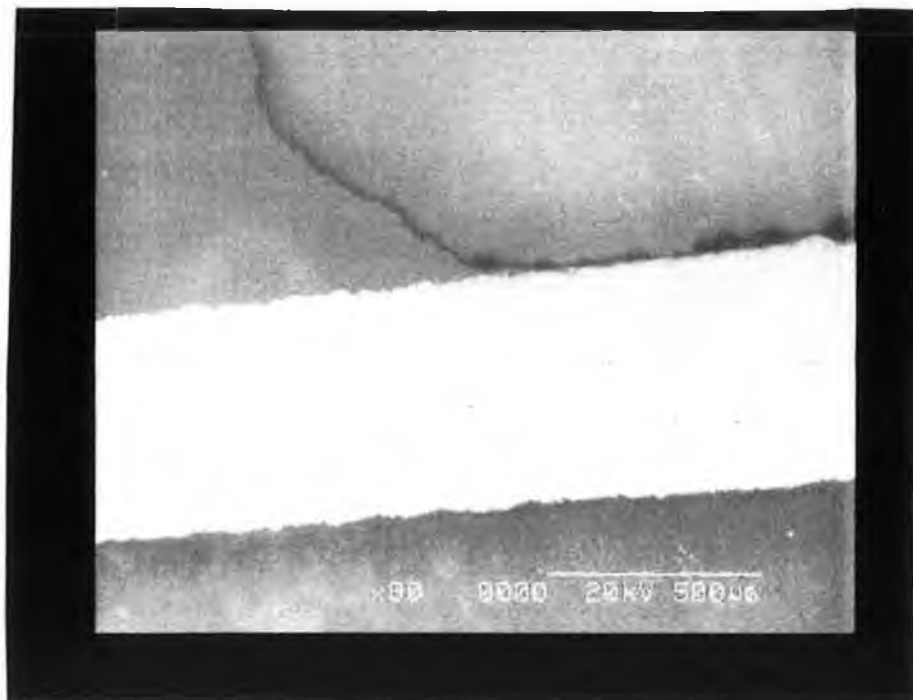
Figure 2.5 Micrograph of WC-Co coating on aluminium sample.

2.5.6 Hypersonic combustion thermal spray process

This is a recent process and consists of burning under pressure, oxygen and a fuel gas. The hot exhaust gases exit down a norrow bore nozzle where finely powdered material is axially introduced. The powder is heated and accelerated by the gas jet and is propelled towards the substrate at velocities of 1000m/s. The thermal and high kinetic energy on impact gives high bonding to the substrates [2.28].

2.5.7 Plasma arc torch

The arc is an ionised gas plasma struck between water-cooled metal electrodes that are not consumed in the process. This produces a high velocity ionised plasma jet. Powdered material is introduced into the flame and transported to the surface [2.28]. This process uses very high temperatures and the heated expanded gas is used to melt and propel the powder particles on to a substrate to form a dense coating. This is a continuous coating process which maintains the properties of the powder because an inert gas is used for feeding the coatings. Coating powder particles are metered in a secondary gas stream (usually nitrogen or argon) into the high velocity, high temperatue plasma flame. The coating is aimed towards the substrate which lies between 20mm and 150mm from the torch nozzle. The process is a line of sight deposition process [2.25]. Porosity is in the region of 1 to 10%.

2.5.8 Applications of Plasma Techniques

Applications for Plasma spraying techniques include wear resistance, fretting and sliding wear, galling, abrasion, erosion, [2.29] and corrosion. Plasma techniques offer the following to components [2.25].

(i)   Increased operating life.

(ii)   Greater scope for design and development engineers.

(iii)   Ability to salvage worn/mismachined parts.

(iv)   Ability to strip and recoat.

(v)   Weight savings.

(vi)   Cost-effective solutions.

2.5.9 Reduced Pressure Plasma Jet Spraying

In conventional practice, plasma spraying is conducted in ambient athmosphere, so that formation of a porous coating of insufficient corrosion and heat resistance has often been inevitable. When executed under a reduced pressure, both the temperature and velocity of the plasma jet can be increased, and more tightly bonded, denser coatings can be formed [2.23].

If the coating time is short, heating of the substrate is minimised, which is caused by the impact of the metal powders cooling on the substrate. In most cases, cooling of the substrate is carried out to prevent dimensional or metallurgical changes occuring.

31

2.5.10 Detonation gun

This involves controlling the detonation of mixtures of oxygen and acetylene in a specially designed chamber. If powder particles are suspended in the gas mixture prior to detonation, the high velocity, hot gas stream can be used to accelerate and melt the powder particles and impact them onto a substrate. The extra kinetic energy of the coating particles generates heat when impacting the substrate. The detonation wave involving a 50/50 mixture of oxygen and acetylene can travel at 2930m/s towards an open ended tube as reported in [2.25]. The speed of the particles depends on the the gas mixture, barrel length of the gun, size of particles, and the position of the powder prior to detonation. The cycle is repeated 4 to 8 times per second, and the coating is very dense, with low porosity, and fine grained with coating thicknesses of 0.1mm to 0.3mm.

2.5.11 Coating properties for thermal and detonation gun processes

The hardness of detonation gun coatings are generally higher than equivalent coatings applied by other flame spraying processes. A rough hardness value for a tungsten carbide cobalt detonation gun coating is over 1,150 HV (Vickers hardness pyramid number). Plasma spraying of similar coatings is in the region of 600 to 800 HV. Combustion spraying is lower still [2.25].

Porosity of detonation gun coatings is of the order of $10\mu m$ diameter, which is well below the porosity expected from plasma sprayed coatings and combustion processes.

The bond strength of detonation gun coatings to their substrate are high (values of 60 to a maximum of 170 MN/m² have been measured). This exceeds plasma coatings (20 to 60 MN/m²). For the detonation gun process, the oxide quantity may be held to 2%. The plasma process using inert gases can range from 1 to 8%. Combustion processes may give a quantity of 10% or greater.

2.5.12 Finishing coatings from plasma and detonation gun processes

Both coating types can be used as-sprayed, for many applications. Roughness values in the as-sprayed form are $3.0\mu m$ CLA (Center Line Average). The roughness can be reduced by brushing with an abrasive-loaded brush. This gives a nodular finish by reducing the peaks of the coating surface without affecting the thickness of the coating.

2.6 WELD SURFACING

Weld surfacing makes use of welding techniques to deposit high performance materials onto selected areas of a component's surface. It is used for repair work and some of the processes include Arc weld surfacing, friction surfacing, and laser surfacing [2.30].

2.6.1 Arc Weld Surfacing

The electroslag strip cladding process, improvements to the plasma MIG process and

33

the availability of hardfacing alloys in strip electrode form are three applications for coating of large surfaces [2.29].

Plasma-MIG combines two conventional welding arcs, a transferred plasma arc and a MIG arc. For surfacing, two modes of operation can be used. The rotating arc metal transfer for solid wire consumables and conventional droplet metal transfer using large electrode extensions for cored wired consumables [2.30]. Both techniques can achieve deposition rates of 12 Kg/hour.

The synergic pulsed MIG process is suitable for surfacing applications because of the improved arc stability and weld quality achieved at low mean currents. It is used for applying corrosion resistant materials such as Inconel, Monel, and Stainless Steel (SS). It is also used for depositing wear resistant materials using cored wire consumables such as martensitic SS and stellite alloys.

2.6.2 Friction Surfacing

This involves pressing a rotating consumable rod on to a moving substrate to deposit a layer [2.30]. It is a solid phase process and can produce thin layers with good adhesion, producing a deposit with the same composition as the consumable used.

2.6.3 Laser surfacing

Lasers can be used for a range of surfacing and surface treatment processes. They are applied for transformation hardening and surfacing of precision components where the heat and deposit must be controlled accurately. The heat also controls the

depth of hardening.

2.7 GASEOUS AND VACUUM PROCESSES

2.7.1 Vapour deposition

Vapor Deposition may be defined as the condensation of elements or compounds from the vapour state to form solid deposits [2.31]. The physical technique includes vacuum metallizing (or vacuum evaporation) and sputtering. Sputtering is based on the bombardment of a target with excited ions. It is a versatile, low temperature vacuum process. Practically any element, alloy or compound which can be formed into a stable sputter target can be deposited. A schematic of a simple DC sputtering system is shown in Figure 2.6.

Sputtering is used to deposit films of high melting point as well as low-vapour-pressure materials, which are difficult to evaporate [2.32]. The deposition process is a versatile and relatively inexpensive method of molecular forming and building of coatings by controlled deposition of matter on an atomic or molecular scale [2.33-2.35]. Conventional sputtering techniques have low deposition rates. Magnetron sputtering sources offer high target erosion rates. The combination of hardness and corrosion resistance of various sputtered coatings make them suitable for tribological applications.

Vapour deposition includes Chemical Vapour Deposition (CVD) and Physical Vapour Deposition (PVD). In PVD processes, the feed vapours must be generated by evaporation from a surface, usually solid. The vapourised material is then
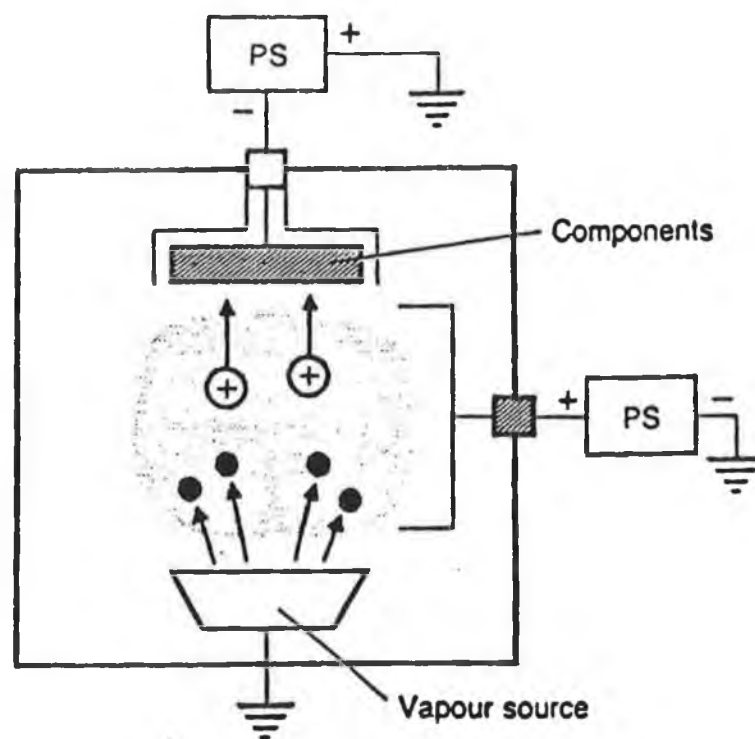
Figure 2.6 Schematic of a simple DC sputtering unit [2.54]

36

transported from the source of the feed to a substrate on which it condenses [2.31]. The vapor-deposited materials are produced and maintained at temperatures below their melting points, and, therefore, structural or compositional effects can be frozen in the deposits. Physical processes are confined to thin film coatings (1μm to 4μm), whereas chemical processes are used both for thin films and thick coatings in excess of 1mm [2.29].

2.7.2 Chemical Vapour Deposition (CVD)

In Chemical Vapour Deposition, the coating is formed by a chemical vapour reaction between gaseous reactants introduced into a vacuum chamber containing the heated component. Tools to be coated are precleaned, placed on coated graphite or high temperature alloy work trays and loaded inside the retort of a CVD reactor. The tools are then heated under an inert, reducing or carburizing athmosphere. The volatile coating material is thermally decomposed or chemically reacts with other gases to produce a non-volatile solid that deposits on the hot tool surface. A wide range of materials can be applied by this process including carbides, nitrides, oxides and borides. The coating thickness deposited and the deposition rates depend upon the reactant concentrations, pressure, temperature and time [2.4]. Reactive gases of either nitrogen or methane, to produce either TiN or TiC, are also introduced into the chamber. It is the main method for coating sintered carbide inserts. Typical coatings for CVD processes are listed in reference [2.17]. High hardness and corrosion protection can be obtained and adhesion is good due to diffusion of the coating into the substrate. The coating process is carried out at 5 to 500 torr pressure

37

but high substrate temperatures are employed and, therefore, many substrates cannot be coated in this fashion. Temperatures of 900 to 1100 °C for instance, are used to coat carbide cutting tools with coating thicknesses to about 10μm. It is not generally practical to deposit coatings on sharp edges when using the CVD process. Rounded edges are recommended, which may limit the precision required [2.4]. Thicker coatings with good adhesion is possible with CVD and irregular geometries are coated with ease. A schematic of a CVD reactor system is shown in Figure 2.7.

2.7.3 Physical Vapour Deposition (PVD)

PVD covers three major techniques, evaporation, sputtering and ion plating [2.17]. In PVD processes, material is physically removed from a source by evaporation or sputtering. The vaporized material then moves through a vacuum or partial vacuum by acquired kinetic energy [2.4]. The vapour then condenses as a film on the surfaces of substrates. PVD is the main way of coating HSS tools because of the low temperatures (150 to 500° C) employed, and the heat cycle does not change the performance of uncoated carbides as reported in [2.2]. The process gives finer grain size coatings than CVD and duplicates the surface finishes of the substrates [2.36]. PVD coatings deposit thinner coatings than CVD processes (1 to 4μm) [2.37]. Coatings do not build up on the edges in this process and sharp corners are permitted as opposed to the CVD process [2.4]. The PVD process is line of sight and, therefore, tools must be rotated for coating purposes. A schematic of a Balzer's PVD system is shown in Figure 2.8.
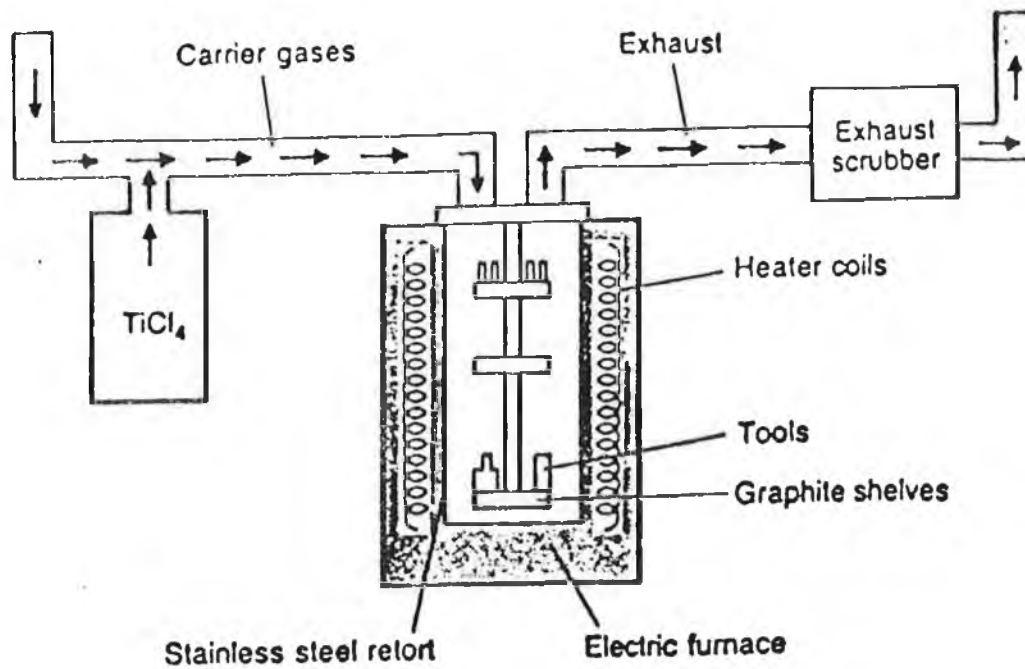
Figure 2.7 Schematic of a CVD reactor system [2.62].
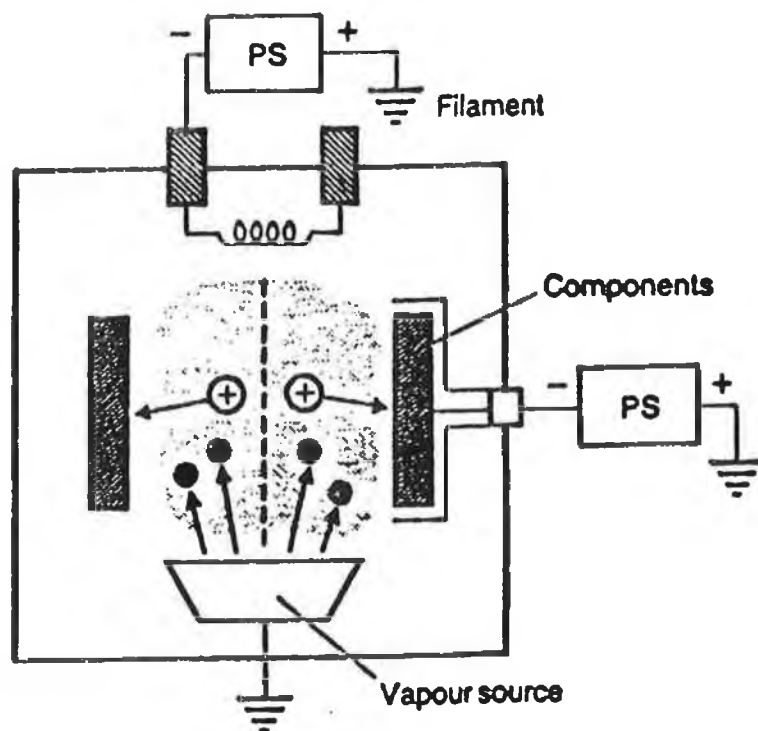
Figure 2.8 Schematic of a Balzer's PVD system [2.54].

2.7.4 Electron Beam Physical Vapour Deposition

This process is used to deposit 100 μm films of alloys such as nickel or cobalt base alloys (NiCoCrAlY or CoCrAlY) on to surfaces to improve corrosion resistance [2:33]. Plasma assisted PVD is used to coat HSS hobs, shaper cutters, shavers, drilling, milling, tapping, reaming, turning tools and broaches as well as punches and dies.

2.7.5 Reaction-ion-plating (PVD PROCESS)

This process allows the deposition of ceramic films at below the tempering temperature of High Speed Steel (HSS) [2.7]. Therefore, cheap tool steels can be coated with excellent adhesion, and uniformity of coating to the substrate.

Reactive-ion-plating methods provide means of increasing the energy of the deposition atoms. An activated reation evaporation (ARE) process involves bombarding a surface with ions of an inert gas, such as argon, prior to evaporating the coating material. This removes surface contaminants and heats the component, which assists adhesion. Biased activated reaction evaporation (BARE) combines ARE with a negative bias on the tools [2.38]. It is shown in [2.49] that if the proportion of ionised to non-ionised species striking the tools can be increased, then the structural and compositional characteristics of the coating can be improved.

2.8 COMPOSITE COATINGS

A number of methods exist for depositing composite coating. One way in which they can be formed is when a metal is deposited electrolytically or autocatalytically from an aqueous solution in which particles are maintained in suspension [2.40,2.41].

2.9 ELECTRODEPOSITED PROCESSES

In electrodeposition, material is deposited on a conductive surface by the discharge of individual ions, which arrive at the surface through a liquid or solvent medium [2.31]. Electrodeposited nickel offers athmospheric protection as well as high temperature oxidation resistance.(e.g. tips for gas soldering irons). Hardness of the deposit may vary from 120 to 400 HV. Electrodeposited nickel applications include ball race bearings, splines, threads, gear and flywheel housings for resalvage work. Pump parts using thicknesses of 10μm and marine components as an undercoat to hard chromium are often employed. The effects of fretting corrosion are reduced by nickel coatings.

2.10 SURFACE COATINGS

2.10.1 Tungsten Carbide Cobalt (WC-Co) Coatings

These coatings were applied for wear testing in the experimental section by the HVOF process described in section 2.5.5. WC-Co coatings have been prepared using

41

numerous surfacing techniques such as plasma spraying in air or vacuum using a variety of carrier gases or hypersonic spraying systems. Each process produces a large range of coatings and coating properties. Spray setting and powder manufacturing processes can be divided into several classes causing wide microstructural differences.

WC-Co type cemented carbides generally exhibit a high hardness, a high rupture strength and a low ductility. At low cobalt content, WC-WC junctions exist whereas at higher cobalt contents, thin cobalt layers separate the WC grains. These layers are of thickness 2-40 nano meters. The thin cobalt layers give rise to the high rupture strength of WC-Co [2.42]. Cobalt is the main binder material used for Tungsten Carbide because it fulfils many of the requirements such as high melting point, high temperature strength and gives a tough binding property. It also forms a liquid phase with WC, and dissolves it. It can also be ground to a very fine state for mixing with the hard WC particles [2.43]. WC-Co are applied mainly for the prevention of wear where fine abrasives (<1mm) are present as either contaminants or in a slurry [2.44]. For intense abrasion by large abrasives (gouging), the thin and brittle WC-Co coatings are regarded as unsuitable, according to Schmid and Nicoll [2.45]. Wear decreases with the carbide size. The generation and propagation of cracks is a function of the crack initiation points present in the coating structure and in the contact zone, which are a function of the sliding speed, friction and applied load. Small carbides do not fracture easily and should a crack develop, it has difficulty developing through the ductile matrix. The Cobalt matrix has allowed a very hard brittle substance, WC, to be used for a large range of applications by altering the toughness of the product, so that one can go from a roughing cutting operation

42

requiring shock loading to a finishing tool requiring high hardness.

2.10.2 PCBN: Poly crystalline cubic boron nitride

Boron nitride is a compound consisting of almost equal numbers of boron and nitrogen atoms, which has a hexagonal structure and can be transformed into crystals of Cubic Boron Nitride by high pressure and high temperature processes with the use of catalysts and solvents to increase the transformation rate. In the mid-1950s, the synthesis of Boron Nitride (BN) with a diamond like structure, cubic BN (cBN) was achieved. Two years later, man-made diamond was produced under high temperature and pressure.

Since then and following a decline in the interest of growing cBN films, new interest has emerged recently due to the excellent properties of these films.

Boron Nitride shows unique structural, mechanical, optical and electronic properties that lend it to industrial applications. Cubic boron nitride was until recently available as a bulky crystal type material. Today, it can be produced as a two dimensional thin film. Polycrystalline cubic boron nitride (PCBN) have a well-established market. The mechanical wear resistance of BN films are highlighted by their super-hardness, high Youngs Modulus of rigidity, and high degree of chemical inertness. One main application of cBN is for low friction films, which are required for a variety of precision thermodynamic engines (stirling, adiabatic diesel engines and gas turbines). PCBN is produced by compacting and sintering the individual crystals together to form a polycrystalline mass. Random orientation of the crystals provides high hardness and abrasion resistance in all directions [2.46]. Different properties can be

43

produced such as hardness, wear resistance and toughness. The hardness and abrasion resistance of cBN is second only to diamond as described in reference [2.47]. Cubic BN is much harder than abrasive materials like Al_2O_3, SiC and boron carbide [2.48]. PCBN has high impact resistance, toughness and hot hardness, and high thermal conductivity. PCBN tools are not recommended for austenitic or ferritic cast irons. Large areas of free ferrite in cast irons will cause rapid wear and short life of PCBN tools. They may also be subjected to chemical wear if machining nickel-based superalloys. They operate well if the microstructure is pearalitic and high cutting speeds are used (488m/min +). Machining of hard (Rc 40-70) abrasive cast iron such as martensitic structures, and martensitic irons such as Ni-hard or high chromium irons are a useful application of PCBN tools. Hard faced, wear resistant alloys applied by weld deposition, plasma spraying or casting which were normally ground are now machined by PCBN tools [2.49-2.52].

2.10.3 Titanium carbonitride

These coatings provide high wear and corrosion resistance as well as resistance to mechanical shock. They can be applied in thick coatings for turning or thin coatings for shock such as in milling applications. In multilayer CVD coatings, the intermediate properties of Ti(C,N) make it a suitable sandwich layer between TiC and TiN [2.4]. Both Titanium Carbide (TiC) and Titanium Nitride (TiN) are isomorphous, and a continuous series of solid solutions can be prepared from them. Both materials can exist in compositions considerably below their stoichiometric values for carbon and nitrogen content, which affects their properties [2.53]. Studies

44

involving cemented TiC base materials have shown that an improvement in physical properties can be obtained by TiN additions. Such improvements include an increase in resistance to plastic deformation, and improved tool life in turning and milling. Some of these features were attributed to grain refining, an increase in thermal conductivity and improved thermal shock resistance as reported in [2.53].

2.10.4 Titanium carbide

TiC, which was introduced during the 1960s for carbide cutting tools, is today applied to forming tools, such as punches and dies, and where abrasive wear is predominant. Threading and grooving operations involving low speeds are also suitable applications. They provide high hardness and abrasion resistance, with low coefficient of friction and resistance to cold welding. Since its thermal expansion is close to that of tungsten carbide (WC) when compared to other hard coatings, it is often used as the first layer in multilayer coatings to minimise thermal stresses at the interface with the WC substrate. The coating also acts as a barrier to prevent the diffusion of carbon from a tungsten carbide substrate to the coating [2.4].

2.10.5 Hafnium nitride

It has a high hardness and chemical stability at at temperatures up to 800°C, with a coefficient of thermal expansion close to that of Tungsten Carbide (WC). It also provides good resistance to abrasive wear, cratering and flank wear [2.4]. A number of PVD methods are suitable for depositing Hafnium Nitride.

45

2.10.6 Titanium

Titanium is a strong, corrosion resistant, and light weight material [2.22]. In pure form, it has an Ultimate Tensile Strength (UTS) of 400 MN/m^2 but when alloyed, its strength can rise to 1400 MN/m^2, which it can maintain at high temperatures.

2.10.7 Titanium Nitride

When coated to materials, it gives an increased life and allows tools to be used at higher cutting feeds and speeds than uncoated tools. Coating thicknesses are between 1μm and 6μm for Physical vapour deposition (PVD). Hardness values over 2000 Hv are achieveable [2.54]. TiN has become the most common coating for HSS cutting tools requiring sharp edges. It is highly inert with no tendency to form alloys with common metals. As a result, the tools resist abrasion, adhesion, galling, welding, cratering and the formation of built up edges [2.4]. Using the Hertz theory of contact, for optimising hardness conditions, Halling [2.55] showed that TiN is a suitable material for coating cutting tools of coating thickness 3-5μm. Its inertness also make it suitable for human implants.

2.10.8 Aluminium oxide

Coatings of Al$_2$O$_3$ are harder than TiN but softer than TiC at low temperatures. At temperatures attained during high speed metal cutting, they have the highest microhardness of all three coating compositions [2.4]. They are the most chemically

stable of all hard coatings at any temperature, making them the most crater resistant. The low thermal conductivity of Al_2O_3 at high temperatures during cutting applications, tends to concentrate the heat in the chips rather than the tools. Flank wear resistance of tools coated with Al_2O_3 is equal to that of solid ceramic tools. Cemented carbide tools coated with them have increased the cutting speeds possible to about 457 m/min.

2.10.9 Zirconium Nitride

This material offers low friction and heat dissipation properties. It gives a very fine coated grain struture to carbides, therby reducing wear and increasing the cutting performance of carbide tools [2.29]. The fatigue life of EN8 steel was increased by a factor of 2 by using Zirconium Nitride coatings as described by Duckworth [2.56].

2.10.10 Diamond and Diamond Like Carbon(DLC) Coatings

The main mechanical properties of diamond are currently exploited by industry in three main areas, namely grinding and polishing, precision machining and drilling [2.57]. The addition of a thin layer of diamond can reduce the amount of wear to ceramic cutting tools and its hardness, low friction and chemical inertness enable it to be used in harsh environments [2.58].

Diamond-like carbon films were first deposited by Aisenberg and Chabot in 1971 [2.59]. These films are used on products such as thin film magnetic recording devices, cutting tools and bearings. Like diamonds, they offer high hardness and

47

wear resistance, and low friction coefficients. Unlike diamond, friction was found to increase for DLC coatings with relative humidity as reported in references [2.60,2.61]. Applications of DLC coatings include low friction coatings on dies, punches and moulds, coating on machine tools for high speed machining of copper and aluminium alloys, protective coatings on medical bone cutting saws and coatings on mechanical seals [2.62]. Carbon films with very high hardness, high resistivity, and dielectric optical properties are now described as DLC. Hardness values are in the range of 3000 to 9000 kg/mm^2. DLC coatings have been produced by rf and dc plasma deposition, ion beam deposition, chemical vapor deposition and sputtering [2.63,2.64]. DLC films are amorphous. Abrasion resistance is one of the main mechanical properties associated with DLC coatings. Some of the DLC coatings show tough characteristics when deposited with titanium. Without titanium, mechanical properties are not as tough as reported in [2.65].

2.11 COATING IMPURITIES

Impurities in coatings may arise from a number of sources. Oxygen, nitrogen, hydrogen and carbon can be present in vacuum processes due to residual gases, vacuum leaks and outgassing. In sputter deposition, the implantation of several atomic per cent of the sputtering gas is common. Carrier gases and unreacted or partially reacted source gases are often incorporated in CVD reaction products [2.47].

Most coatings will be in a state of thermal stress due to the difference in the thermal expansion coefficients of the coating and the substrate materials, and an intrinsic

48

stress due to crystallographic flaws built into the coating during deposition. Thermal stresses form on cooling from the deposition temperature, while the intrinsic stress is due to the deposition process.

CHAPTER 3

WEAR OF MATERIALS AND WEAR TEST EQUIPMENT

3.1 INTRODUCTION

Leonardo da Vinci measured the frictional forces of bodies sliding on horizontal and inclined planes [3.1,3.2]. The coefficient of friction between rubbing solids was further developed by Guillaume Amontons and Coulomb [3.3]. Contact theory was initiated by Hertz and later developed by Johnson and Kalker [3.4]. Other Scientists such as Euler, Reynolds, Sommerfeld and Bowden along with many others have contributed to the historical development of current theories and knowledge of adhesion, friction, lubrication and wear, or more commonly known today as tribology [3.1,3.4-3.6].

Wear occurs to the hardest of materials including diamond. Much of the attention in wear studies has been focused on the surface damage in terms of material removal mechanisms, including transfer film, plastic deformation, brittle fracture and tribochemistry [3.7]. Properties which influence the wear of materials include the presence or absence of crystallinity, crystal orientation, anisotropy in mechanical properties as well as surface chemistry and changes therein. Bond dissociation in the surface layers influence wear. A reduction of hardness within materials can be achieved even with adsorbed gases, such as with hydrogen on diamond.

Wear can be defined simply as the loss of material which occurs by way of displacement and detachment at component surfaces [3.8], and one of the main uses of coatings is to reduce wear. Where metal detachment occurs, one or more of the

50

following will be operational [3.8,3.9].

i)   Abrasive wear.   ii) Adhesive wear.

iii)   Erosive wear.   iv) Fretting wear.

v)   Surface fatigue.   vi) Delamination.

Some of these processes are shown schematically in Figures 3.1-3.5. Figure 3.1 highlights the wear associated with different forms of motion between bodies along with types of erosion wear. Figure 3.2 shows the basic effects of material wear due to contact of components. Figure 3.3 shows the effects of adhesive wear and its progression due to sliding contact while Figure 3.4 compares a working system to a typical model of wear between two moving components. Figure 3.5 shows the results of different wear parameters on materials due to contact and impact operating conditions. Low friction and the use of suitable lubricants will result in low wear generally but parts may need replacement after a small amount of material has been removed or if surfaces are roughened while in operation. In polymer processing equipment, adhesion, erosion, abrasion, lubricated sliding and corrosion have been identified [3.10].

Resistance to impact tends to decrease with increasing hardness and can lead to cracking or chipping of a surface coating [3.11]. Materials and alloys that are resistant to repeated impacts generally are not very resistant to abrasion and vice versa [3.12]. Some solid lubricants can under certain conditions act as abrasives. The loss of material by abrasive and erosive wear of valves, dies, pump impellors and cutting equipment causes significant reductions in the efficiency and useful lifetime

51
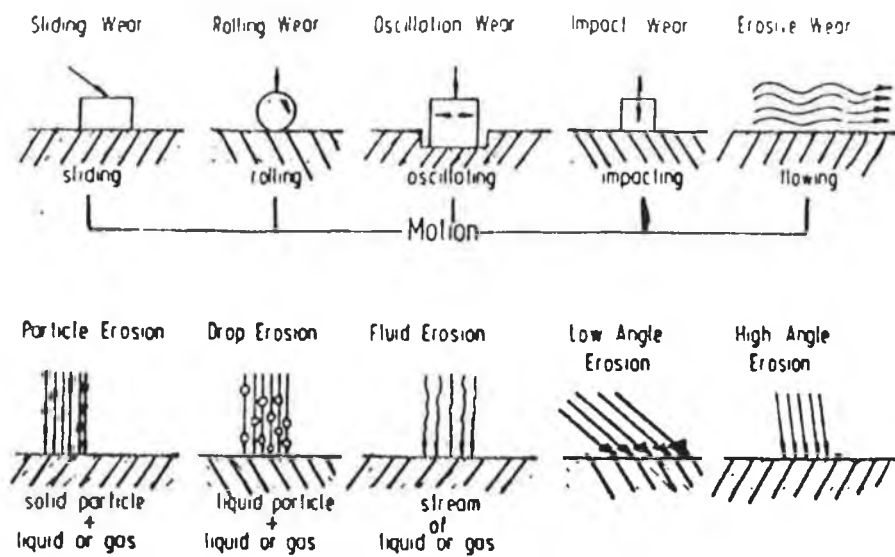
Figure 3.1 Classification of wear processes by wear modes [3.1].
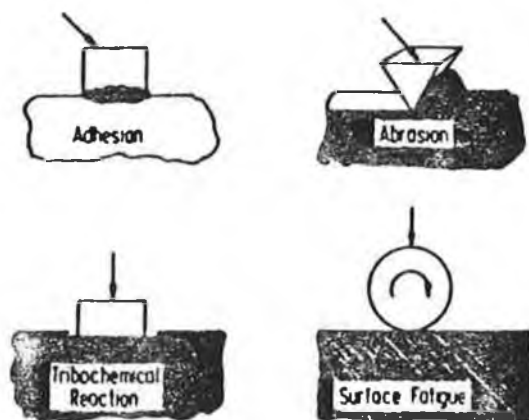
Figure 3.2 Schematic description of four wear mechanisms [3.1].

52
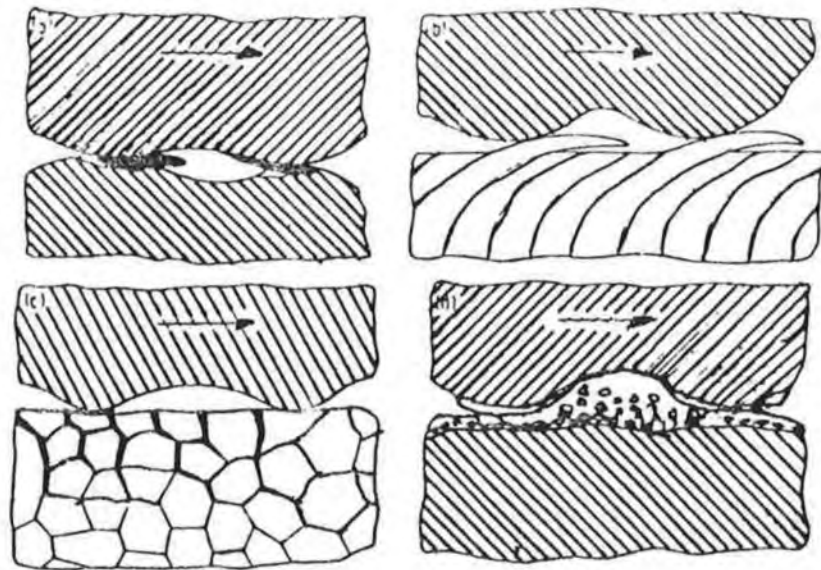
(a) Adhesive junctions, material transfer and grooving.
(b) Surface fatigue due to repeated plastic deformation on ductile solids.
(c) Surface fatigue results in cracking on brittle solids.
(d) Tribochemical reaction and cracking of reaction films.

Figure 3.3 Mechanisms of wear during sliding contact [3.1].
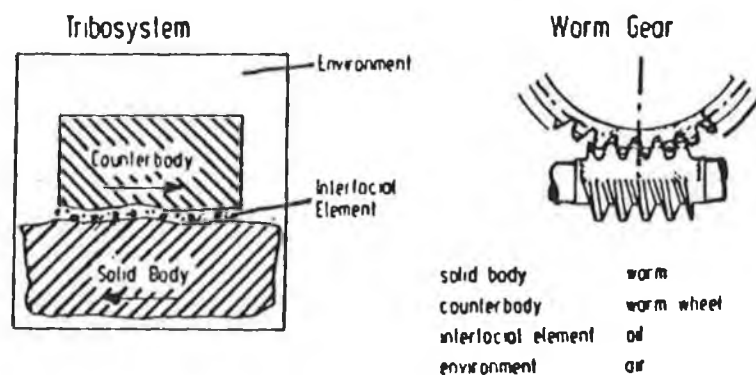
The system consists of four main elements:

1. Solid body.
2. Counterbody.
3. Interfacial element.
4. Environment.

Figure 3.4 Schematic of the elements of a tribo-system [3.1].

53

tribochemical reaction

abrasion
(ploughing,
cutting)

severe

mild

adhesion
(shearing,
material transfer)

fatigue
(crack initiation,
crack growth)
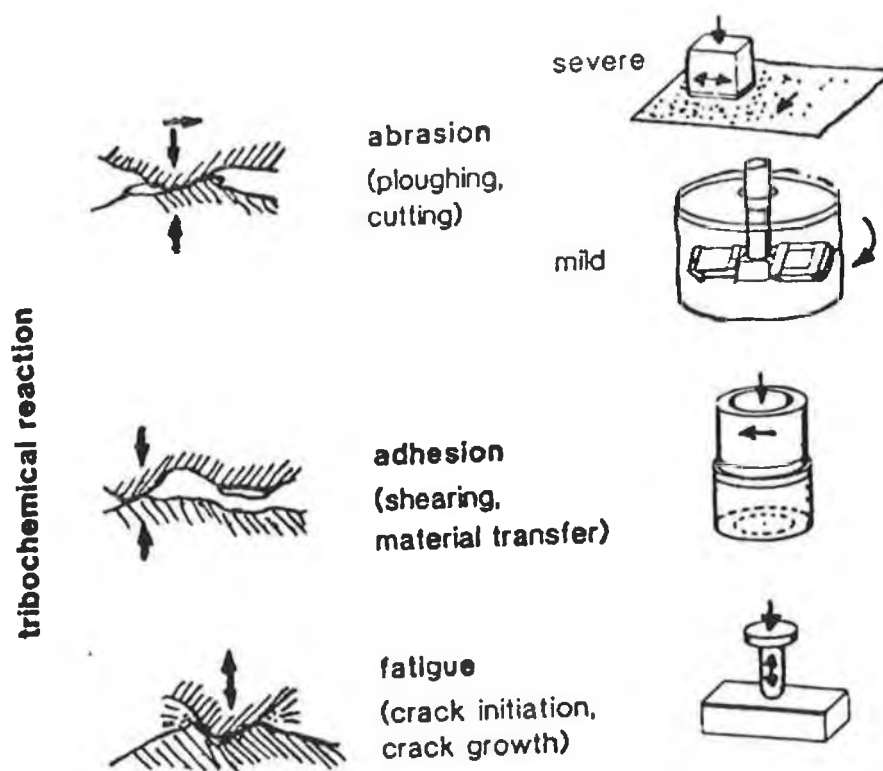
Figure 3.5 Schematic representation of abrasion, adhesion and fatigue [3.13].

54

of machinery. The surface of a specimen will only lose material when two conditions have been satisfied. The strain imposed must reach a critical value at which microfractures are initiated. These microfractures must then propogate in order that the fragments are released. An ideal wear resistant material will, therefore, have an ability to absorb strain prior to the initiation of microfractures and have a toughness which resists the propagation of the microfractures. In cutting tools, the cutting edges must show high resistance to abrasive wear and to cracks caused by mechanical and thermal fatigue. Wear damage in components is often caused by vibrations. In the case of very small amplitudes (in the μm-range) of relative motion, fretting corrosion can occur. This is often accompanied with tribochemical processes and the production of oxidized wear particles [3.14]. In rubbing conditions, wear is influenced by the frictional properties of the materials in contact, the presence or absence of lubricants, the mechanical properties of the materials, the coating adhesion, and the velocity of rubbing.

As seen from the preceeding facts, the nature and quantity of wear will also depend upon the materials in contact, the composition of their surfaces and the environment in which they are used, along with the type of wear forces applied.

The investigation of coating systems to provide wear and impact abrasion resistance at extreme temperatures was discussed in the previous chapter. This chapter discusses some of the main wear parameters that components and tools are subjected to in service. It also lists and describes equipment developed both in the form of standard and in-house laboratory wear test rigs. This equipment is compared with the Test Rig developed for the experimental work conducted in this research.

3.2 TYPES OF WEAR

3.2.1 Friction and wear

Friction and wear lead to the deterioration of material surfaces and coatings. Friction has been mathematicallly defined by many pioneers and researchers and relates to the resistance of relative motion. For movement between two surfaces, friction is considered as sliding friction and rolling friction for bodies rotating relative to each other. Under conditions of temperatures, vacuum, humidity, normal forces, coating properties and surface topography and roughness, frictional conditions become complicated. Wear parameters such as tribochemical effects [3.15] also complicate frictional values.

3.2.2 Abrasive wear

This occurs when a soft surface with hard particles slides along a hard surface ploughing a series of groves in that surface. These particles penetrate the surface and displace material in the form of elongated chips [3.9,3.11,3.16-3.18]. Abrasive wear can be divided into two and three body type wear and their effects are shown schematically in Figure 3.6. Two-body abrasive wear results when a rough surface or fixed abrasive particle slides across another to remove material. The roughness of the harder material has an influence on the wear rate in these conditions. In three-body abrasive wear, particles are loose and mobile during their interaction with the wearing surface [3.19]. Three-body abrasion as shown in Figure 3.7 can be

56

divided into "closed" and "open". Closed three-body abrasive wear occurs when loose particles are trapped between two sliding or rolling surfaces which are close to each other. Open three-body abrasive wear occurs when the two surfaces are far apart or when only one surface is involved in the wear process [3.19]. Open three-body abrasive wear causes gouging, involving a combination of abrasion and impact force [3.20-3.23]. Abrasive wear is related to hardness, with wear resistance increasing with hardness [3.24]. In publications [3.25,3.26] it is shown that hardness or its equivalent cannot uniquely characterise the magnitude of wear under the conditions of abrasive impact [3.27]. Rickerby and Burnett have shown in [3.28] that it is also necessary to consider the load bearing capacity of the coating/substrate system.

3.2.3 Adhesive wear

When two atomically clean metal surfaces are brought into intimate contact, bonds between atoms of both surfaces are established and adhesion takes place. If an asperity of one metal is slid across the other material, adhesion between them can lead to a transfer of material from one to the other producing adhesion wear [3.3,3.29-3.32]. Crystal structure [3.33] and crystal orientation [3.34] has an influence on adhesive wear with Hexagonal metals giving the best adhesion conditions. Adhesion becomes more pronounced at hot working temperatures characterized by high atomic mobility. If contact is restricted to a few high spots and if there are forces acting on the surfaces, micro or pressure welding may occur. Small surface projectories weld together, work harden and fracture therby

57
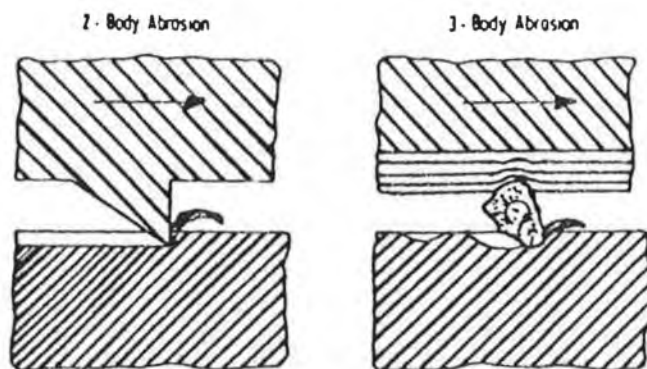
Figure 3.6 Two-body and three-body wear patterns [3.1].
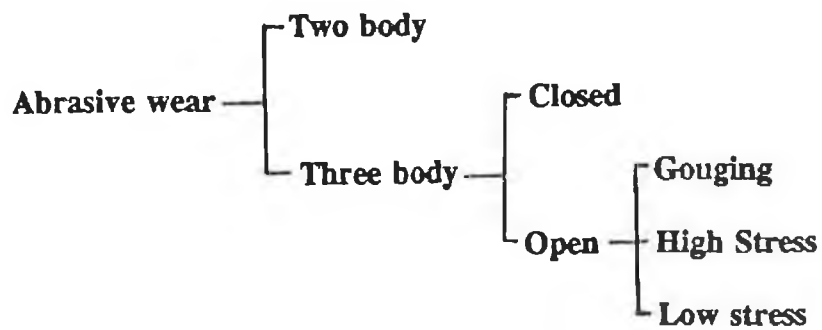
Figure 3.7 Classification of abrasive wear types [3.19].

58

transferring material from one surface to another. This leaves projections on one surface, cavaties on the other and the possibility of further damage [3.8]. Components requiring a close tolerance fit are particularly susceptible to this form of wear [3.10]. When dissimilar materials are in contact, the weaker of the two materials will in general transfer particles to the stronger material [3.34]. Factors influencing the wear mechanisms during sliding contact are shown in Figure 3.8., and the metallurgical properties affecting sliding wear shown in Figure 3.9.

3.2.4 Gouging wear

When abrasive lumps or particles rub against a surface with sufficient force, gouging wear or abrasion occurs [3.35]. It may develop from the impact of such particles on the mating surface, so a method to resist fracture due to impact, and a need for hardness to resist gouging, is required.

3.2.5 Erosive wear

The mechanical removal of material as a result of the impact of abrasive particles carried in a contacting fluid is called erosion [3.8,3.10,3.36]. Processes resulting in wear loss due to single or multiple impact of particles causing erosive wear are described in Figure 3.10. Solid particle erosion can be divided into three regimes according to the ferocity of attack of the particles [3.37]. A low stress regime occurs when large particles strike materials at low velocities giving elastic interaction between the particle and material. The second regime involves elastic/plastic

59
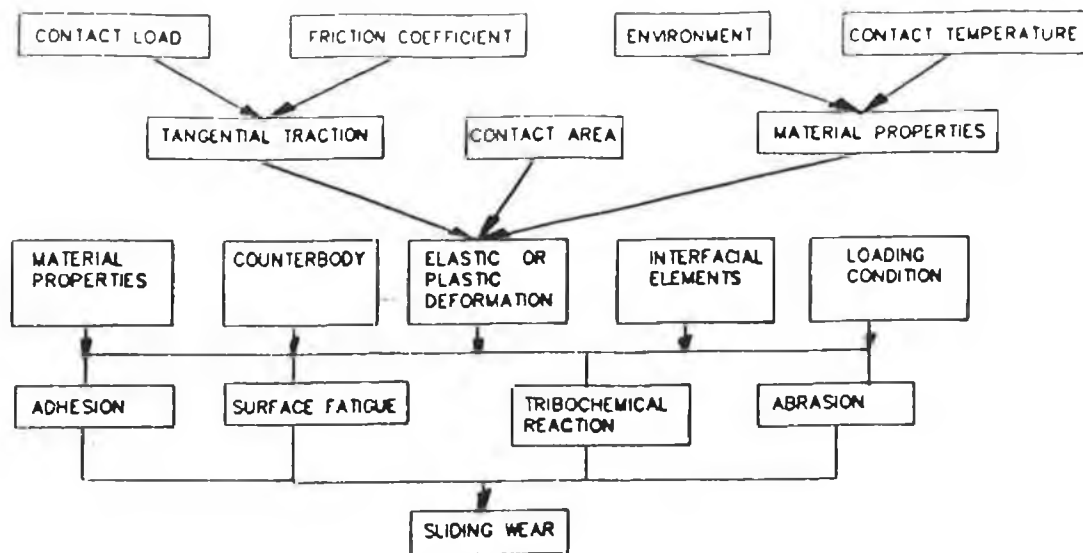
Figure 3.8 Factors influencing wear during sliding contact [3.3].
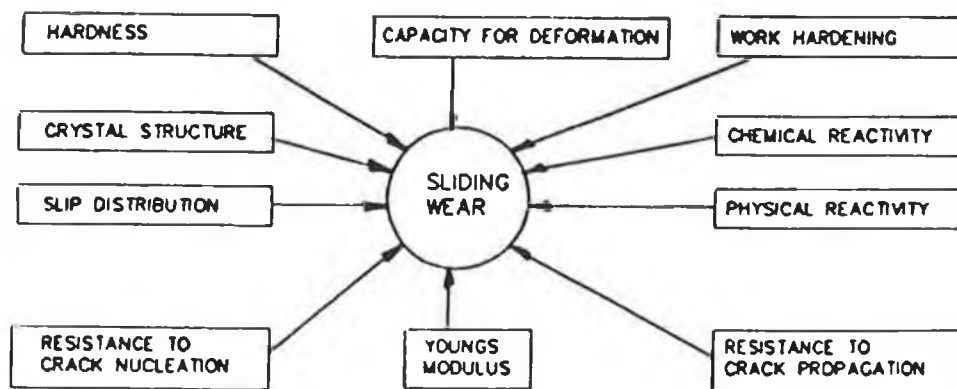
Figure 3.9 Metallurgical properties influencing sliding wear [3.3].
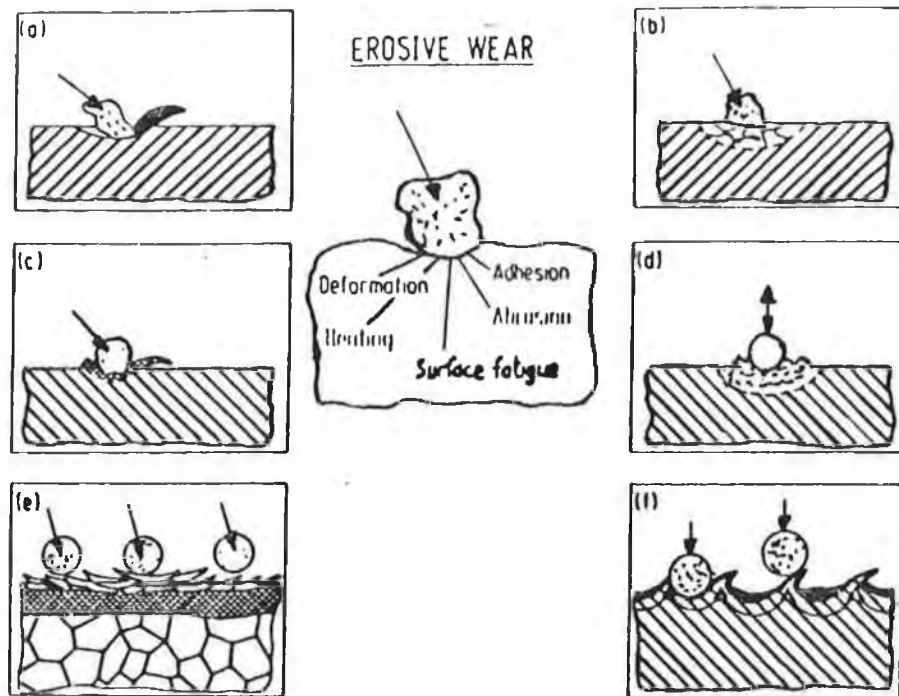
Wear due to single or multiple impacts of particles.

(a) Microcutting and microploughing.
(b) Surface cracking.
(c) Extrusion of material at the exit end of the impact craters.
(d) Surface and subsurface fatigue cracks due to repeated impacts.
(e) Formation of thin platelets due to extrusion and forging by repeated impact.
(f) Formation of platelets by a backward extrusion process.

Figure 3.10 Particle erosive wear [3.17].

61

interaction and the third regime occurs when very small particles strike materials at high velocities producing high strain rates [3.38]. The effects of erosion have become a problem associated with airfoils and shrouds in various fans, in compressors and turbines, on helicopter blades, in centrifugal pumps, on valve components and in pipe joints and bends. The extent of erosion depends on the composition, size, and shape of the eroding particles, their velocity and angle of impact, and the composition and microstructure of the surface being eroded [3.39,3.40]. In brittle materials, such as ceramics, microcracking develops due to erosion. When the eroded surface is a sprayed coating, most authors report a brittle tendency for carbides and ceramics, but the erosion mechanism is affected by other factors such as porosity or cohesive strength, as reported in [3.41,3.42].

3.2.6 Fretting wear

When components are subjected to very small relative vibratory motion at high frequencies, fretting wear occurs. Fretting wear is dependent on the sliding conditions and on the nature and properties of surfaces. It occurs by continuous small displacements (in the region of 5 to 50μm) of contacting surfaces and is assisted by adhesion and abrasion. Corrosion also assists the fretting process. Oxide layers can lubricate if they remain intact but if displaced, they can become abrasive particles [3.8]. Cracking due to fretting can be offset by the use of hard coatings such as TiN and DLC coatings according to Fouvry et al [3.43].

3.2.7 Fatigue

Kragelsky [3.44], was the first person to publish a paper on the fatigue theory for the wear of solids. Fatigue is associated with loading and unloading of a material and is caused by cyclic pressure or stresses. It is characterised by the detachment of particles to leave pits or spalled areas [3.45,3.8]. It occurs on surfaces which come into repeated contact at stresses higher than the fatigue limit [3.9,3.16]. It can result in cracks or fracture as shown in Figure 3.11. Cracking in a component will begin from a point where the shear stress is a maximum and gradually work itself out to the surface. Imperfections within the materials will assist this process. The fatique resistance of metals can be improved by incorporating compressive stresses in the surface layers. Grit blasting of samples prior to spraying, compressively stresses its surface and this can improve fatique life and a suitable coating can combat the corrosive factors in applications where corrosion-fatigue conditions apply [3.46]. Subsurface and surface fatigue wear are the dominant failure modes in rolling element bearings. For fluctuating loads, failure is likely to occur at a lower stress level than that estimated for static conditions. The mechanism of fatigue is generally considerd to consist of three phases.

i)   Commencement of crack due to material weakness.

ii)   If allowed to proceed, the crack spreads causing the crack propogation period.

iii)   At a certain stage in this period the area remaining can no longer support the applied load and fracture occurs. Contact fatigue, percussive wear, cavitation erosion and delamination are all related to fatigue wear.

3.2.8 Impact, shock and cavitation

Impact refers to the collision of two masses with initial relative velocity. In some cases, impact occurs due to clearance between parts such as in the rattling of mating gear teeth. This can lead to fatigue failure on the impact surfaces. Resistance to impact tends to decrease with increasing hardness and can lead to cracking or chipping of a surface coating [3.11]. Shock is used to describe any suddenly applied force or disturbance. Homogeneous materials with high toughness, such as martensitic steels, with coatings of high concentrations of a ductile matrix and consisting of hard particles, may be suitable for impact conditions. In impact, energy can be absorbed without causing severe fatigue wear or spontaneous fracture. As the matrix decreases, the toughness decreases and the materials are sensitive to impact loads and repeated load cycles (fretting, rolling or sliding under hertzian contact conditions) leading to surface fatigue. With increasing content of hard phases, wear is enhanced due to impact [3.45]. Failure may result due to a normal, steady-state fatigue process occurring within the layer or due to high brittleness and insufficient binding to the bulk material. A summary of indentation processes consisting of impact and abrasion conditions are shown in Figure 3.12. Cavitation occurs when gases trapped in fluids generate into bubbles under mechanical agitation. These bubbles collapse and impact against solid surfaces with energy sufficient to cause material wear.
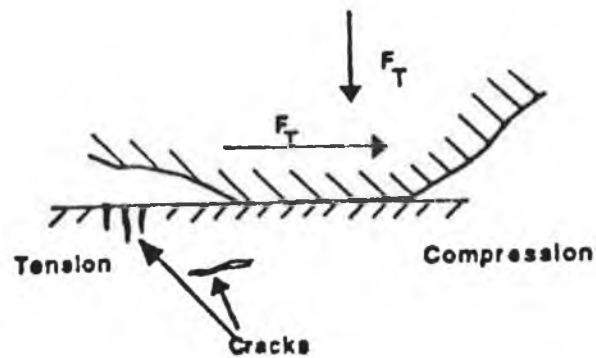
Figure 3.11   Schematic of fatigue wear mechanism.
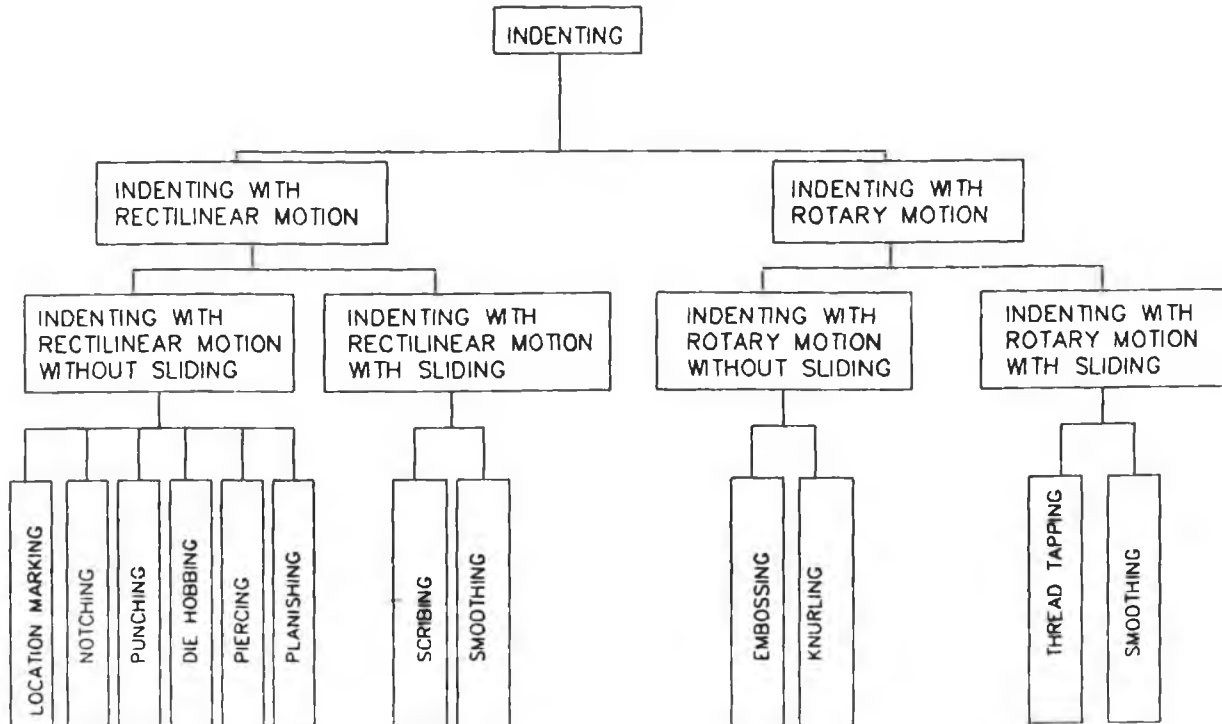
Figure 3.12   Summary of indentation processes   [3.3].

3.2.9 Delaminations

Delaminations is caused by high contact stresses, plastic deformation and work hardening in shear and cracking when flakes of material become detached [3.8].

3.2.10 Diffusion wear

Solid-state diffusion is the mechanism by which atoms in a metallic crystal shift from one lattice point to another causing a transfer of the element in the direction of the concentration gradient. Diffusion is time and temperature dependent and is influenced by the bonding affinity of surfaces in contact.

3.2.11 Corrosive wear

Corrosion wear has been defined as the reaction of a metal or alloy with its environment [3.46,3.47]. Corrosion tends to leave a pitted surface [3.9,3.11]. The wear rate of a corroded surface will often be higher than that of an uncorroded surface, and the corrosion of a worn surface will often be higher than that of an unworn surface. Many common forms of corrosion for coated and uncoated tools are identified in [3.48]. The total rate of loss of material in corrosive wear can be high and it tends to be more serious at higher temperatures [3.35,3.49]. Hot corrosion occurs on turbine blades and nozzle guide vanes during normal operation. In applying corrosion resistant films, it is important to avoid pinholes which assist the process of corrosion [3.50].

3.2.12 Scuffing

Scuffing is defined as the seizure and galling caused by solid phase welding between sliding surfaces without local surface melting [3.51].

3.2.13 Hardness

Hardness is often used as an initial guide to the suitability of coating materials for applications requiring a high degree of wear resistance. The effect of hardness of a wearing material however is complicated as different wear mechanisms can prevail in service. For instance, softer materials will deform plastically at lower loads, which favours the formation of a large area of contact. Since thin wear resistant coatings are in the order of 5μm thick, microhardness measurement results in substrate deformation in the process leading to a composite hardness number [3.52,3.53]. Stoichiometry of a coating is important for consistent hardness throughout a system. Although hardness is important in the calculation of the wear of materials, it has been shown that the wear resistance is not only influenced by hardness but also by fracture toughness. Hard materials may also undergo plastic deformation and result in wear similar to softer materials. Hardness may not control the occurrance of adhesive wear but is known to effect the wear particle size. Surface roughness also influences the tribological performance of a mechanical system. If the harder member is rough, for instance, in a contact situation, the counterface may wear by abrasion due to micro cutting or ploughing. It has also been shown for thin, hard coatings that the rougher the surface finish, the lower the

67

coating adhesion, as measured by scratch testing methods. When a hard coating is applied to a rough surface, it is more easily removed than when applied to a smooth surface. Although low surface roughness of tools improve the surface finish of the workpiece they leads to a cost increase.

3.2.14 Built Up Edge (BUE)

At low speeds, work material welds on to cutting tools and will be pulled or pushed aside at the exit or re-entry of the cutting edge. As a result, a breakage of the tool may occur [3.54]. Coatings avoid contact between the workpiece and the substrate, thus giving protection against abrasion, adhesion and the damage caused by built up edges.

3.2.15 Stress of Thin films

All films will be in a state of internal stress. They experience shear, tensile and compressive stresses and in extreme cases, the interfacial shear stresses may exceed the adhesion strength of the coating-substrate interface. This will lead to cracking and delamination of the coating. Compressive stresses are known to increase coating hardness [3.55]. If coatings are deposited in a stressed state on a thin substrate, the substrate will bend to a certain degree. A tensile stress will bend, giving the coated surface a concave shape and compressive stresses will bend it to produce a convex shape [3.56].

3.3 EFFECTS OF COATING AND GRAIN SIZE ON WEAR RESISTANCE

Crater resistance is approximately proportional to coating thickness but resistance to flank wear generally levels of when thicknesses reach about 8μm [3.57]. The strength of cutting edges usually reduce as the coating thickness increases. If the thickness exceeds 12μm, brittle properties can dominate. Thicknesses between 2 to 12μm can produce a combination of properties [3.58]. Multiple layers can be tougher than one thick layer, as the grain structure may be more refined and they may possess better elastic behaviour over the single thick coating [3.57,3.58]. For interrupt cutting operations, the resistance to wear and the impact strength of the cutter tool are critical. Cutting edges must show high resistance to abrasive wear and to cracks caused by mechanical and thermal fatigue [3.51]. In some cases, coatings can lead to crack initiation, which can result in failure faster than an uncoated sample as for example in bandsaw blades [3.59]. It was shown in this paper that Hard Chromium plating to bandsaw blades resulted in a reduction in the fatigue limit of the blades by over 50%. Titanium nitride coatings on the other hand increased the fatigue limit by 44% over uncoated blades. Cudden and Allen [3.60] have reported that the wear resistance of cemented carbide varies widely depending on the binder content and grain size. Large grains expose large binder areas and thus lead to faster wear rates of that binder. Tungsten carbide grains, which are poorly supported by the removal of binder through abrasion and corrosion, are susceptible to shear forces and are easily torn away from the surface. Any relative motion of grains can manifest in triangular cracking and, thus, loss of grains. Larger tungsten carbide grains have lower fracture toughness and may crack more easily. Thicknesses of

69

various coating applied by surface treatment processes are shown in Figure 3.13.

3.4 WEAR TEST EQUIPMENT

Most wear tests are designed to remove material in a controlled manner. However, different wear patterns emerge for different tests and wear tests remove material in many different ways. Advanced coating processes are increasingly being applied to solve wear problems on tools. Methods of wear testing for cutting tools seem to be well developed, especially for thin coatings. Methods for other tools and components are widespread and less well developed [3.61]. In selecting a suitable wear test, the following points may be considered:

i)   Is the test selected measuring the desired properties of the material.

ii)   Is the material in bulk form or a thick or thin coating?.

iii)   What forces and stress limits are suitable for the test?.

iv)   Will abrasives be present?. Abrasive size, form and the velocity of the abrasive should also be considered.

v)   Is the contact between the components rolling, sliding, impact or erosion only or a combination of these?. The surface finish of the test samples should be similar to that of the actual components.

vi)   Are temperature and humidity factors important?.

vii)   Is the test environment similar to the actual working environment.

viii)   What is the duration of the test.

ix)   Is the materials used in the test typical of the actual materials used in the machine parts etc.

If wear tests have been carried out with a high degree of simulation, of the service situation, then the results can be used with considerable confidence in selecting the best wear resistant coating system.

3.4.1 Material tests

Some of the techniques for testing materials in a non destructive way include:

i) Acoustic techniques.   ii) Dimensional changes.

iii) Magnetic particle.   iv) Die penetrant.

v) Visual.

Tests are used for quality control functions such as thickness, porosity, adhesion, strength, hardnesss, ductility, chemical composition, stress and wear resistance. Some of the available techniques for mechanical and tribological characterisations of coatings are given in Table 3.1 as reported in [3.62].

Coating Property	Characterisation method.
Hardness.	Microindentation & Nanoindentation.
Fracture toughness.	Palmqvist indentation.
Adhesion to the substrate.	Pull test, Indentation test, Scratch test.
Residual stress.	X-ray, $Sin^2\psi$ method.
Thickness.	Ball grinding, cross section measurements.
Wear resistance.	Pin-on-disk, erosion tests.

Table 3.1 Mechanical and tribological tests for coatings.

71
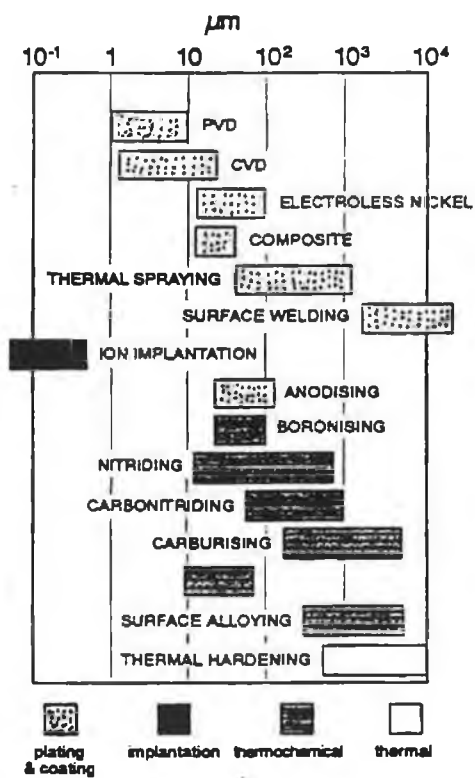
Figure 3.13 Thickness of various coating and surface treatment processes [3.58].

3.4.2 Test methods

Many tests for coated and uncoated cutting tools are conducted on machine tools, including lathes, mills, drills, punches and saws [3.63-3.74]. These test processes perform almost identical conditions to those experienced in manufacturing. It is also important to note that unlike common wear test equipment available, the machining tests subject the cutting tools to many wear parameters including impact and shock, abrasion, adhesion and hot corrosion. The limitations of these tests depend on the machine power available and quality of the machine tool. There are a considerable amount of other components subjected to coating processes which are not used as cutting tools and whose wear properties must be examined by laboratory wear tests. Many pieces of test equipment are currently available on a commercial scale including nano and micro hardness testers, fatigue testers, acoustic, and scratch-type test equipment etc. Most, if not all, simulation test processes will require some compromise.

3.4.3 Abrasive and Adhesive test equipment

Scratch hardness is the oldest form of hardness measurement and depends on the ability of one solid to scratch another. Mohs [3.93] categorised materials using this process giving diamond a maximum scratch hardness of ten. Most scratch type tests developed from this simple technique.

Abrasive tests are described by Kato et al [3.5] and others [3.12,3.45,3.75]. A review of test methods for abrasive wear is discussed by Spero et-al [3.76]. Other

methods involving adhesion, indentation and scratch tests for coatings are modelled and analysed by Rickerby and Matthews [3.52].

Adhesion is characterised by both scratch and indentation tests as reported in the literature [3.78-3.80]. In indentation adhesion tests, a mechanically stable crack is introduced into the interface of the coating and subsrate. The resistance of propogation of the crack along the interface is used as a measure of adhesion. In the scratch adhesion test method, a stylus is drawn over the surface under a continually increasing normal load until the coating fails. The wear areas can be examined by optical microscopy and scanning electron microscopy.

Depending on the shape of the product, different wear tests will be required. For instance, a simple polishing test, performed by Krokoszinski [3.81] and also described in [3.82] was carried out on coated test resistors. Measurements of the thickness after definite periods of time were used as indications of wear resistance of CVD and PVD applied coatings.

3.4.4 Pin-on-Disc

Most pin-on-disc machines are used for measuring sliding wear and friction properties. Under sliding wear, a coated or uncoated pin presses against a rotating plate. Almond et al [3.83] used a pin-on-disc apparatus for testing ceramics and cemented carbides on alumina discs using the pin as the test material. Using a diamond tip for the abrading tool, Kato et al [3.5] used a pin-on-disc test to operate within the chamber of a Scanning Electron Microscope to examine the abrasion effects. Scratch testing in conjunction with SEM provides a useful method of

analysing single point wear mechanisms of coated systems through an assessment of the deformation and fracture produced [3.84,3.85]. In a pin-on-disc apparatus described by Bouslykhane et al [3.86], hard Ti_xN were tested in atmospheric conditions with a rotation speed of 5 rev/min under loadings of 0.5, 2 and 4 N. In this experiment a ruby ball of 5 mm in diameter was used in an unlubricated condition. The wear rate was defined as the wear linear density (WLD) measured by a profilometer. The duration of this test was 1000 revolutions. In a two-body abrasion test, a coated pin is pressed on to a rotating abrasive paper making a spiral path to avoid overlapping [3.86,3.87]. This test process is very common for thin coatings. Makela and Valli [3.88] used a pin-on-disc apparatus to evaluate the wear resistance of TiC coatings on tool steel using a pin tip of radius 50 mm, sliding speed of 0.2m/s and sliding distance of 250m. A normal pin force of 5 N was used on a combination of various coated surfaces. The test results showed that the wear rate of TiC was greater than TiN. The friction of a TiC coated pin was low against a TiN coated disc (0.2), however the same did not apply for the reverse, i.e. TiN coated pin and TiC coated discs. Figure 3.14 is a schematic of a simple pin on disc wear test process. Watanabe et al [3.89] describe a similar type of test rig used for friction testing. In this apparatus, a vertical force is applied to a round nose or ball indenter while the specimen is moved horizontally back and forth by a hydraulic ram. Figure 3.15., shows a typical surface crack caused by a pin-on-flat scratch tester. Research conducted by Glaeser and Ruff [3.90] reported that pin-on-disc were the most widely used wear test processes followed by pin on flat. Other applications of pin-on-disc include material wear and friction properties at elevated temperatures and in controlled athmospheres as reported in [3.91].

3.4.5 Pin-on-drum abrasive wear test

In this test, one end of a cylindrical pin specimen is moved over an abrasive paper with sufficient load to abrade material from the specimen and crush the fixed abrasive grains [3.12]. This test simulates the wear that occurs during crushing and grinding of ore in which the abrasive (the ore) is crushed [3.75]. The pin also rotates while traversing as indicated in Figure 3.16. This ensures that the pin always contacts fresh abrasive. This test is considered a high stress abrasion type test, as the load is sufficient to fracture the abrasive particles.

3.4.6 Repeated impact wear test

Some research was undetaken in the past for ascertaining the effects of pure impact on alloy steels and cast irons. Equipment described by Blickensderfer and Tylczak [3.92] involved balls made from alloys being dropped 3.4 m on to a column of balls, with each successive ball receiving an impact on each side. The first ball receives maximum impact while the last one receives the least. This test, as shown in Figure 3.17 highlights the effects of spalling due to impact and shock only. This impact tester does not take account of the orientation of the samples used which can be up to 50mm in diameter. The effects of rebound was not addressed either in the test work.

The method of Dynamic Hardness Measurement as described by Tabor [3.93], makes use of an indenter striking a surface. The hardness is expressed in terms of the energy of impact and the size of the remaining indentation.

76
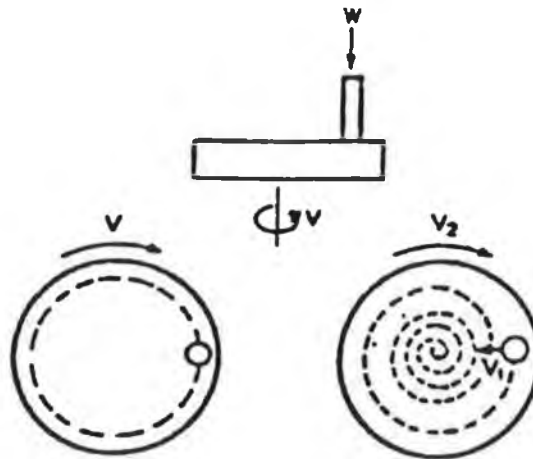
Figure 3.14 Schematic of pin-on-disc apparatus [3.86].

100μm
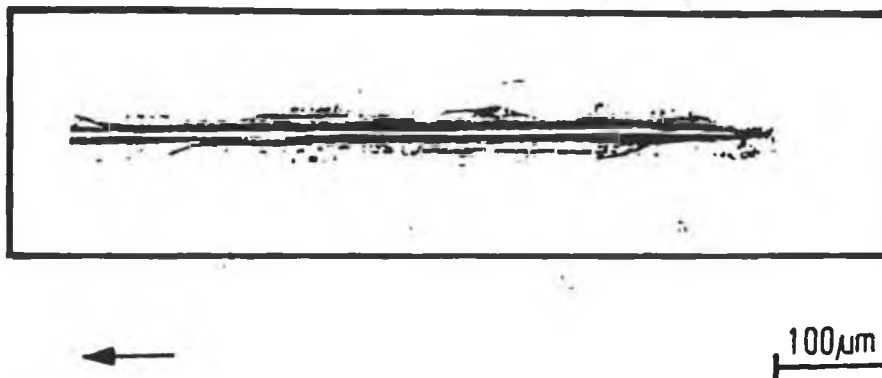
**Surface cracking caused by a diamond tip sliding
under a normal load of 3N across a coated surface.**

**Figure 3.15 Surface cracking due to diamond sliding on
surface coating [3.90].**
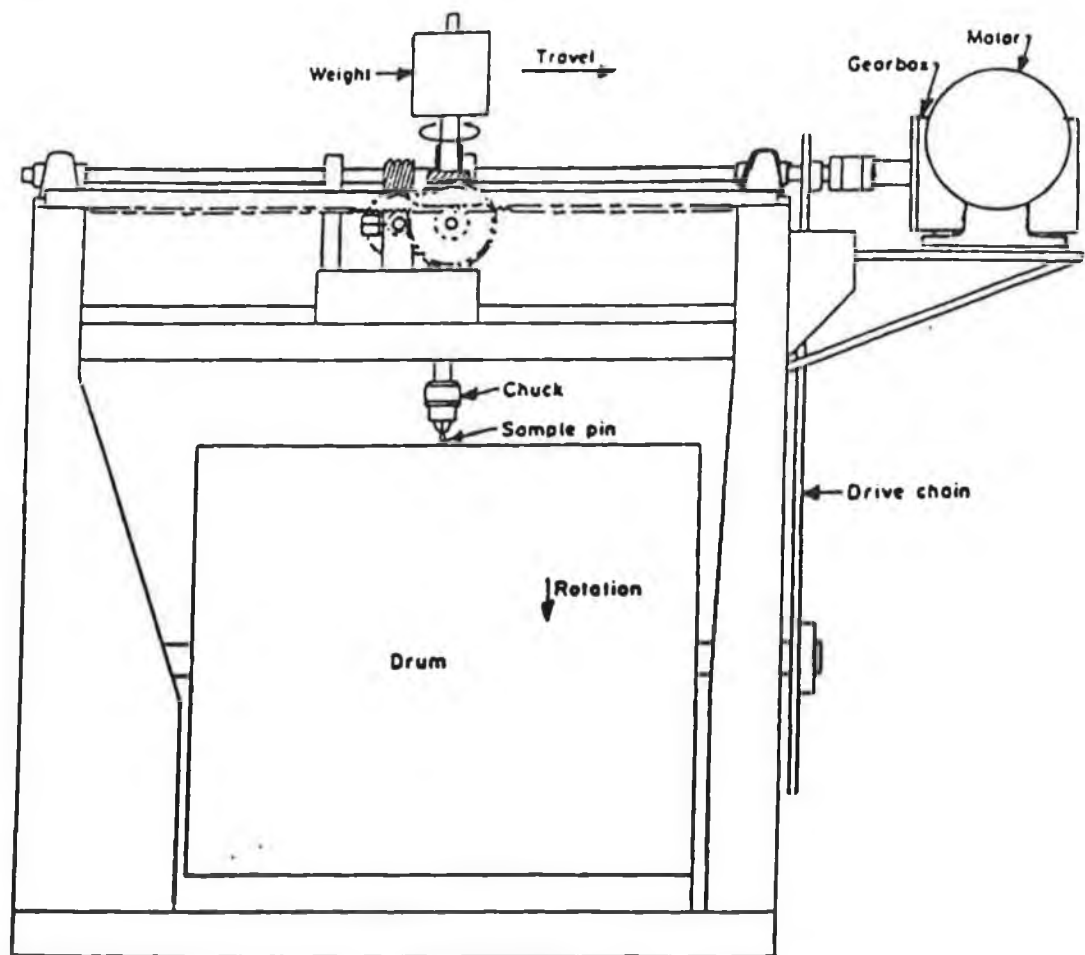
Figure 3.16 Schematic of pin-on-drum apparatus [3.12].

78
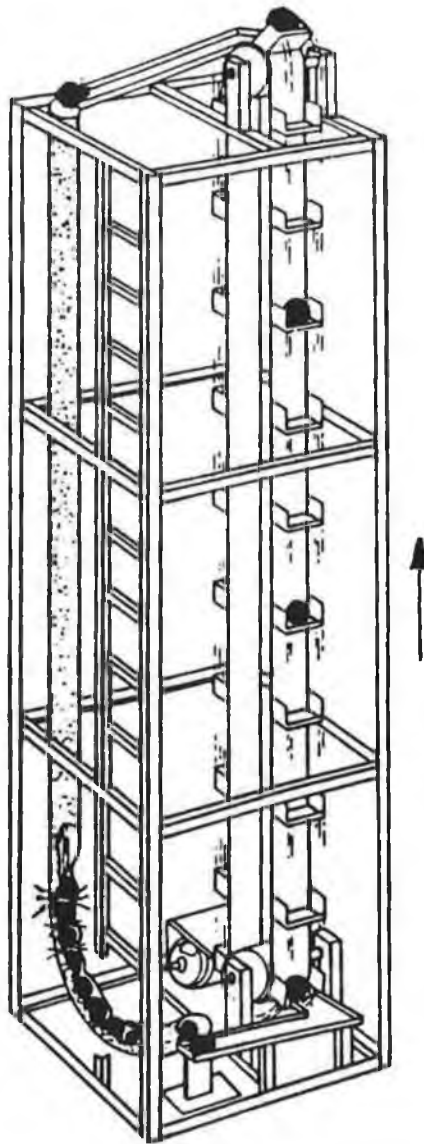
Figure 3.17 Schematic of impact tester [3.92].

The wear resistance of a material's surface layer can be increased by the impact effect itself, as this may cause distortions of the crystalline lattices and the formation of elastic deformation fields, which can lead to an increase of the strength properties of a material, as described by Clark and Wood [3.94]. An impact test machine for determining the dynamic cushioning properties of plastic foams is reported by Shestopal and Chilcott [3.95] and shown in Figure 3.18. Again, this process is pure impact and has many limitations, as described in the reference paper. Brenner et al [3.96] used a test rig to combine impact and its effect on adhesion at elevated temperatures for iron spheres impacting on an iron plate. The shock of the impact of the colliding bodies was transmitted to a piezoelectric transducer, which produced a pulse on the screen of an oscilliscope proportional to the applied force as shown in Figure 3.19.

3.4.7 Impact-abrasion test

A test rig described by Fiset et al [3.97] uses abrasive belts as the impact-abrasive surface. This test performs combined impact-abrasion tests only and unlike the rig developed for this research, cannot perform pure impact. The specimens are used as a hammer to impact the abrasive paper as shown in Figure 3.20. and the test is used to simulate ore grinding.
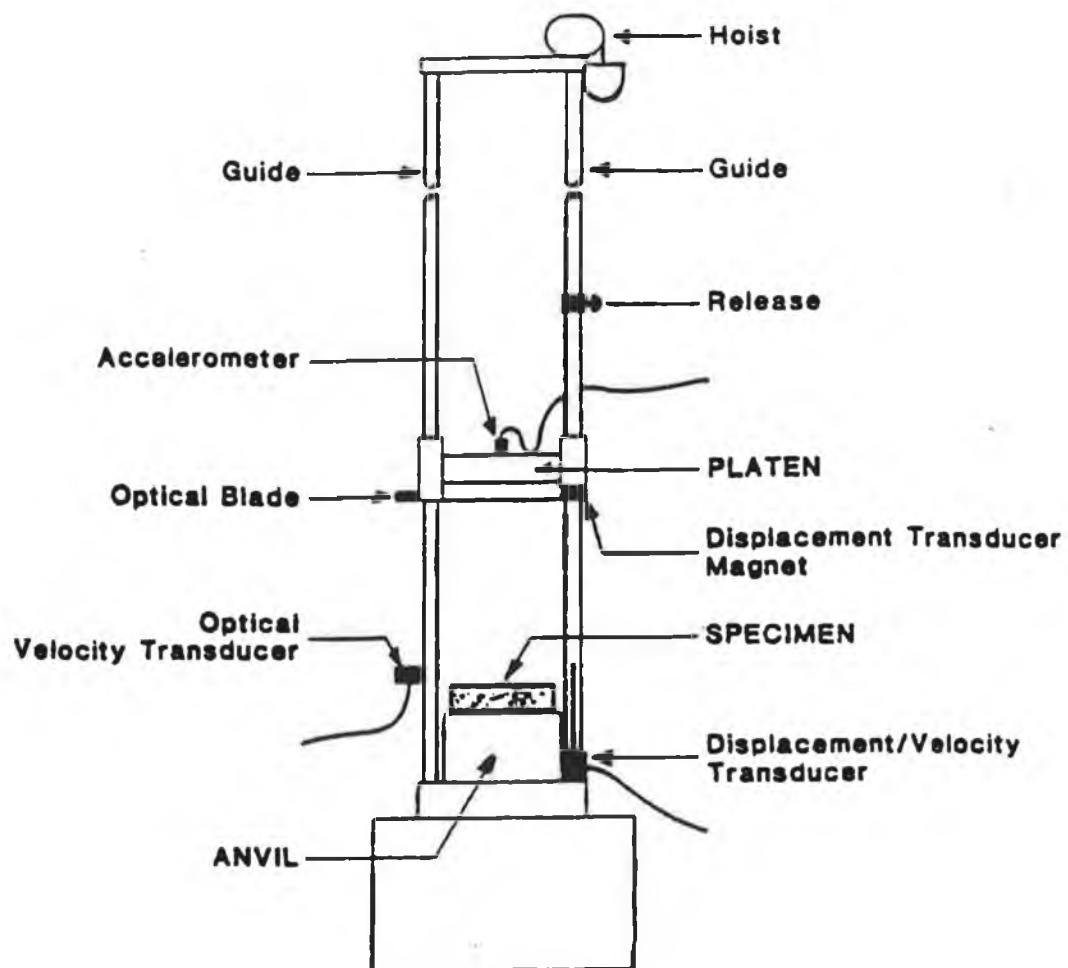
Figure 3.18 Dynamic testing of plastic foams [3.95].
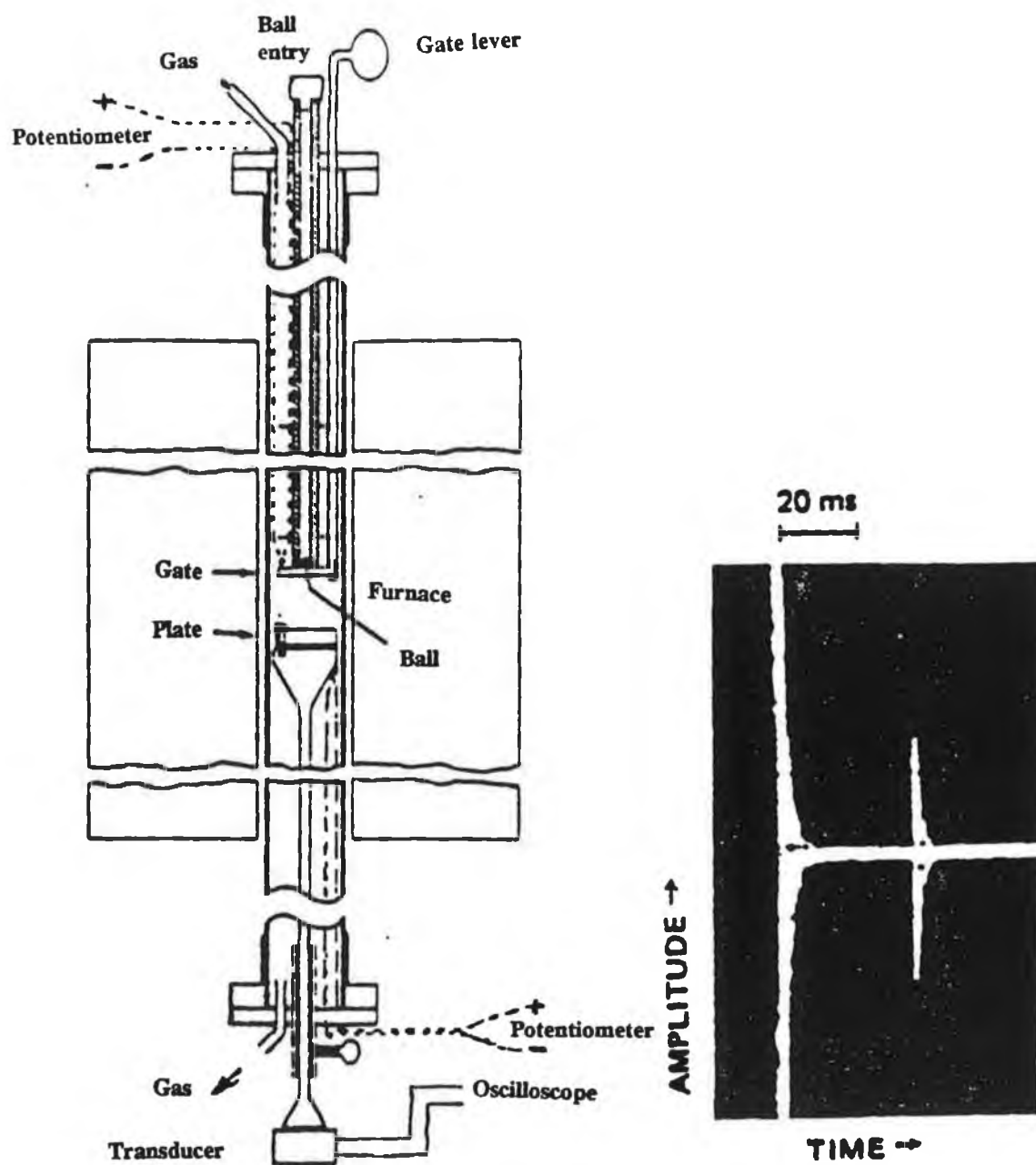
Figure 3.19 Apparatus for dropping spheres onto plates to measure impact and adhesion [3.96].

3.4.8 Adhesion tests using Acoustic emission monitoring

Acoustic emmision monitoring is used with scratch testing to determine a critical normal load for the onset of coating failure and decohesion. Experiments conducted by Diniz et al [3.98] used acoustic emmission to monitor the change of workpiece surface roughness caused by an increase in tool wear during turning. Adhesion tests conducted by Kubo and Hashimoto [3.99] used a modified scratch test with a steady increasing load. This test is designed to evaluate thin film properties such as adhesion [3.100,3.101], and the critical load at which the film becomes detached is detected by acoustic emission. A diamond indenter tip of 0.2mm radius was used in this test process, along with a camera and SEM to observe how the films were scratched as shown in Figure 3.21. The relative mechanical strength of thin coatings and of the coating-substrate interfaces may be evaluated by scratch testing by measuring the cohesive load to initiate cracking within the coating [3.102]. Figure 3.22. is a schematic of a scratch coating adhesion test using acoustic emission.

3.5 SLIDING WEAR AND FRICTION

3.5.1 Rubbing tests

An ASTM standard test method for wear testing with a crossed cylinder apparatus [3.103], was adopted for testing similar and dissimilar metals, alloys and coated systems in unlubricated conditions. A rotating cylinder as shown in Figure 3.23. and turning at 100 r.p.m. is forced at right angles against a stationary cylinder and the

83
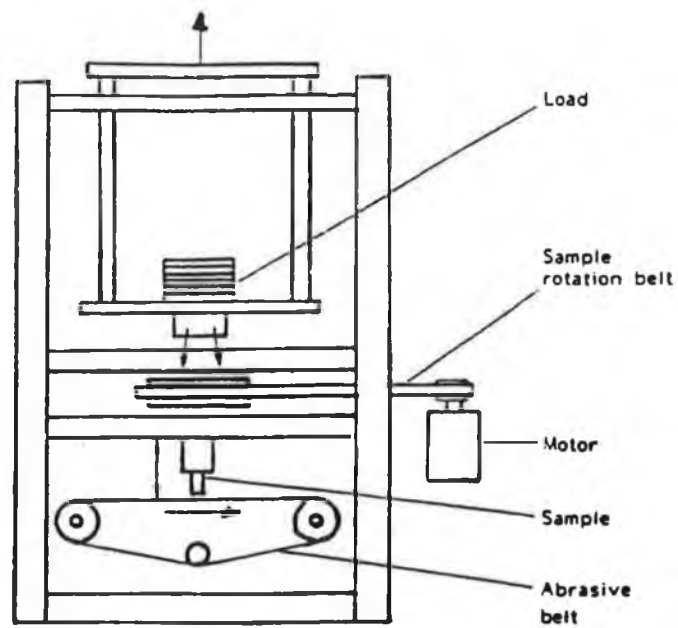
Figure 3.20 Schematic of combined impact-abrasion tester using sanding belts [3.97].
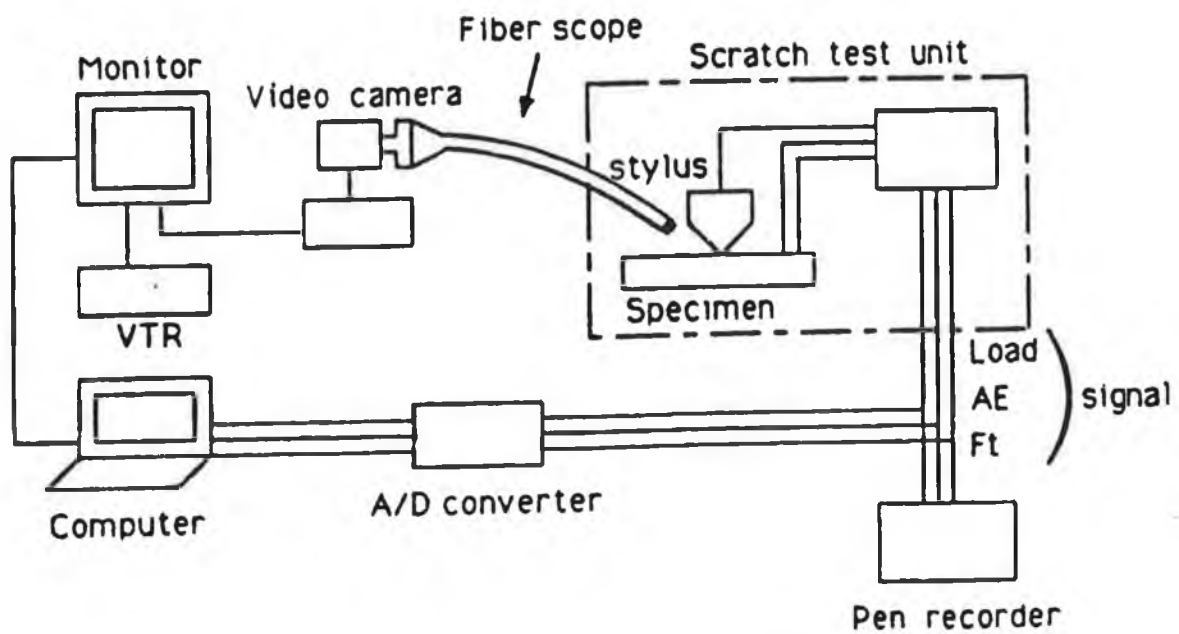
Figure 3.21 Block diagram of modified scratch tester [3.99].

Acoustic emission vs
load profiles
for two coatings.
The higher critical
load P_{cr} corresponds
to the coating
with better adhesion.
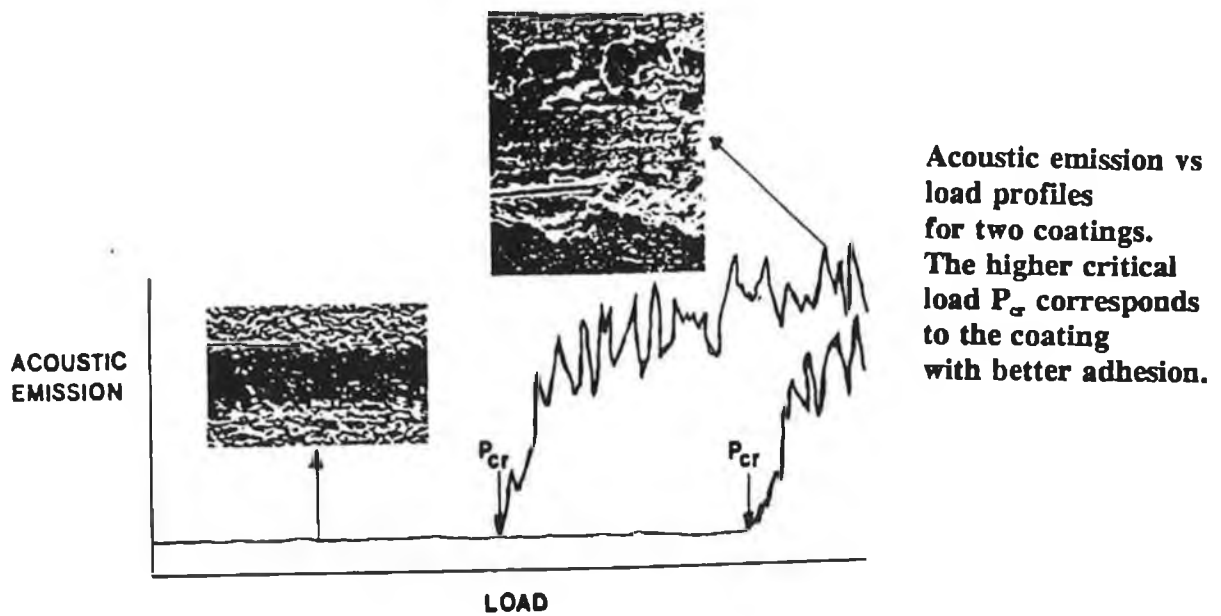
Figure 3.22 Schematic of scratch coating adhesion test using
acoustic emission [3.98].
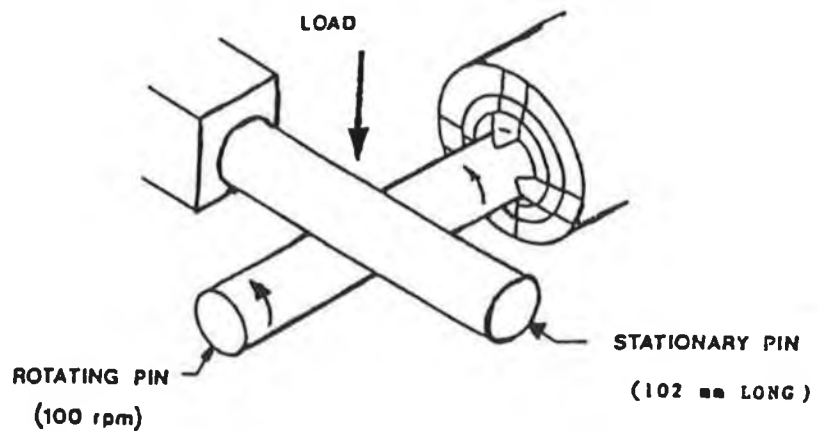
Figure 3.23 Schematic of a crossed cylinder test apparatus [3.103].

85

volume of material loss is determined by formulae. Friction and wear tests conducted by Shimura and Mizutani [3.104] describe a plate-on-plate wear test apparatus used to measure friction and adhesion of ceramic coated materials.

3.5.2 Block-on-ring test

In this test, a rotating metal ring is loaded against a fixed block, making a line contact when the test begins, as shown in Figure 3.24. This test is very versatile, allowiing variations in materials, speeds, loads, lubricants, coatings and different operating athmospheres [3.105]. An ASTM G77-83 is available for this test [3.106]. Wear is again calculated by using volume loss of the block and weight loss of the ring from the standard.

3.6 LOW ABRASION LOW STRESS TESTS

3.6.1 Taber test

The Taber Abraser is used to measure low stress abrasive wear resistance of materials and coatings. Low stress abrasive wear occurs when hard particles are forced against and move along a solid surface where particle loading is insufficient to cause fracture of the hard particles. The Taber apparatus is shown in Figure 3.25. and involves the abrasive wear of a flat plate specimen by the action of a pair of rubber bonded abrasive wheels loaded normal to the specimen. The specimen which is coated or uncoated, is rotated, causing the abrasive wheels to drag and abrade the

86
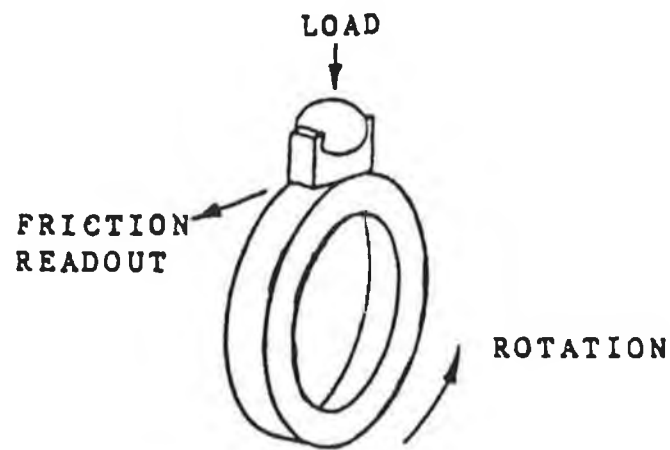
Figure 3.24 Schematic of a block-on-ring tester [3.106]
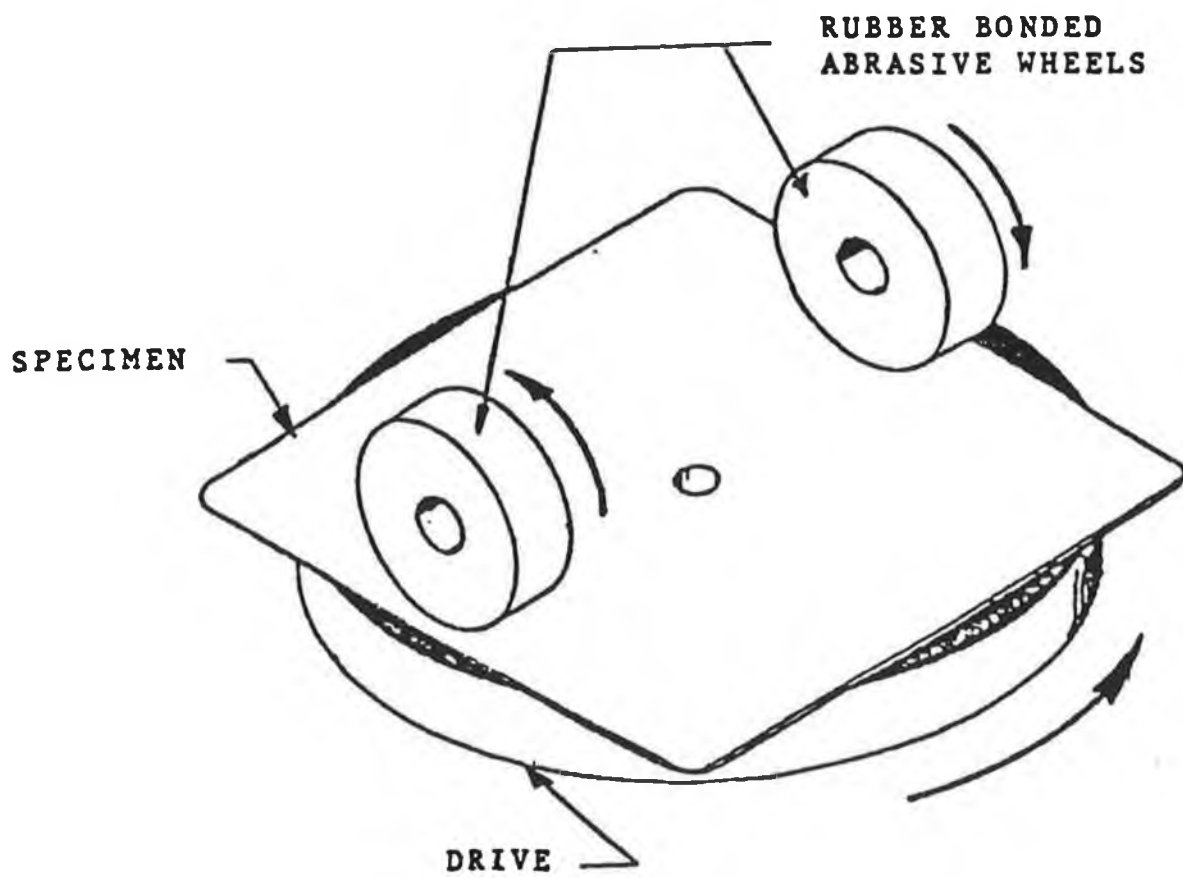
Figure 3.25 Schematic of a taber abraser apparatus [3.91].

surface. Wear is determined by weight loss. A standard test method is available for the Taber Tester (ASTM 1044). The test also allows loose abrasive particles to be incorporated in the wear track, giving rise to three body abrasion.

3.6.2 Dry sand rubber wheel test

This test, ASTM 65-81 is used to rank the abrasion or scratch resistance of materials to silica sand. It is a low stress abrasion test and is ideal for dry wear test conditions. Figure 3.26. shows a schematic of the tester. In operation, sand particles are trapped between the specimen and a rubber wheel and dragged along as the wheel rotates. The specimen is held against the wheel with a constant force. Cerri et al [3.107] describe wear tests on WC coatings characterised with a dry sand rubber wheel abrasion tester. In the reference they examine the abrasion resistance of carbide powders with several materials and coatings used for similar applications in an abrasive environment. Swanson [3.108] used a dry sand rubber wheel test to compare laboratory and field tests under sandy soil working conditions, and concluded that there was a close correlation between the two and that the test adequately simulates the abrasive wear of materials used in sandy soil conditions with low moisture content.

3.6.3 Alumina Slurry Test

An alumina Slurry test, standard ASTM 611 is used to simulate high abrasive conditions in a liquid medium [3.91]. The test rig which is shown in Figure 3.27,

88
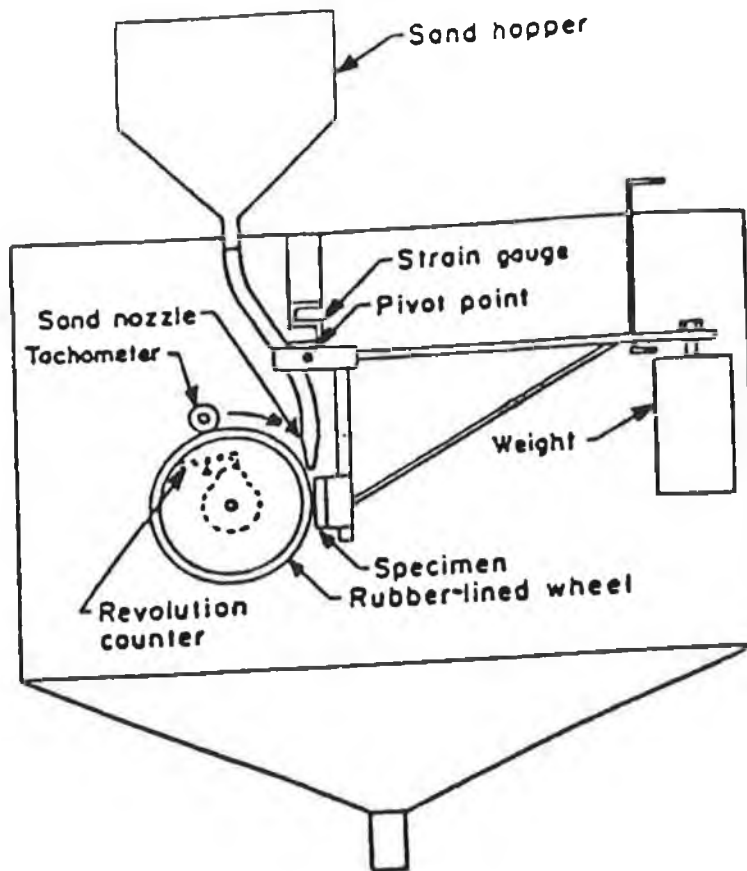
Figure 3.26 Schematic of a dry sand rubber
wheel apparatus [3.106,3.108].
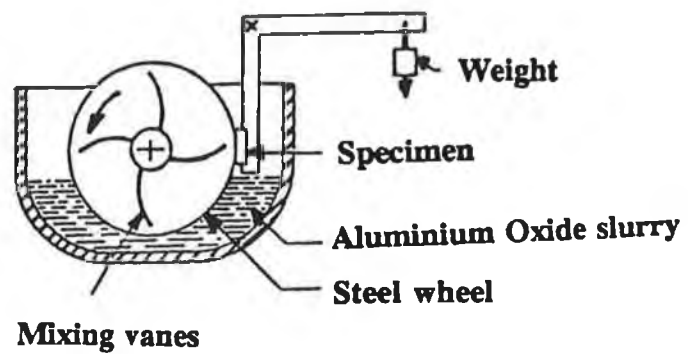
Figure 3.27 Schematic of an alumina slurry abrasion
test apparatus [3.109].

uses a steel wheel which rotates against a flat coated specimen in a slurry containing sharp alumina particles. Many applications of coatings are used in components handling slurry such as pumps, valves, and piping etc., causing erosion of parts and a wide range of such testers are available as reported by Kelley et al [3.91].

3.7 COMMON WEAR TEST PROBLEMS

Every wear test, whether for bulk material or coatings can be complicated by equipment problems, test procedures, sample preparation, inconsistency in abrasive materials and the wrong interpretation of the test results.

Many of the abrasive wear tests already described depend on their accuracy and repeatibility on the consistency of the abrasive paper used. Slight difference in the particle size, shape, and surface texture can cause test results to vary. The slurry erosion tests depend on the consistency of the mix and distribution of the erodent particles. In many real situations, the slurry is moving continually and wear particles in the mix attacking machine parts are sharp and, therefore, more abrasive. The initial problem of the briquette die depended on the combination of many wear factors as discussed in section 1.5 and some parts of the die experienced higher wear than others. Thick coatings, such as those produced by thermal spray and weld facing, seldom experience penetration during the above mentioned tests. Thin coatings on the other hand require greater care during a test process in order to avoid penetration.

3.8 MAIN FEATURES OF NOVEL TEST RIG

The novel wear test rig developed for this research work and discussed in detail in Chapter four has many unique features over the test equipment described above. Such features include the combined and individual actions of impact and abrasion, a variable linear velocity of the abrasive stylus, and a facility to assess the performance of materials and coatings under the effects of rebound. Most impact situations involve a secondary impact effect caused by the rebound of particles following the first impact. This effect can result in high wear and shock on components and may need to be addressed by coating designers. Chapter six, discusses the main effects of rebound on samples tested. Normal loads applied to the samples can be changed instantly along with the impact velocity. The test rig may operate under dry or lubricated conditions and three body abrasion wear tests can be performed. The reciprocating action of the stylus with a variable velocity addresses many practical problems such as a piston and cylinder. Most existing wear test rigs only apply abrasive or scratch tests in a single direction and others avoid contacting the previously abraded area.

The test rig developed can be used for thick and thin coatings as well as bulk material and penetration of thick coatings have been successfully achieved. Most scratch testers are applied over a small surface area, whereas this test rig is used for examining materials over a larger area, giving an improved representation of the performance of a coating for larger products. The on-line data acquisition feature, although not unique, allow immediate measurements of the applied load at any time during the test process. The clamping mechanism on the test rig allows the same

sample to undergo a number of similar tests which help improve the reliability of the wear test and results.

Wear testing of coated and uncoated components requires an ability to apply wear conditions which can address an individual wear problem or a combination of such problems. Test rigs which are designed only to address individual wear problems may be limited in simulating the complex wear problems experienced by components in service today.

3.9 MEASURING WEAR OF SPECIMENS

3.9.1 Weight loss

One of the simplest ways of measuring wear is based on weight loss during and after a test. This is simple and direct provided the materials considered are similar and care is taken in the measurements. The mass loss of specimens can be measured at intervals during the testing period by removing the specimens, cleaning, drying and weighing. The mass loss can be converted to volume loss and the wear rate calculated with respect to time. Some of the tests conducted during the experimental stage of this thesis were performed in this way. For coating applications, if the coating is penetrated, the weight loss is a combination of both substrate and coating(s). In some cases, wear may occur but no mass loss may be experienced as in the case of plastic flow or deformation. Measurement of the wear area by volume loss will indicate the material loss in this case.

3.9.2 Volume loss

This can be calculated from formulae based on the wear scar shape. If the scar shape is regular and symmetrical, accuracy with this approach is possible. The volume of material removed can be measured at intervals using equipment for measuring the depth and width of the wear scar or impact zone. The dimensions of the abrading tool can also be checked to assist in the volumetric loss in mm³. Volume loss can be converted to weight loss, if the material density is known. However, many coatings and substrate combinations have different densities and compositions and in a multi-layer system, densities will differ throughout. Therefore, weight loss using volume and density alone becomes a complicated task. If one consideres the total system of coating and substrate, then volume loss of the combined system can be used. A computer programme shown in Appendix B. is used to calculate the volume loss of material on a specimen based on a number of measured and known dimensions of the abrasive stylus and wear scar produced.

3.9.3 Wear scar depth

Depth of wear scar is considered a reliable method for material loss and results obtained for this thesis used a surface profilometer to measure and record these values on a range of samples. A more exact method using a profilometer and computer control equipment was developed by George and Radcliffe [3.110]. This process produces an isometric plot of the wear scar and the wear scar volumes are calculated by computer automatically. Most cutting tools are assessed under wear

93

scars in the form of crater or flank wear.

3.9.4 Prediction of wear life

The method most commonly used is to calculate a wear coefficient k, where:

$$k = \frac{Volume}{Load * Sliding\ distance} \quad (\frac{mm^3}{N-m}) \tag{3.1}$$

This coefficient is based on the assumption that the volume wear varies directly with the contact load and the sliding distance or the wear depth varies directly with the contact pressure and the sliding distance. It was recommended by Holmberg and Matthews [3.111] that the volumetric wear divided by the total sliding distance and the normal force should be used as a standard for calculating wear rates on materials. This wear factor definition is used by many researchers today [3.14,3.35] and in some of the results achieved in this thesis. In other results obtained, the mass loss in grams (g) was used. The relative wear resistance of each material can also be calculated using the reciprocal of the steady-state wear rate for a reference standard. i.e. relative wear resistance equals the steady state wear rate of a particular material divided by the steady state wear rate of a test grade. Therefore, the relative wear resistance of different grades can be compared [3.60].

Another approach to measuring wear life uses the following equation:

$$L = \frac{(Sr)(Pr)}{(S)(P)} *Lr. \tag{3.2}$$

where L and Lr are the predicted and test lifes, S and Sr the service and test speeds,

94

and P and Pr the service and test loads (limited within certain speeds and loads). These relationships only apply to homogeneous materials and where a component has a hardened surface, the wear rate may be different once the hardened layer has been penetrated.

CHAPTER 4

TEST RIG DEVELOPMENT AND OPERATING PROCEDURES

4.1 MAIN DESIGN OBJECTIVES

Following an investigation into existing wear test equipment for applying dynamic wear conditions to materials and components such as those described in section 1.5, most facilities did not address such complex testing. Since it is common for coated and uncoated components to be subjected to a wide range of loading and wear conditions in applications today, the need for a dynamic type tester is appropriate at this time. As a result, the following objectives were decided upon for the design of the test rig.

i)   To provide a variable linear velocity of the abrasive stylus.

ii)   To produce a reciprocating action of the stylus on a surface.

iii)   To perform pure impact loading.

iv)   To perform combined impact abrasion.

v)   To allow dry and lubricated operating conditions.

vi)   To perform two or three body abrasion wear.

vii)   To allow some flexibility in the sample size for testing.

viii)   To measure the impact load instantly and allow it to be changed for different tests.

ix)   To allow for dynamic rebound of materials under impact.

x)   To allow impact conditions to be applied at different linear velocities of the reciprocating stylus.

4.1.1 Test Rig Facilities

The novel Test Rig (Photograph 4.1 and 4.2) was designed, manufactured and developed for the experimental work in this thesis to combine the effects of Impact and Abrasive wear, producing dynamic wear testing. A front elevation of the test rig is shown in Figure 4.1, highlighting the main components. Detailed drawings of the test rig are supplied in appendix A. As already discussed, engineering components are subjected to a range of loads and wear combinations in service and the ability to combine some of these wear patterns in a test rig is now desirable and necessary. It is also required in order to simulate, in a laboratory situation, wear problems experienced by components in service. The Impact action combines many wear parameters such as shock loading, fatigue, gouging, fracture and spalling while the sliding action combines abrasion, adhesion, and fretting wear [4.1]. Unlike most test equipment described in the literature, this rig uses a reciprocating stylus whose velocity is changing continually over the test surface.

4.2 TEST RIG OPERATION

With reference to Photographs 4.1 and 4.2 and Figure 4.1, samples are prepared and held in position by two clamps and a locating fixture, fixed to the wear test table. The abrading stylus is located over the sample, in a linear drive unit, driven by the motor. The load cell is placed over the stylus housing in a fixture and the normal applied load is then placed over this. The normal load is held on a bearing system in two guides, fixed to the linear drive unit. At the motor shaft, the linear
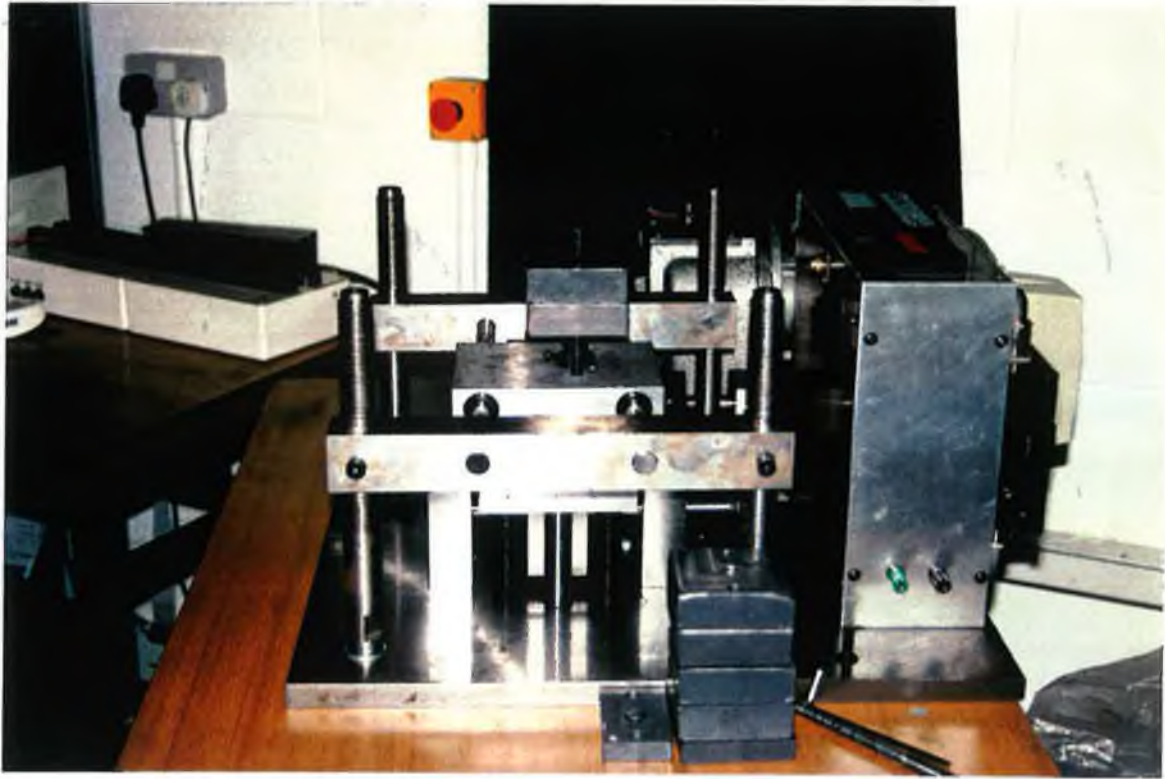
Photograph 4.1   End view of wear tester.
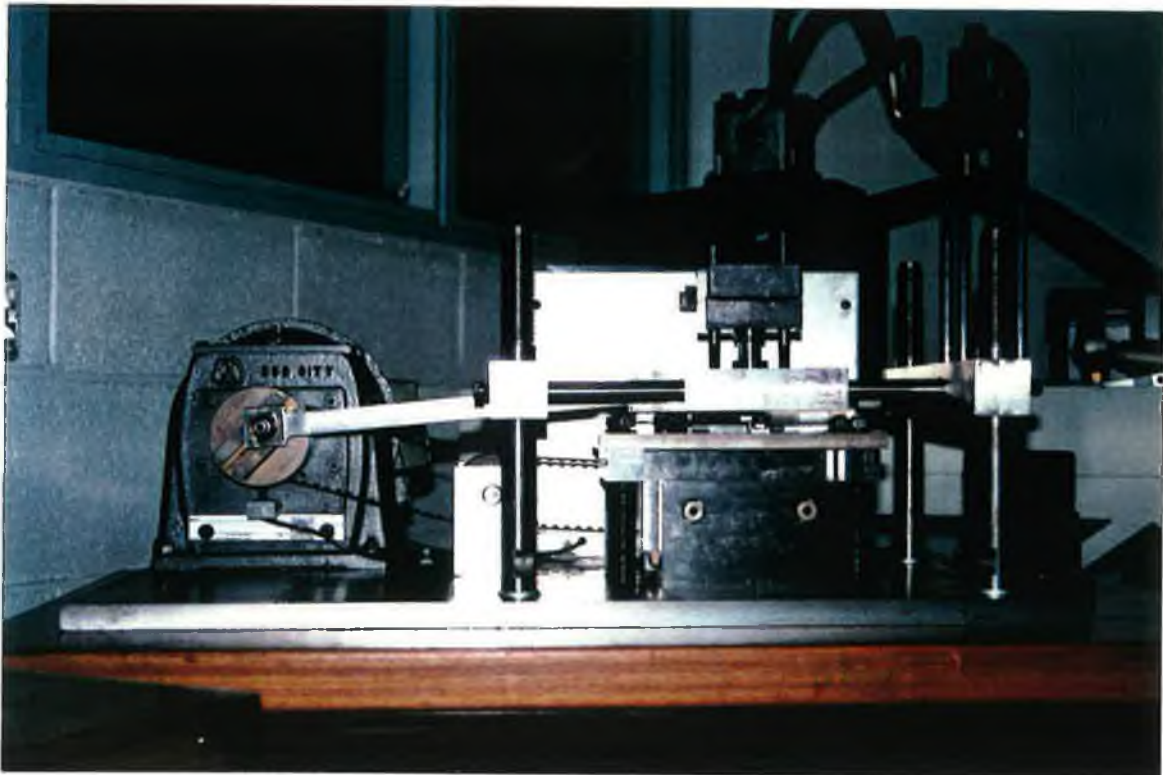
Photograph 4.2   Front view of wear tester.

TEST RIG ASSEMBLY DRAWING.

PART	DESCRIPTION	PART	DESCRIPTION
1	MOTOR	9	BEVEL WASHERS
2	DRIVE UNIT	10	BEARINGS
3	TIMING BELT DRIVE SYSTEM	11	MAIN PILLARS
4	INTERMEDIATE DRIVE SHAFT	12	TIMING BELT PULLEYS
5	CAMS	13	STYLUS
6	KNIFE EDGES FOR CAMS	14	LINEAR DRIVE UNIT
7	TABLE FOR SAMPLES	15	TEST MASS
8	BASE PLATE	16	STYLUS HOLDER
		17	DRIVE SHAFT

99
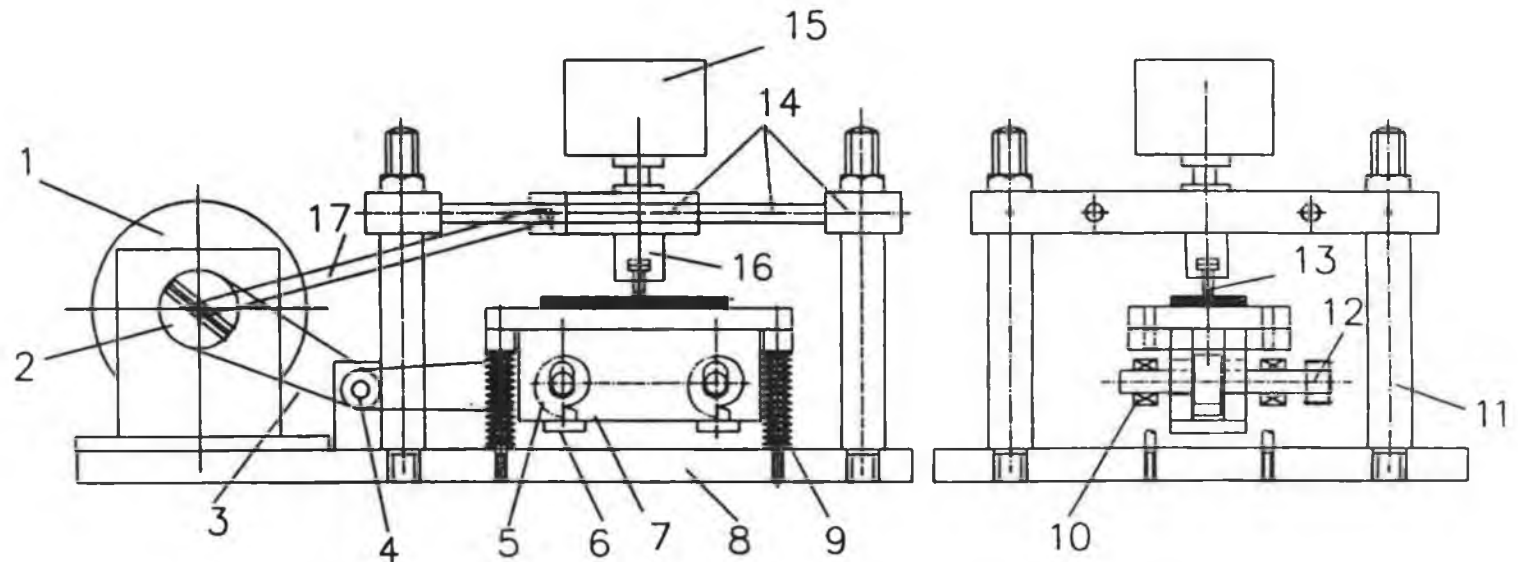
Figure 4.1   Impact abrasion wear tester.

displacement of the stylus can be set by adjusting the linear drive unit relative to the to the shaft center. In operation, the stylus impacts the test sample and then rubs or abrades along the sample as shown in Figure 4.2. The test rig performs the following main functions.

i)   Direct impact.

ii)   Direct abrasion (sliding contact).

iii)   Combined impact-abrasion or dynamic abrasion conditions.

iv)   Impact loading at specified abrasion velocities.

Photographs 4.3 and 4.4 show a typical cratering effect and abrasive track respectively due to the wear actions of the test rig.

In direct or pure impact only, the sliding velocity is reduced to zero, and the stylus impacts the sample in the same place each time. The number of cycles per minute is 106 but this can be changed with motor speed.

Under sliding conditions, the impact operation is removed and pure rubbing occurs, producing a wear scar only. Sliding action in this test rig is reciprocating, causing abrasion in both directions. This form of wear is considered more severe than one directional processes [4.2].

Tests can be applied to both coated and uncoated substrates under identical conditions. Other applications of the Test rig include a facility to change the sliding velocity and apply impact loads at any location along the abrasive wear scar. The test procedure is relatively fast and the applied forces of impact can be changed to suit test conditions. Other testing may include lubricated conditions to measure the effects of coolant or a lubricant on the wear conditions.
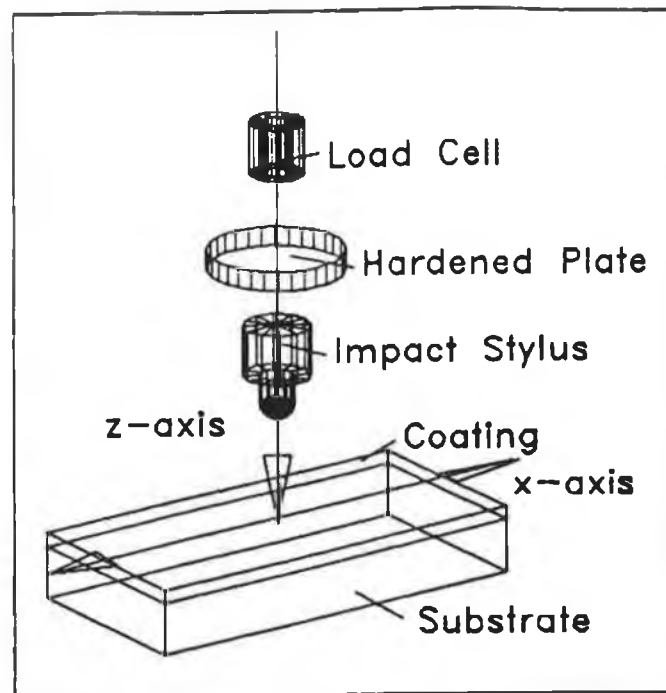
Figure 4.2   Stylus motion under impact and abrasion conditions.
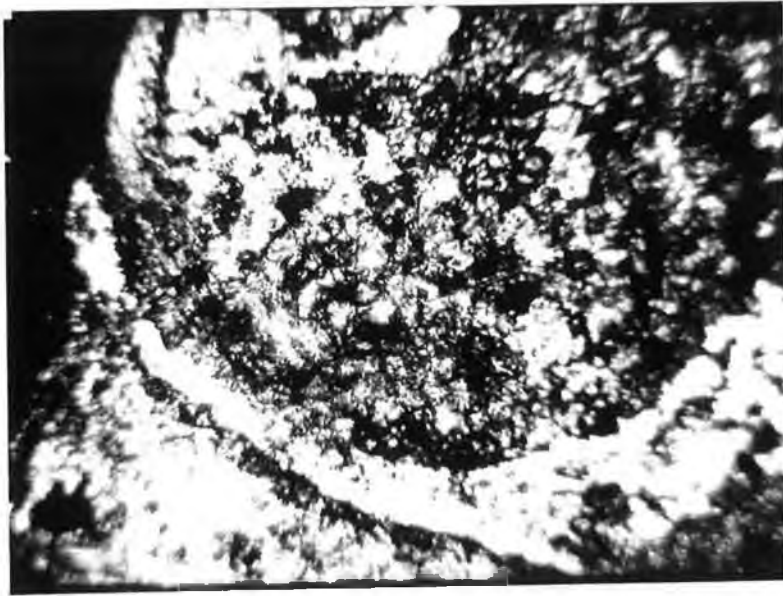
Photograph 4.3 Crater in coated sample.   1 mm
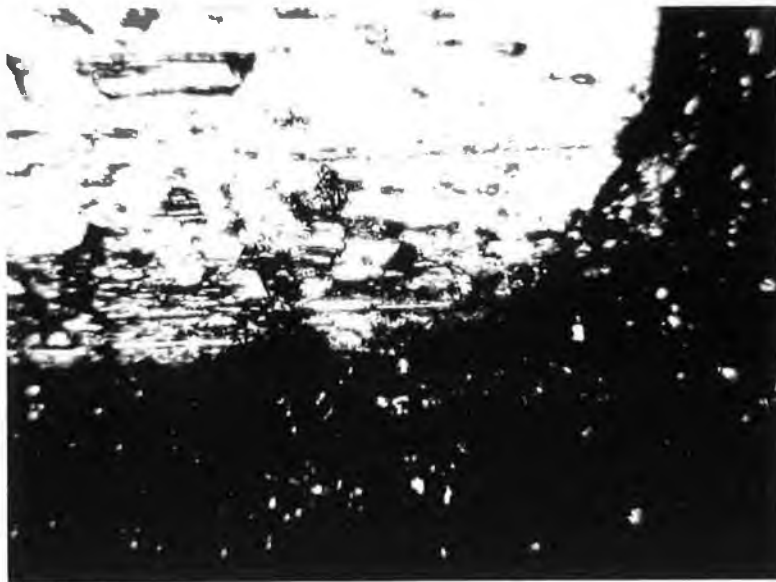
Photograph 4.4 Abrasion scar on coating.   1mm

4.3 TEST RIG COMPONENTS

4.3.1 Drive system

A' three phase, 750 watt electric motor was selected to drive both the linear and impact mechanisms together in order to syncronise both actions. A high power, high torque, low speed motor was selected in order to facilitate high test forces and prevent any chatter occuring during testing. Toothed belts were selected to drive the intermediate shaft and cam's producing the impact conditions. The drive mechanism from the motor to the cam shafts, to initiate the impact effect are shown in photograph 4.5. A counter was installed to record the number of cycles during each test process. Figure 4.3 shows the complete drive system for the test rig.

4.3.2 Intermediate shaft

This shaft is used to direct the drive system to the cam shafts and also allow adjustment of the cams so that impact can occur anywhere along the wear scar. This feature is very useful as it allows the impact force to occur while the stylus is traversing the sample with linear velocity.

4.3.3 Cam shafts

Two cam shaft's are used for balancing the impact mechanism. They were machined, heat treated in a vacuum furnace, and ground. The cam faces were machined by an

Figure 4.3   Drive system for the test rig.

104
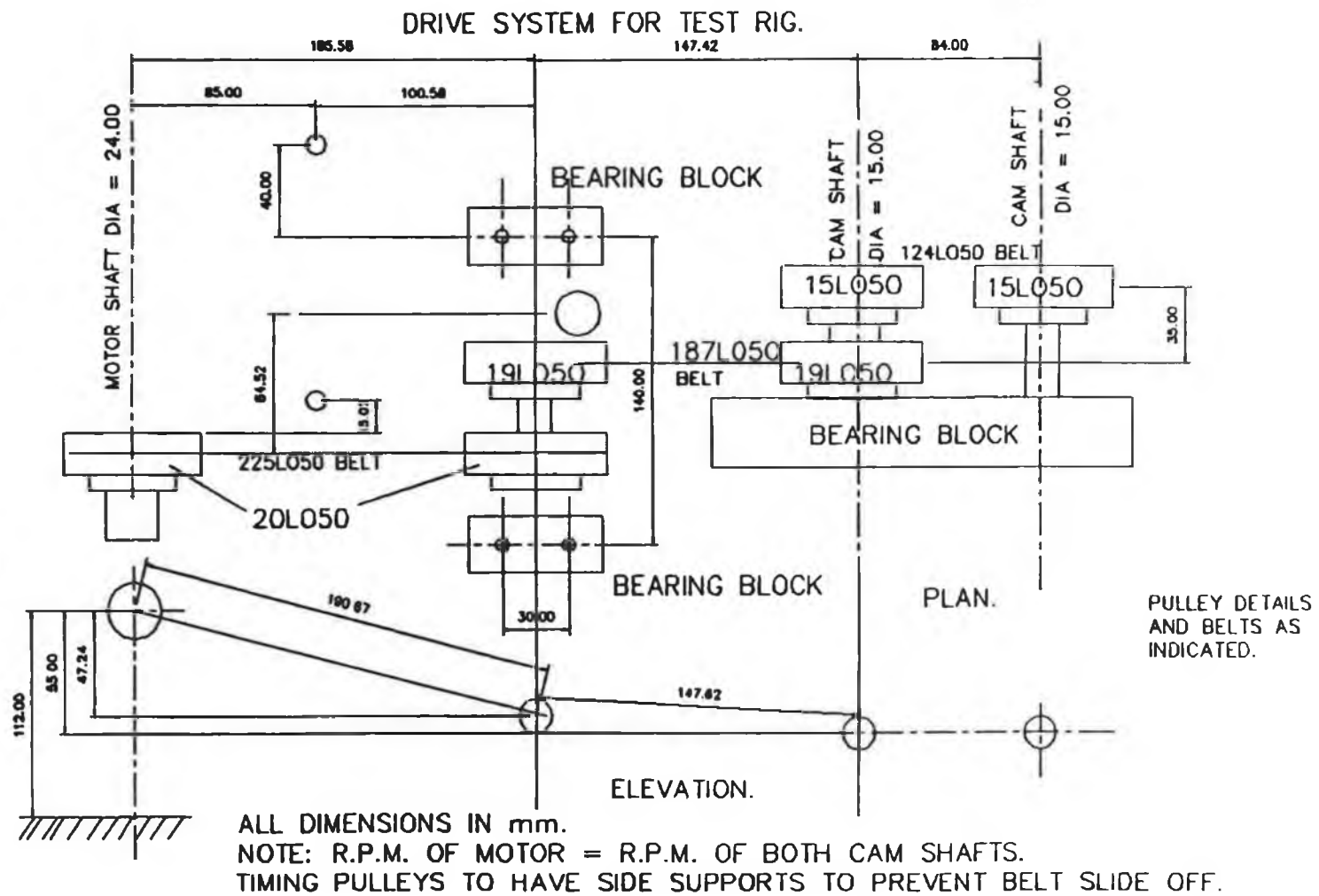
Electrical Discharge Machining process. Figure 4.4 shows the general shape of the cam profiles produced.

4.3.4 Impact table

This table is used for locating and clamping the test samples and is positioned on the test rig base plate by four vertical pillars and linear guide bearings. The pillars are fixed to the base plate of the test rig. These pillars allow the table to move vertically only for impact, driven by the cams through the use of knife edges fixed to the table. Bevel washers (TF 20*10.2*1.1) were selected to act as a spring force to drive the table vertically upwards, producing impact while the cams are used to drive it downwards, opposing the spring action. Photographs 4.5 and 4.6 shows the impact table for holding the specimens, and the stylus holder respectively. If abrasion (sliding) testing is required, the table can be clamped to the base plate. This makes the cam operation redundant. The material used for the table, and supports is an AISI-D2 tool steel which was also heat treated. The bevel washers were calibrated using an Instron compression test and a calibration chart for the Bevel washers is shown in Figure 4.5.

4.3.5 Linear guide unit

The linear guide unit producing sliding contact is driven from the motor by a simple link mechanism and is shown in photograph 4.2. This mechanism can be adjusted to change the length of the wear scar produced by the stylus, and thus, the sliding
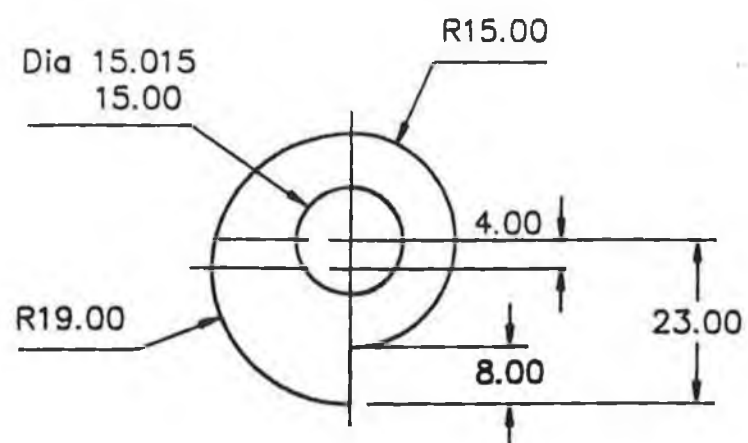
Figure 4.4   Cam profile for impact unit.
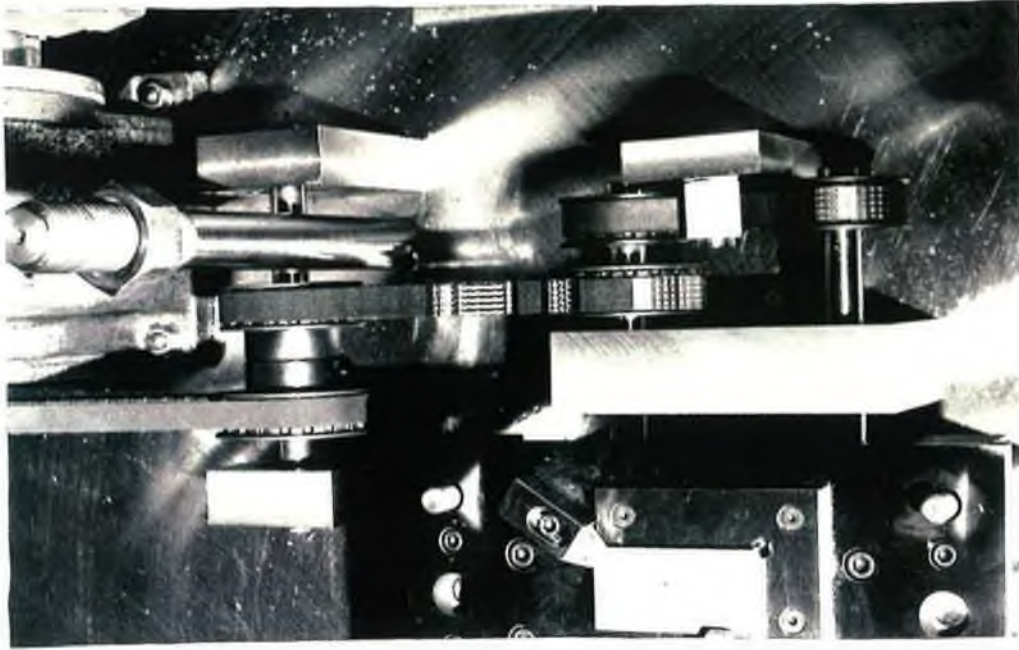
Photograph 4.5 Drive for cams producing impact effect.
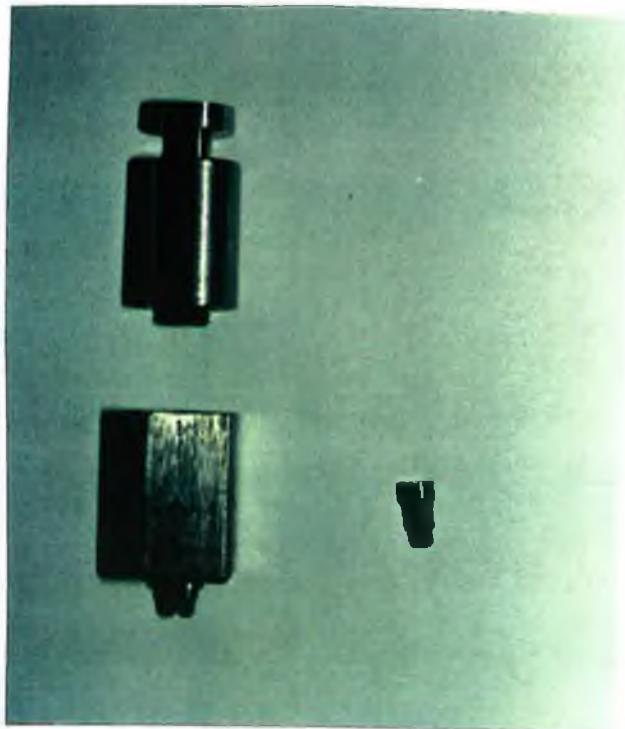
Photograph 4.6 Stylus and holder.

20 mm

BEVEL WASHERS CALIBRATION
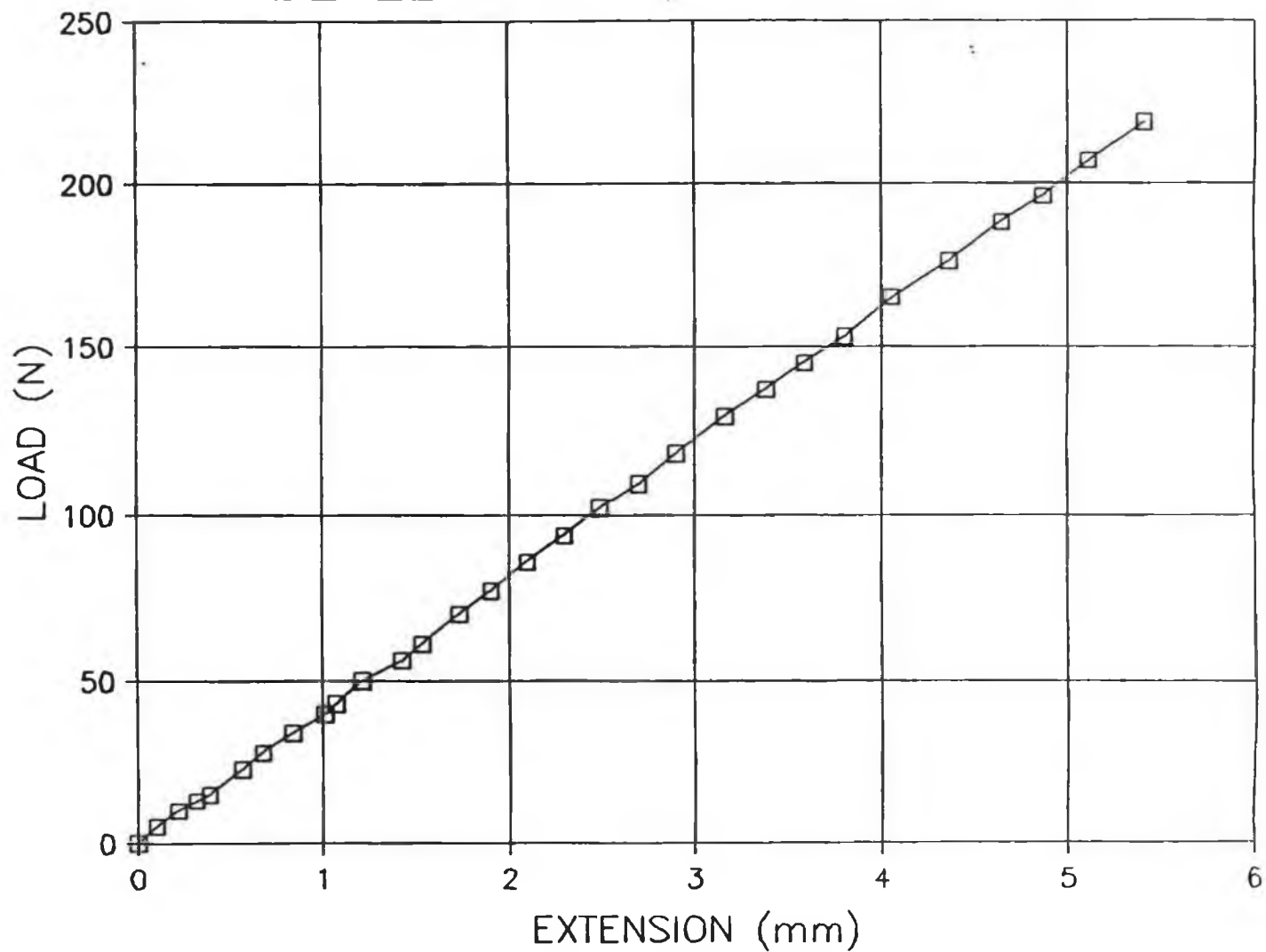
Figure 4.5   Calibration chart for the bevel washers.

or linear velocity. The linear guide unit is used for locating the stylus in relation to the test piece. It is attached to and supported by four pillars, which allow vertical adjustment of the linear unit. These pillars are fixed to the base plate of the test rig.

4.3.6 Stylus and stylus holder

The stylus used for the main testing in the thesis consisted of a 2mm radius, round nose tool. It is located in a tool holder using a lock screw to ensure it cannot move independently during the impact tests. There is no restriction on the shape of the stylus tip, and any material, coated or uncoated could be used for the stylus. The stylus used for testing purposes is shown in Figure 4.6. It is produced form a Tungsten Carbide of ISO Grade, P50, recommended for high metal removal rate and unfavourable conditions such as shock loading [4.3].The stylus holder is produced from an AISI-D3 tool steel, and heat treated to 58 HRc and shown in Photograph 4.6. Figures 4.7 to 4.9 show typical displacement, velocity, and acceleration characteristics of the stylus under abrasion conditions.

4.3.7 Load Cell

The load cell used is a 7.5 kN, Piezo Electric type 9001A quartz load washer [4.4], designed for measuring a sudden change in force or impact force. It is located in a housing as shown in Figure 4.10 and is connected to an amplifier and data acquisition card, fixed in a computer. If a force is applied to opposite faces of a quartz crystal, charges of opposite polarity are generated on the faces and the size

Figure 4.6   WC-Co Stylus.

110

4.00

6.00

4.00

R2.00

dia=6.5
dia=5
dia=4
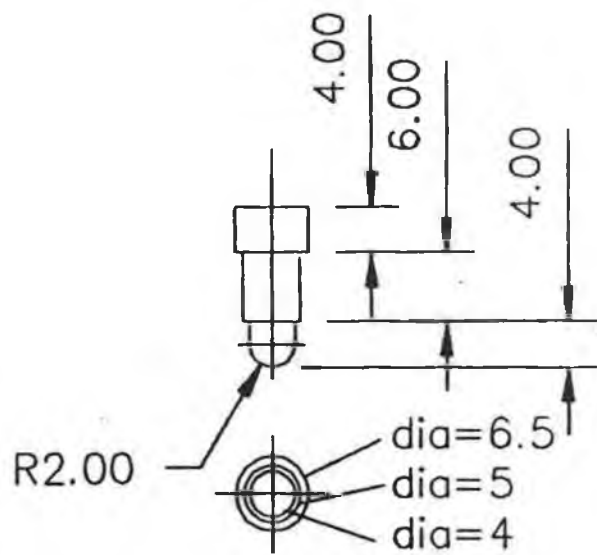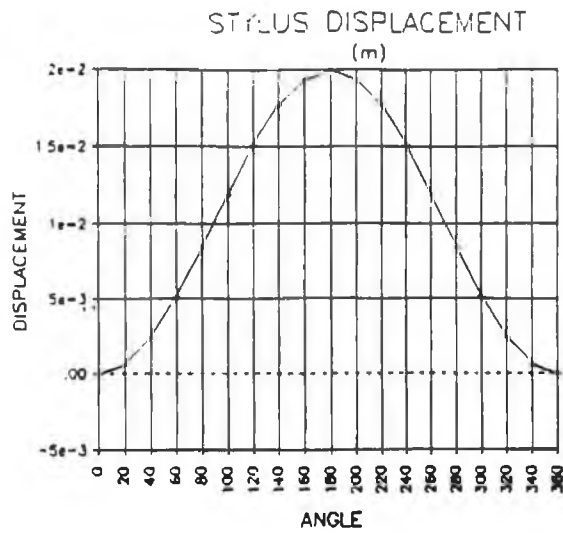
Figure 4.7 Displacement graph of stylus.

Figure 4.8 Velocity graph of stylus.
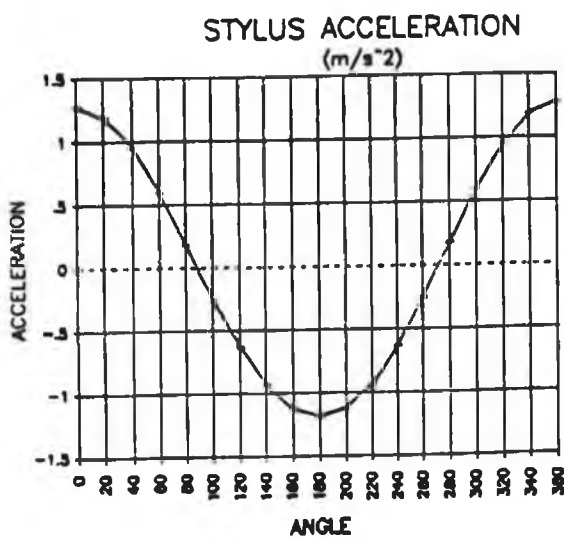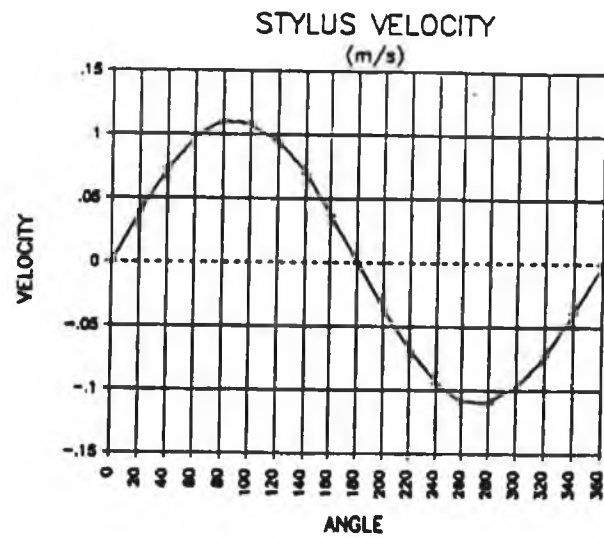
Figure 4.9 Acceleration graph of stylus.

111
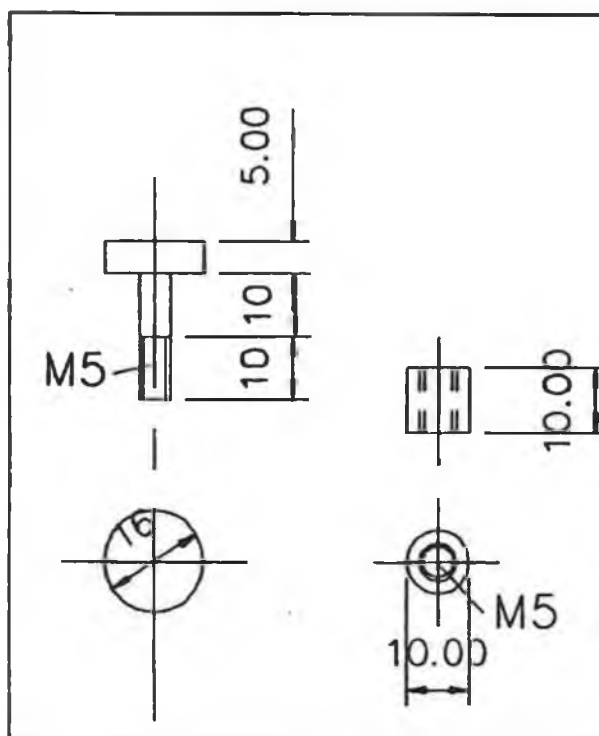
Figure 4.10 Load cell holder.

10.00
20.00

15.00
30.00

M8*10
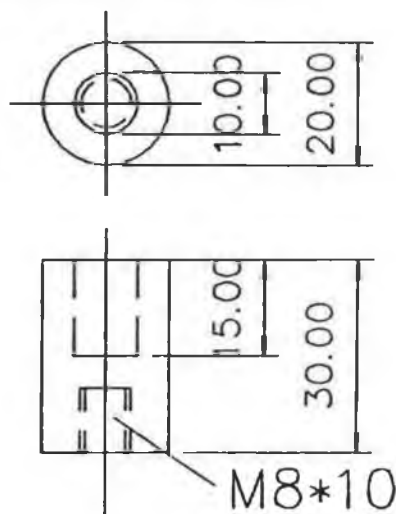
FIXED TO STYLUS HOLDER
WITH M8 THREADED SHAFT.

of the charge is proportional to the applied force. This is called the piezoelectric effect. To facilitate connection to a measurement circuit, the charges are collected on metallic electrodes which are deposited on the two faces of the crystal. These electrical charges are converted to voltages. A programme code was produced to read in and record the signals from the load cell, and display the normal force during testing on a computer screen. The computer hardware configuration for the force measurements are shown in Figure 4.11.

4.3.8 Data acquisition card

The card used for data acquisition purposes was a Keitley Metrabyte DAS8 card [4.5]. This was placed into the computer and computer software (see appendix B) was generated to link it with the load cell. The software produces a real time graphical presentation of the force response under both impact and abrasion conditions on a computer screen. It also allows this data to be stored on disc for future graphical representation and analysis.

4.3.9 Bearings

All rotating shafts and linear guided components are supported in bearings, details of which are given in appendix A.

HARDWARE CONFIGURATION
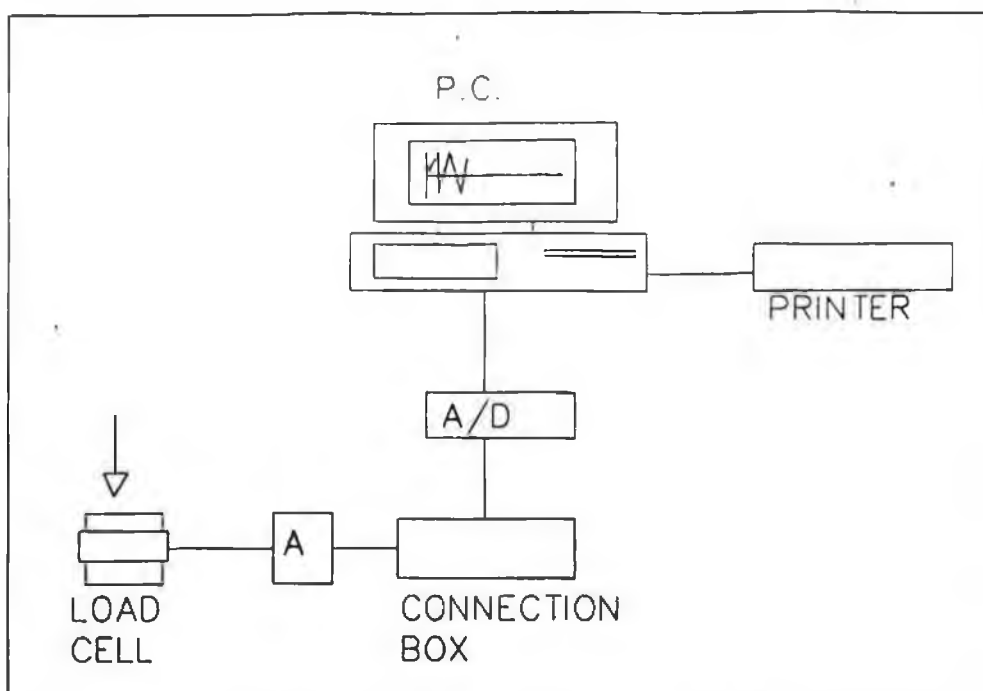
A: Amplifier.
A/D: Analog to digital control

**Figure 4.11 Computer hardware configuration for data
acquisition.**

4.4 SAMPLE SIZES

The sample sizes can vary but must be longer than the stroke of the stylus when reciprocating on the surface under test. Two clamps are used to hold the samples in position against a base plate and a fixed locating face as shown in Photograph 4.5. It was decided to clamp the samples from above rather than the side in order to avoid shifting during the impact process. Typical sample dimensions are 80mm +/- 20mm in length, 35mm +/- 5mm in width, and 10mm +/- 3mm in thickness. Circular samples can also be accomodated and small samples such as cutting inserts can be fixed to a suitable base plate before testing. Some of the initial testing conducted with the test rig can be found in the literature [4.6].

4.5 OTHER EQUIPMENT USED IN THE RESEARCH

4.5.1 Hardness tester

Hardness is not a fundamental property of a material as it depends on yield strength, elastic modulus and ultimate strength. It can be described as the resistance to indentation or abrasion by a body or indenter. These tests are localised compression tests and consist of forcing a spherical or conical indenter into a material with the size of the indented area or depth taken as a measure of hardness. The most common forms are Brinell, Vickers and Rockwell tests. In coating technology the depth of penetration must be minimised to get a more accurate picture of the coating hardness, independent of the substrate. Microhardness instruments are frequently

used for such hardness testing.

When the ratio D/t (D= indentation depth and t= coating thickness) of the indentation depth to the film thickness exceeds a critical value, the measured hardness, H is influenced by the substrate material and is no longer a characteristic of the coating. The critical D/t ratio varies between approximately 0.07 and 0.2. The most unfavourable conditions for hardness testing is that of a hard coating on a soft substrate, which is typical of WC-Co on an aluminium substrate.

Nanoindenters, unlike conventional hardness testers produces continuous curves of load versus indentation. When the depth is plotted for increasing and decreasing load, a hysteresis curve is produced, the area of which represents the plastic work performed [4.7].

4.5.2 Surface roughness testing

Surface roughness measurements were carried out with the use of a Mitutoyo Surftest 402, Series 178 instrument (see Photograph 4.7). Measurements of average surface roughness R_a values were also recorded from this instrument.

4.5.3 Surface profile testing

A profilometer instrument was used for showing and recording the surface profile of specimens under wear testing. The instrument is the same as that described in section 4.5.2 with the added feature of a chart recorder. This provides profile and roughness curves of the surface.

4.5.4 Optical Microscope

The Vickers micro hardness tester described in section 4.5.1 incorporates a microscope suitable for measuring the width of wear scars, the size of hardness indentations and general observation of the surface area on a microscopic scale.

4.5.5 Scanning Electron Microscope(SEM)

Scanning Electron Microscopy is a popular method for the direct observation of surfaces because they offer better resolution and depth of field than optical microscopes. SEM processes are commonly used to measure wear. The SEM has a magnification in the order of 100,000X, resolution of 200 to 250A, and a depth of field at least 300 times more than that of the light microscope, all of which result in the characteristic photographs of three dimensional quality.

The process principally involves the generation of a primary beam of electrons from an emission source which are then accelerated by a voltage of between 1-30 KeV and directed down the centre of an electron optical column consisting of two or three magnetic lenses [4.8]. These lenses allow a fine electron beam to be focused onto the specimen surface. Scanning coils are made to pass through the corresponding deflection coils of a Cathode Ray Tube (CRT), so as to produce a similar but larger raster on the viewing screen in a synchronous fashion. Various phenomena occur at the surface of the sample including secondary electron emission which is used to form the image. There is a one to one correspondence between the number of secondary electrons collected from any particular point on the specimen surface and

117

the brightness of the analogous point on the CRT screen. As a result, an image of the surface is built up. Some of the electrons are inelastically scattered by the K,L or N electrons shells in the atom losing their energy in the form of x-rays and it is these which are detected in energy dispersive x-ray analysis (EDX). The theory and analysis of the SEM instruments and their method of operation are detailed in the following reference [4.9].

Samples analysed with the SEM were cut to a suitable size using a diamond studded wheel and lubricant operated at low cutting speeds and forces to prevent any distortion of the sample examined. The samples were then polished, mounted, and enclosed in the vacuum chamber of the instrument.

The Scanning Electron Microscope used in this work (S-2400 HITACHI Scanning Electron Microscope) and shown in Photograph 4.8, consists of the vacuum chamber and components within, screen, surface profile recorder and computer and software (Oxford Link ISIS Labbook supplied by Oxford Instruments Ltd, U.K.) used for data acquisition and analysis of the recorded information. All tests made use of the Secondary Electron Excitation mode. This instrument allowed detailed analysis of the wear area and showed the distribution of elements in the coatings and substrate materials using the speed map features of the software. It was also used to supply a spectrum of the elements in the coated systems inspected using the X-Ray Analyser features.
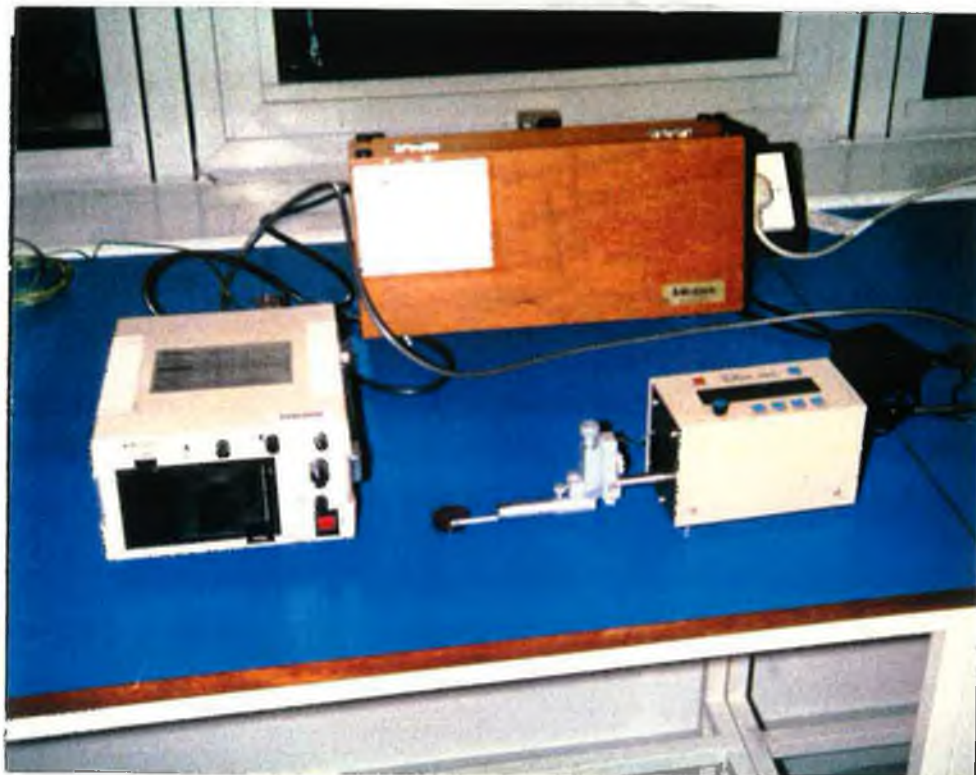
Photograph 4.7 Surface profile measurement equipment.

Photograph 4.8 SEM unit used for inspection of samples.

119

4.5.6 HVOF Thermal Spraying process.

The Thermal spraying process used in applying coatings for this thesis and discussed in Chapter 2. was used for applying thick coatings of Tungsten Carbide Cobalt (WC-Co) and Nickel Chrome (Ni-Cr) coatings. Incorporated in the spraying area is a surface preparation unit for grit blasting the specimens prior to coating. A thermocouple was used to measure the substrate temperature during the coating process as excess heat can lead to coating failure due to thermal stresses. The coating process was manually performed and details on the surface roughness, hardness and thickness before and after the coating process were recorded. Measuring substrate thickness before the coatings were applied allowed accurate measurement of the coating thickness before testing. These coating thickness values were confirmed by using the Scanning Electron Microscope described in section 4.5.5.

4.5.7 Sample Surface preparation.

Surface preparation for the Thermal Spray Process consisted of the following procedure.

i)   Preliminary clean (grit blast).

ii)   Pre-machine.

iii)   Degrease.

iv)   Grit blast.

v)   Spray within two hours.

The substrates used for the thin coating applications were prepared by commercial

suppliers but a typical coating process for these films include,

i)   Wet cleaning

ii)   Heating

iii)   Etching

iv)   Coating

v)   Cooling

CHAPTER 5

MATHEMATICAL ANALYSIS

5.1 WEAR MEASUREMENT EQUATIONS

5.1.1 Abrasion test conditions

Under pure abrasion tests, the stylus continually traversed the surfaces for a specified number of cycles and the wear rate measured at regular intervals. Metal removal was measured by weight loss and volume loss. The depth of the wear scar was also recorded for these tests.

The approximate volume of the wear scar, a cross section of which is shown in Figure 5.1a, formed by abrasion contact may be given by equation (5.1) which was developed from an equation in reference [5.1].

$$Volume = 0.5S[r^2\beta - W(r-h)] \tag{5.1}$$

where

r = stylus radius.

W = width of the wear scar at the surface.

h = depth of the wear scar.

S = sliding distance.

β = included angle.

A computer programme was written (see appendix B) for calculating the volume

wear under abrasion conditions using the above formula.

For continuous use, the stylus tip would be expected to wear and the shape to change to that shown in Figure 5.1b. This wear of the tool was experienced in the test process and had to be taken into account when measuring the wear volume. From Figure 5.1b., the equation for calculating the cross sectional area of the wear scar, which is a development of equation (5.1) is equal to:

$$CSA = \frac{1}{2}r^2[\beta - \sin(\beta) - \alpha + \sin(\alpha)]$$

(5.2)

where β and α are the included angles as shown. The volume is found from the product of this and the sliding distance (S).

The actual volume is calculated from the width of the wear scar at the surface (W), the width of the tip of the stylus (W1), and the radius (r) of the stylus, and substituting these values into the above equation for $\sin(\beta)$ and $\sin(\alpha)$.

A programme for calculating the wear scar volume based on this tool shape was written in Basic and is given in Appendix B. The width of the tip of the stylus was measured between tests to note any change in its shape.
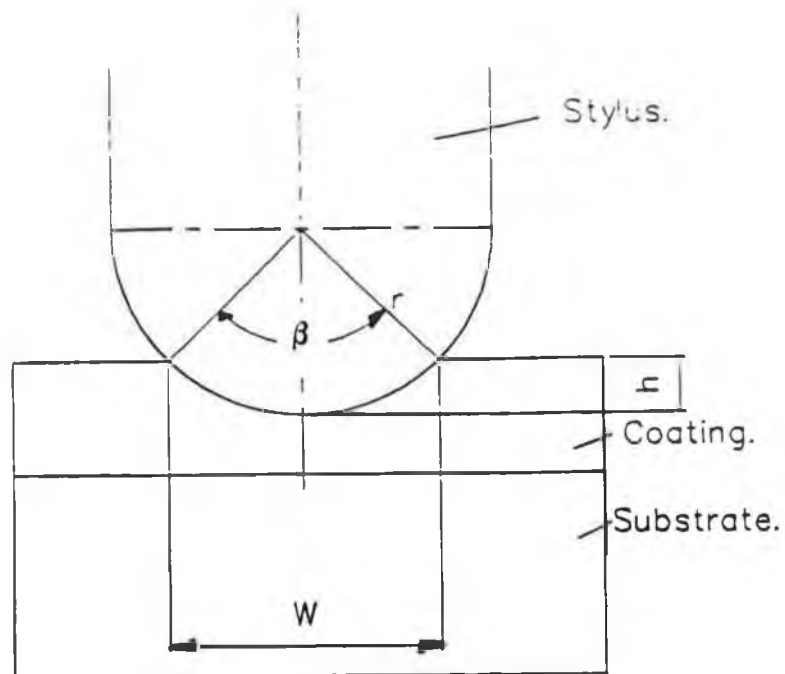
Figure 5.1a   Abrasion wear scar cross section.
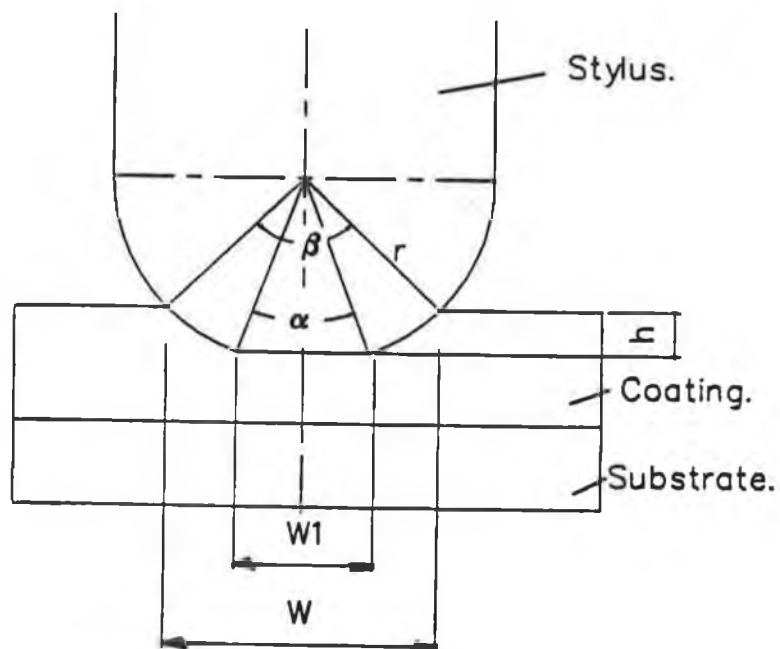
Figure 5.1b   Abrasion scar for worn stylus.

124

5.1.2 Impact conditions

Under impact conditions, for a perfectly hemispherical tip continually impacting a samples, the volume of the resulting crater is given by equation (5.3) from reference [5.1].

$$Crater\ Volume\ =\ \pi h_c^2 r\ -\ \frac{\pi h_c^3}{3} \qquad (5.3)$$

where

r = radius of the impact stylus.

h_c = depth of the crater as shown in Figure 5.2a.

In the event of the tip of the stylus becoming flattened during the test process, the crater shape would be modified and the following formula used to calculate the volume produced as shown in Figure 5.2b:

$$Volume\ =\ \frac{\pi h_c}{6}(h_c^2 + 3(\frac{W1}{2})^2 + 3(\frac{2a}{2})^2) \qquad (5.4)$$

This represents the volume of a frustrum of a sphere where:

h_c = crater depth.

W1 = width at tip of stylus.

2a = crater diameter at the surface.

The surface area of the crater produced is approximately:

$$Surface\ area\ =\ 2\pi r h_c \qquad (5.5)$$

125

5.1.3 Combined impact abrasion

Samples were subjected to combined impact-abrasion tests for a specified number of cycles and the wear rate measured at regular intervals. The crater and abrasive wear scars were measured seperately and recorded and the weight loss also noted. The wear volume produced due to combined impact abrasion for a hemispherical tip as shown in Figure 5.2a, approximates to:

$$Volume = \pi h_c^2 [r - \frac{h_c}{3}] + 0.5 S_1 [r^2 \beta - W(r-h)] \qquad (5.6)$$

where $S_1 = S-2a$ and

$2a$ = crater diameter at the surface.

For a modified stylus tip, the combined wear volume would be the sum of the volumes for equations (5.2) and (5.4).

Impact can occur while the stylus is stationary at the start of the wear scar or can be applied as the stylus traverses the sample at different velocities and positions. Experimental work considered impact at the start and at the center of the wear scar to measure the effects of linear velocity of the stylus on the material loss and wear scar produced. A computer programme (see appendix B) was written for calculating the wear volume under combined impact and abrasion.

5.2 MATHEMATICAL MODEL FOR CONTACT WEAR

One of the most widely used equations for measuring the wear volume for contacting surfaces is the Archard or constant wear volume equation which has been adapted
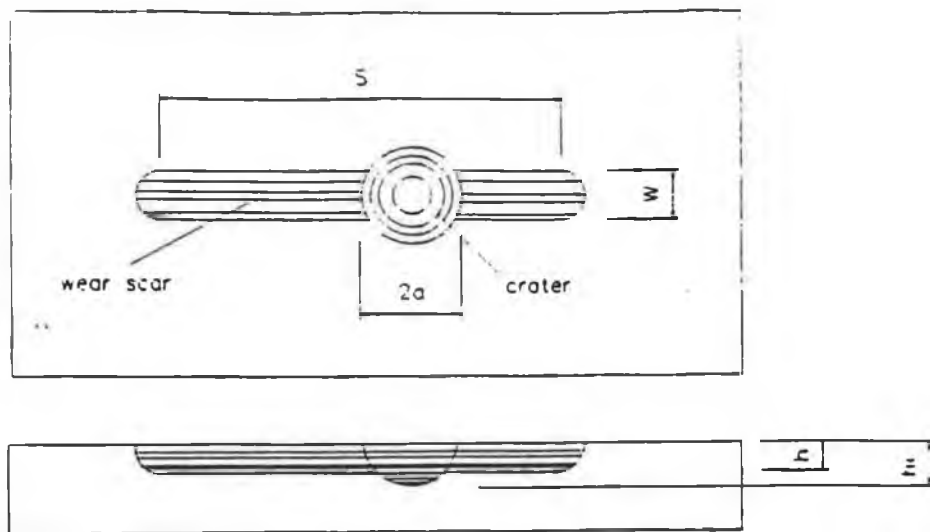
Figure 5.2a   Combined impact abrasion wear scar.
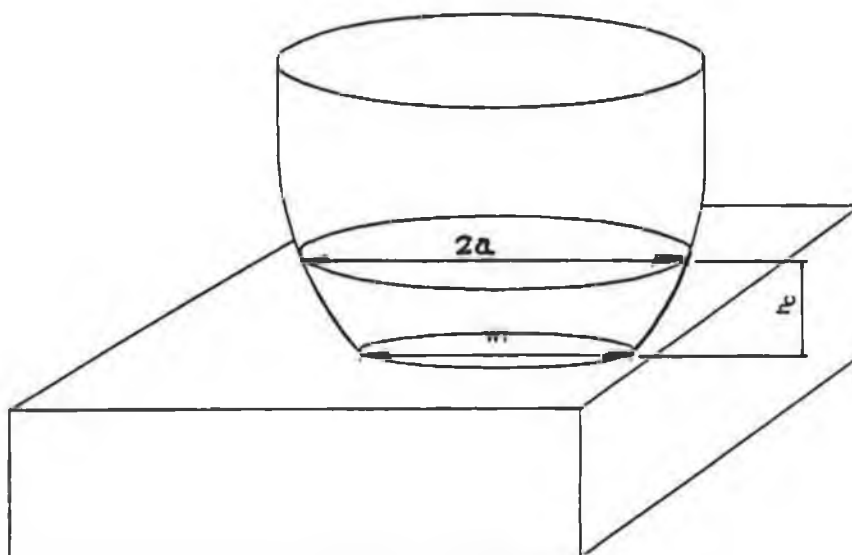
Figure 5.2b   Crater size for worn stylus.

by many authors [5.2 - 5.8]. The standard equation appears as follows,

$$\frac{V}{S} = K \times \frac{L}{H}$$

(5.7)

where

$V =$ volume of material worn off (mm^3)

$S =$ sliding distance (m).

$L =$ Normal Load (N)

$H =$ Hardness (N/m^2)

$K =$ wear coefficient.

This equation shows that the wear increases with both the applied load and the sliding distance.

K can be replaced by the wear constant, k as

$$k = \frac{K}{H}$$

(5.8)

therefore:

$$\frac{V}{S} = k \times L$$

(5.9)

Inhomogeneous materials such as those with a modified surface or a coating should not be expected to yield constant k values. The k-value will then become a weighed mean of the individual wear constants of the coating and the substrate (k_c & k_s respectively) as described by Kassman et al [5.4].

In the wear test used for this experimental work, the sliding velocity is not constant and a new wear constant k_1 is used to take account of velocity changes. This

128

interpretation of the wear equation has been suggested by authors in the past [5.8,5.9] but to date has not been applied to a reciprocating stylus whose linear velocity is changing. It is well accepted that the cutting velocity of machine tools for instance has a bearing on the life of the tool.

Considering a small volume change corresponding with a change in sliding distance:

$$let \quad \delta V = volume \ change$$

$$let \quad \delta S = sliding \ distance \ change$$

Therefore:

$$\frac{\delta V}{\delta S} = k_1 * v * L \qquad (5.10)$$

also

$$\delta S = v * \delta t$$

thus giving:

$$\frac{\delta V}{\delta t} = k_1 * L * v^2 \qquad (5.11)$$

from which

$$dV = k_1 * L * v^2 \ dt \qquad (5.12)$$

This gives the wear volume V as:

$$V = k_1 * L * \int_0^t v^2 \ dt \qquad (5.13)$$

With reference to Figure 5.3, the velocity of the abrading stylus is;

$$velocity \ v \ = \ w*r*(\sin\theta + \frac{\sin2\theta}{2*n}) \qquad\qquad \text{(5.14)}$$

where

ω = angular velocity of the motor in radians/sec.

n' = the ratio l/r.

r = crank radius.

l = con rod length.

If the velocity is squared, the wear volume equation becomes;

$$V \ = \ k_1 L \int_0^t w^2 r^2 (\sin^2\theta + \frac{2\sin^2\theta\cos\theta}{n} + \frac{\sin^2 2\theta}{4n^2})dt \qquad \text{(5.15)}$$

also

$$dt \ = \ \frac{d\theta}{w} \qquad\qquad \text{(5.16)}$$

and the time, t is proportional to the number of cycles.

Integrating for θ from 0 to 2π for one full cycle the wear volume becomes:

$$V \ = \ k_1 * L * w * r^2 * 2\pi \qquad\qquad \text{(5.17)}$$

This value can be multiplied by the number of cycles to calculate the total wear volume at any test interval.

The equation can also be written as:

$$V \ = \ k_1 * L * v * 2\pi r \qquad\qquad \text{(5.18)}$$

where v is the velocity (m/s) of a point at the end of the motor arm, and $2\pi r$ is the circumference of the circle produced by this point in one revolution, and is proportional to the sliding distance of the stylus on the surface of a test sample.

130
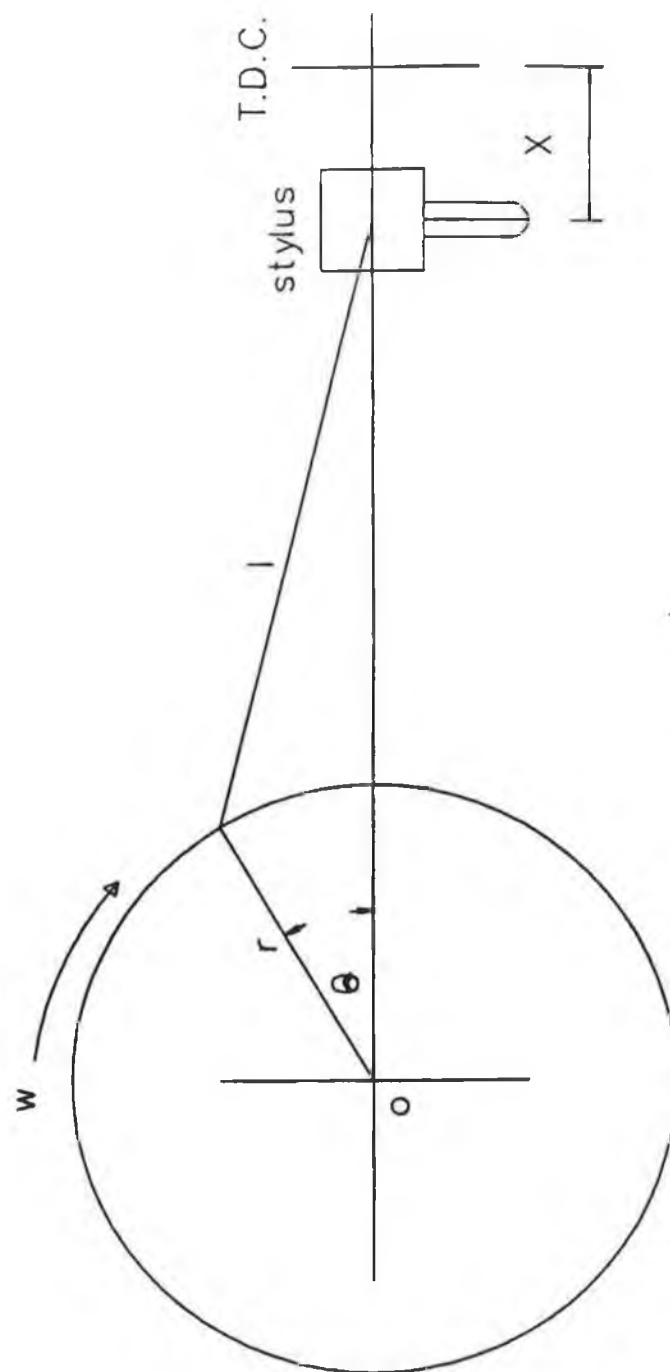
Figure 5.3   Drive mechanism for the test rig.

If the normal load L is 100 N, the crank radius r, 0.01 m, and the motor speed 106 revolutions per minute (r.p.m.) then the wear volume, V, for one cycle is:

$$V = 0.698k_1 \qquad \qquad (5.19)$$

and the value of k_1 can be found by measuring the wear volume in the experimental tests. The units of k_1 in this case are:

$$\frac{mm^3}{N-m-m/s}$$

From inspection of uncoated aluminium samples subjected to abrasion under a variable linear velocity, it was observed that the depth of the wear scar changed with displacement or velocity of the abrasion stylus. This is discussed in Chapter six.

5.3 IMPACT ANALYSIS

A collision between two bodies which occurs in a very small time interval, and during which the two bodies exert on each other relatively large forces is called an impact [5.10].

5.4 DYNAMIC INDENTATION

When two elastic bodies such as a sphere and a flat specimen are pressed against each other and the load exceeds a critical value, the elastic limit, a plastic zone develops and an indentation in the surface may result. At first the region of contact will deform elastically, and if the impact is low enough the surface will recover

132

elastically and seperate without residual deformation. The collision in this case is purely elastic.

Tabor [5.11] and later Brenner et al [5.12] showed that a lubricant film or thin oxide films do not affect the deformation produced by impact of a sphere on a surface. However such coatings are likely to reduce any adherence or sticking between two impacting surfaces.

5.5 DYNAMIC HARDNESS

The dynamic hardness of a material is defined by Tabor [5.13] as the resistance to local indentation when the indentation is produced by a rapidly moving indenter. The volume of the indentation formed is directly proportional to the kinetic energy of the indenter. This implies that a material offers an average pressure of resistance to an indenter equal numerically to the ratio;

$$\frac{Energy \ of \ indenter}{Volume \ of \ indentation} \tag{5.20}$$

For a hemisphericl indenter, applying a constant dynamic impact pressure P, if at any instance the projected area of the indentation is A, the force exerted on the material is PA. At the next cycle, the indenter will penetrate a further distance dx, the work done will be PAdx and the total work in forming the indentation is

$$\int PAdx = P\int Adx = PV_1 \tag{5.21}$$

where V_1 is the volume of indentation. This can be equated to the energy of impact

133

as given in reference [5.13], so that

$$P = \frac{Energy \ of \ impact}{V_1}$$ (5.22)

There may be a change in the volume of the indentation due to elastic recovery if there is some rebound involved. If the impact results in the mean pressure exceeding about $1.1Y$, where Y is the yield stress or elastic limit of the material, slight plastic deformation will occur. As the impact energies increase, deformation becomes plastic resulting in the total kinetic energy of the indenter being absorbed in deformation. Finally, a release of elastic stresses in the indenter and in the indentation takes place as a result of which some rebound occurs.

Following impact, the volume of the remaining permanent indentation is V_r, the work done as plastic energy in producing this indentation is given by

$$W_3 = PV_r$$ (5.23)

where W_3 is the difference between the energy of impact, W_1 and the energy of rebound W_2. The volume V_r of the permanent indentation left in the surface, as derived by Tabor and applied by others [5.14] approximates to;

$$V_r = \frac{\pi a^4}{4 r_2}$$ (5.24)

where

a = radius of indentation crater

r_2 = radius of curvature of the indentation given by:

$$r_2 = \frac{(\frac{(2a)^2}{4} - h_c^2)}{2h_c} \qquad (5.25)$$

h_c = depth of crater.

5.5.1 Contact area on impact

When two surfaces are brought together, they meet at the tips of the higher asperities and the total area of contact is determined by the deformation of the material in these regions under the applied load. In many experimental works a spherical shape is normally used as the abrading tool so that the total area of contact is confined to a single circular area. As the loads increase, this area increases in size [5.5].

The radius, r_2, of the circular area of contact formed when a sphere of radius r is pressed against a flat surface under a force L is given in [5.15] by,

$$r_2 = 1.1 * \sqrt[3]{0.5*Lr(\frac{1}{E_1} + \frac{1}{E_2})} \qquad (5.26)$$

when the deformation is elastic and

E_1 = Youngs modulus for the abrading tool.

E_2 = Youngs modulus for the contacting surface.

When the deformation is plastic the radius becomes.

$$r_2 = \sqrt{\frac{L}{\pi * p_m}}$$
(5.27)

where

p_m = Mean pressure of the deformable member over the area of contact.

5.5.2 Time of impact for plastic conditions

Considering an indenter of spherical shape and radius r, impacting a sample and penetrating a distance x, it produces a crater of radius a, as shown in Figure 5.4. The value 2rx approximates to a^2 [5.13]. The decelerating force on the sample is equal to $P\pi a^2$ or $P\pi 2rx$, where P is the average yield pressure. The equation of motion for the system is given in [5.13] as;

$$\frac{d^2x}{dt^2} + \frac{2P\pi r}{m}x = 0$$
(5.28)

and the solution is given by;

$$x = A\sin\sqrt{\frac{2P\pi r}{m}}t$$
(5.29)

The sphere is brought to rest when dx/dt = 0, and therefore,

$$t = \frac{\pi}{2}\sqrt{\frac{m}{2P\pi r}}$$
(5.30)

136
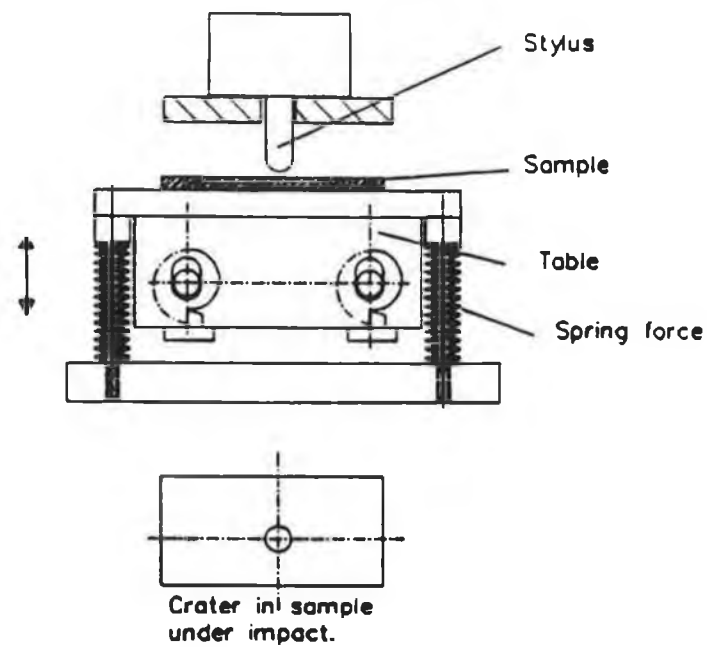
Figure 5.4   Method of applying impact craters.

t = time of impact

m = mass of the indenter.

Tabor [5.13], in deriving this approximate equation assumes that the indenter is completely undeformable and all elastic strains are neglected.

For a plastically deforming sphere striking a rigid plate, Richmond [5.15] has shown that the time of impact is given by;

$$t = 0.65r\sqrt{\frac{\rho}{\sigma_f}} \qquad (5.31)$$

ρ = density of the sphere material

σ_f = flow stress

r = radius of the sphere.

Both equations show that the duration of the impact does not depend on the impingement velocity v.

5.5.3 Plastic zones formed in impact

The plastic zones beneath the abraded area are formed below the impact or indenting tool [5.16,5.17]. A plastic zone of uniform depth is formed whose size, Q is proportional to the diameter of the crater, 2a, formed on the eroded surface by the impact tool. That is;

$$Q = 2a*c \qquad (5.32)$$

where c is a constant.

For a spherical particle of radius, r, and density, ρ, impacting a test piece of average

hardness, H, the energy balance equation is given in [5.15] as;

$$HV = \frac{2\pi}{3}r^3\rho v^2 \tag{5.33}$$

V = crater volume.

HV is the energy in forming the crater and the Right Hand Side of the equation is the kinetic energy of the incident particle and v is the impact velocity.

5.6 IMPULSE AND MOMENTUM

In applications where an impulsive force is applied over a very short time, lasting from $t=t_0$ to $t=t_1$ to a mass m, from Newtons 2nd law,

$$\int_{t0}^{t1} f(t)dt = \int_{t0}^{t1} m*\frac{dv}{dt}dt = \int_{v0}^{v1} m*dv = m(v_1-v_0) \tag{5.34}$$

where f(t) is the force function.

If the mass centres are located on the common normal to the surfaces in contact, the impact is considered a central impact. If the velocities of the particles are directed along the line of impact, the impact is said to be a direct impact. Otherwise the impact is said to be oblique impact [5.18].

The main stages of combined impact-abrasion are shown in Figure 5.5.

5.6.1 Direct central impact

For two bodies, a and b of mass m_a and m_b moving in the same straight line and heading towards each other with velocities v_a and v_b, the collision on impact may

cause the two bodies to deform. At the end of the deformation period, they will have the same velocity, u. A period of restitution will then take place, following which the bodies will regain their original shape or stay deformed. If there is no impulsive, external force, the total momentum of the two particles is conserved as follows,

$$m_a v_a + m_b v_b = m_a v1_a + m_b v1_b \qquad (5.35)$$

where $v1_a$ and $v1_b$ are the final velocities of particles a and b respectively after the period of restitution.

In the analysis here, particle a (the stylus) is stationary before impact and therefore has an initial normal velocity, v equal to zero, therby reducing the momentum equation to.

$$m_b * v_b = m_b * v1_b + m_a * v1_a \qquad (5.36)$$

Since the only impulsive force acting on a is the force F exerted by b then,

$$-\int F dt = m_a * u \qquad (5.37)$$

u = velocity during deformation.

The force exerted by particle b (the table and sample mass) on a, during the period of restitution, denoted by R is given as

$$m_a u - \int R dt = m_a v1_a \qquad (5.38)$$

where

$$\int R dt \leq \int F dt \qquad (5.39)$$

The ratio of these impulses correspond to the period of restitution and the period of deformation is the cefficient of restitution, e.

$$e = \frac{\int R dt}{\int F dt} \qquad (5.40)$$

where e is between 0 (for pure plastic) and 1 (for pure elastic conditions). The coefficient of restitution depends on the materials involved, the impact velocities and the particle shape as described in reference [5.18].

The relative velocity of the particles before impact is equal to v_b and the relative velocity after impact is $v1_b$-$v1_a$, then

$$e = \frac{u - v1_a}{-u} \qquad (5.41)$$

Considering the effects of particle a on particle b, and combining equations, the coefficient of restitution becomes,

$$e = \frac{v1_b - v1_a}{-v_b} \qquad (5.42)$$

This property can be used to determine the value of the coefficient of restitution experimentally of the two materials colliding under impact. The final velocity of particle b after impact and the period of restitution is,

$$v1_b = \frac{v_b(e * m_a - m_b)}{m_b + m_a} \qquad (5.43)$$

and the velocity of particle a after restitution is,

$$vl_a = \frac{m_b v_b (1+e)}{m_a + m_b}$$ (5.44)

Since under the experimental work carried out in this research, there is a combination of elastic and plastic conditions, the total energy of the particles is not conserved, and the kinetic energy before and after impact is expected to differ due to heat produced and elastic waves generated within the colliding particles. Some rebound of the stylus and its attached load occured in the experimental work, following which, a secondary impact took place, completed by contact abrasion until the next impact cycle. This rebound depends on the stored elastic energy in the colliding bodies which is equivalent to the kinetic energy of rebound. Hertz [5.19] expressed this elastic energy E_e as,

$$E_e = \frac{3}{5} \frac{\pi^2 a^3 P^2}{E(1-v^2)}$$ (5.45)

where;

E = Young's Modulus.

v = Poissons ratio.

P = Pressure under which the metal flowed plastically during impact.

a = Radius of impact crater.

and the kinetic energy of rebound E_r , is given by,

$$E_r = \frac{m * vl_a^2}{2}$$ (5.46)

This energy is applied to the samples in producing a secondary impact effect.

142

MAIN STAGES OF COMBINED IMPACT ABRASION

a. Before Impact.   b. Impact.   c. After Impact.   d. Abrasion.
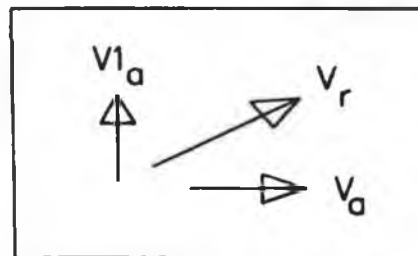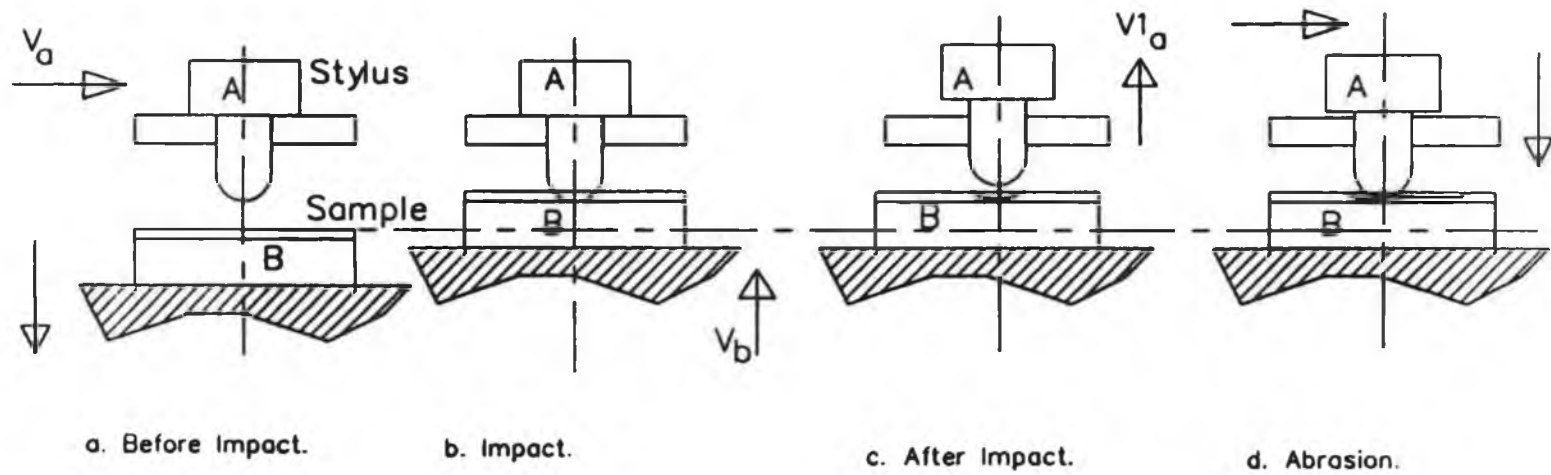
Stylus after impact.

Resultant of normal
and tongential velocity
of stylus.

Figure 5.5   Main stages of combined impact abrasion.

5.6.2 Oblique central impact

When the velocities of the two colliding bodies are not directed along the line of impact, impact is said to be oblique. This is common to combined impact abrasion. The direction of the velocities of the bodies before and after impact are as shown in Figure 5.5. If the bodies are assumed frictionless, the only impulse exerted on the particles during impact are due to internal forces directed along the line of impact (normal axis). The components along the tangential axis of the momentum of each particle is conserved.

In the normal direction:

$$m_b v_b = m_b * v1_b + m_a * v1_a \qquad (5.47)$$

and also:

$$v1_b - v1_a = e(-v_b) \qquad (5.48)$$

since $v_a = 0$.

Considering the tangential component, the velocity of the stylus before impact is equal to the velocity just after impact;

$$v_a \ before = v_a \ after \qquad (5.49)$$

From the above equations, if the masses, m_a and m_b, are known, along with the initial velocities, v_a and v_b, and the coefficient of restitution, e, then the velocities just after impact can be determined.

Due to the normal and tangential components of the velocity of the particle a, its actual velocity and direction is the resultant of these two components as shown in Figure 5.5. Figure 5.6 shows a schematic of the effects of the dynamic

144

rebound caused by the combination of impact conditions and linear velocity on the stylus.

Combined Impact Abrasion wear scar.

Double crater effect due to impact and rebound
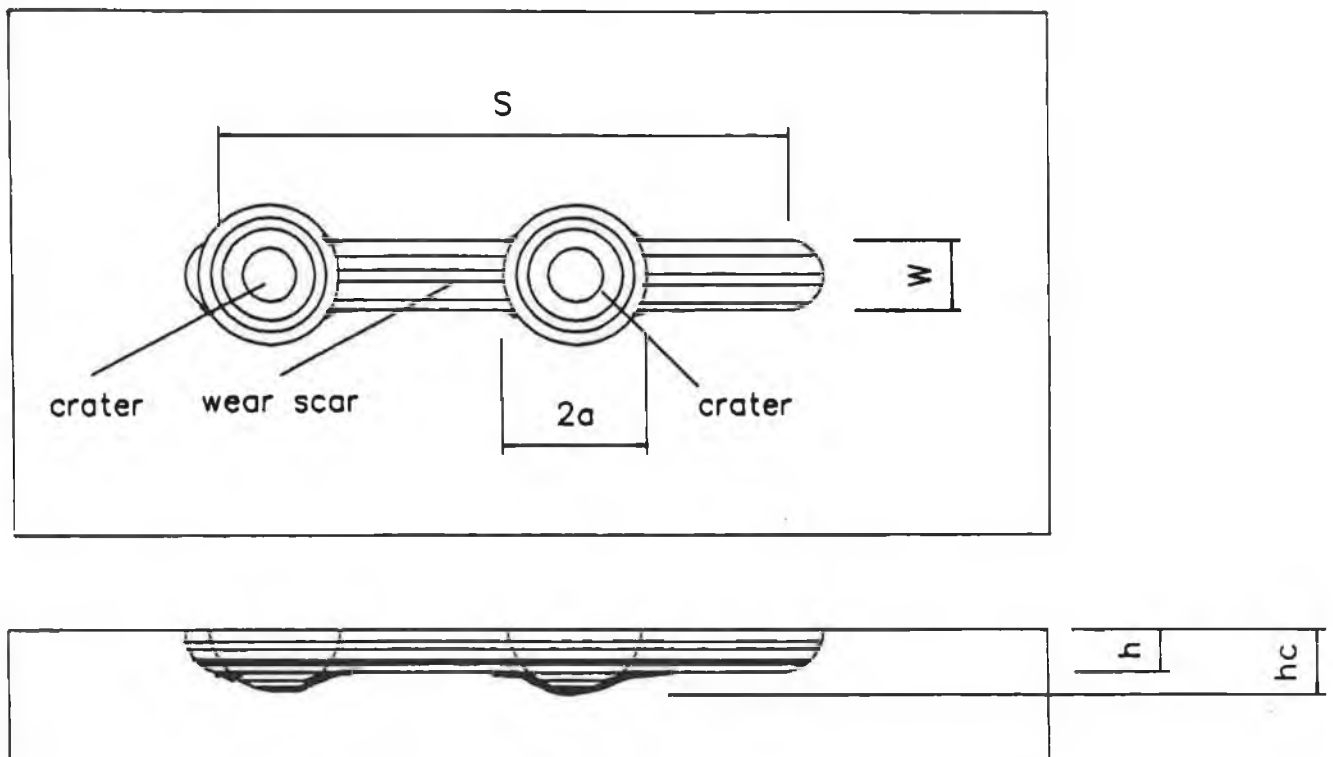
Figure 5.6 Cratering due to dynamic rebound on samples.

CHAPTER 6

WEAR TESTING OF SAMPLES AND

DISCUSSION OF RESULTS

6.1 INTRODUCTION

Various coating were applied to substrates and thickness values were measured and recorded prior to wear testing. Surface roughness values and hardness values of the substrate and coatings were also recorded using a surface profileometer and hardness tester respectively. The profileometer was also used for measuring the depth and examining the profile of the wear scars and craters following each test. Microhardness measurements for the experimental work were taken on a Vickers hardness tester using a diamond pyramid indenter and Macro hardness values measured with an Omag hardness tester. Material loss and volume loss values were recorded at regular intervals and the values plotted against the number of wear cycles. Uncoated samples were also tested and compared to the coated specimens. Most coatings were tested to destruction which resulted in either coating failure, removal or penetration.

6.2 OPERATING PROCEDURE

6.2.1 Applied loads

Normal loads of 100 Newtons were applied to the samples during testing. Other loads applied during the testing are as stated.

6.2.2 Sliding distance and velocity range

The sliding distance of the stylus was set at 20 mm for most experimental work which gave a reciprocating velocity range shown in Table 6.1 for the stylus. The displacement and acceleration values corresponding with the velocity range are also given.

6.2.3 Impact velocity

A Uniphase helium gas laser was used for measuring the velocity just before impact occured in each test. The impact distance (1.5 mm) and spring force were identical for each test. Recorded impact velocities were 0.22 m/s. From the calibration chart for the bevel washers in Figure 4.5, the calculated spring constant C (N/m) for the impact system is 161.40 kN/m. The mass of the impact table is 5.2 kg. This applied an upward force on the stylus and its mass of 240 N. Following impact, the stylus mass is pushed upwards freely a distance, depending on the coefficient of restitution. Typical rebound heights were in the

147

order of 1 to 1.5 mm, measured by an electronic displacement gauge. The falling

mass, then strikes the sample at a velocity of 0.14 to 0.2 m/s. The stylus then

abrades the sample until the cams seperate them and the cycle repeats itself.

Operating speeds are 106 cycles per minute.

```
Crank Radius r =          .01
Con rod length l =        .3

n = l/r =                 30
Speed of rotation         106          (R.P.M.)
w (rad/sec) =             11.10
```

ANGLE (DEG)	DISPLACEMENT (m)	VELOCITY (m/s)	ACCELERATION (m/s^2)
0	0	0	1.273
20	.0006	.0392	1.189
40	.0024	.0732	.9510
60	.0051	.0977	.5955
80	.0084	.1099	.1754
100	.0119	.1087	-.253
120	.0151	.0945	-.637
140	.0177	.0695	-.937
160	.0194	.0368	-1.13
180	.02	0	-1.19
200	.0194	-.037	-1.13
220	.0177	-.070	-.937
240	.0151	-.095	-.637
260	.0119	-.109	-.253
280	.0084	-.110	.1754
300	.0051	-.098	.5955
320	.0024	-.073	.9510
340	.0006	-.039	1.189
360	0	0	1.273

Table 6.1 Reciprocating velocity range for stylus.

6.3 HARDNESS VALUES

The hardness measurements for the coated specimens were conducted with a Leitz Miniload Vickers micro hardness tester [6.1]. The Vickers hardness number Hv, from this reference is given by:

$$H_v = 1854.4 * \frac{f}{d^2} \qquad (6.1)$$

f = applied load in grams

d = mean value of a diagonal in μm

6.4 MATERIALS TESTED

6.4.1 Substrates

Substrate materials of Aluminium, Mild Steel and Tool Steels (AISI D2, AISI D3, VANADIS 4, and VANADIS 10,) were used. All substrates were cut to size, and prepared for coating purposes. The composition of the substrate materials and hardness values (HRc) for the uncoated samples are given in Table 6.2.

	Contents %							Hardness
Material	C	Si	Mn	Cr	Co	W	V	(Rc 150 kgf)
AISI D2	1.55	0.3	0.3	12	0.8		0.8	63
AISI D3	2.05	0.3	0.8	12		1.3		60
Vanadis 4	1.5	1.0	0.4	8.0	1.5		4.0	62
Vanadis 10	2.9	1.0	0.5	8.0	1.5		9.8	63
Mild Steel	0.2	0.15	0.30					62 HRb
Aluminium		5.0	0.55					60 HRf

Table 6.2 Substrate materials.

6.4.2 Coatings

Coatings applied and tested in the experimental work include:

1. Titanium Nitride TiN.   (Thin coatings 2 to 4 μm).

2. Titanium Carbide Ti_xC.   (Thin coatings 2 to 4 μm).

3. Tungsten Carbide-Cobalt. (Thick coatings).

4. Nickel Chrome.   (Thick coatings).

The Tungsten Carbide-Cobalt, and Nickel Chrome coatings were applied by the High Velocity Oxy Fuel Process described in section 2.5.5, and the Titanium Nitride and Titanium Carbide (Ti_xC where x = 0.05) coatings were applied by a PVD process (Teers Coatings, U.K.). For the High Velocity Oxy Fuel process, Diamalloy 2003 [6.2], Tungsten Carbide-Cobalt Metal/carbide powder and Diamalloy 2001 [6.3], Nickel Chrome Thermal spray metal powder were used. Details of these materials are supplied in Tables 6.3 and 6.4 respectively.

DIAMALLOY 2003.	Contents.	Relative Density.	Melting Pt
Tungsten Carbide	88.5%	4.5-6.3.	1200-1260°C
Cobalt	11.5%		
Powder size	less than 40μm with coarse appearance.		

Table 6.3.   WC-Co Metal/carbide powder.

DIAMALLOY 2001	Contents	Relative Density	Melting Pt.
Nickel	72%	4.4	980-1150°C
Chromium	17%		
Silicon	4%		
Boron	3.5%		
Iron	1%		
Cobalt	1%		

Table 6.4. Ni-Cr Thermal spray metal powder.

6.5 CONTACT ABRASION TESTS

6.5.1 TiN and TiC coated tool steels

Abrasion wear tests were performed on four tool steel materials of AISI D2 and D3 and Vanadis 4 and Vanadis 10. Coatings of Titanium Nitride (TiN) and Titanium Carbide (TiC) were applied to each material using a PVD process. Wear

151

tests on the coated and uncoated samples were conducted on each sample using a round nose tool stylus of radius 2 mm, made from Tungsten Carbide. A normal load of 5.5 kg was applied to the samples until such time that the coating was penetrated. The sliding contact distance was set at 20 mm. Wear tests on each material showed that the TiC coated samples demonstrated greater wear resistance, with the TiC coated Vanadis 4 providing the best wear resistance. Factors assisting the low wear of these samples was the combined coating/substrate hardness and the quality of the coating. TiN coated D2 and D3 samples showed very little improvement in wear resistance over the uncoated samples.

Figures 6.1 to 6.4 show the results of wear scar depth versus number of wear cycles for D2, D3, Vanadis 4 and Vanadis 10 respectively. From these figures it is evident that the Titanium Crabide coatings offered the greatest wear resistance with the best performance on Vanadis 4. In comparison, the uncoated and Titanium Nitride coated samples offered much lower and similar wear resistance. For the uncoated samples, the D3 material showed the least wear resistance. On the TiC coated samples, the D3 substrate material proved the least wear resistant, and the Vanadis 4 providing the best wear resistance. For the TiN coated samples, the most wear resistant material was also Vanadis 4, followed by Vanadis 10. Similar wear resistance was noted for the TiN coated D2 and D3 samples.

WEAR TRACK DEPTH VS NUMBER OF CYCLES
COATED AND UNCOATED SPECIMENS

Legend:
- ☐ Ti C COATED D2
- ✕ TiN COATED D2
- ▽ UNCOATED D2

Y-axis: DEPTH (microns)
X-axis: CYCLES
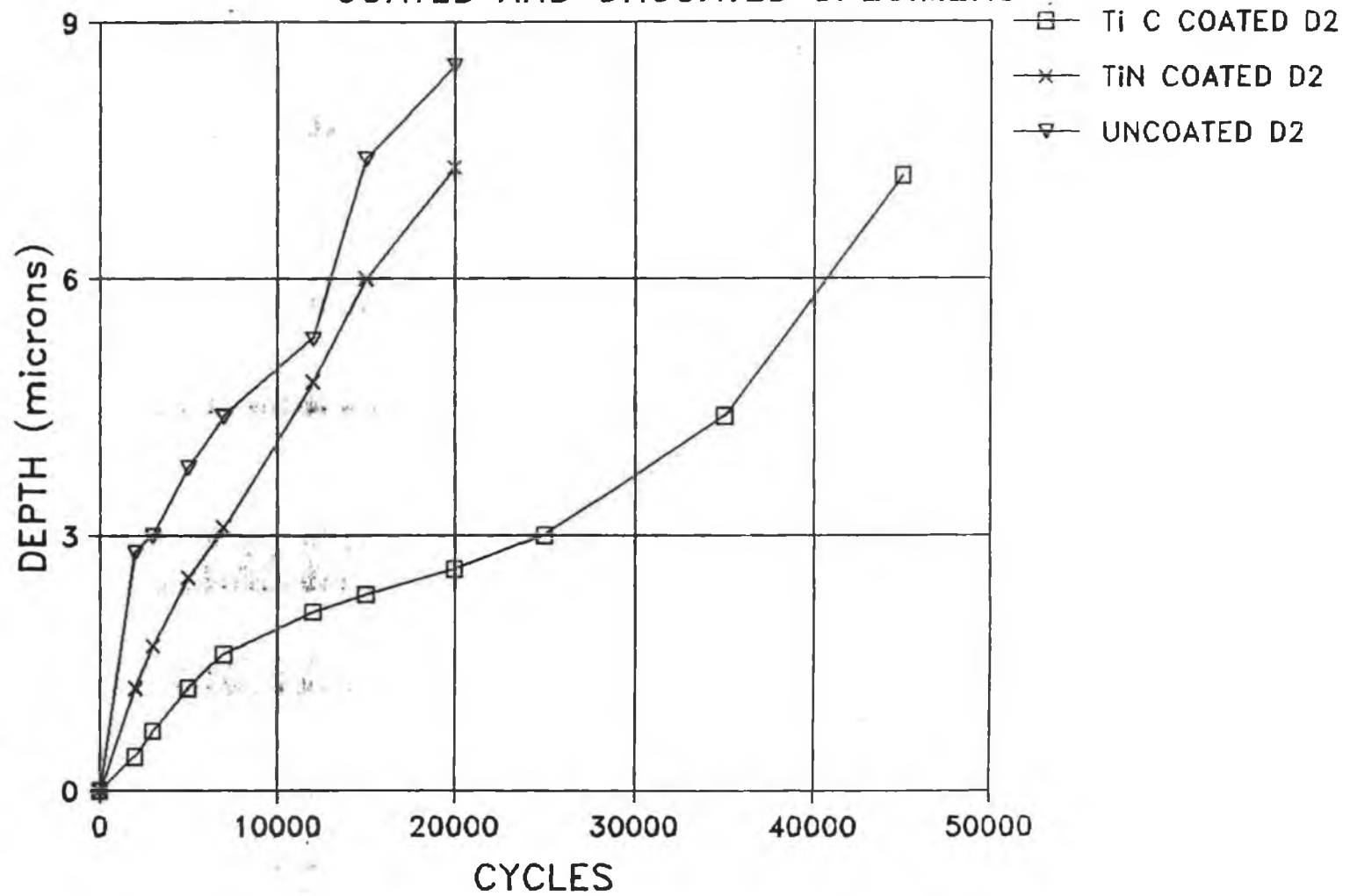
Figure 6.1 Wear track depth for AISI D2 coated and uncoated samples.
Depth (μm) vs number of cycles (5.5 kg load).

153

WEAR TRACK DEPTH VS NUMBER OF CYCLES
COATED AND UNCOATED SPECIMENS
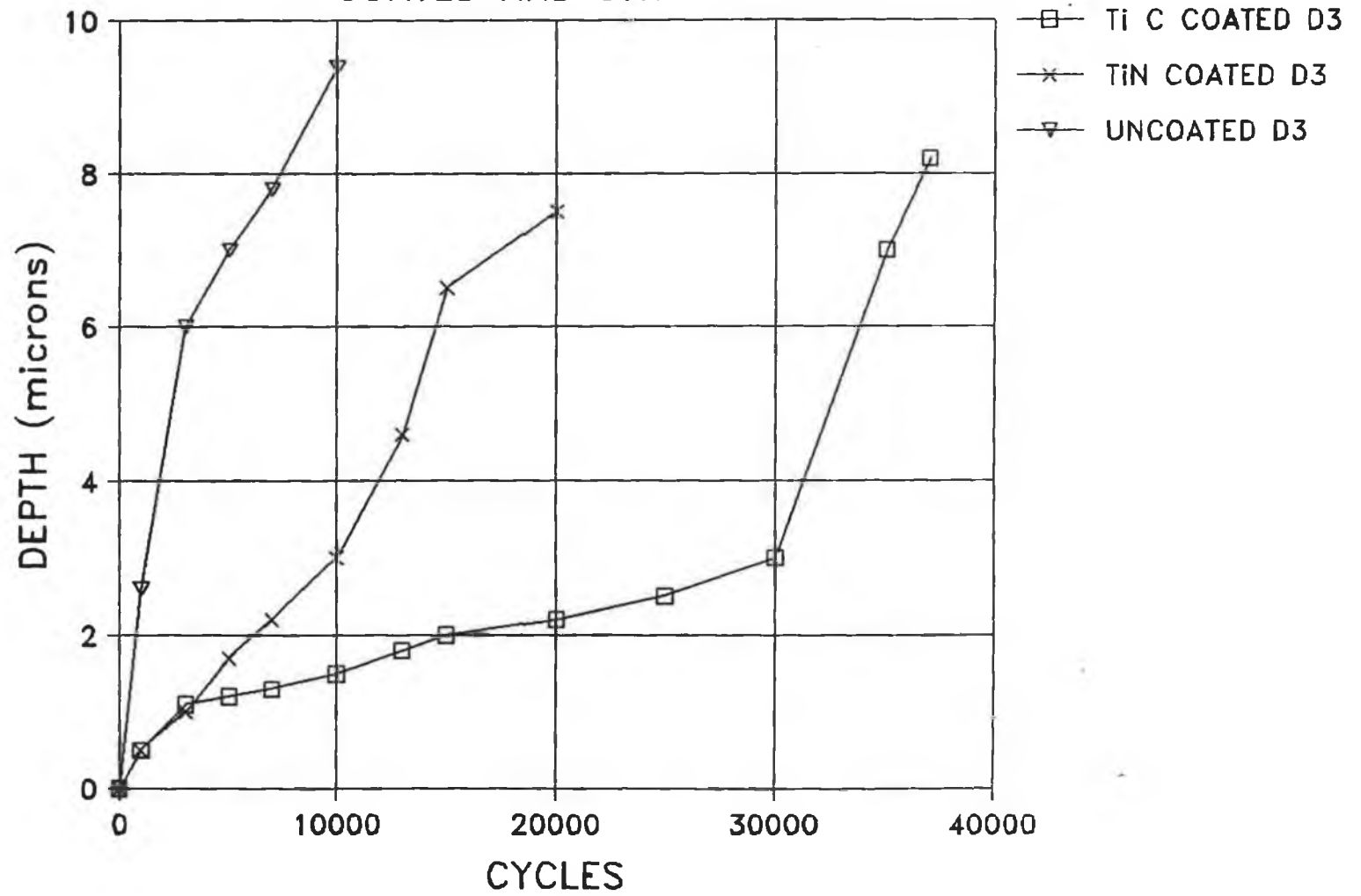
Figure 6.2 Wear track depth for AISI D3 coated and uncoated samples.
Depth (μm) vs number of cycles (5.5 kg load).

154

WEAR TRACK DEPTH VS NUMBER OF CYCLES
COATED AND UNCOATED SPECIMENS
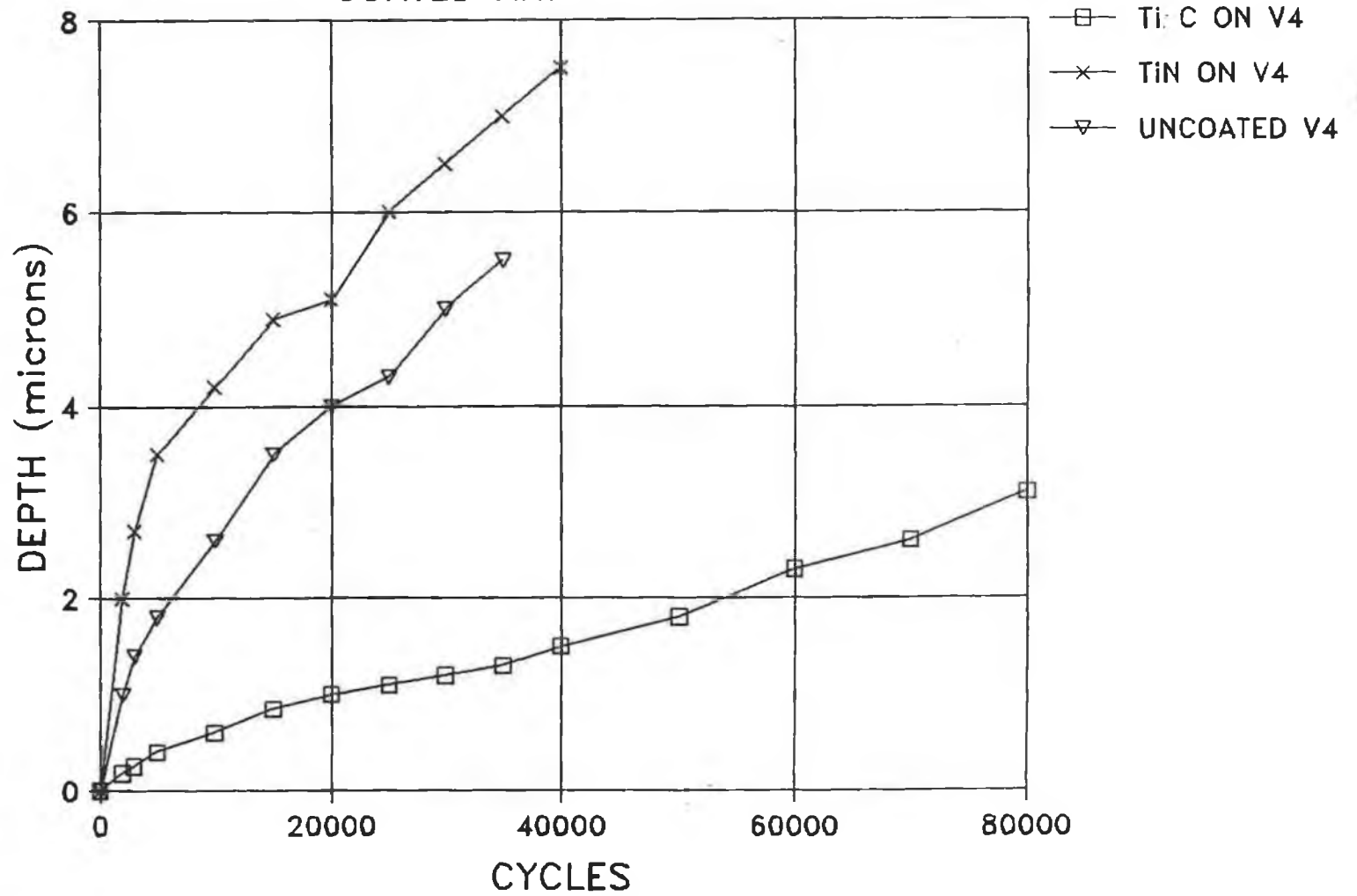
Figure 6.3 Wear track depth for Vanadis 4 coated and uncoated samples.
Depth (μm) vs number of cycles (5.5 kg load).

155

WEAR TRACK DEPTH VS NUMBER OF CYCLES
COATED AND UNCOATED SPECIMENS
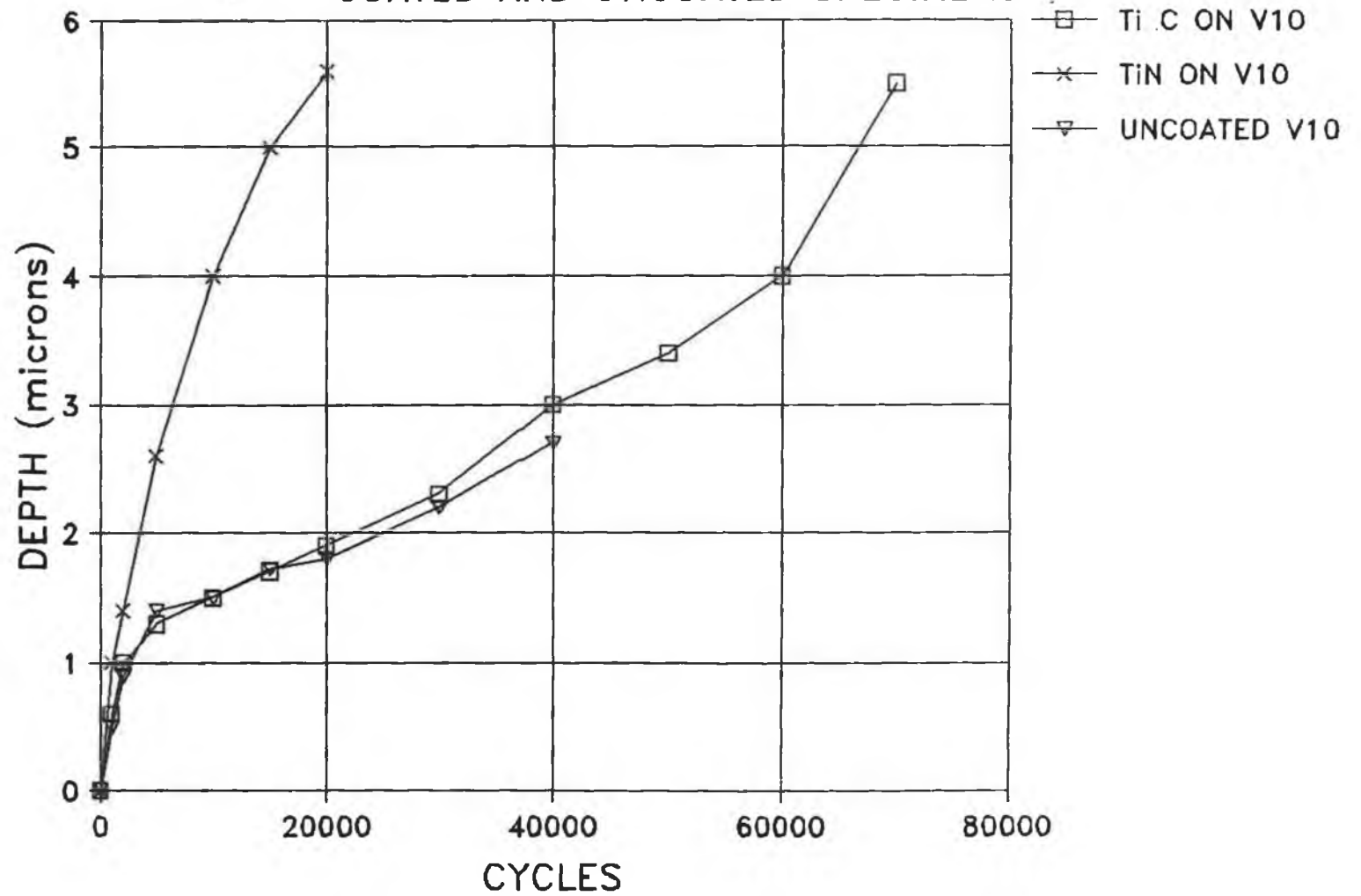
Figure 6.4 Wear track depth for Vanadis 10 coated and uncoated samples.
Depth (μm) vs number of cycles (5.5 kg load).

156

6.5.2 Hardness and wear resistance

The hardness values of the combined coating/substrate samples are shown in Figure 6.5. The lower hardness value of the combined TiC/D3 sample corresponds with a lower wear resistance for this sample in the wear tests conducted. Figure 6.5 also shows lower hardness values for the uncoated samples over the coated ones, which contributed to their lower wear resistance. Although the TiC coated D2, Vanadis 4 and Vanadis 10 show similar hardness values, the wear resistance varied considerably for each sample. It is noticeable that the hardness values for the TiN coated samples are considerably lower than the TiC coated samples. This is a contributory factor to their higher wear rates which brought them more closely to the wear rates of the uncoated samples. Inspection on the surface of the coated samples before testing showed some pitting in the case of the TiN coatings. The same effect was not noticeable on the TiC coatings. The presence of these pits contributed to the low wear performance of the TiN coated samples. As a result, the uncoated samples were just as wear resistant as the TiN coated samples tested. In contrast, the TiC coatings improved the wear resistance significantly of all substrate materials.

6.5.3 Tungsten Carbide Cobalt coated samples

Initial tests were carried out on WC-Co samples using an applied load of 100 N and sliding distance of 20 mm. Weight loss in grams were measured on the worn samples. Table 6.5 gives the details of the coated and uncoated samples of
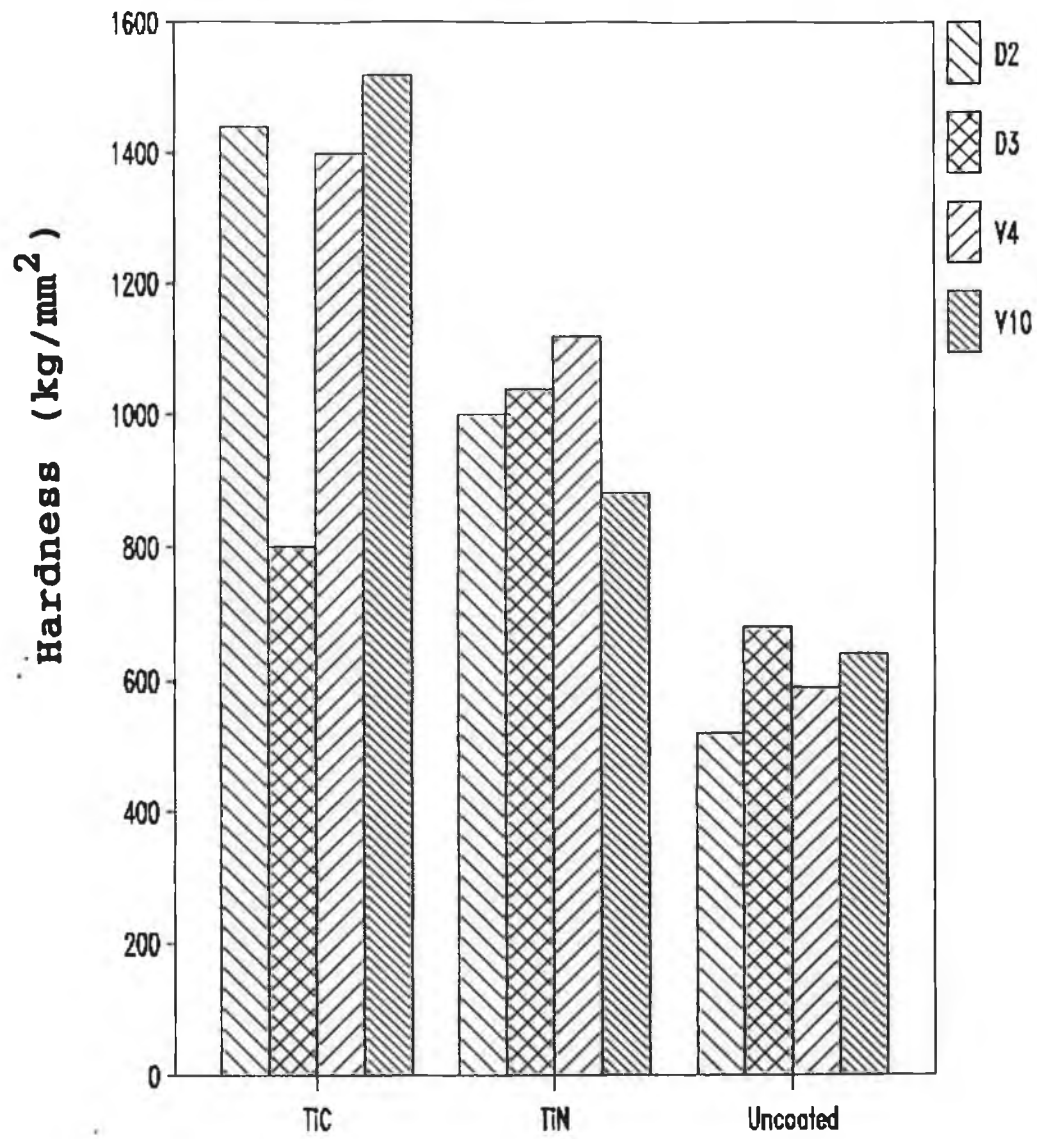
Figure 6.5 Hardness of combined coating/substrate system.

aluminium (Al) and mild steel (MS). Figures 6.6 to 6.9 show the weight loss for abrasion and impact abrasion of the aluminium and mild steel samples. Apart from the uncoated samples, the wear rate for each sample is similar. Due to combined impact and abrasion, the coatings on the softer substrates experienced considerable wear. This was due to cracking, cratering, gouging, abrasion and plastic deformation. This effect is shown in Photograph 6.1. Results show that thin coatings performed best on soft aluminium substrates subjected to impact abrasion conditions whereas the thicker coating performed better on the harder, mild steel sample for the same test. Figures 6.10 and 6.11 show the depth of the wear scar and craters for abrasion and impact abrasion respectively, showing a large crater depth for the .42 mm thick coating on aluminium, caused by coating detachment and substrate penetration under impact conditions.

Sample.	Surface roughness. Ra values substrate (μm)	Coating thickness (mm)	Ra values coating. (μm)	Micro hardness. Hv 300. substrate.	coating.
Al-1	5.5	0.517	4.5	70	1089
Al-2	5.5	0.42	4.5	80	945
Al-3	5.5	0.232	4.5	70	1157
Al-4	5.5	0.043	4.5	90	974
M.S.-1	6.2	0.384	4.5	220	1370
M.S.-2	6.2	0.460	4.5	220	1272
M.S.-3	6.2	0.171	4.5	220	1400
M.S.-4	6.2	0.048	4.5	220	1183

Table 6.5. Surface roughness, hardness and coating thickness of test samples.

CONTACT ABRASION
ALUMINIUM SAMPLES

Legend:
- al (.232 mm coating)
- al uncoated
- al (.517 mm coating)
- al (.42 mm coating)
- al (.043 mm coating)

Y-axis: WEAR (g) — .015, .01, .005, 0

X-axis: NUMBER OF CYCLES — 0, 636, 1272, 1908, 2544, 3180
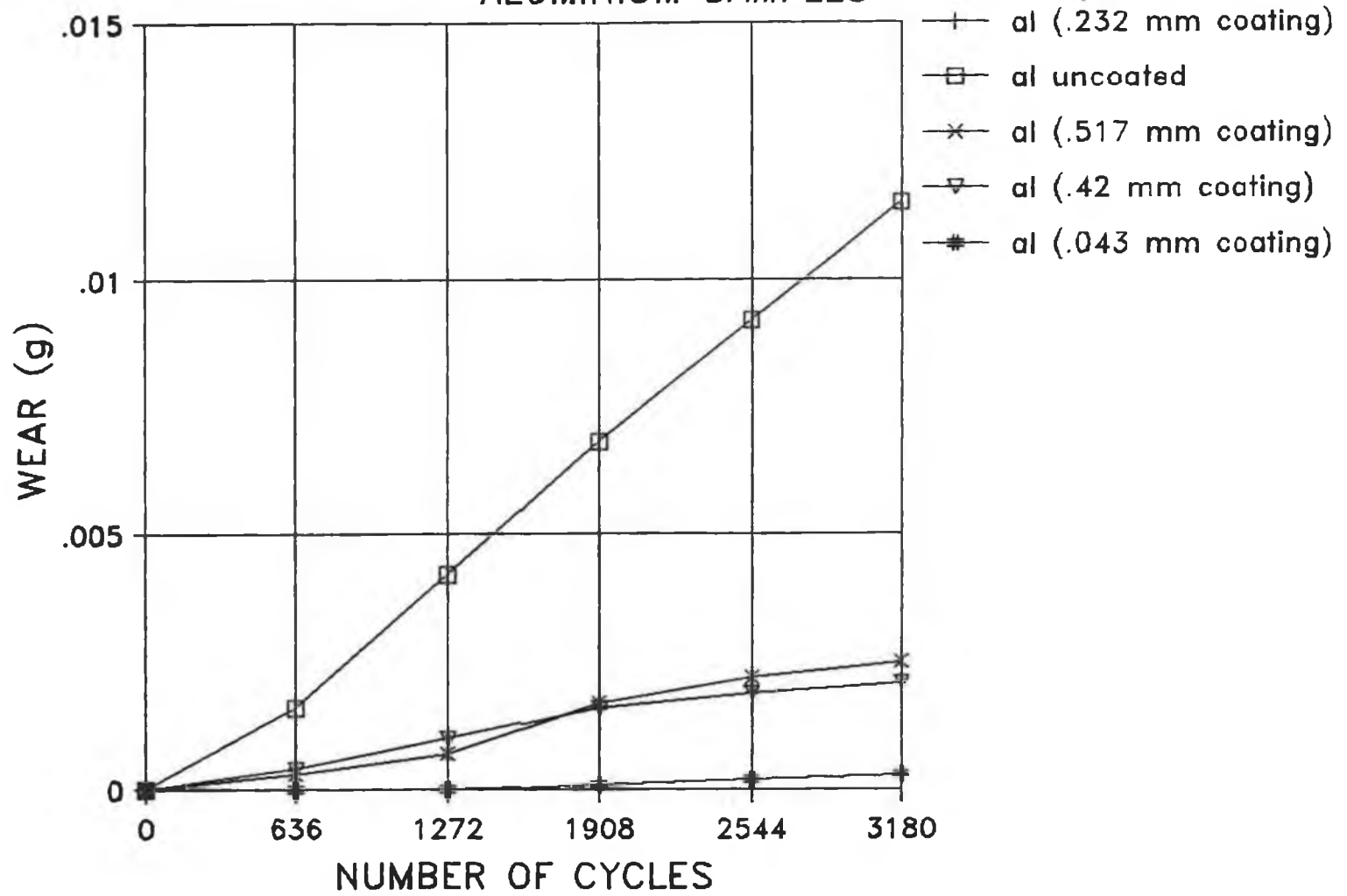
**Figure 6.6 Contact abrasion of aluminium samples
Wear (g) vs number of cycles.**

160

IMPACT ABRASION
ALUMINIUM SAMPLES

Legend:
- ⊟ al uncoated
- ✳ al (.517 mm coating)
- ▽ al (.42 mm coating)
- ✳ al (.043 mm coating)

WEAR (g)

.15

.1

.05

0

NUMBER OF CYCLES

0   636   1272   1908   2544   3180
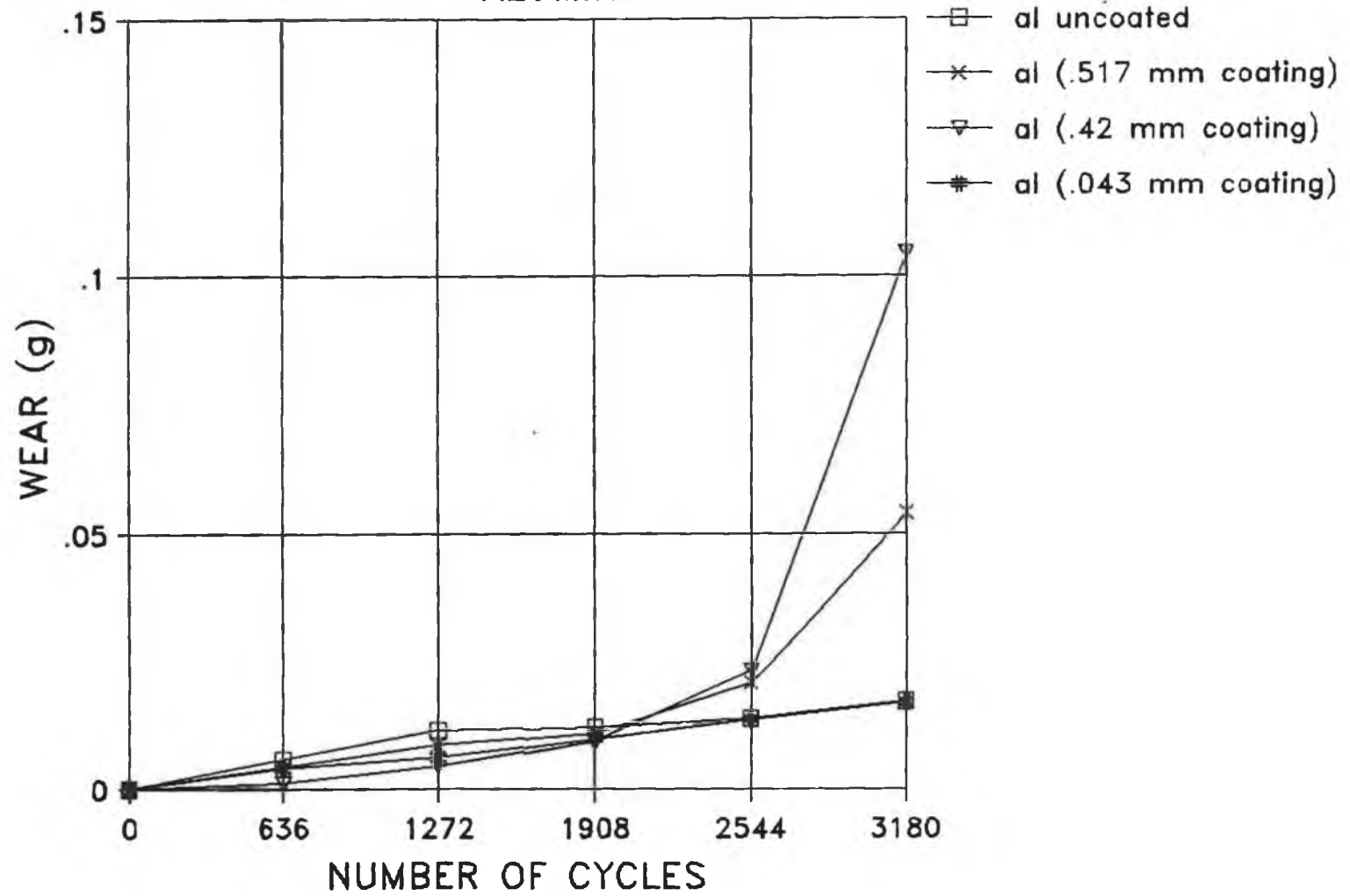
Figure 6.7 Impact abrasion for aluminium samples Wear (g) vs number of cycles.

161

MILD STEEL IMPACT ABRASION

Legend:
- m.s. (.46 mm coating)
- m.s. (.171 mm coating)
- m.s. uncoated
- m.s. (.048 mm coating)
- m.s. (.384 mm coating)

WEAR (g) vs NUMBER OF CYCLES
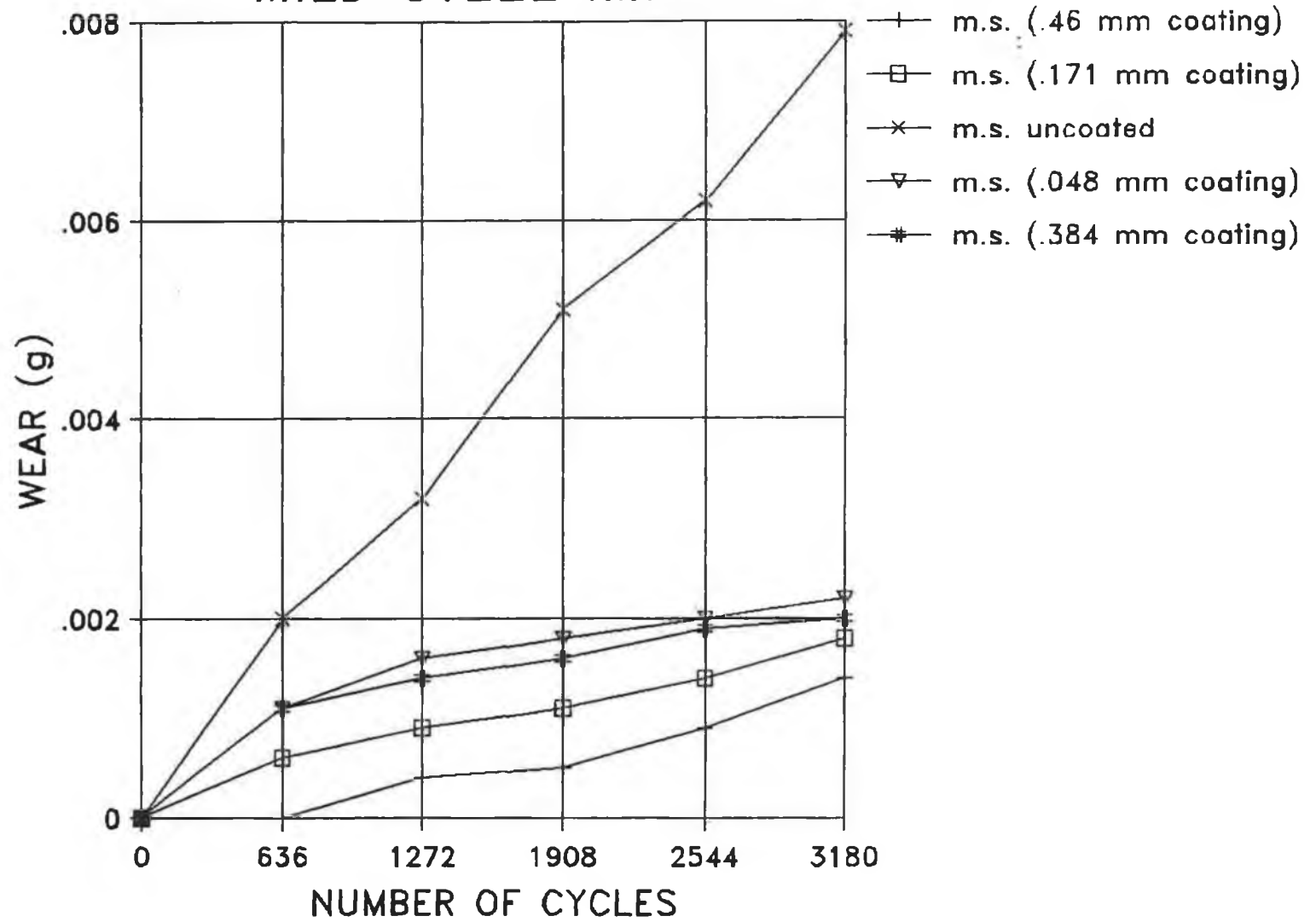
Figure 6.8 Impact abrasion for mild steel samples
Wear (g) vs number of cycles.

162
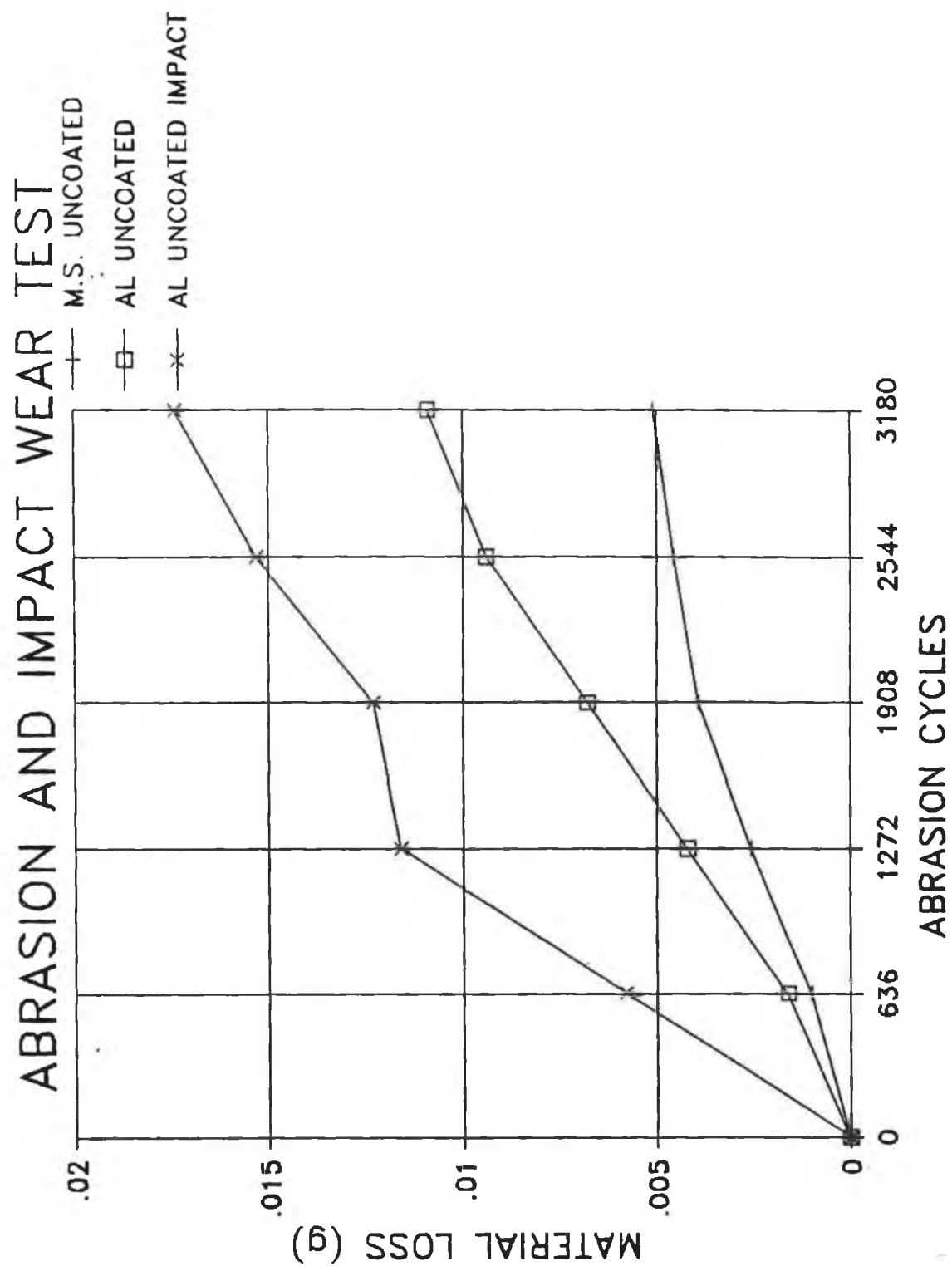
Figure 6.9 Abrasion of mild steel and aluminium uncoated samples compared to uncoatd aluminium under Impact abrasion.

163
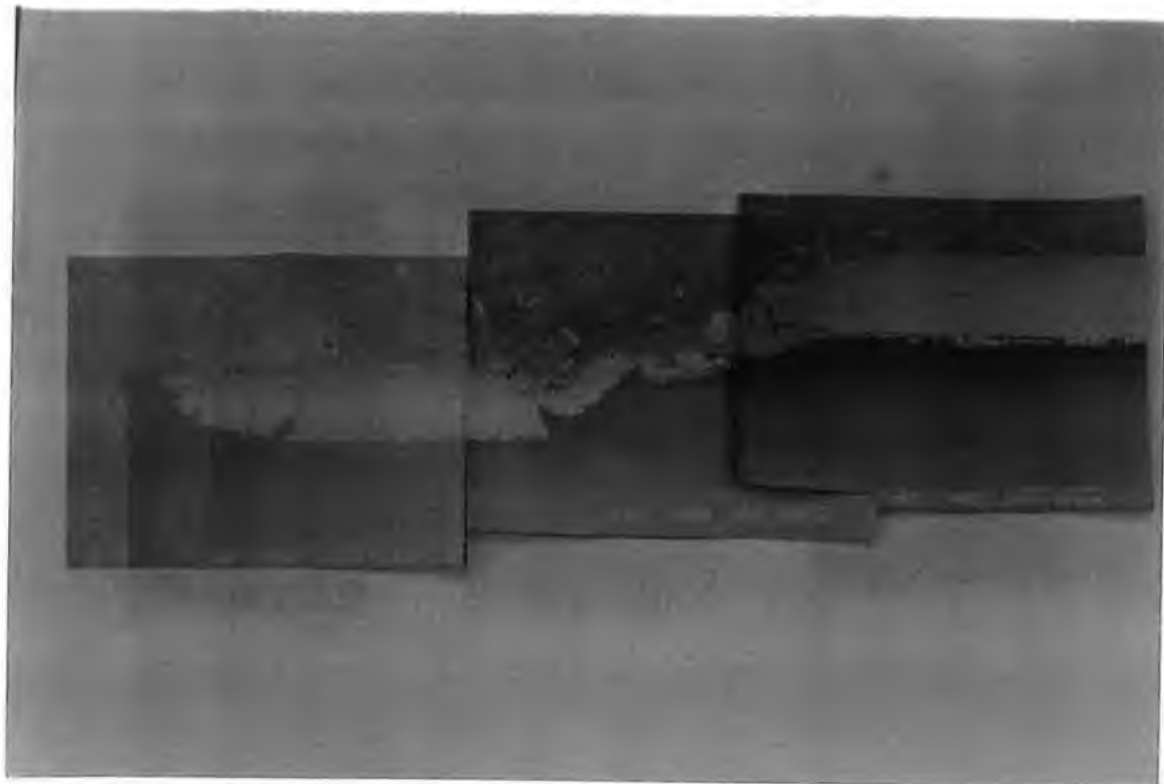
**Photograph 6.1 Cratering and coating failure of WC-Co on
aluminium substrate subjected to impact abrasion.**
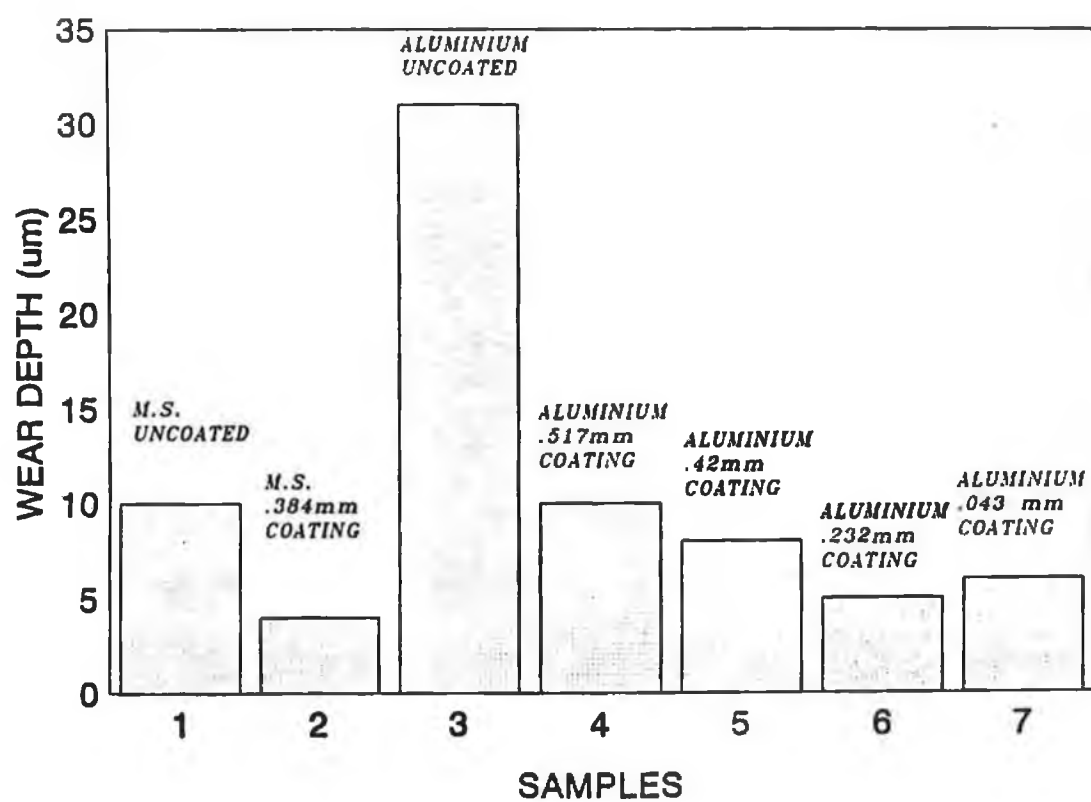
Figure 6.10 Wear track depth for aluminium and mild steel
samples subjected to abrasion wear tests.
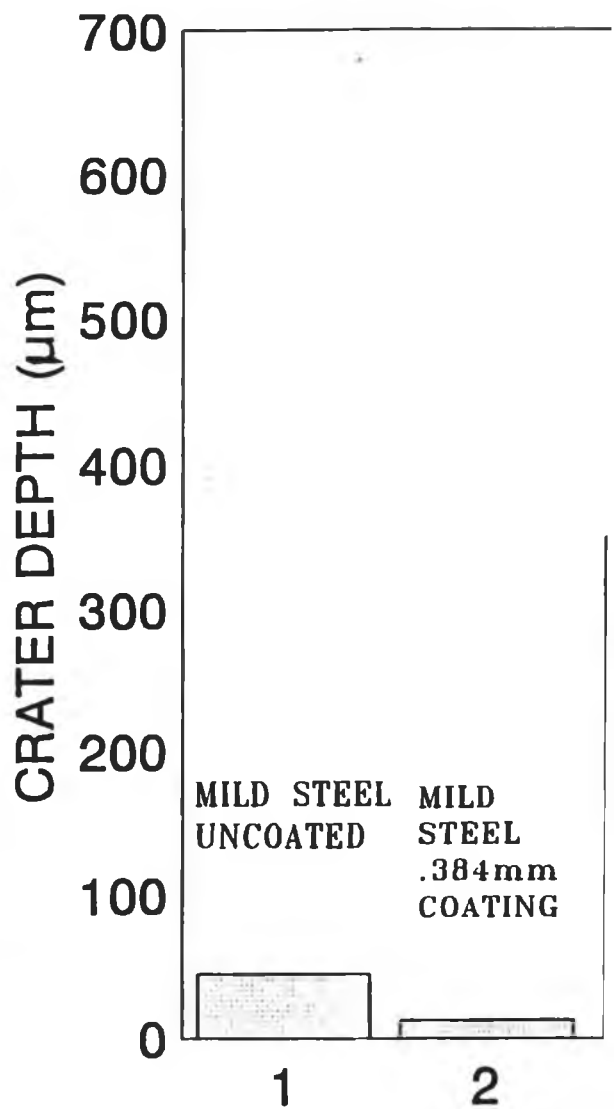
Figure 6.11 Crater depth for aluminium and mild steel samples subjected to impact abrasion.

166

ALUMINIUM   .42mm
             COATING

ALUMINIUM   ALUMINIUM   ALUMINIUM
                                                  .043mm
                                                  COATING

ALUMINIUM   ALUMINIUM   ALUMINIUM
UNCOATED   .517mm   .232mm
             COATING   COATING

3   4   5   6   7
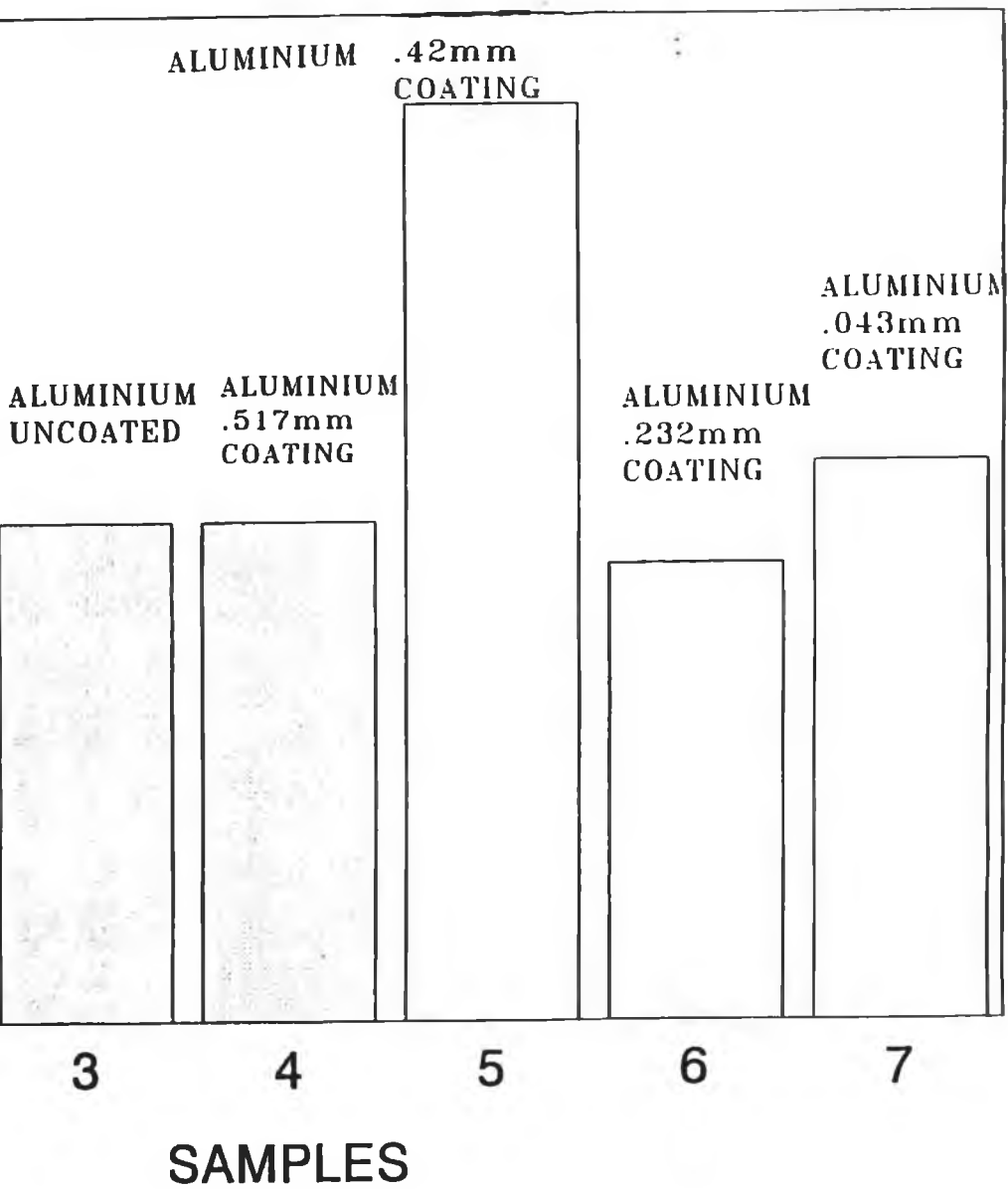
SAMPLES

6.6 WEAR VOLUME FOR WC-Co AND Ni-Cr COATED SAMPLES

Coatings of WC-Co and Ni-Cr were applied to substrates of aluminium and mild steel. These samples were subjected to contact abrasion, pure impact, and combined impact abrasion at different linear velocities as discussed in section 5.6.2. Samples, coatings, thickness of coatings and hardness values are given in Table 6.6. Using equations (5.1) to (5.4) and (5.6), wear volume, crater volume and wear volume for combined impact abrasion values were calculated from the wear scars and craters produced. Experimental work considered impact at the start and at the center of the wear scar to measure the effects of linear velocity of the stylus on the material loss and wear scar produced. At the start of the wear scar, the linear velocity is equal to zero and at the center of the wear scar, the linear velocity is a maximum.

The impact distance set by the cam driven impact mechanism was 1.5 mm for all samples and a normal load of 100 N applied. Figures 6.12 to 6.14 show the effects of abrasion and impact abrasion at different linear velocities on aluminium substrates coated with WC-Co and Ni-Cr. Figures 6.15 to 6.17 show similar effects on mild steel samples. Figures 6.18 and 6.19 show results for the crater volume produced by pure impact and Figure 6.20 compares the effects of wear on the combined impact abrasion at different linear velocities and the wear volume due to impact and abrasion as seperate wear tests on a WC-Co coated aluminium sample.

The influence of rebound following impact, combined with the linear velocity of the reciprocating stylus has a major effect on the wear rates of the samples tested.

167

It was observed during the testing that when the linear velocity of the reciprocating stylus was equal to zero, one crater was produced in the test samples. However when impact loading was applied at maximum linear velocity, two main craters were produced in the samples along the wear scar, the second of which was due to the rebound effect. The dynamic effects resulted in gouging on impact, producing craters whose length were greater than their width, unlike pure impact which generated symmetrical crater shapes on samples. It was found that the indentation crater left in the metal surface has a larger radius of curvature than that of the indenting sphere. This effect is referred to as shallowing and is due to the release of elastic stresses in the metal specimens. Applying impact loads on samples led to rapid failure of poorly adhered coatings. These same coatings performed satisfactorily under abrasion conditions. This highlights the importance of impact loading as a test for coated samples. The loads applied under the test conditions were relatively high and as a result led to rapid failure and breakage of the coatings and in some cases, damage to the substrates. The WC-Co alloy coatings proved very successful under the test conditions compared to Ni-Cr coatings applied to aluminium and mild steel samples, which failed more rapidly under similar circumstances. Under combined impact abrasion conditions, the detached particle sizes were large compared to pure abrasion.

From the results obtained it is shown that the characteristics of the substrate material has an influence on the wear resistance of the coatings examined under impact conditions. The coatings employed improved the wear resistance of the samples under the test conditions.

Sample.	Surface roughness. Ra values substrate (μm)	Coating thickness (mm)	Surface roughness. Ra values coating. (μm)	Hardness. substrate. (HB-60kgf)	coating. (μHv 300)
Al-1(WC-Co)	5.5	0.210	4.5	55	1089
Al-2(WC-Co)	5.5	0.076	4.5	54	945
Al-3(Ni-Cr)	5.5	0.088	4.5	56	860
Al-4(Ni-Cr)	5.5	0.131	6.5	34	900
Al-5(Ni-Cr)	5.5	0.2	6.4	33	846
Al-6(WC-Co)	5.5	0.245	4.5	56	1050
Al-7(WC-Co)	5.4	0.246	4.3	35	1023
Al-8(Ni-Cr)	5.5	0.242	6.5	50	850
Al-uncoated	5.5	-	-	54	-
				(HB-100kgf)	
MS-2(Ni-Cr)	6.0	0.131	4.5	99	850
MS-4(Ni-Cr)	6.2	0.190	4.5	106	890
MS-5(WC-Co)	6.0	0.151	4.5	107	1250
MS-7(WC-Co)	6.2	0.373	5.3	104	1010
MS-8(Ni-Cr)	6.2	0.250	5.3	107	870
MS-11(WC-Co)	6.2	0.265	4.5	107	1380
MS-uncoated	6.2	-	-	98	-

Table 6.6 Test samples for wear volume measurements
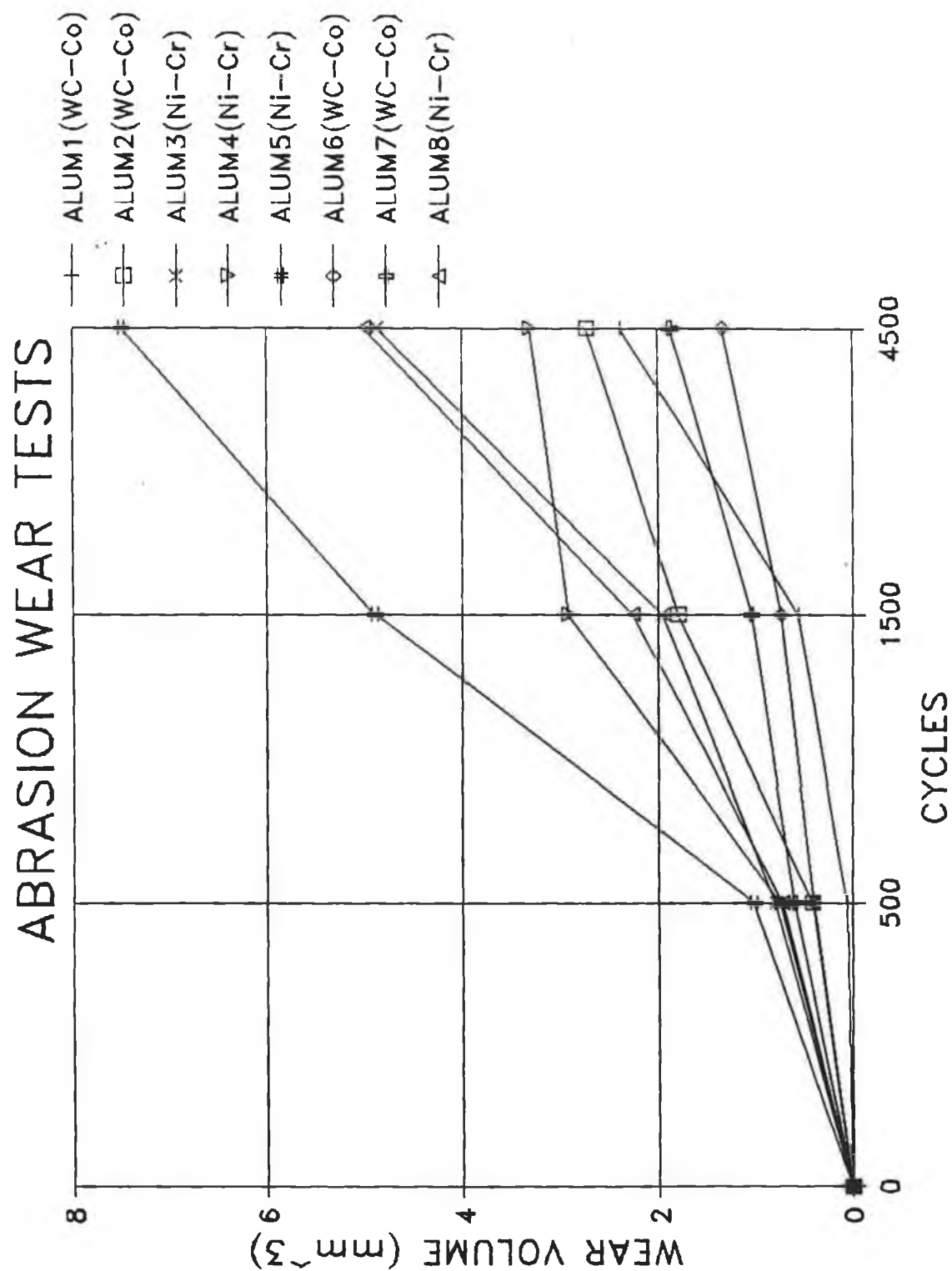
Figure 6.12 Abrasion wear tests for aluminium samples
Wear (mm³) vs number of cycles.

170
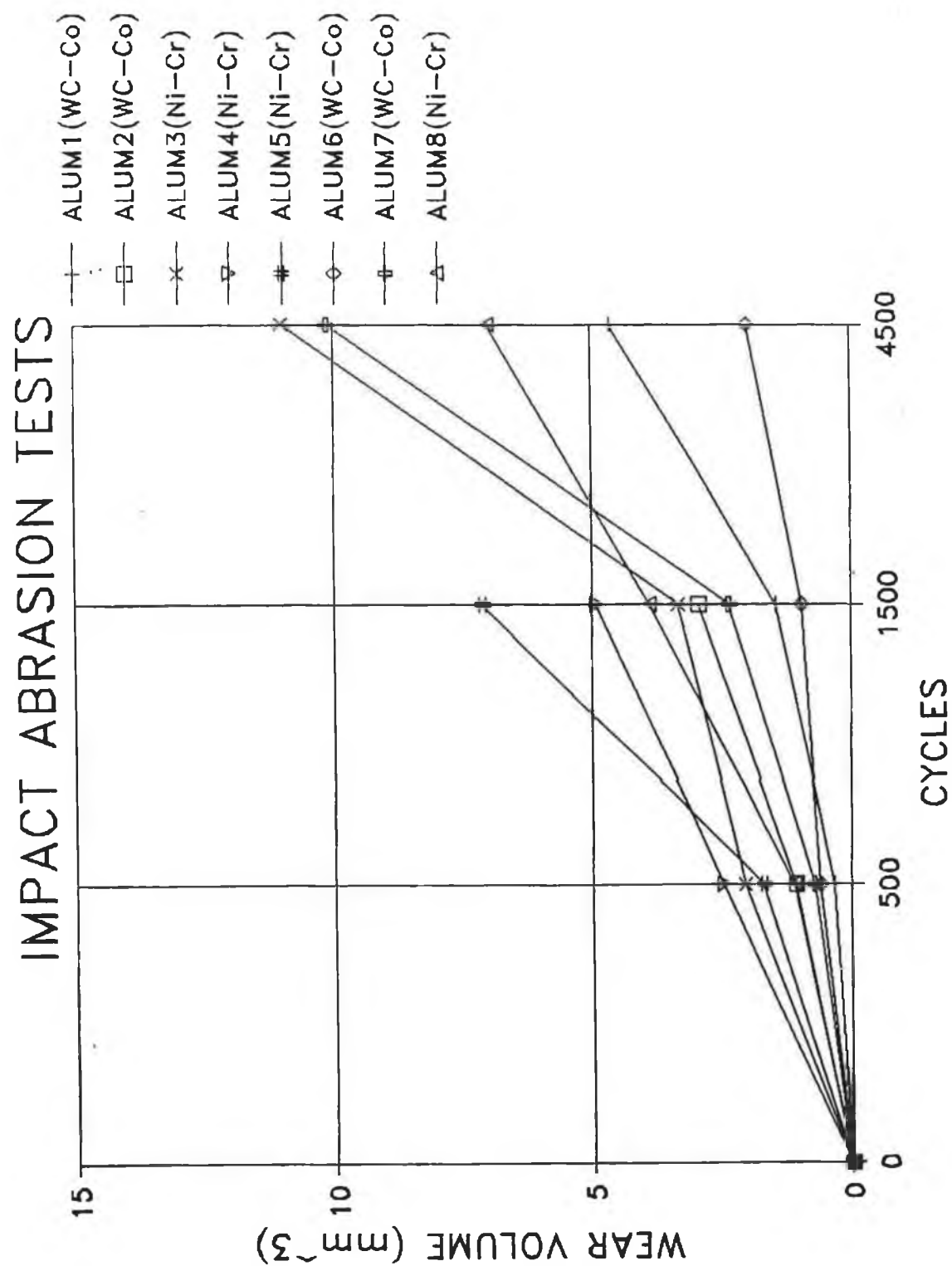
Figure 6.13 Impact abrasion tests of aluminium samples
Impact at start of wear scar
Wear (mm³) vs number of cycles.

171
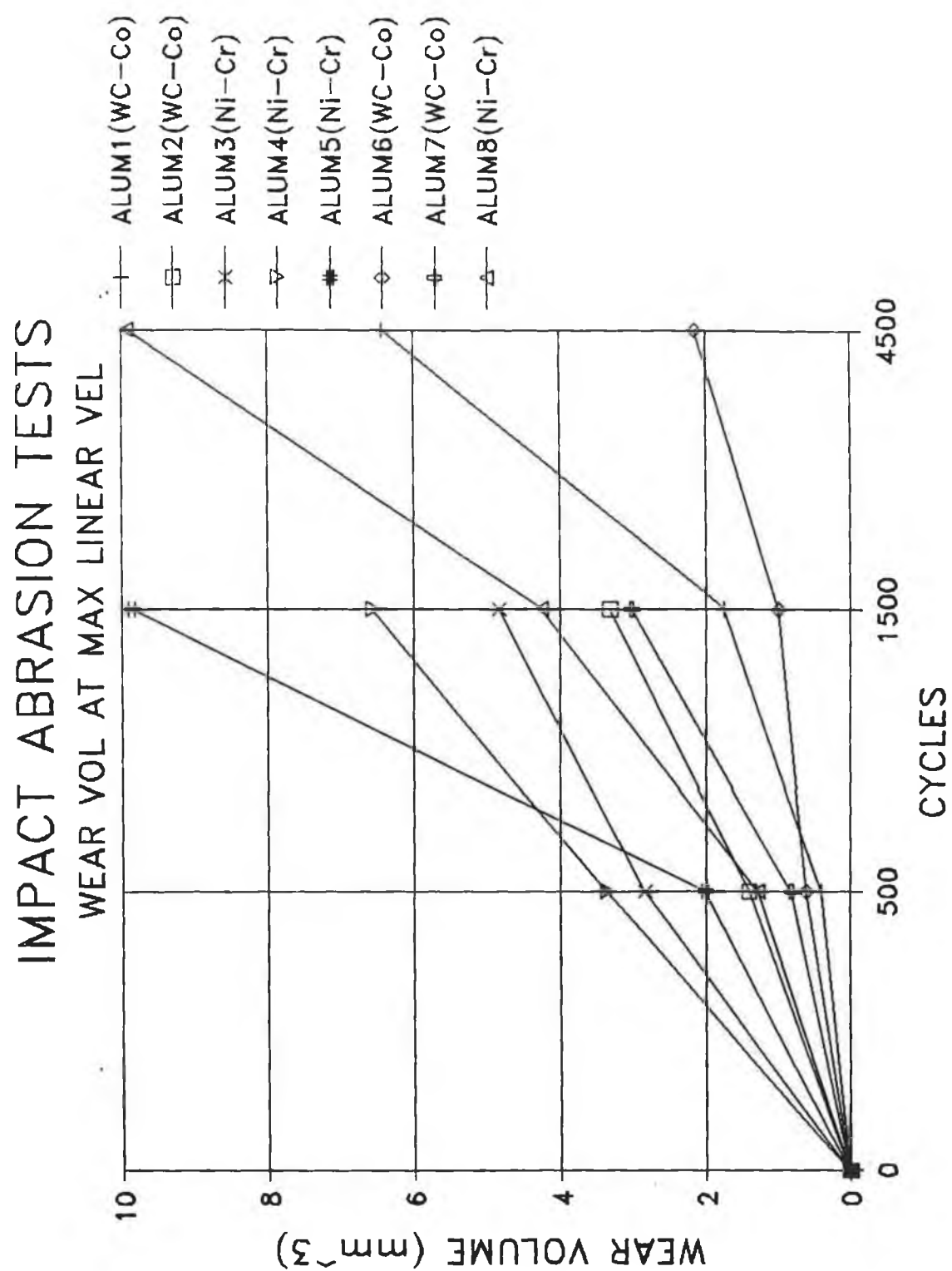
Figure 6.14 Impact abrasion tests of aluminium samples
Impact at center of wear scar
Wear (mm³) vs number of cycles.

172

ABRASION WEAR TESTS

Legend:
- M.S. 4(Ni–Cr)
- M.S. 8(Ni–Cr)
- M.S. 11(WC–Co)
- M.S. 5(WC–Co)
- M.S. 2(Ni–Cr)
- M.S. 7(WC–Co)
- MILD STEEL UNCOATED
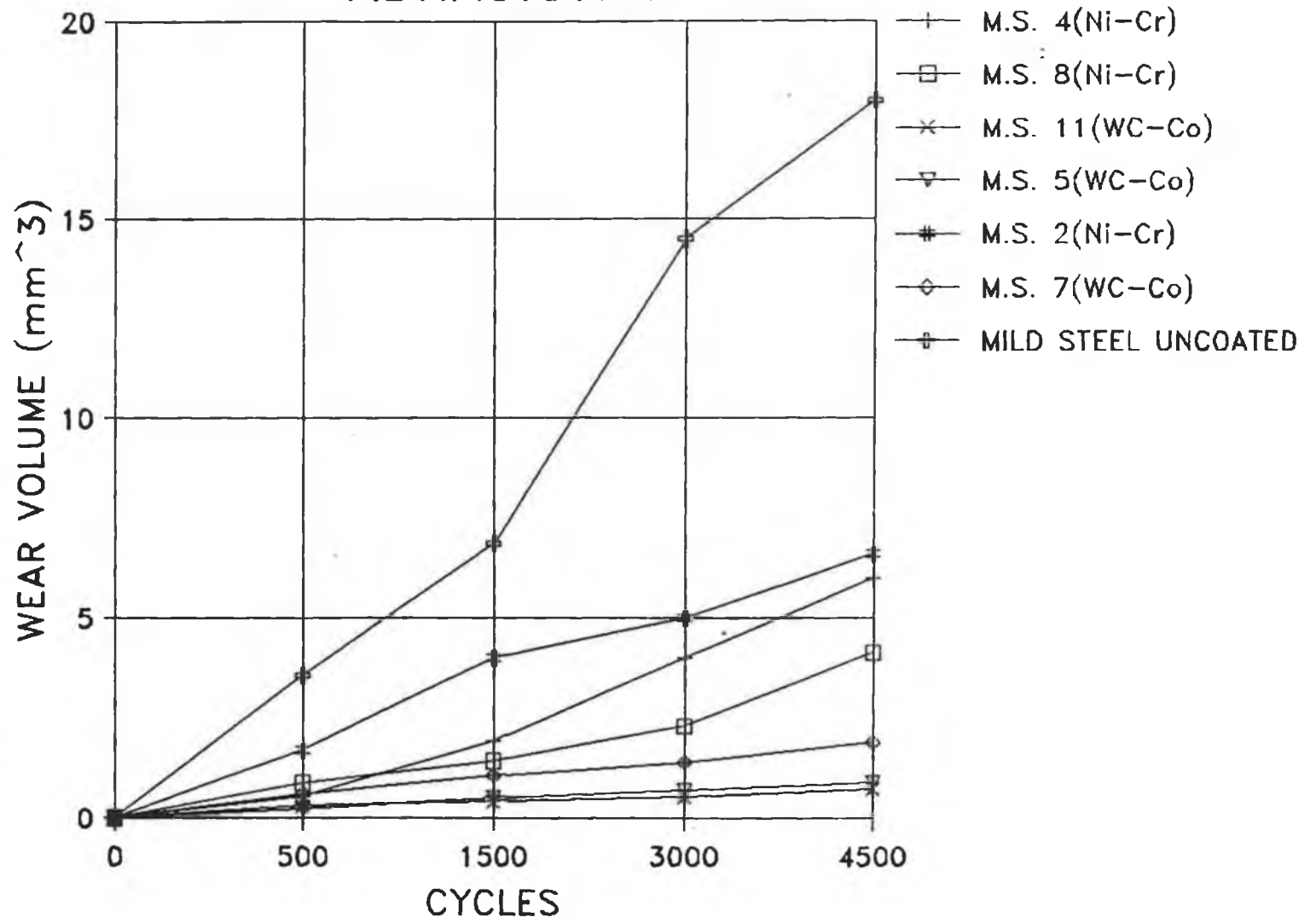
Figure 6.15 Abrasion wear tests of mild steel samples
Wear (mm^3) vs number of cycles.
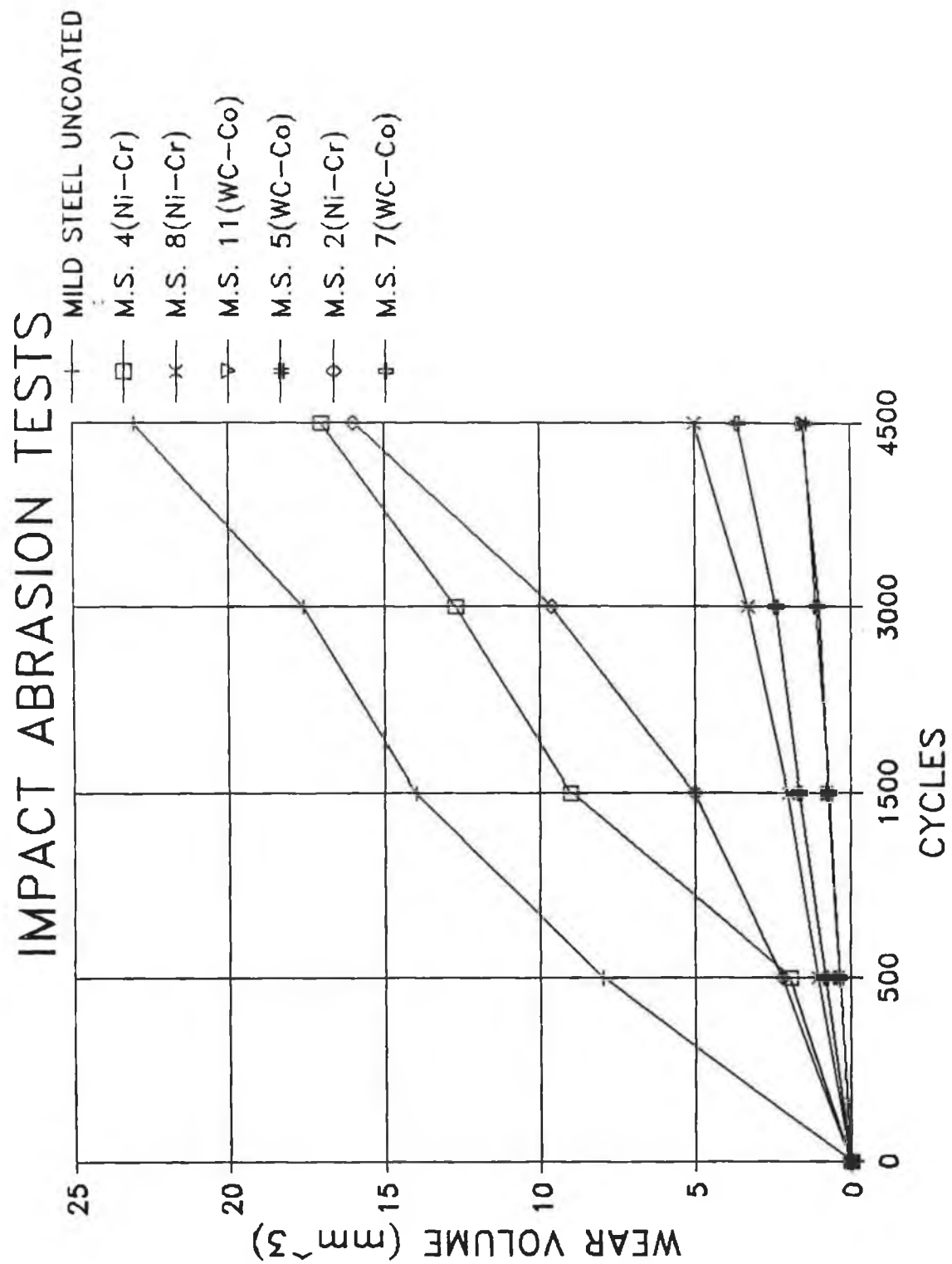
Figure 6.16 Impact abrasion tests of mild steel samples
Impact at start of wear scar
Wear (mm³) vs number of cycles.

174

IMPACT ABRASION TESTS
WEAR VOL AT MAX LINEAR VEL

Legend:
- + MILD STEEL UNCOATED
- M.S. 4(Ni-Cr)
- M.S. 8(Ni-Cr)
- M.S. 11(WC-Co)
- M.S. 5(WC-Co)
- M.S. 2(Ni-Cr)
- M.S. 7(WC-Co)

Y-axis: WEAR VOLUME (mm^3)

X-axis: CYCLES
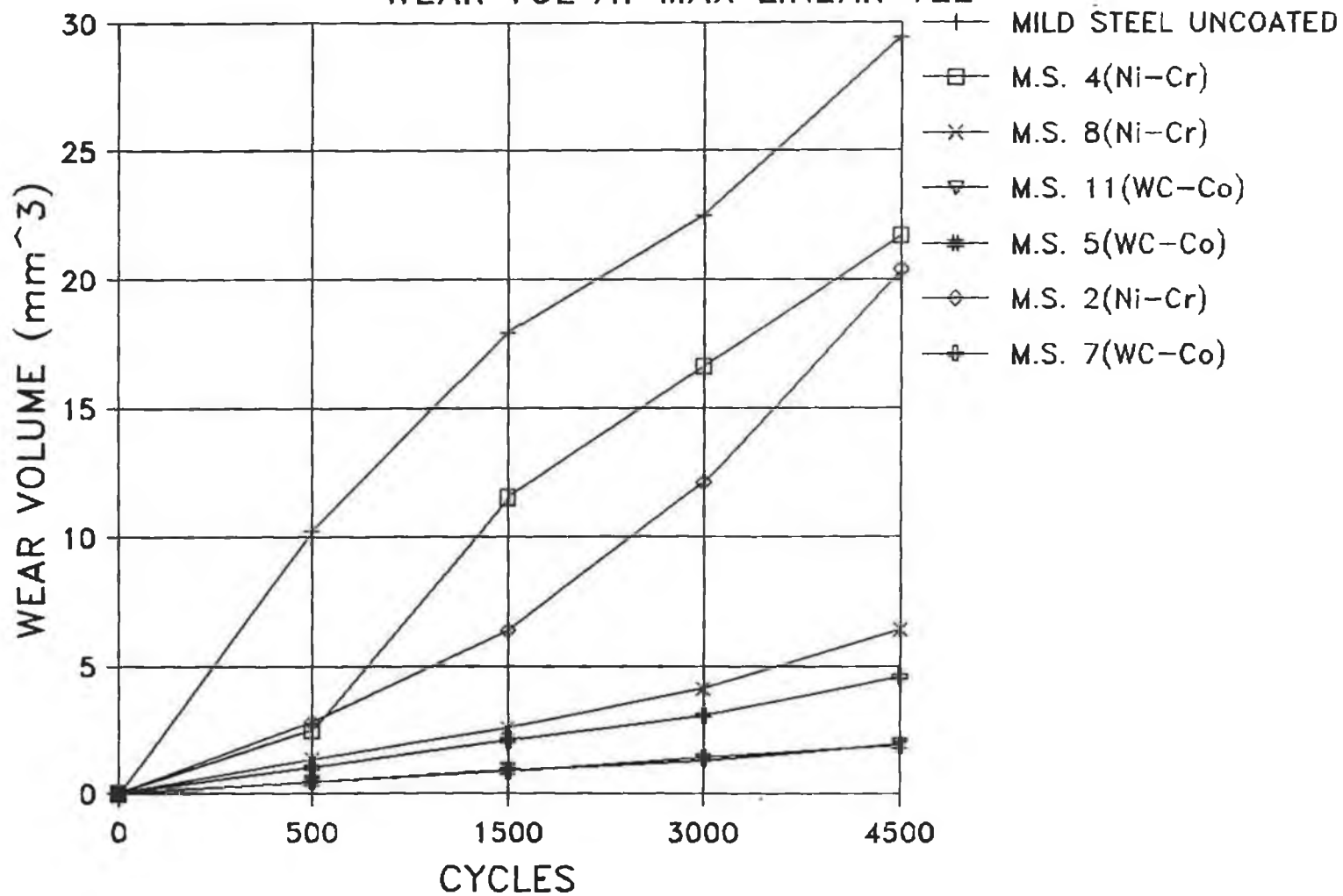
Figure 6.17 Impact abrasion tests of mild steel samples
Impact at center of wear scar
Wear (mm³) vs number of cycles.

175
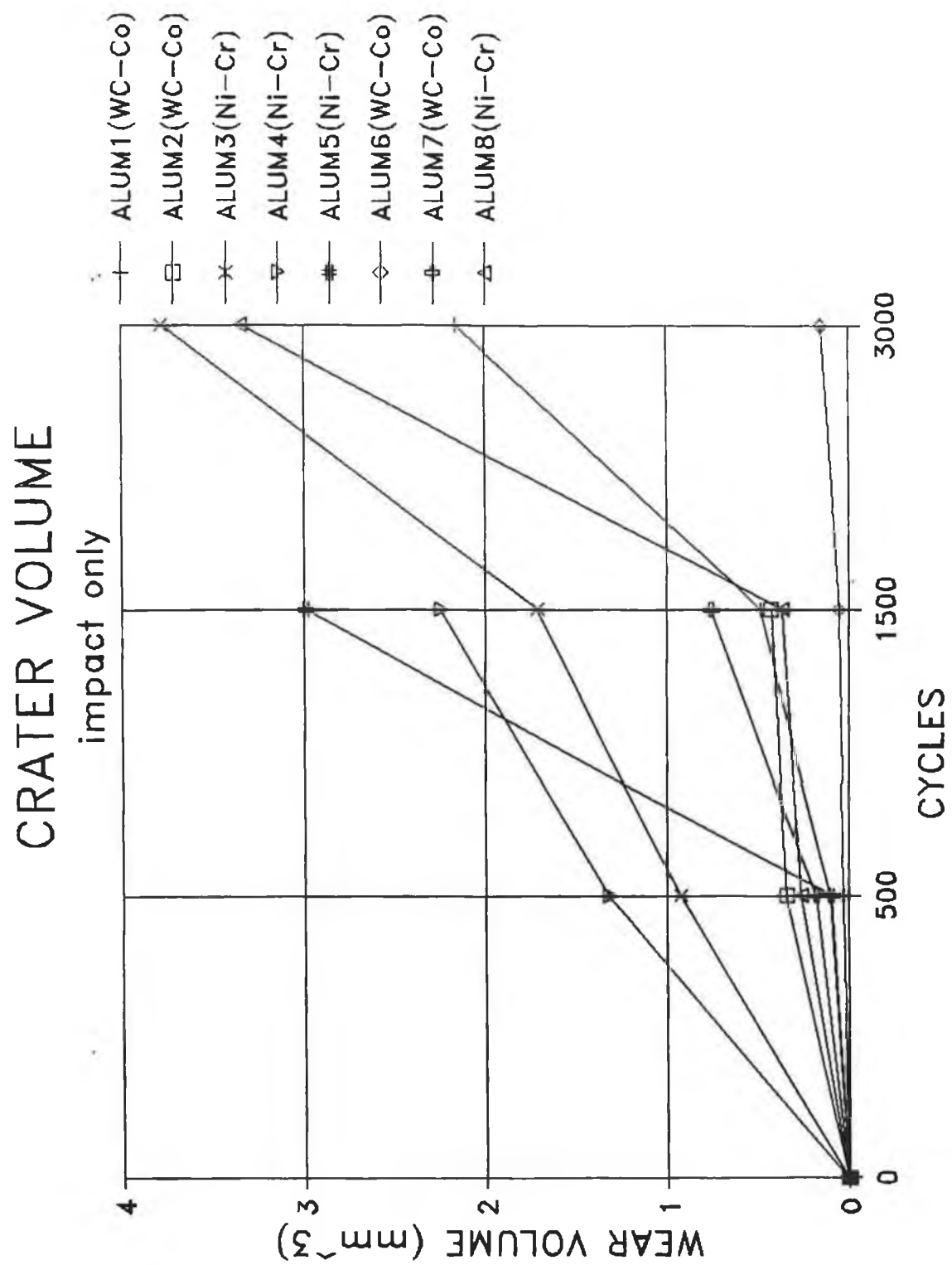
Figure 6.18 Crater volume for aluminium samples
Pure impact conditions
Wear (mm³) vs number of cycles.

176
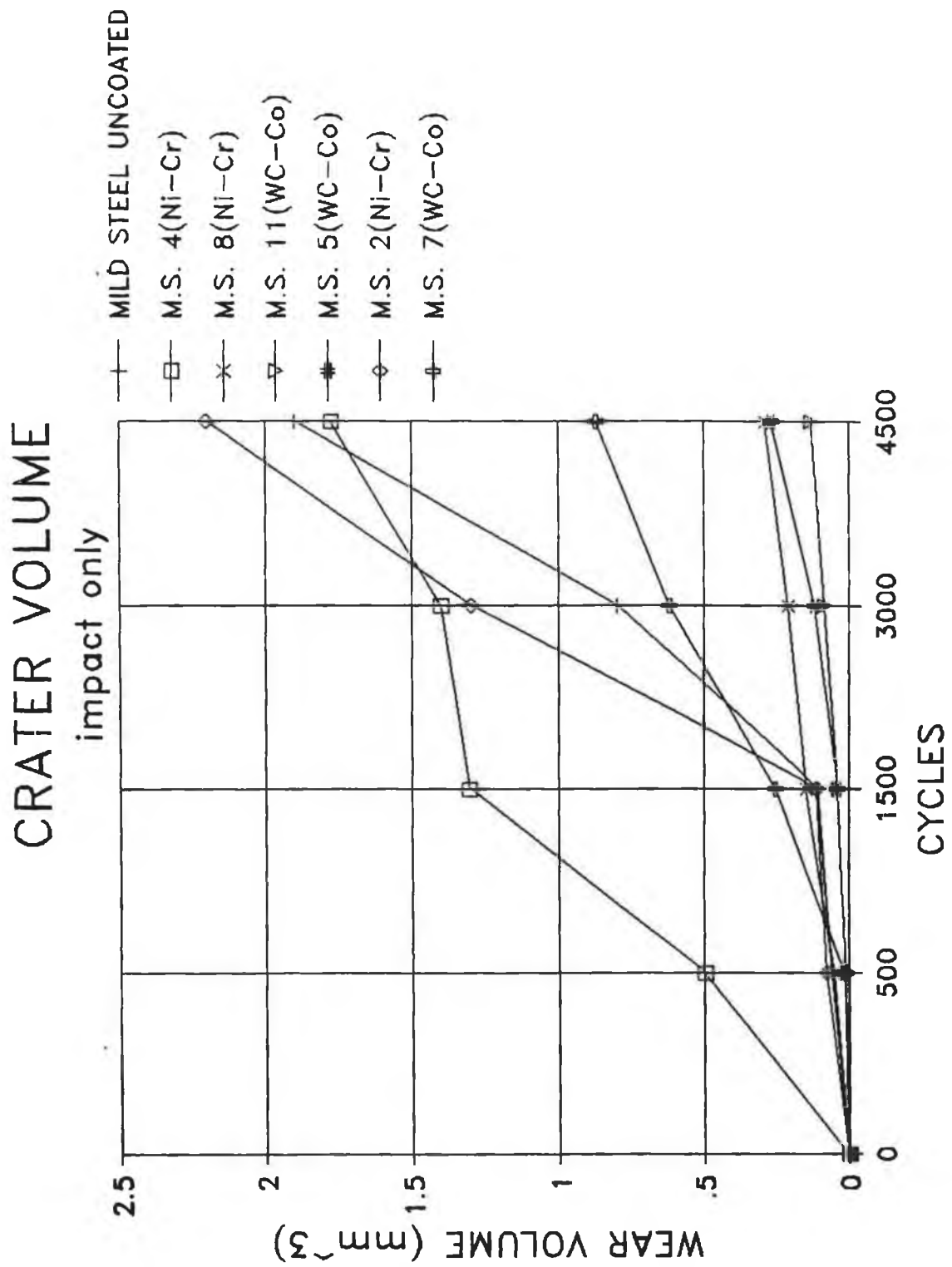
Figure 6.19 Crater volume for mild steel samples
            Pure impact conditions
            Wear (mm³) vs number of cycles.
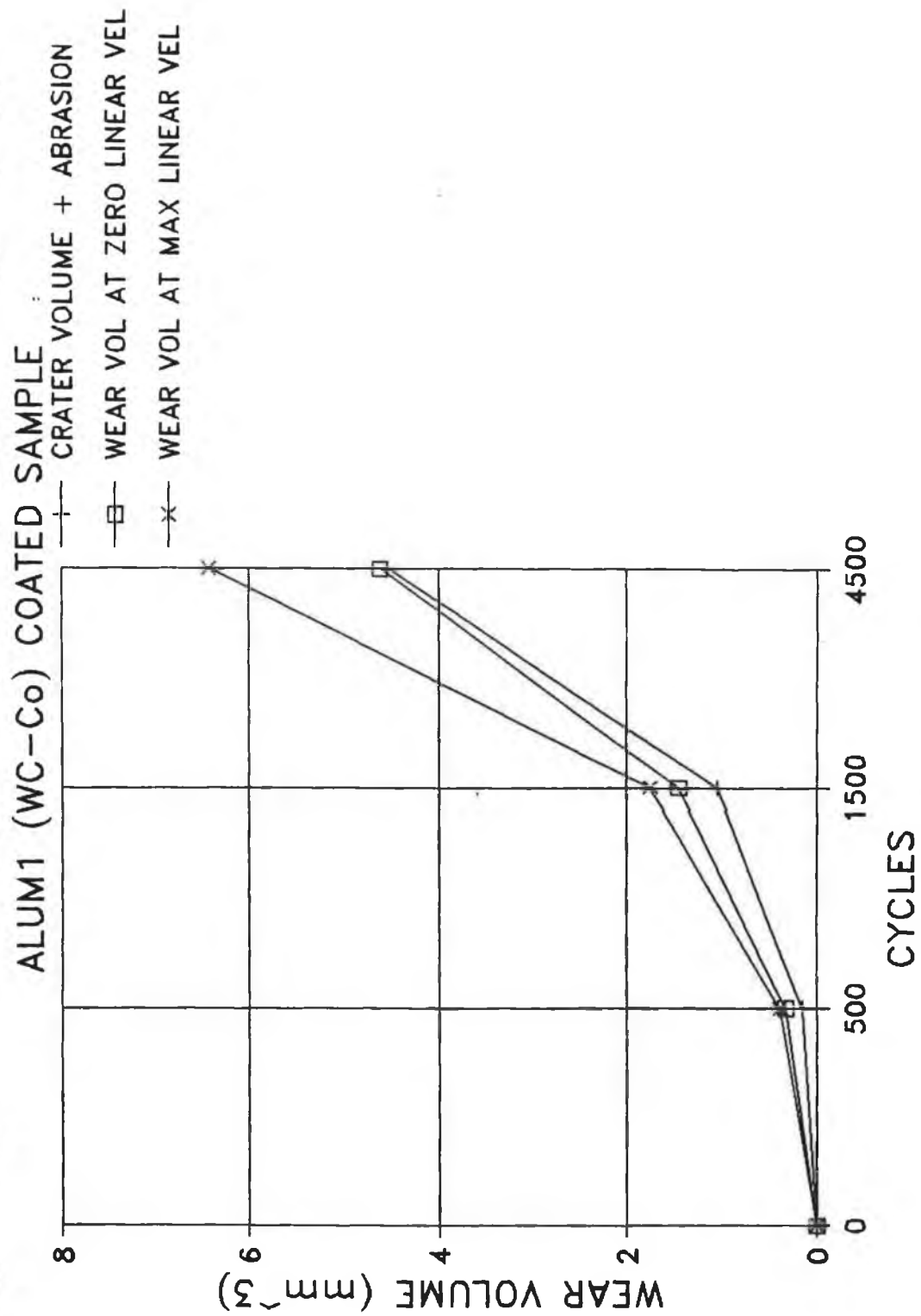
Figure 6.20 Comparison of aluminium coated sample for:
1) Crater and abrasion volume
2) Wear volume for impact at start of wear scar
3) Wear volume for impact at center of wear scar
Wear (mm³) vs number of cycles.

178

From the results of wear for the different forms of testing applied, it is shown that the impact abrasion with impact occuring at maximum linear velocity (impact in center of wear track) produces maximum wear. Due to the dynamic abrasion effect, some of the aluminium samples experienced severe gouging, especially when the coating was penetrated. Photograph 6.1 shows the effects of impact, on the soft substrate, where the coating was pushed down into the material, and cracked due to its brittle nature.

6.7 WEAR COEFFICIENTS

6.7.1 Standard wear coefficient

Under contact abrasion, the wear coefficient, k, for samples were calculated using equation (5.9), based on the applied normal load (N), the sliding distance (m), and the wear volume (mm^3). Average wear coefficients for samples are given in Table 6.7. These values were determined by measuring the width and depth of the wear scars at the center of the wear tracks. Using equations (5.1), and (5.9), the wear coefficients were found.

These coefficients correspond with the wear volume loss for different substrate/coating combinations tested. TiC coated and uncoated Vanadis 4 samples offered the highest wear resistance and lowest wear coefficient.

Materials showing least wear resistance and high wear coefficients are uncoated mild steel and aluminium. The wear coefficients represent the combined coated system.

179

Aluminium samples	Wear coefficients
Uncoated aluminium	2.63×10^{-2}
Al-1 (WC-Co)	0.84×10^{-4}
Al-2 (WC-Co)	2.19×10^{-4}
Al-3 (Ni-Cr)	3.33×10^{-4}
Al-4 (Ni-Cr)	3.47×10^{-4}
Al-5 (Ni-Cr)	5.83×10^{-4}
Al-6 (WC-Co)	1.23×10^{-4}
Al-7 (WC-Co)	1.58×10^{-4}
Al-8 (Ni-Cr)	3.70×10^{-4}
Mild steel samples	
Uncoated mild steel	2.28×10^{-3}
M.S.-2 (Ni-Cr)	5.15×10^{-4}
M.S.-4 (Ni-Cr)	3.06×10^{-4}
M.S.-5 (WC-Co)	0.93×10^{-4}
M.S.-7 (WC-Co)	1.97×10^{-4}
M.S.-8 (Ni-Cr)	3.0×10^{-4}
M.S.-11 (WC-Co)	0.87×10^{-4}
Tool steel samples	
AISI D2 Uncoated	9.86×10^{-5}
AISI D2 (TiN)	3.42×10^{-5}
AISI D2 (TiC)	1.23×10^{-5}
AISI D3 Uncoated	1.66×10^{-4}
AISI D3 (TiN)	3.09×10^{-5}
AISI D3 (TiC)	2.16×10^{-5}
Vanadis 4 Uncoated	1.95×10^{-5}
Vanadis 4 (TiN)	1.31×10^{-5}
Vanadis 4 (TiC)	6.57×10^{-6}
Vanadis 10 Uncoated	8.5×10^{-6}
Vanadis 10 (TiN)	3.69×10^{-5}
Vanadis 10 (TiC)	8.6×10^{-6}

Table 6.7 Standard wear coefficients for contact abrasion

6.7.2 Modified wear coefficients

Due to the velocity of the reciprocating stylus continually changing over the abraded surface, the modified wear coefficient, k_1, given in equations (5.18) and (5.19), were considered. For example, Figure 6.21 shows the wear scar depth profile produced by an abrasion test on aluminium, and shows that the depth is not constant along the wear scar length.

The modified wear coefficient values are given in Table 6.8. The volume of the wear scars are average values, based on a number of cross sectional areas taken across the wear scar.

Due to the operating conditions of the test rig, and the limited number of researchers applying the wear coefficient, k, to wear testing, there is very limited information available on the wear coefficients of the materials tested.

Most testing still applies crater wear, weight loss, depth of wear scar, flank wear and erosion wear as the means of measuring wear resistance. Based on the materials in contact during rubbing wear, and the operating loads and conditions of the test rig, the order of the wear coefficients achieved are typical and comparable to the type of tests mentioned above.

Aluminium samples	Modified Wear coefficients (k_1)
Uncoated aluminium	3.70×10^{-2}
Al-1 (WC-Co)	2.4×10^{-4}
Al-2 (WC-Co)	0.65×10^{-3}
Al-3 (Ni-Cr)	0.9×10^{-3}
Al-4 (Ni-Cr)	0.99×10^{-3}
Al-5 (Ni-Cr)	1.66×10^{-3}
Al-6 (WC-Co)	3.82×10^{-4}
Al-7 (WC-Co)	0.55×10^{-3}
Al-8 (Ni-Cr)	0.97×10^{-3}
Mild steel samples	
Uncoated mild steel	3.2×10^{-3}
M.S.-2 (Ni-Cr)	1.88×10^{-3}
M.S.-4 (Ni-Cr)	0.89×10^{-3}
M.S.-5 (WC-Co)	1.88×10^{-4}
M.S.-7 (WC-Co)	3.8×10^{-4}
M.S.-8 (Ni-Cr)	0.65×10^{-3}
M.S.-11 (WC-Co)	1.96×10^{-4}
Tool steel samples	
AISI D2 Uncoated	1.17×10^{-4}
AISI D2 (TiN)	0.53×10^{-4}
AISI D2 (TiC)	1.91×10^{-5}
AISI D3 Uncoated	2.62×10^{-4}
AISI D3 (TiN)	4.72×10^{-5}
AISI D3 (TiC)	3.16×10^{-5}
Vanadis 4 Uncoated	3.01×10^{-5}
Vanadis 4 (TiN)	2.92×10^{-5}
Vanadis 4 (TiC)	1.01×10^{-5}
Vanadis 10 Uncoated	1.15×10^{-5}
Vanadis 10 (TiN)	0.58×10^{-4}
Vanadis 10 (TiC)	1.33×10^{-5}

Table 6.8 Modified wear coefficients for contact abrasion
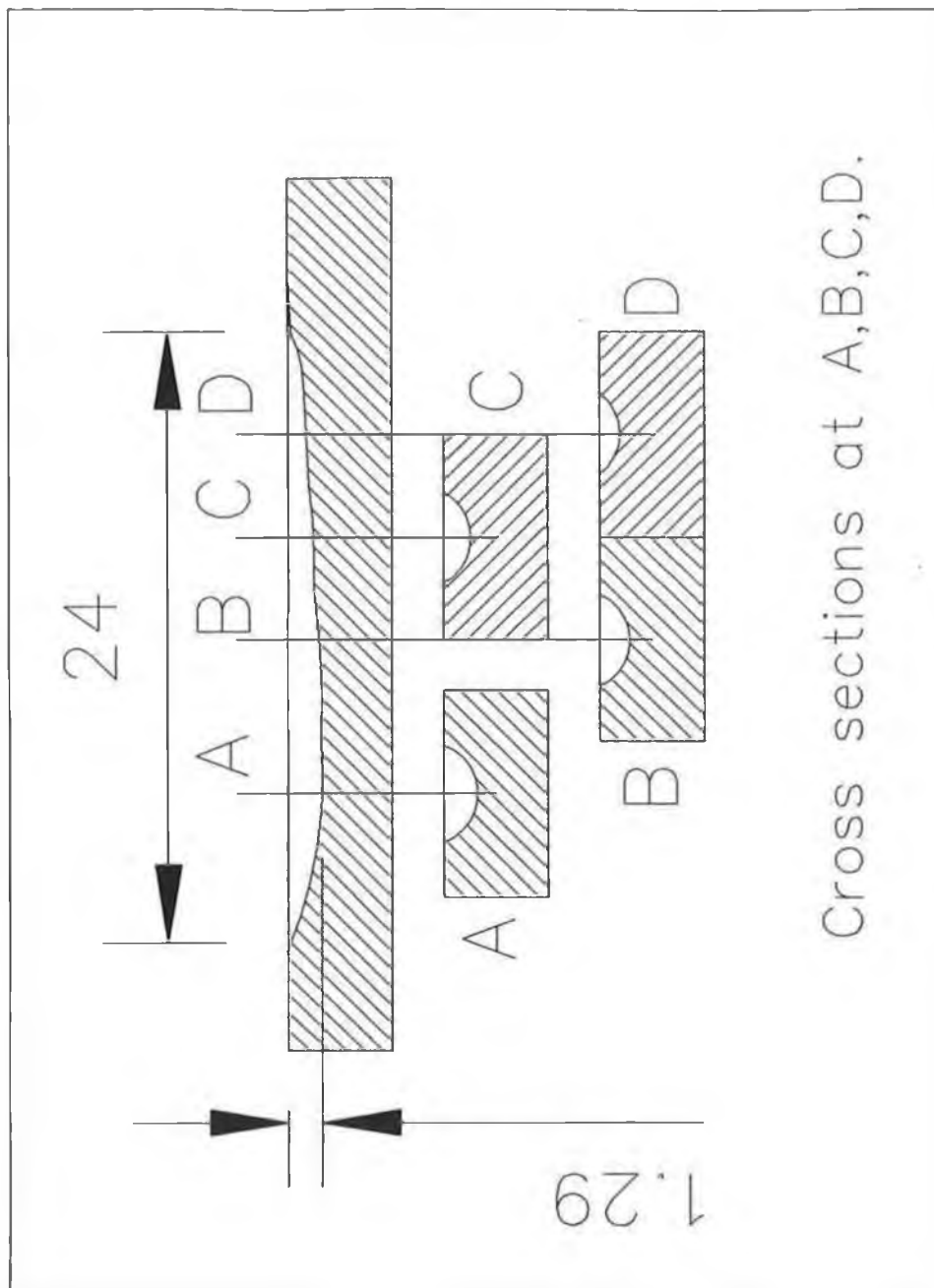
Figure 6.21 Wear scar depth profile for uncoated aluminium sample produced by abrasion test.

6.7.3 Wear volume for modified wear coefficients

Using the integral of equation (5.15), and the modified wear coefficients from Table 6.8, graphs of wear volume were produced. Figure 6.22 and 6.23 show the wear volumes against linear velocity for one cycle of abrasion. Figure 6.22 shows a sample of a WC-Co coated mild steel (MS-11) and Figure 6.23, shows a WC-Co coated aluminium specimen (Al-6). The volume loss for each specimen at 4500 cycles is also given in the figures which show close approximation to the wear values measured.

6.7.4 Surface roughness profiles

Figures 6.24 to 6.27 show surface roughness profiles following abrasion tests on coated samples of mild steel and tool steel.

The WC-Co and Ni-Cr coated mild steel samples were both subjected to 4500 abrasion cycles with a load of 10 kg.

The TiN and TiC coated tool steel samples were subjected to 5700 and 15000 cycles of abrasion under a load of 10 kg respectively.

The TiC coated sample shows a large improvement in wear resistance over the TiN sample. Similarly, the WC-Co sample shows improvement over the Ni-Cr coated mild steel sample. The appearance of the surface profiles shows the enhanced surface finish of the thin coatings over the thick coatings applied. The physical shape of the wear scar profile is semi-circular.

184

```
Degrees    rads        volume (mm^3)
---------------------------------------------
0          0           0
20         .3490659    .0000111
40         .6981317    .0000207
60         1.047198    .0000278
80         1.396263    .0000327
100        1.745329    .0000366
120        2.094395    .0000412
140        2.443461    .0000479
160        2.792527    .0000573
180        3.141593    .0000684
200        3.490659    .0000794
220        3.839724    .0000888
240        4.188790    .0000955
260        4.537856    .0001001
280        4.886922    .0001040
300        5.235988    .0001089
320        5.585054    .0001160
340        5.934119    .0001256
360        6.283185    .0001367

Volume for 4500 cycles =    .6152
```
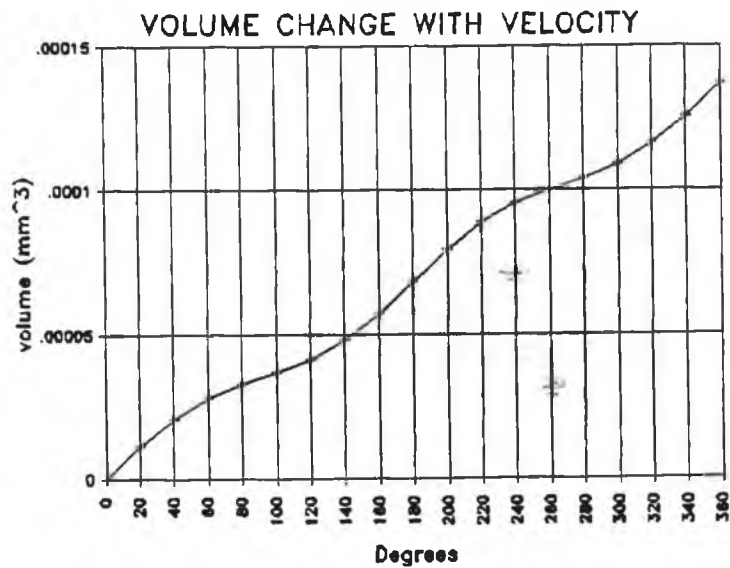

Figure 6.22 Wear volume for one cycle of abrasion on a
WC-Co coated mild steel sample
Volume change vs velocity.

```
Degrees   rads        volume (mm^3)
--------------------------------------------
0         0           0
20        .3490659    .0000217
40        .6981317    .0000403
60        1.047198    .0000542
80        1.396263    .0000637
100       1.745329    .0000713
120       2.094395    .0000802
140       2.443461    .0000934
160       2.792527    .0001116
180       3.141593    .0001332
200       3.490659    .0001548
220       3.839724    .0001730
240       4.188790    .0001862
260       4.537856    .0001951
280       4.886922    .0002027
300       5.235988    .0002122
320       5.585054    .0002261
340       5.934119    .0002448
360       6.283185    .0002664

Volume for 4500 cycles =    1.2
```
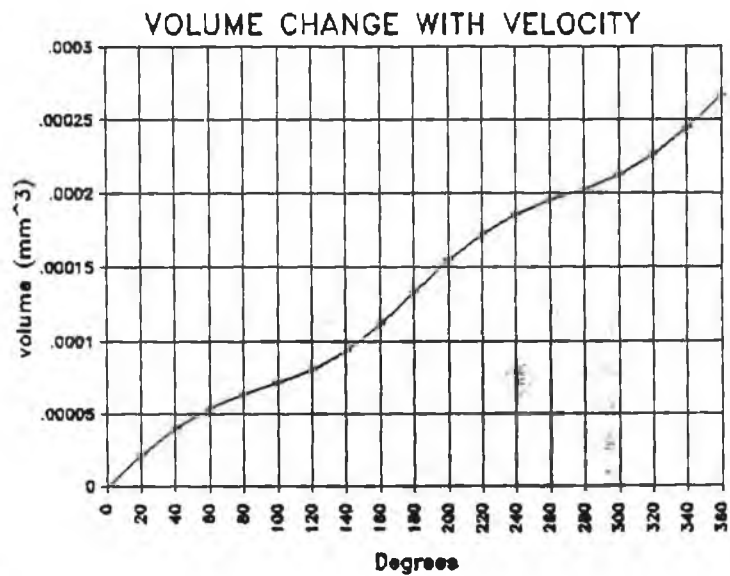

Figure 6.23 Wear volume for one cycle of abrasion on a
WC-Co coated aluminium sample
Volume change vs velocity.

186

Figure 6.24 Surface profile of WC-Co coated mild steel
$R_{max} = 17.6\ \mu m$, depth $= 25\ \mu m$.
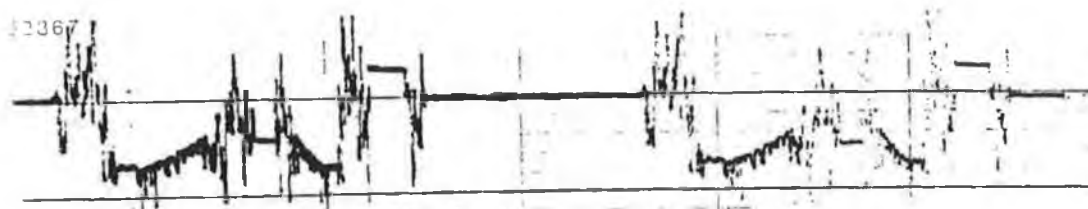
Figure 6.25 Surface profile of Ni-Cr coated mild steel
$R_{max} = 22\ \mu m$, depth $= 31\ \mu m$.
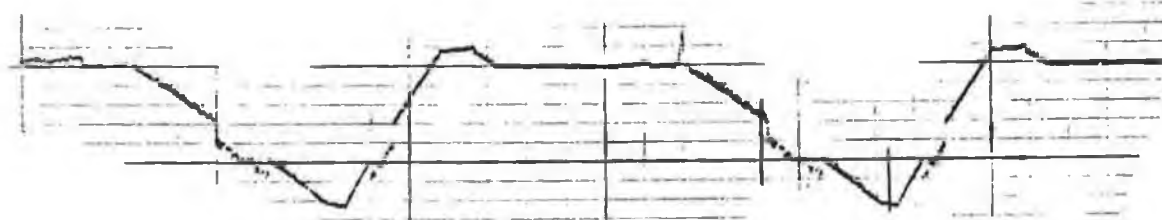
Figure 6.26 Surface profile of TiN coated tool steel
$R_{max} = 6\ \mu m$, depth $= 15\ \mu m$.

Figure 6.27 Surface profile of TiC coated tool steel
$R_{max} = 3.6\ \mu m$, depth $= 15\ \mu m$.

187

6.8 SURFACE ANALYSIS OF COATINGS

6.8.1 Abrasion surface

Photographs 6.2 and 6.3 show a plan and cross section respectively of a WC-Co coated tool steel (AISI D3) sample. The abrasion and scuffing of the coating are shown along with the wear depth caused by the abrasive tool after 3000 cycles under a 10 kg load. The thermal sprayed coating showed good adhesion to the substrate. Photograph 6.4 shows tool steel samples coated with TiC and TiN before testing and their appearance following abrasive wear tests is shown in Photograph 6.5. The TiN coated sample was subjected to 5700 cycles under a load of 10 kg, while the TiC coated specimen received 12000 cycles. The TiC coated sample showed superior wear resistance over the TiN coated specimen. Both coatings were of similar thickness (2-4μm) and applied to the same material (AISI D3).

Photograph 6.6 shows the abrasion wear of uncoated aluminium and mild steel samples. The aluminium sample was subjected to 500 cycles while the mild steel sample received 4500 cycles. Considerable wear occured on the aluminium sample compared to coated aluminium samples under abrasion conditions. Photograph 6.7 shows the effects of abrasion wear on mild steel samples coated with Ni-Cr and WC-Co thermal sprayed coatings respectively. Both samples received 4500 cycles at 10 kg. The enhanced wear resistance of the WC-Co sample is clearly shown by the photograph.

30 mm

**Photograph 6.4   TiN and TiC coated tool steel samples
before abrasion tests.**

30 mm
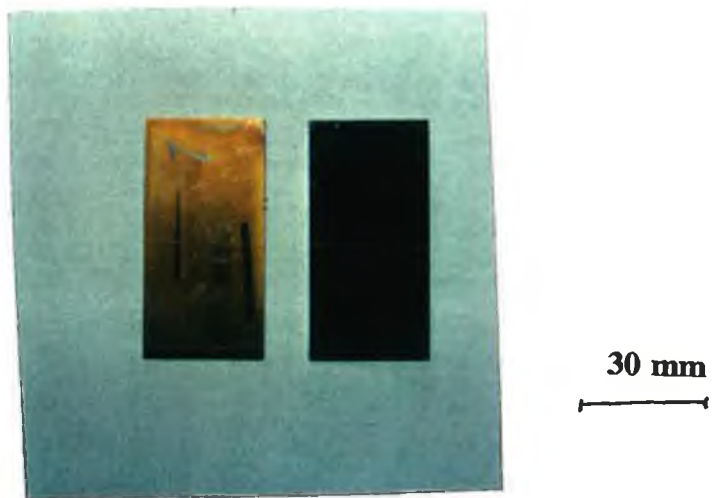
**Photograph 6.5   Abrasion wear scars on TiN and TiC samples
TiN sample = 5700 cycles at 10 kg
TiC sample = 12000 cycles at 10 kg.**

190

30 mm
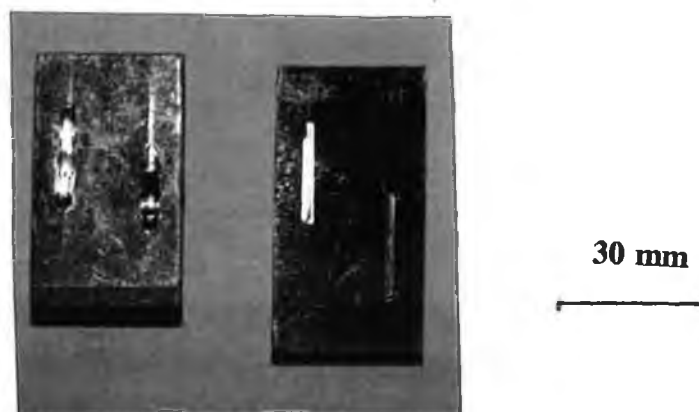
Photograph 6.6 Wear scars on uncoated aluminium and mild steel samples.

30 mm

Photograph 6.7 Abrasion scars on Ni-Cr and WC-Co coated mild steel samples.

191

6.9 SEM ANALYSIS

Photograph 6.8 and 6.9 show a WC-Co coated aluminium sample before and after abrasion tests under a Scanning Electron Microscope. The coating is in the order of 0.5 mm thick and shows good adherence to the substrate. The final coating thickness following the test is 0.1 mm.

Using the Secondary Electron mode and the data capture facility of the SEM software, a speedmap of the coating and substrate was produced and is shown in Figure 6.28. This shows the general location and distribution of the coating particles (W and Co) relative to the substrate (Al). Figure 6.29 shows an X-Ray spectrum of the same sample.

6.9.1 Defects in coatings

Using the SEM facility, some defects were observed in coatings before wear testing. Photograph 6.10 shows a longitudinal crack, parallel to the surface in a WC-Co coating under a magnification of 300. Photograph 6.11 shows cracking in a coating parallel and normal to the substrate. Such defects, caused by internal stresses and lack of bonding would lead to easy removal of portions of the coating.

Photograph 6.8   WC-Co coated aluminium before abrasion wear testing.

Photograph 6.9 WC-Co coated aluminium after abrasion test.
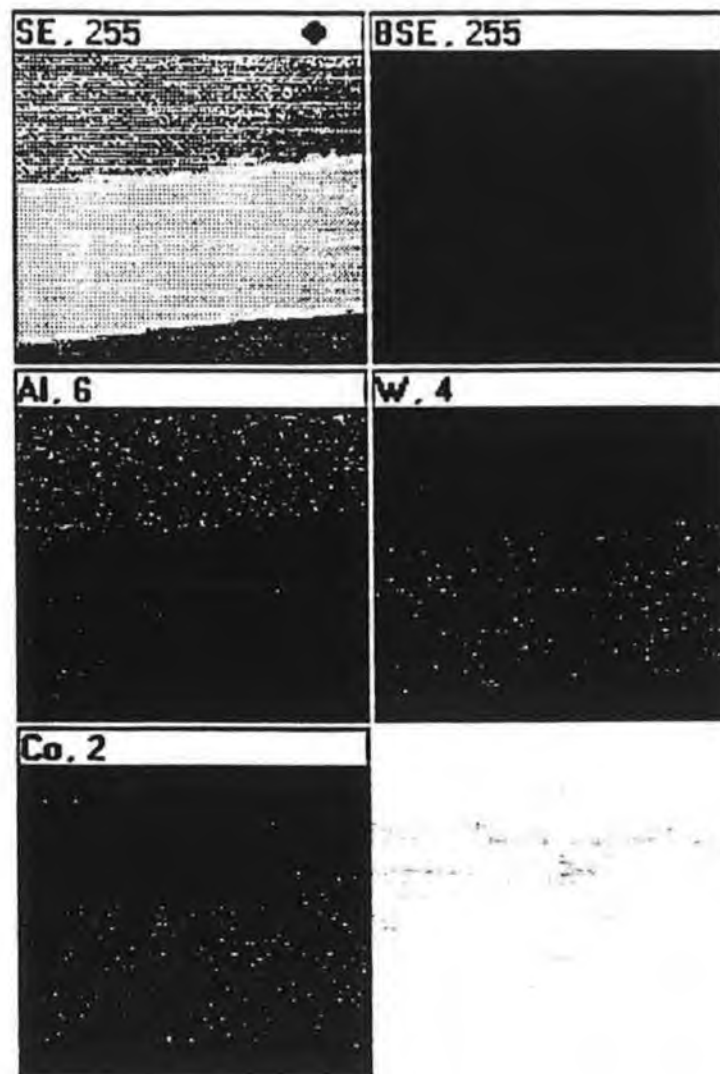
Figure 6.28 Speedmap of WC-Co coated aluminium sample.
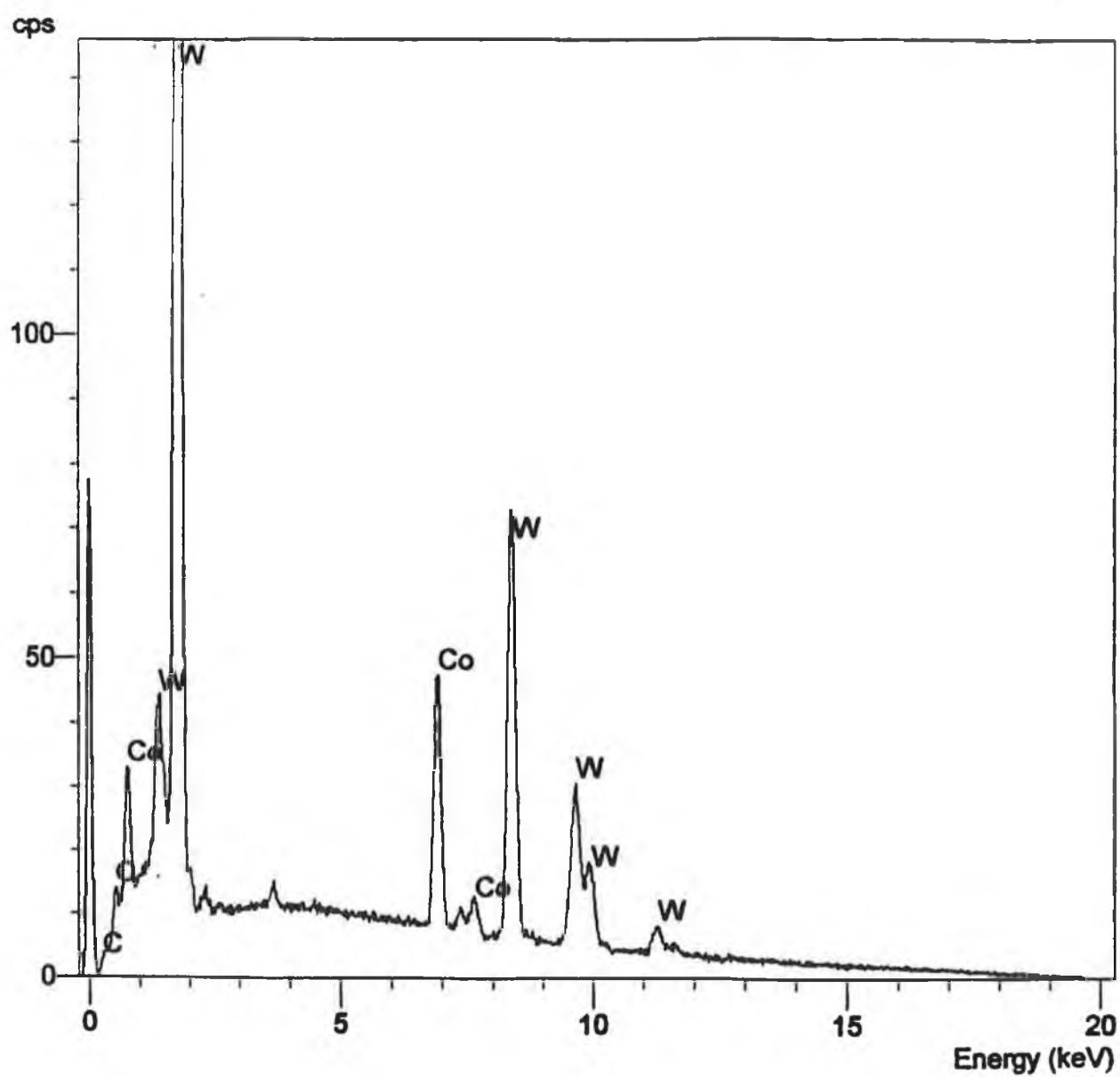
Figure 6.29 X-ray spectrum of WC-Co coated aluminium sample.
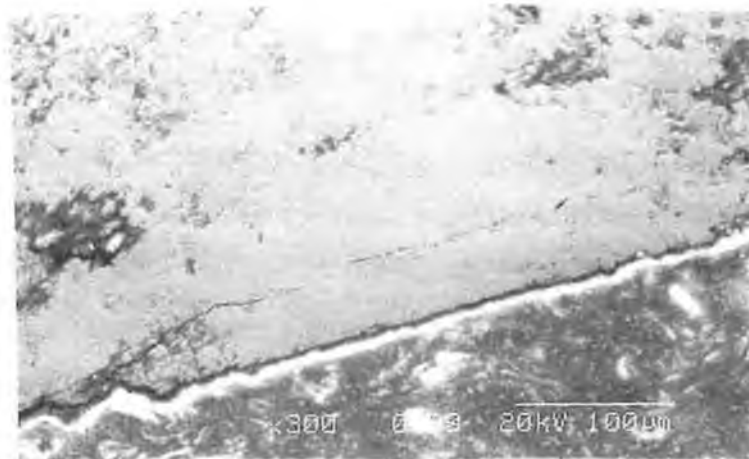
**Photograph 6.10 Internal cracking in WC-Co coating parallel
to the surface.**

**Photograph 6.11   Internal cracking in WC-Co coating parallel
and normal to the surface.**

6.10 IMPACT ABRASION

Photograph 6.12 shows wear scars for abrasion and combined impact abrasion. The samples consist of Ni-Cr and WC-Co coated aluminium respectively. The Ni-Cr coated sample which showed most wear under both test conditions shows considerable cratering and damage in the impact region caused by impact loading and gouging. Some plastic flow is also evident on the surface of the sample. The WC-Co coated sample shows greater wear resistance to both impact and abrasion with a much smaller and more uniform impact crater on the surface. The shape of this crater is shown in Photograph 6.13. Photograph 6.14 shows a crater produced on a WC-Co coated mild steel sample subjected to 4500 cycles under a load of 10 kg while Photograph 6.15 highlights plastic flow and abrasion scars in a mild steel sample produced by contact abrasion. Ni-Cr coated tool steel samples are shown in Photograph 6.16. These coatings were subjected to 1500 impact abrasion cycles under a 10 kg load, which led to spalling, fracture and detachment of large parts of the coating. Identical samples, subjected to pure abrasion did not reveal the same defects. This highlights one advantage of subjecting coatings to impact loading for testing adhesion and fracture resistance of the combined coated system. Photograph 6.17 shows a similar defect on a WC-Co coated aluminium sample where cracking and detachment of large pieces of coating were removed adjacent to a crater. In this case the impact loads resulted in fracture of the coating at the edge of the crater. By inspection of the wear tests, impact loading results in large pieces of coating to become detached
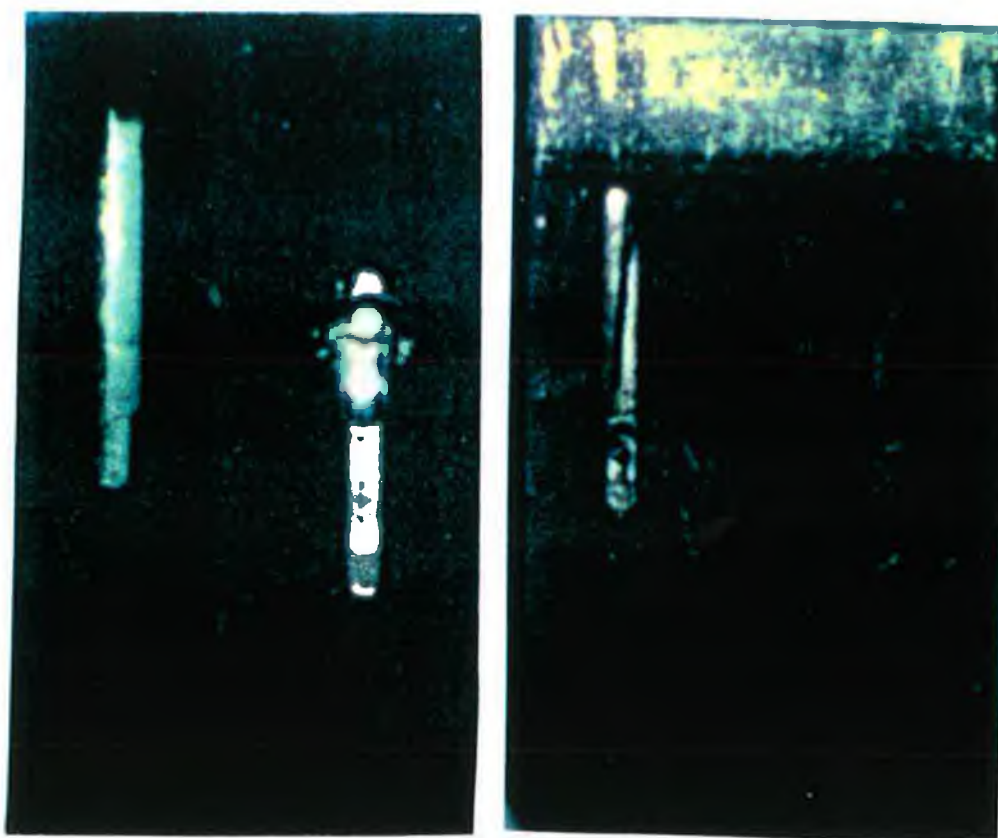
Ni-Cr sample   WC-Co sample

30 mm

Photograph 6.12 Impact abrasion wear scars on Ni-Cr and WC-Co
coated aluminium samples.

198
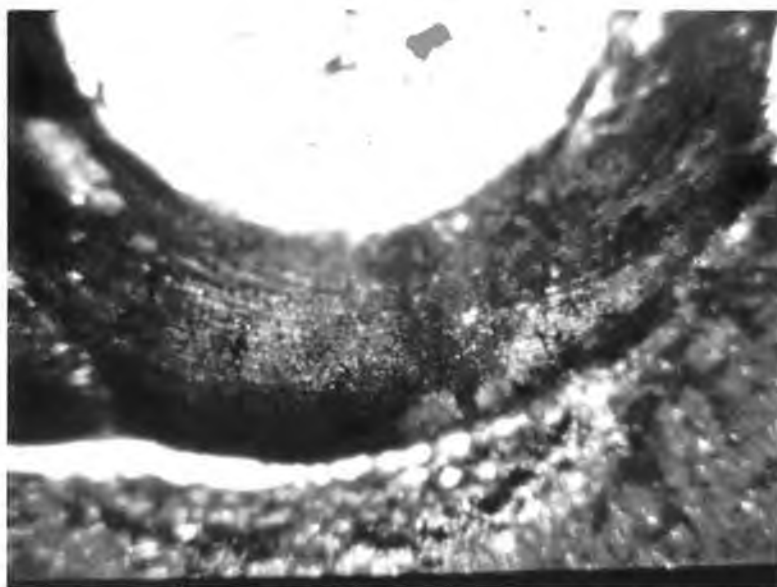
2 mm

**Photograph 6.13 Impact crater in WC-Co coated aluminium sample
showing substrate and wall of crater.**
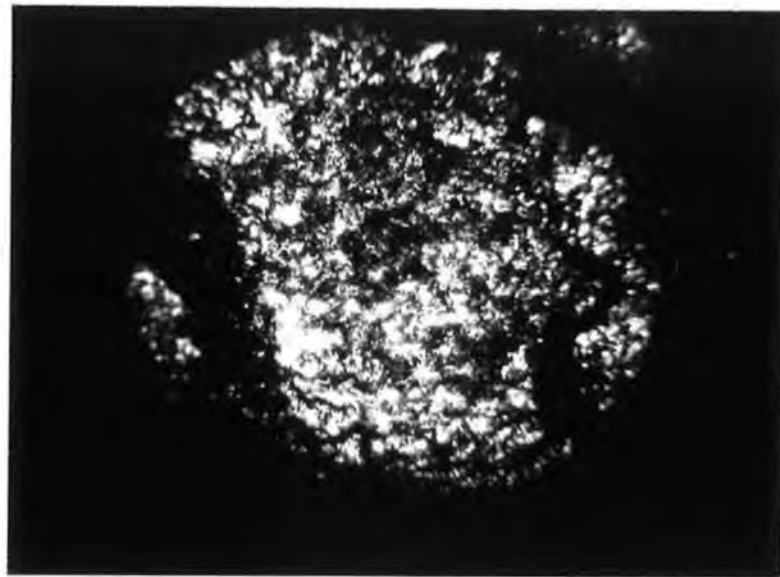
2mm

Photograph 6.14   Crater on WC-Co coated mild steel.

1mm

Photograph 6.15   Abrasion scar and plastic flow on mild steel sample.

30 mm
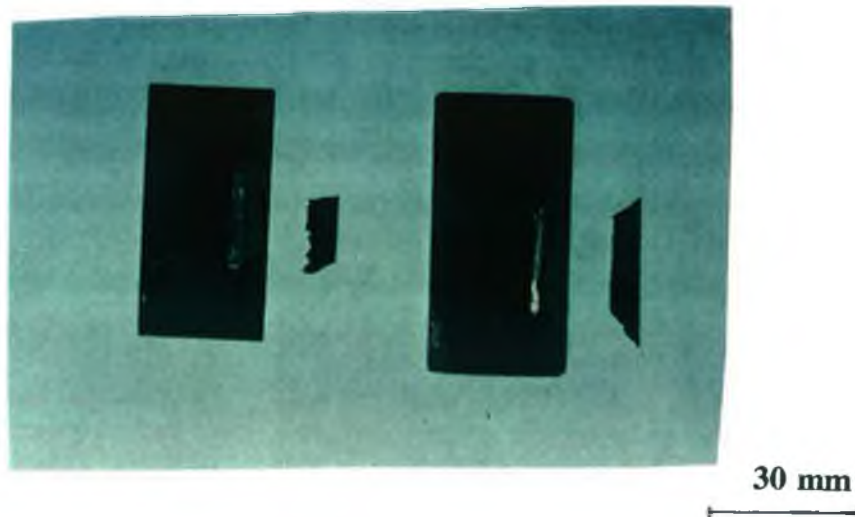
**Photograph 6.16 Ni-Cr coating detachment from tool steel
substrates subjected to impact abrasion.**

2mm
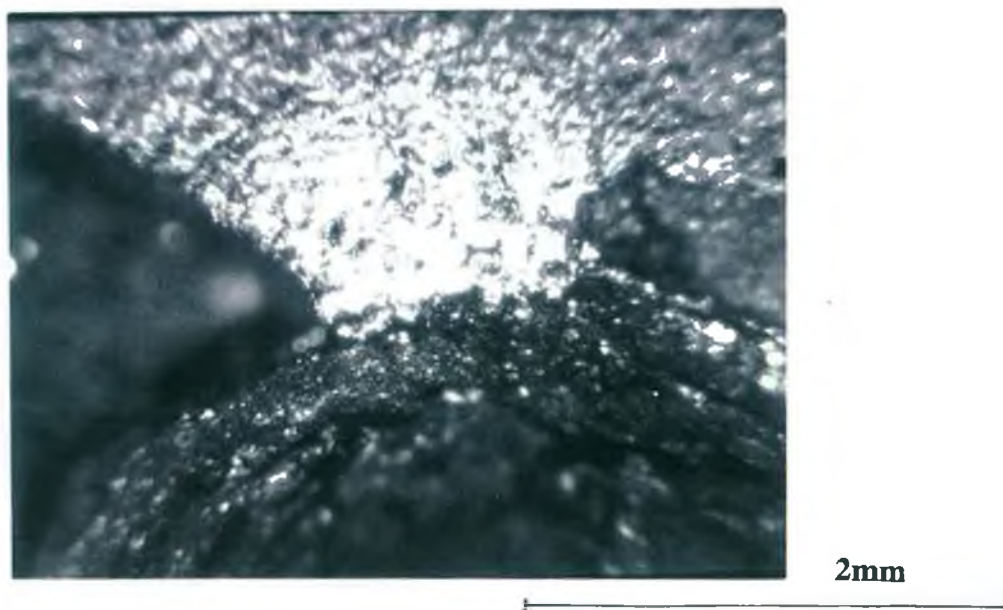
**Photograph 6.17 Large detachment of coating adjacent to crater
produced by impact loading of WC-Co
aluminium coated sample.**

201

while pure abrasion removed small particle sizes. The effects of combined impact abrasion of a hard coating on a soft substrate are shown in Photographs 6.18 and 6.19. In these cases the coating has become immersed in the substrate due to the impact loads sinking the coating into the substrate, followed by the abrasive effect causing plastic flow of the substrate material over the coating. Severe cracking of the coated parts are noticeable. Under the test conditions, the substrate was unable to support the coating which led to penetration of the coating into the aluminium substrate.

The brittle nature of the WC-Co coating caused it to crack due to the applied loads and collapse of the substrate support. A TiN coated D3 tool steel sample subjected to impact abrasion is shown in Photographs 6.20 and 6.21. A top view and cross section of the impact region is shown. The sample was subjected to 4500 cycles at 10 kg. The substrate in this case is able to support the coating and minimal yielding of the substrate is evident. The coating has only detached in parts corresponding to where it received direct impact. This caused the coating to crack and spall, leaving the substrate exposed in places. Coating detachment only occured in specific areas.

Photograph 6.18 Hard WC-Co coating immersed in soft aluminium substrate under impact loading.

Photograph 6.19 WC-Co coating covered by aluminium substrate due to plastic flow and abrasion wear.

203
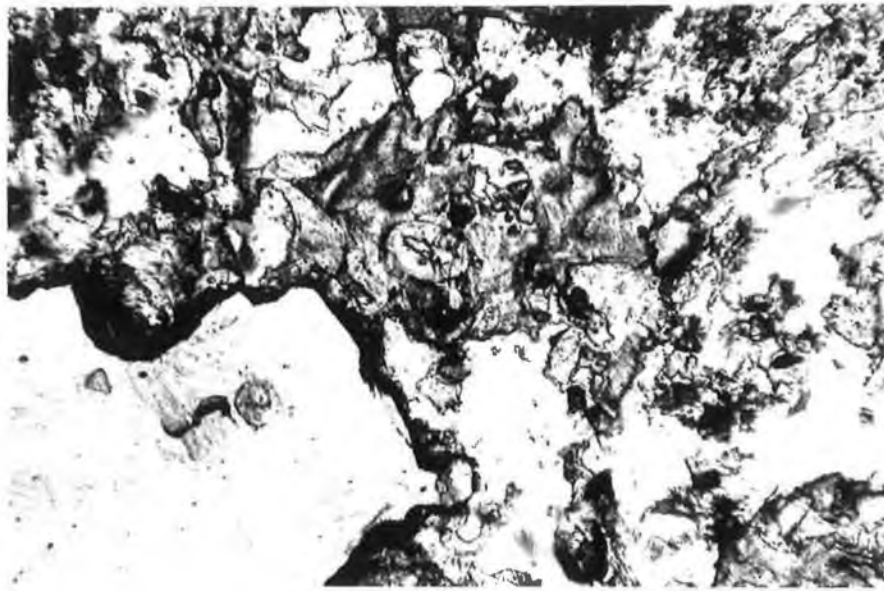
Photograph 6.20 Impact of TiN coated tool steel showing coating detachment and adhesion regions.

Photograph 6.21 Cross section of TiN coated tool steel showing coating detachment.

CHAPTER 7   CONCLUSIONS

7.1 INTRODUCTION

From the results obtained it is shown that the characteristics of the substrate material has a major effect on the wear resistance of the coatings examined under impact conditions. The coatings employed improved the wear resistance of the samples under contact abrasion conditions. Coatings that performed satisfactorily under contact abrasion showed high wear rates under impact abrasion conditions. Hard WC-Co coatings applied to soft substrates such as aluminium will result in rapid destruction and high wear rates of the material under the influence of impact forces.

The main aims and objectives of this study were:

(i)   to develop a novel test rig for testing coated and uncoated engineering materials under the conditions of dynamic abrasion wear testing, and incorporate a method of measuring the applied forces during these test methods.

(ii)   to compare the effects of coated with uncoated samples under dynamic abrasion test conditions.

(iii)   to examine the performance of the coating-substrate combination and the effects of different substrates on the overall wear resistance of the system.

(iv)   to assess the performance of different coating thicknesses on substrates under dynamic abrasion wear tests.

(v) to investigate how surface coatings perform under impact conditions compared with pure contact abrasion and pure impact.

(vi) to compare the performance of coated and uncoated specimens under dynamic test conditions for unlubricated conditions.

(vii) to describe the main wear parameters produced during the dynamic abrasion testing.

(viii) to compare the separate effects of impact and abrasion with the combined effects of impact abrasion on coated and uncoated materials.

These objectives were carried out during the experimental and analysis stages of the thesis and the following conclusions can be drawn from the work.

7.2 GENERAL CONCLUSIONS

(i) Applying impact loads on samples led to rapid failure of poorly adhered coatings. These same coatings performed satisfactorily under abrasion conditions. This highlights the importance of impact loading as a test for coated systems.

(ii) The results of the study show that the impact abrasion test apparatus can be used to test the wear resistance of coated and uncoated specimens.

(iii) The impact effects were useful for identifying poor coating adhesion and caused rapid failure of such samples.

(iv) The combined effects of impact-abrasion make the test rig more applicable to industrial applications and unique as a wear test, compared to other available equipment.

(v)   It was found that the indentation crater left in the surface has a larger radius of curvature than that of the indenting sphere. This effect is referred to as shallowing and is due to the release of elastic stresses in the metal specimens.

(vi) On impact, some adherence of the coating to the stylus occured immediately which results in a transfer of material between the colliding bodies. Shearing due to sliding or abrasion action disrupts the surface films on materials.

(vii) For the WC-Co coated samples, the tests confirmed literature findings that these coatings are prone to scuffing even at light loads [7.1].

(viii) Substrate properties have an influence on the wear of the combined coated/ substrate system.

Under pure impact conditions, a symmetrical crater as expected is produced. Under combined impact and abrasion the stylus is striking the samples at force and abrading the surface. This resulted in a number of effects and gouging or ploughing of the samples became predominant. This effect was more noticeable on substrates of soft materials. The gouging resulted in the stylus shearing the coating from the surface. As observed, the impact of the stylus forced the stylus below the coating/substrate interface and produced severe abrasion of the coating. It was noticeable on substrates of aluminium that a step effect was produced, from the crater due to impact and gouging of the stylus on the specimens. It was stated by Swick et al [7.2], that combined impact abrasion resulted in less wear of a specimen than if the two effects were performed seperately. Measurements taken in this research work on samples indicated that due to gouging and ploughing, of the sample, following impact resulted in greater wear loss than if both impact and abrasion were conducted seperately.

7.3 THESIS CONTRIBUTION

The main work and contributions of the thesis to wear testing are as follows:

(i)   Development of a new wear test rig for applying dynamic abrasion loading to coated and uncoated engineering materials was developed and tested.

(ii)   Experimental testing of the effects of dynamic rebound on impact loading was conducted to measure its contribution to dynamic abrasion of materials.

(iii)   Applying impact and abrasion tests under a variable linear velocity in a reciprocating motion was carried out.

(iv)   Comparisons of wear testing for coated and uncoated materials under abrasion and impact abrasion were investigated.

The thesis has highlighted the effects of impact abrasion as opposed to pure contact abrasion and shown in some instances that impact conditions can isolate poorly adhered coatings that seemed to function satifactorily under abrasion contact.

The advanced operation of combined impact-abrasion on samples allows the wear tester to be used for combined wear testing. Wear tests for impact-abrasion conditions that required the use of two or more different rigs in the past can now be performed with one piece of equipment, given improved accuracy to the results. Such tests arise in intermitten cutting or milling as described by Knotek et al [7.3].

7.4 RECOMMENDATIONS FOR FURTHER WORK

Further research for lubricated conditions under abrasion and dynamic conditions could be undertaken to assess the difference in wear rates for coated and uncoated samples.

Having experimentally conducted tests on pure impact and abrasion, modelling the dynamic conditions using a Finite Element Method would be a good comparison, especially for coated samples to analyse the stresses and loading of the materials in such conditions.

APPENDIX A

TEST RIG DETAIL DRAWINGS

BASE PLATE

THICKNESS = 18mm.

Figure A-1. Test rig base plate.

211

NOTE: Unless stated, all dimensions +/− .025 mm

MAIN PILLARS FOR TEST RIG

M 20. OUTER DIA = 25 M20.

20 | 20

17.50 175.00 85 00
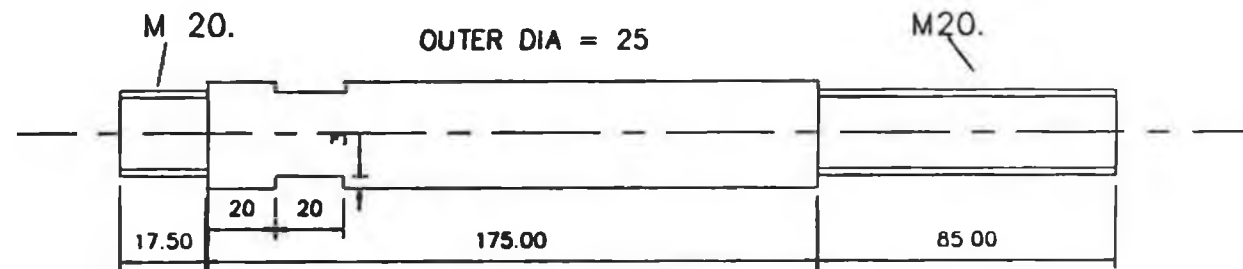
MAIN PILLARS: 4 OFF

note: Unless stated, all
dimensions +/- .025

Thread M8 1.50 2*45.

20 | 15

17.50 130.00 OUTER DIA = 10
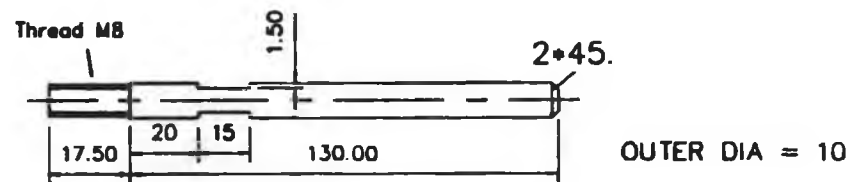
PILLARS FOR TABLE: 4 OFF.

Figure A-2. Support pillars for linear guide unit.

212

BASE TABLE FOR SAMPLE

ELEVATION

ENDVIEW

NOTE: Unless stated, all dimensions +/− .025

Figure A-3. Base table for samples.

213
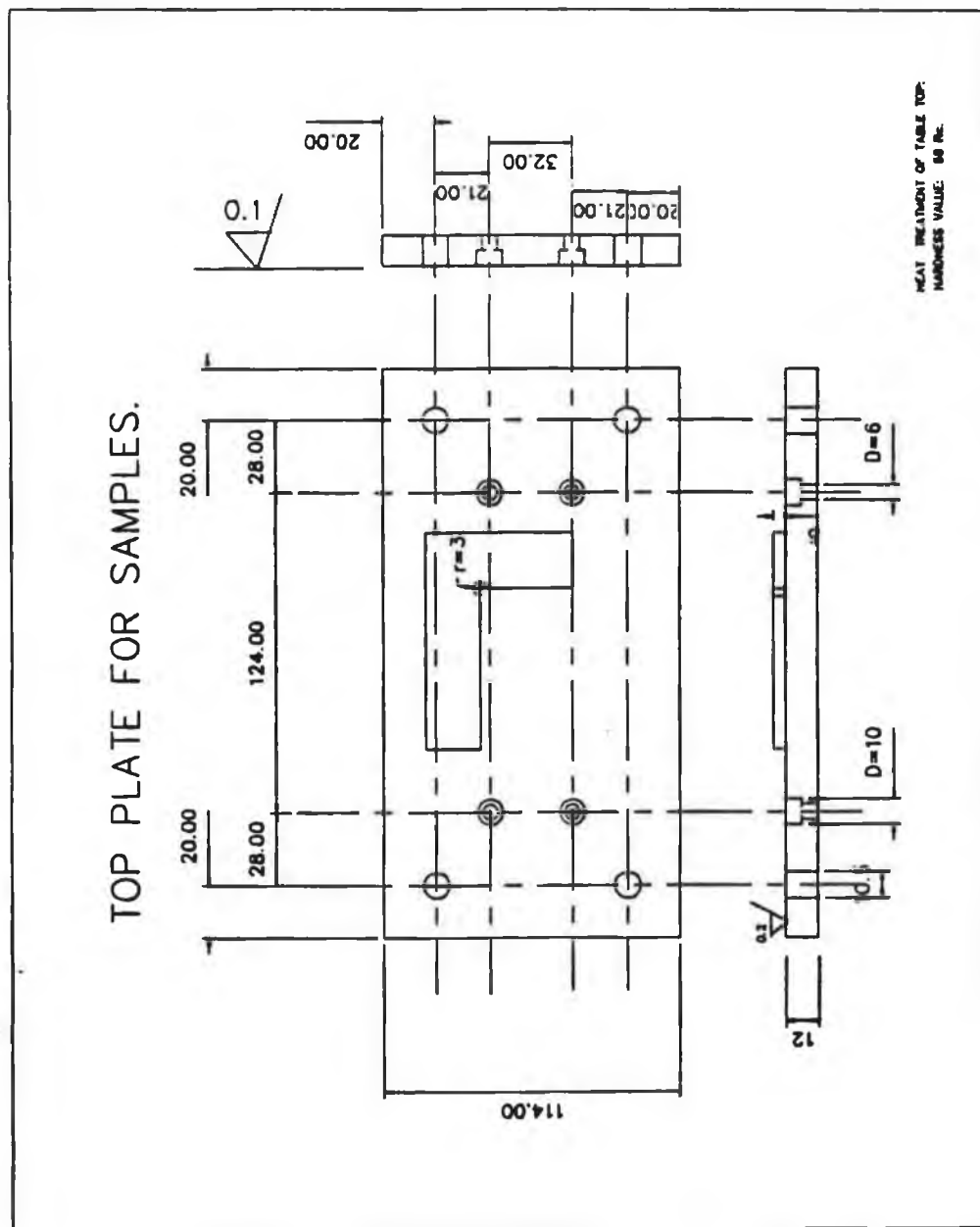
Figure A-4. Sample location plate.

214

LOCATION PLATE:
FIX TO BASE WITH 3 M4 SCREWS.

20.00

114.00

35.00

20

35

r=3

20

60.00   60.00
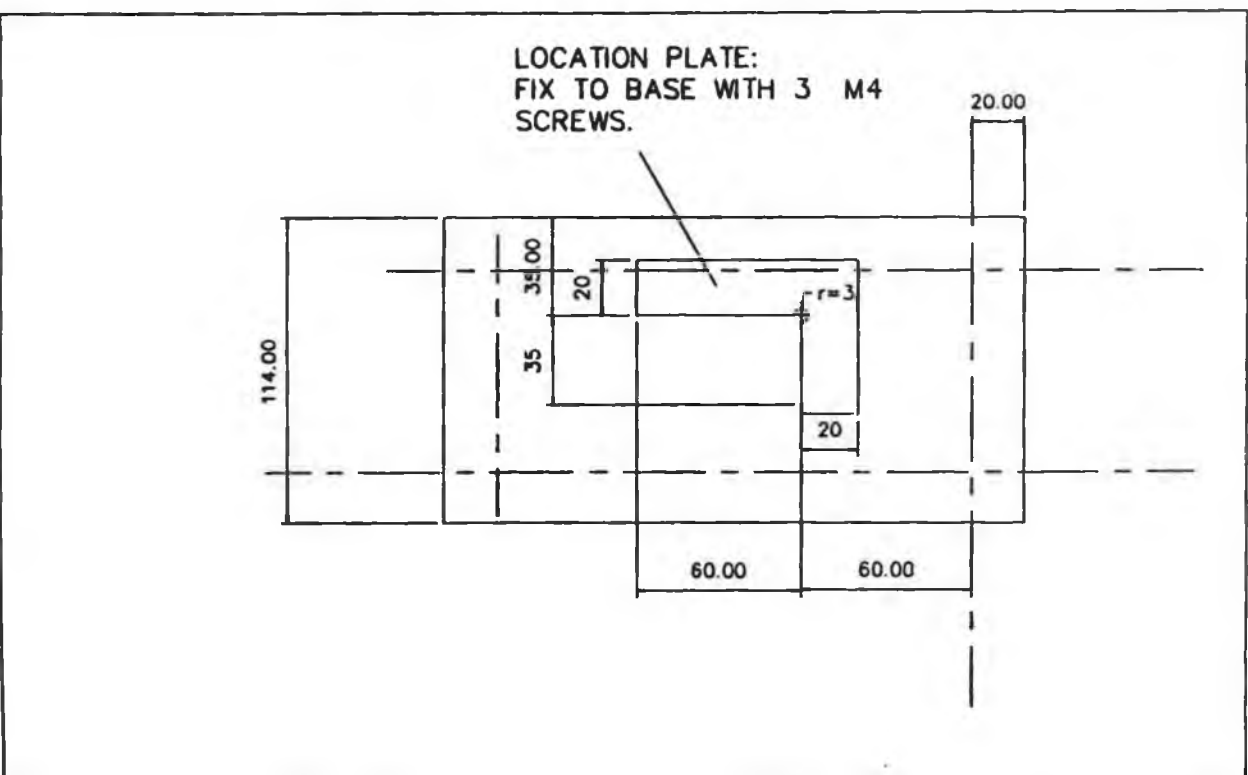
Figure A-5.   Detail of sample support fixture

215
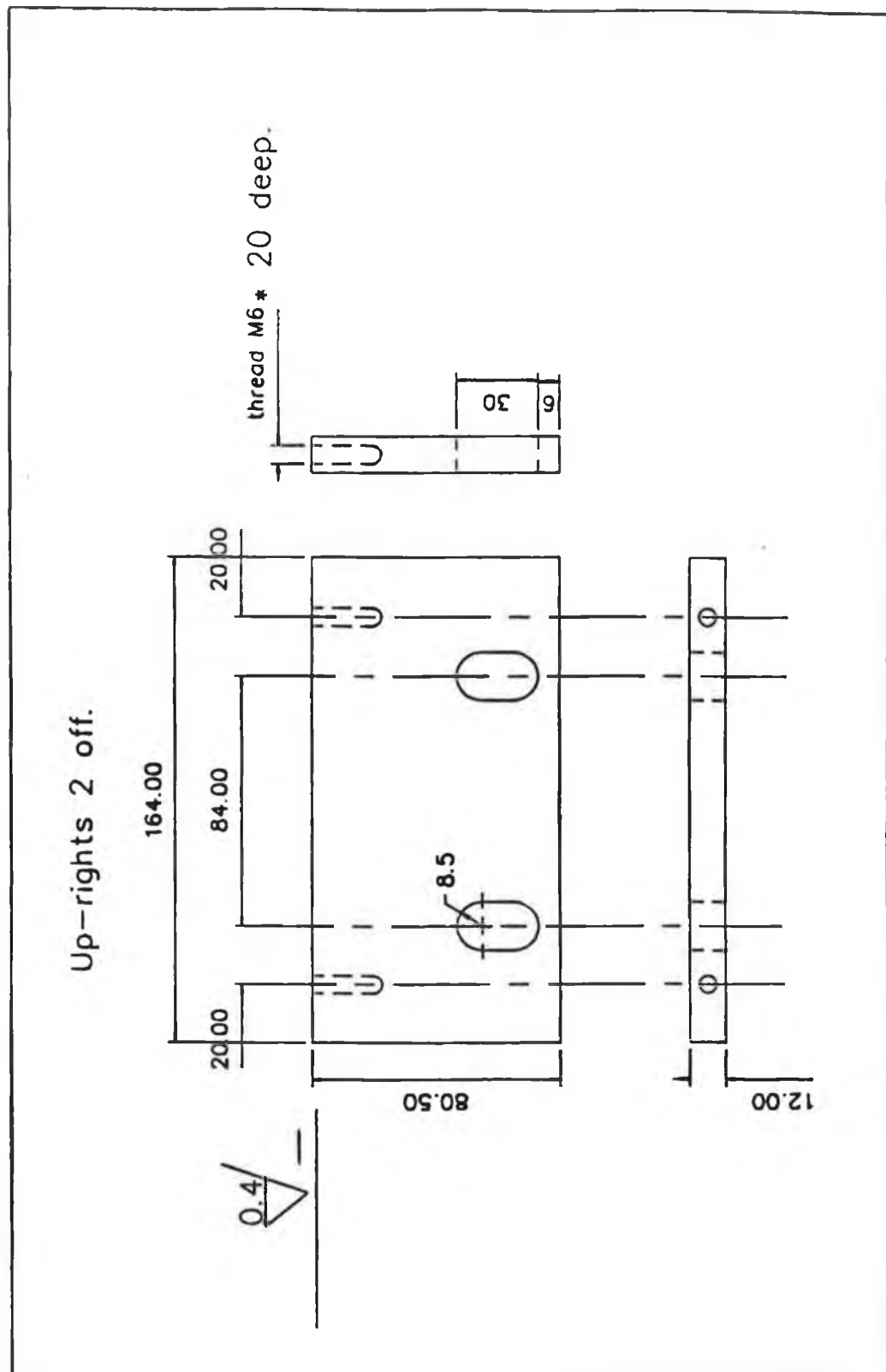
Figure A-6.   Uprights for sample table

216

SLIDER UNIT FOR ABRASION TOOL.

R1.50

M5 * 20 mm.

52.00

20.00

20.00   50.00

125.00

21.00

110.00

21.00

30.00

17.50   20.00   2 HOLES M4 COUNTER SUNK.

12.5 10

35.00

40

10

25

BRACKET FOR
FIXING SLIDER UNIT TO
CONNECTING ROD.

2 off.

Figure A-7.   Reciprocating unit for stylus

217
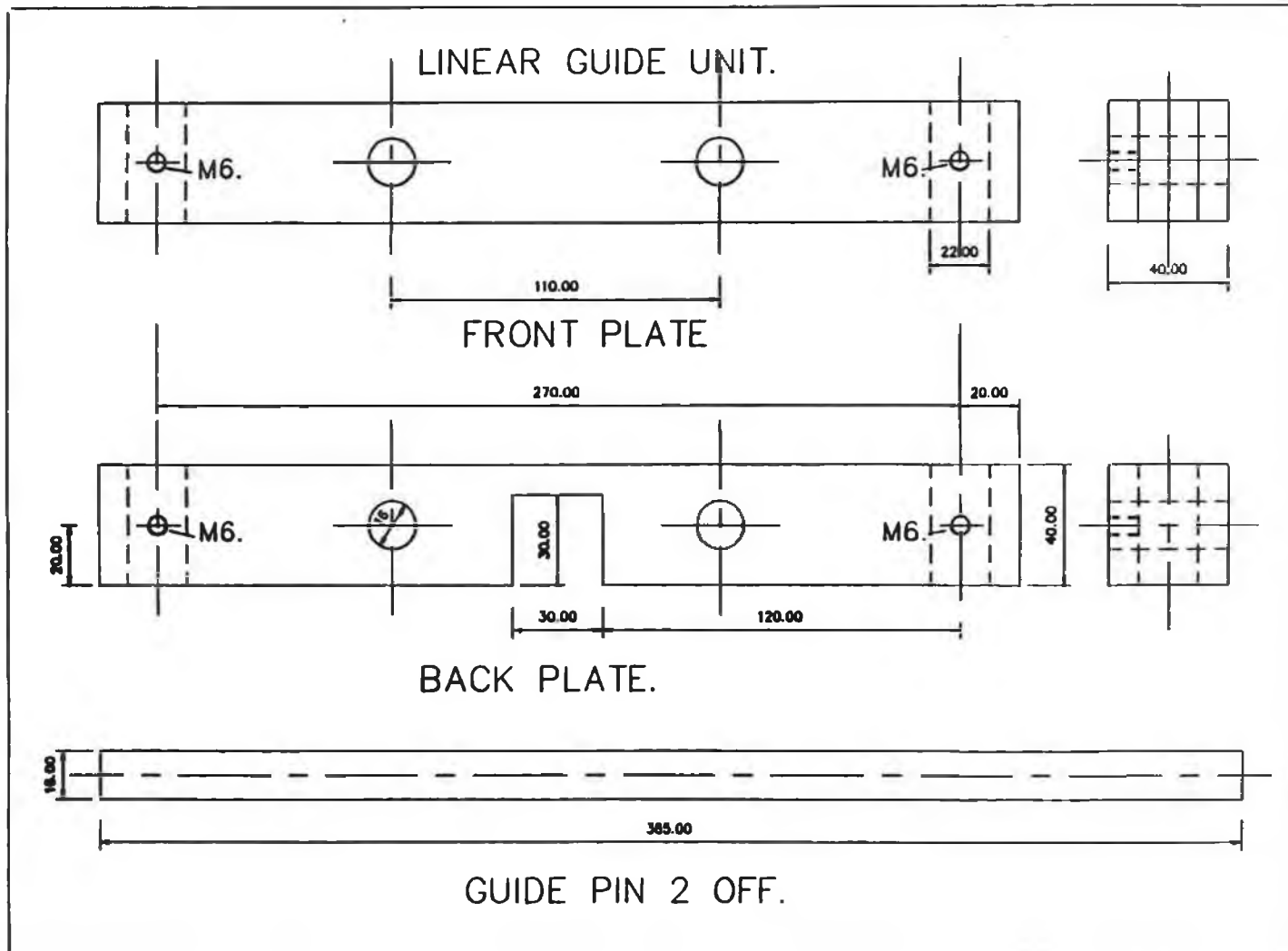
Figure A-8.   Linear guide unit

218

LINEAR GUIDE UNIT.

M6.   M6.

22.00

110.00

40.00

FRONT PLATE

270.00   20.00

M6.   M6.

30.00   120.00

30.00

40.00

20.00

BACK PLATE.

16.00

385.00

GUIDE PIN 2 OFF.

Figure caption text visible in the drawing:

Drive unit from motor.

section A – A.
END–VIEW.

ELEVATION.

KEY DETAILS

PLAN.

NOTE: Unless stated,
all dimensions +/- .025

Heat Treat to 58 Rc.

Dia to suit I.D. of needle bearing.

2*45deg taper.

Machine for Circlips.

Tap M5.

3

17

12.5

5

5

19

10

25
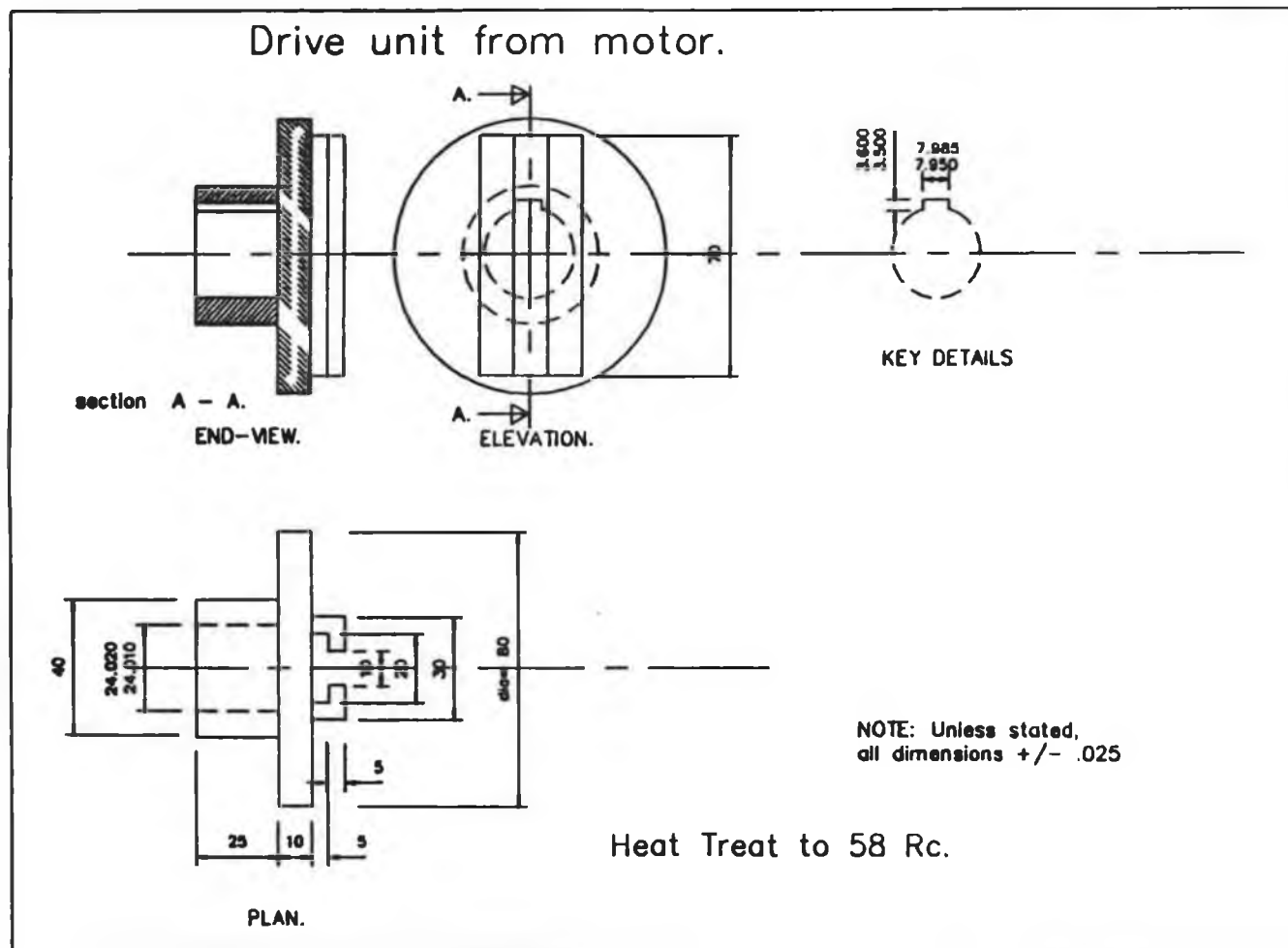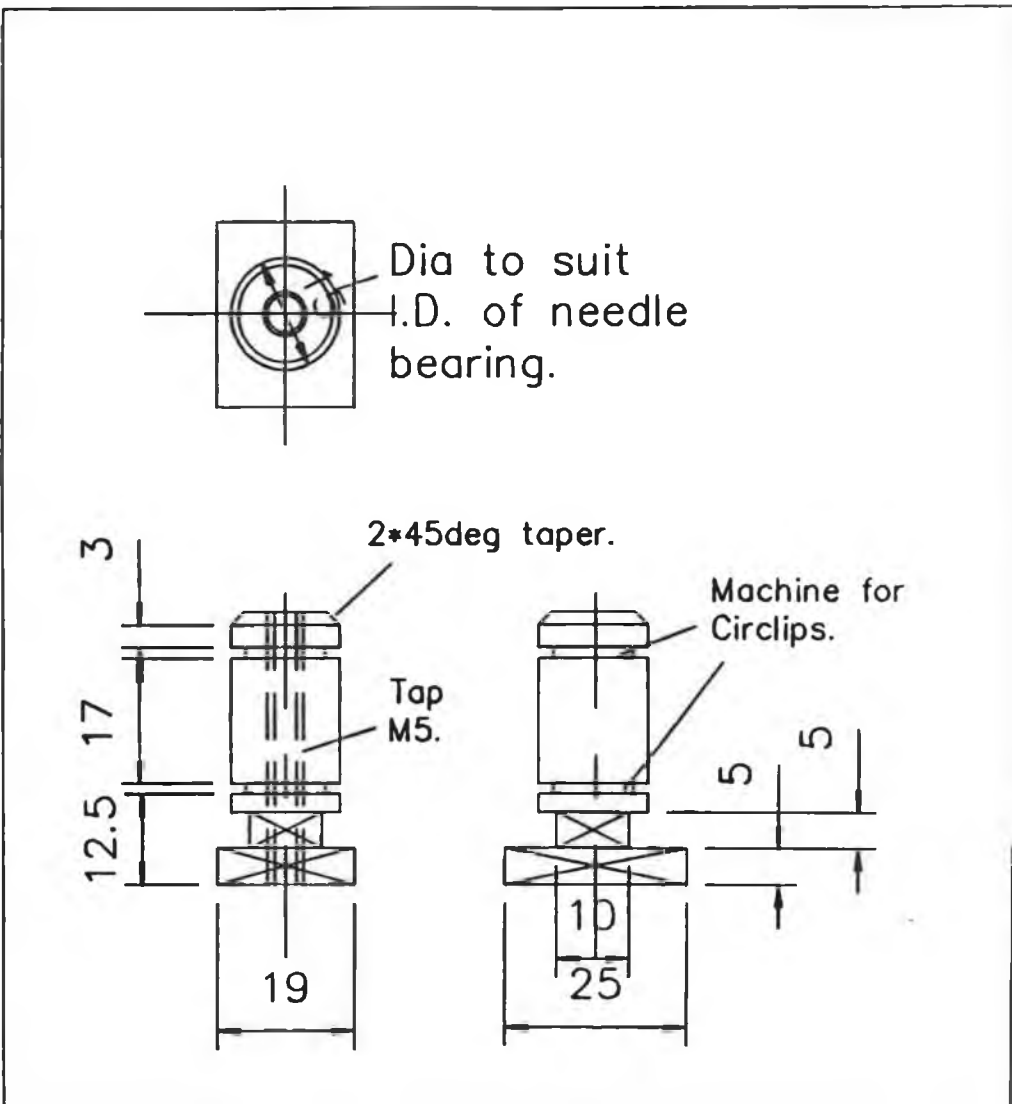
Figure A-10. Locking unit for connecting rod
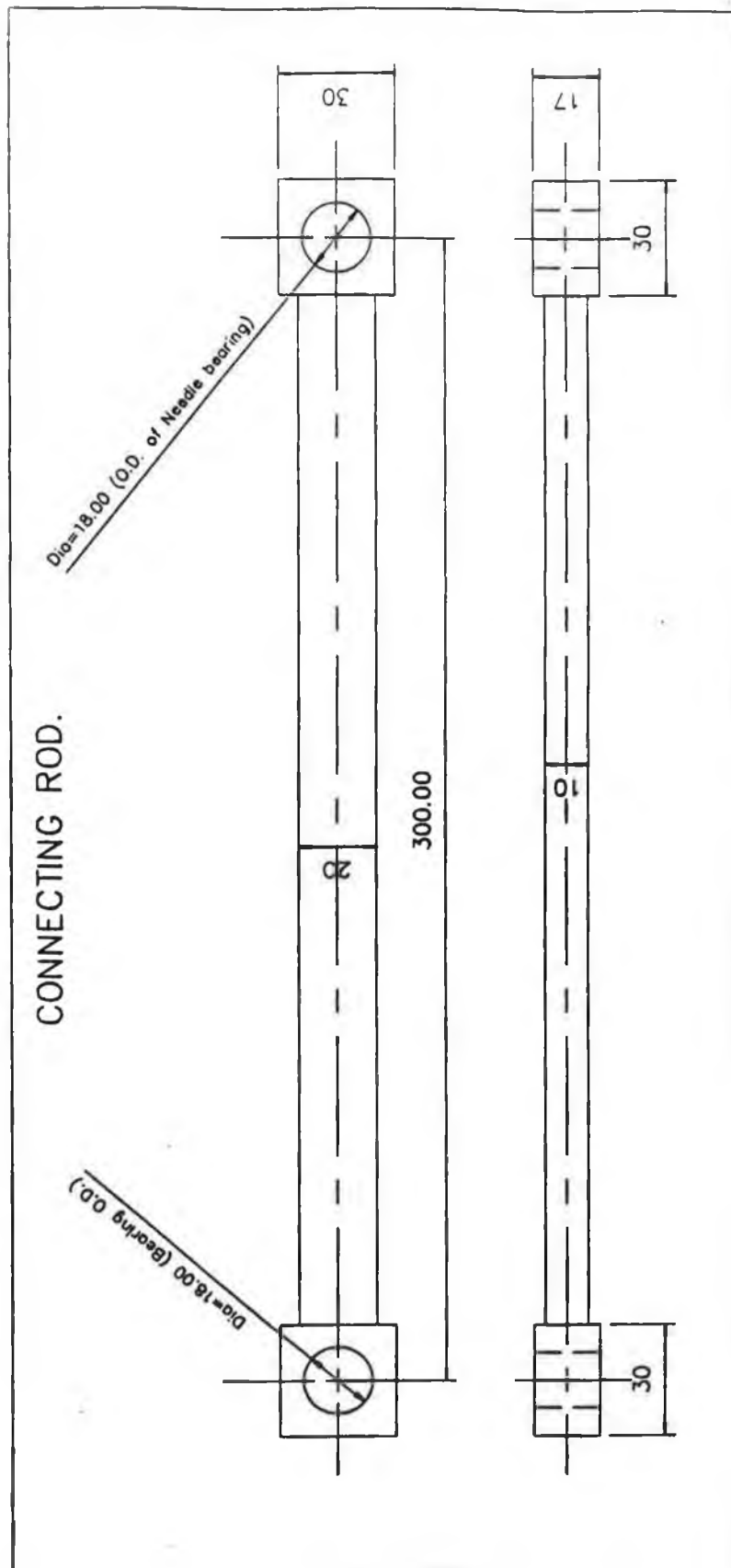
Figure A-11. Connecting rod

221

CAM DETAILS: 2 OFF

R15.00
R19.00
4.00
23.00
8.00

0.1
0.2
0.2

5.015
15.000

85.00
18.00
145.00
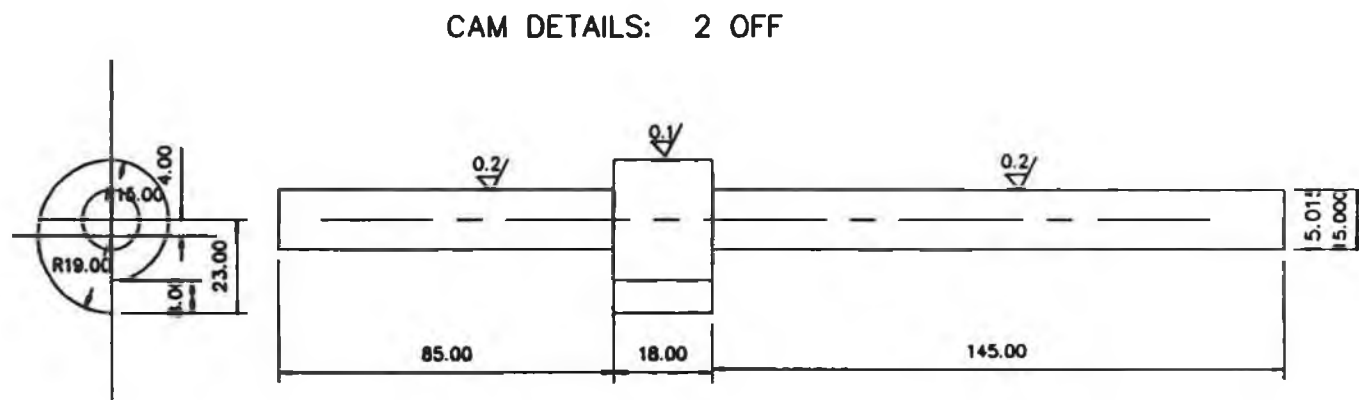
CAM DETAIL

1. no rise for first 180 deg's.
2. Rise from 15 to 23mm for next 90 degrees.
3. No rise for final 90 degrees.

CAM FACE HARDNESS: 58 Rc.

NOTE: UNLESS STATED, ALL
DIMENSIONS +/− .025mm.
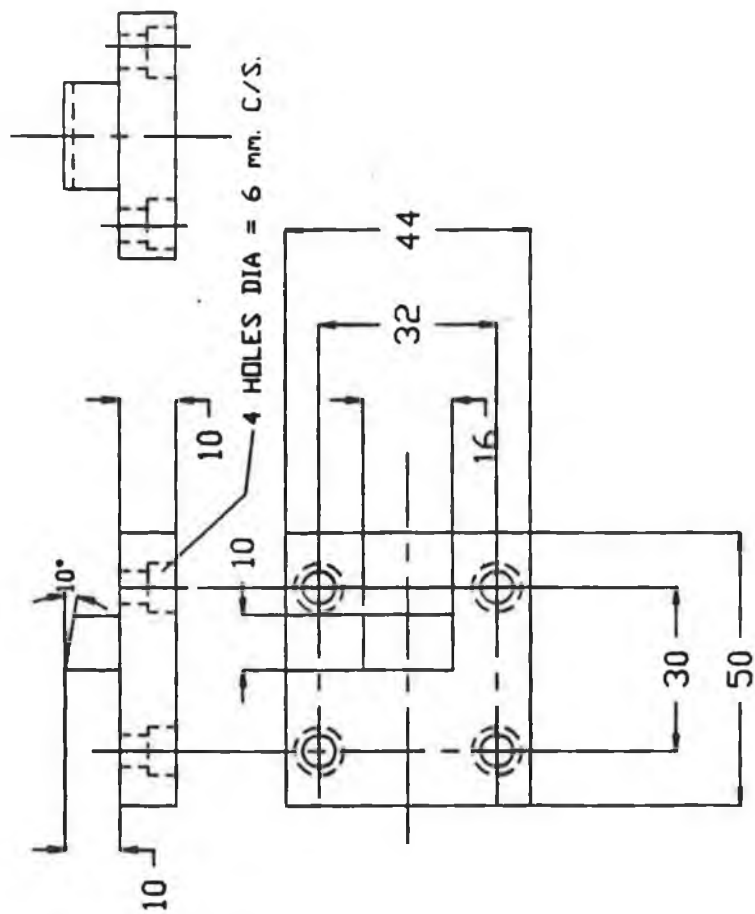
Figure A-13.   Cam follower (knife edge)

BEARING BLOCK FOR
CAM SHAFTS: 2 OFF.

23.00   84.00   23.00   32.00

23.00

57.00

20.00

80.00

13

M 8

16

Heat treat to 58 HRc.

NOTE: UNLESS STATED,
ALL DIMENSIONS, +/- .025mm.

Figure A-14. Bearing blocks for cam shafts

224
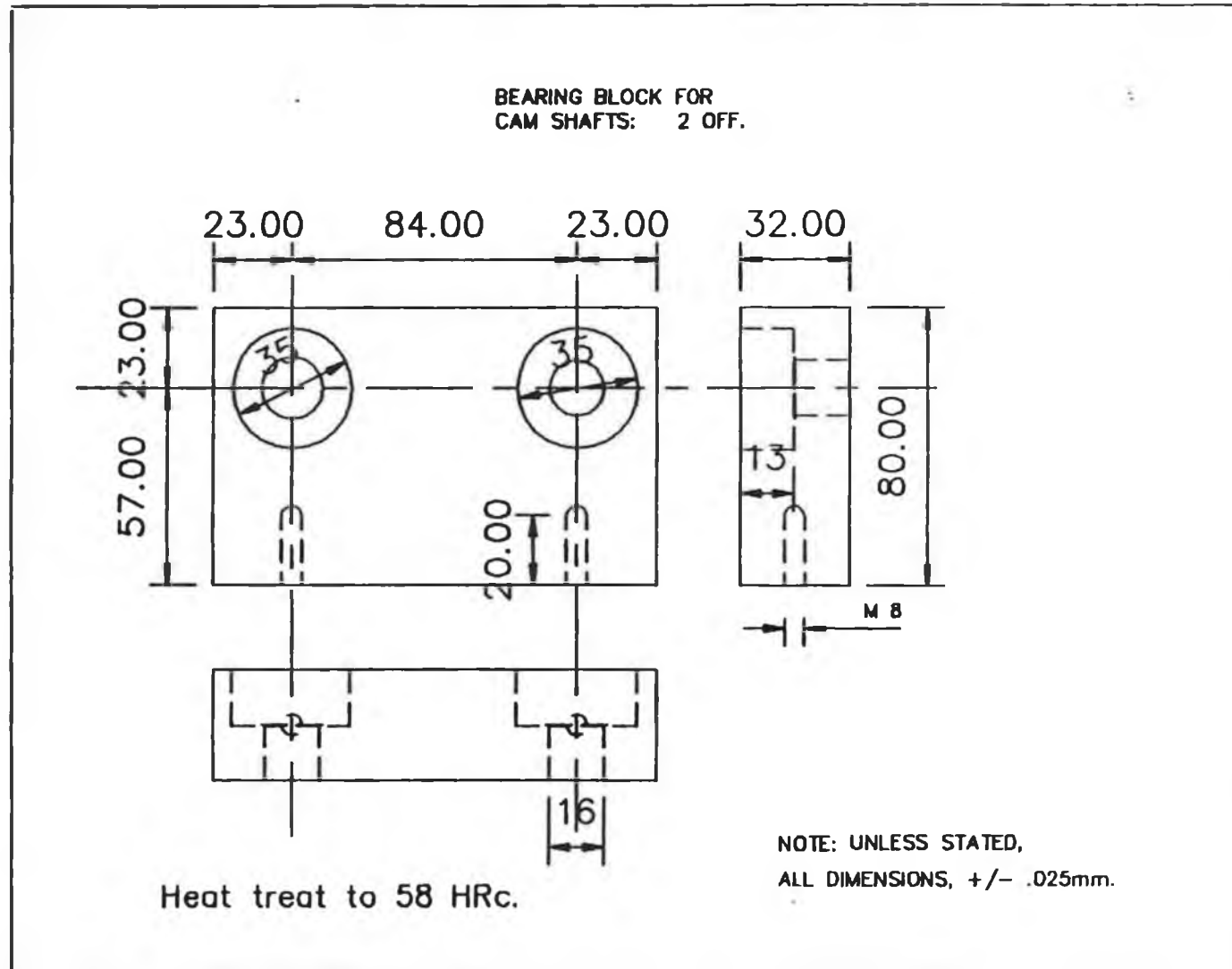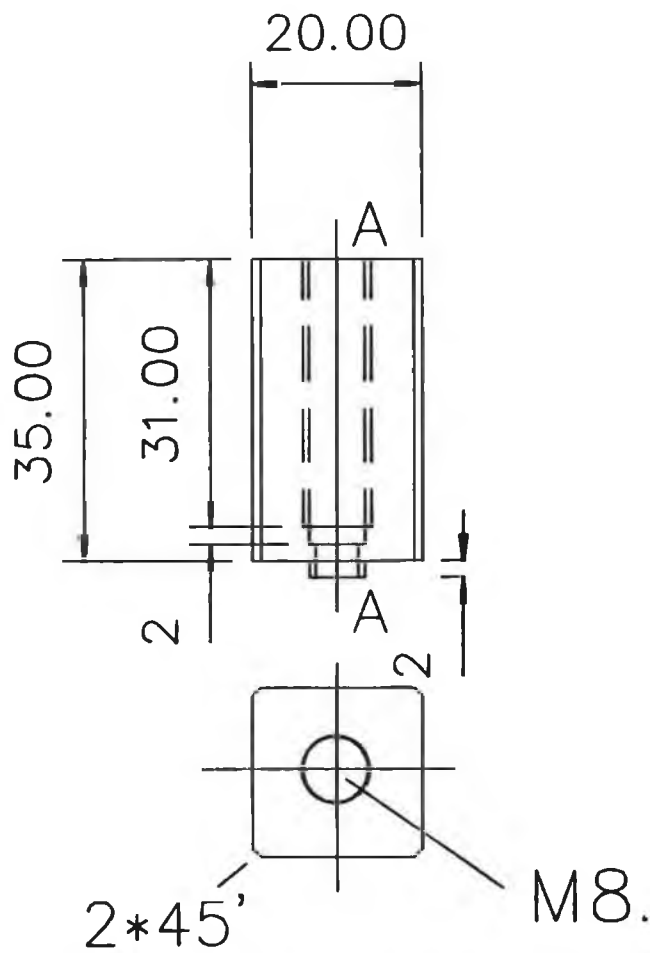
Figure A-15. Stylus holder

20.00

A

35.00

31.00

2

A

2

2*45'

M8.

20.00
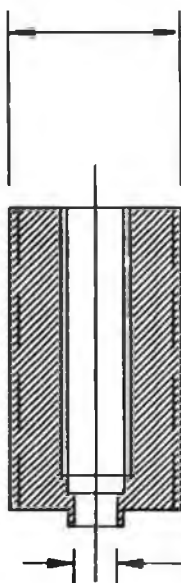
5.00

SECTION A—A
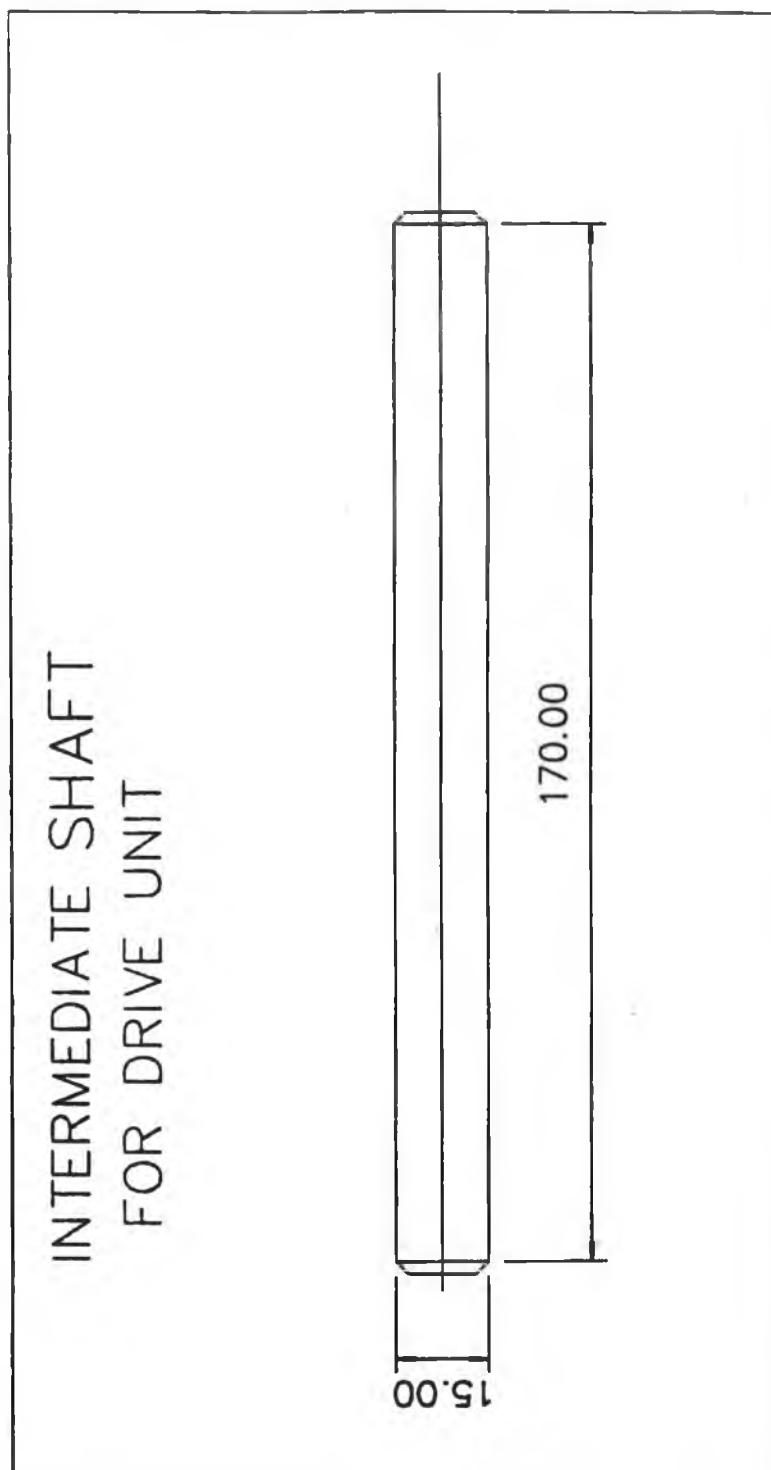
Figure A-16. Intermediate drive shaft

BEARING BLOCKS.
2 OFF. FOR INERMEDIATE
SHAFT.
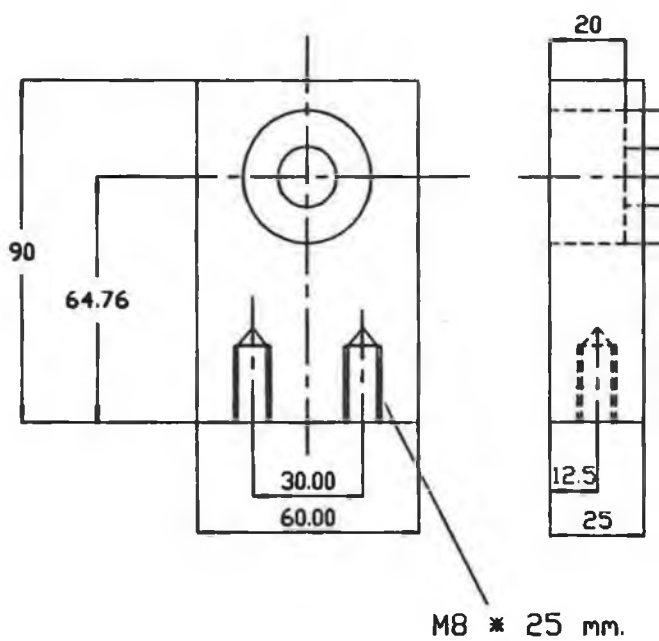
Figure A-17. Bearing block for intermediate shaft

227

16   35.00
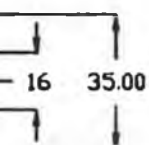
BEARINGS FOR TEST RIG

1. Cam shaft bearings:
   SKF Deep groove ball bearings.
   Bearing wheel reference: 6202, 22R
   I.D. 15 mm. O.D. 35 mm. Width = 11 mm.
   4 off.

2. Bearings for linear unit:
   SKF Needle roller bearings.
   Bearing wheel reference: RK 15*18*17F.
   I.D. 15 mm. O.D. 18 mm. Width = 17 mm.
   2 off.

3. Bearings for guiding table:
   I.D. 10 mm. O.D. 18 mm. Width = 25 mm.
   Plain bearings or linear guide bearings.
   4 off.

TOOTHED BELTS AND SPROCKETS

1. From motor to intermediate drive shaft:
Pulley on motor:	20L050
Pulley on intermediate shaft:	20L050
Timing belt:	225L050

2. From intermediate to first cam shaft:
Pulley on intermediate shaft:	19L050
Pulley on first cam shaft:	19L050
Timing belt:	187L050

3. From first cam shaft to second cam shaft:
Pulley on first cam shaft:	15L050
Pulley on second cam shaft:	15L050
Timing belt:	124L050

Messunterlagscheibe
Rondelle de charge
Load washer

Type **9001 A**   SN **416644**

Kalibrierter Bereich Gamme etalonnee Calibrated range	[N]	0...7 500	0 750	0...75
Empfindlichkeit Sensibilite Sensitivity	[pC/N]	−4,02	−3,89	
Linearitat Linearite Linearity	< ± % FSO	0,5	0,3	

Betriebstemperaturbereich
Gamme de temp. d'utilisation [°C] -196 200
Operating temperature range

Kalibriert bei
Etalonne a   20 °C
Calibrated at   by Wg Date 20.7.92

1N(Newton)=1kg·m·s⁻¹=0,1019...kp=0 2248...lbf
1kp=1kgf=9.80665 N
1lbf (pound force)=4.448 N
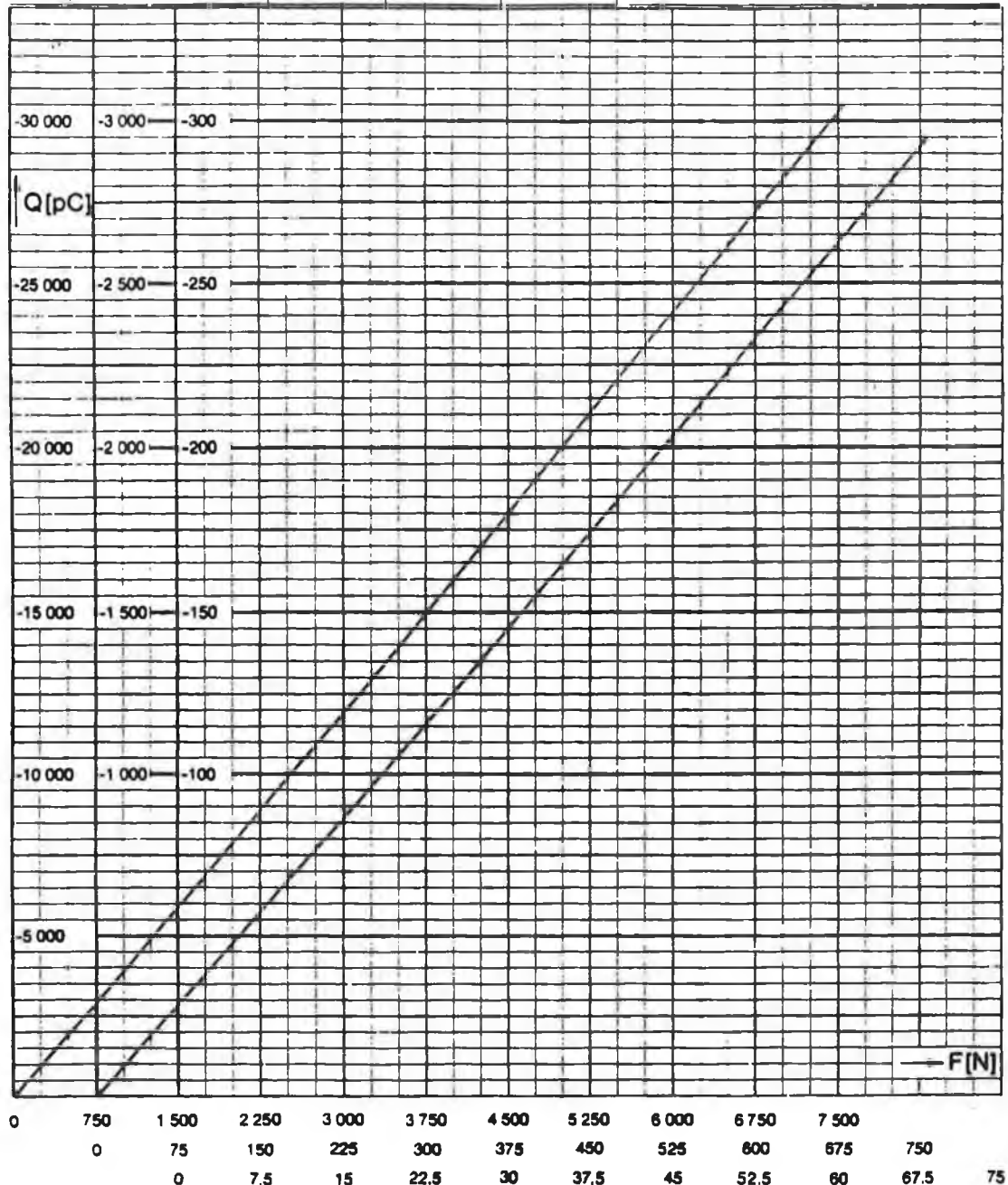
Calibration sheet for piezo electric load cell.

APPENDIX B

BASIC PROGRAMMES FOR DATA ACQUISITION

AND MEASURING WEAR LOSSES

QBASIC PROGRAMME FOR READING DATA FROM LOAD CELL.
D. KENNEDY.
FILE NAME = DK988.EXE.

```
DECLARE SUB DAS8 (MODE%, BYVAL dummy%, FLAG%)
10 CLS
20 PRINT
30 PRINT
40 PRINT " Written by  David Kennedy"
50 PRINT
60 PRINT " School of Mechanical & Manufacturing Engineering"
70 PRINT " Dublin City University"
80 PRINT " Ph.D Student 1994"
90 PRINT
100 PRINT " This programme performs the following tasks"
110 PRINT
120 PRINT " (1)... Reads data from data acquisition card"
130 PRINT
140 PRINT " (2)... Sends data to a text file for graphical presentation etc"
150 PRINT
160 PRINT " (3)... Displays on screen real-time-data of test procedures"
170 PRINT
180 PRINT " (4)... Measures the normal force acting on a test piece"
190 PRINT
200 PRINT " PRESS ANY KEY TO CONTINUE"
210 A8$ = INKEY$: IF A8$ = "" THEN GOTO 210
220 DIM DI%(8)
230 DIM NY(8)
240 DIM NY1(8)
250 CLS : PRINT SPC(79);
260 NCHAN% = 8
270 U% = 0
280 OPEN "DAS8.adr" FOR INPUT AS #1
290 INPUT #1, basadr%
300 CLOSE #1
310 DIM S%(6)
320 S%(0) = basadr%
330 FLAG% = 0
340 MD% = 0
350 CALL DAS8(MD%, VARPTR(S%(0)), FLAG%)
360 LOCATE 12, 1: PRINT SPC(79);
420 PRINT " START PROGRAMME"
430 PRINT
440 PRINT " SEND DATA TO FILE AND DISPLAY FORCE ON SCREEN"
450 PRINT
460 PRINT " PLEASE ENTER THE FILENAME : "
470 INPUT FILE$
```

```
480 OPEN FILE$ FOR OUTPUT AS #5
490 DIM D%(7)
500 DIM DIO%(7)
510 COLOR 1, 2, 4: CLS
520 VL = 1
530 DIM CH%(16)
540 DIM YL%(16)
550 FOR I% = 0 TO 16: YL%(I%) = -32768: NEXT I%
560 LOCATE 25, 1: PRINT ""; : LOCATE 1, 1
570 PRINT "which channel do you want plotted <e.g. 0-3-7 >?:", x$
580 x$ = INKEY$: IF x$ = "" THEN GOTO 580
590 x$ = "-" + x$
600 L% = LEN(x$)
610 FOR I% = 1 TO L%
620 IF MID$(x$, I%, 1) = " " THEN MID$(x$, I%, 1) = "-"
630 NEXT I%
640 FOR I% = 0 TO NCHAN% - 1: CH%(I%) = 0: NEXT I%
650 CR% = ASC(LEFT$(x$, 1))
660 IF ((CR% > = 48 AND CR% < = 55) AND (VAL(x$) < = NCHAN% - 1 AND
VAL(x$) > = 0)) THEN CH%(VAL(x$)) = 1: L% = LEN(x$): x$ = RIGHT$(x$,
L% - (1 + INT(VAL(x$) / 10)))
670 IF I% < NCHAN% - 1 THEN N% = ASC(MID$(x$, I + 1, 1))
680 L% = LEN(x$)
690 IF L% > = 1 THEN x$ = RIGHT$(x$, L% - 1): GOTO 650
700 IF U% > = 48 AND U% < = 55 AND N% > = 48 AND N% < = 55 THEN
CH%(10 * (U% - 48) + N% - 48) = 1: I = I + 1
710 SCREEN 2: CLS
720 LOCATE 25, 1: PRINT "PRESS + TO SPEED UP, - TO SLOW
DOWN,<ESC> TO EXIT"
730 x% = 32: U% = 1: C% = 1: LOCATE 23, 50: PRINT "GRID IN 1 SECOND
INTERVALS";
740 DATA 250,200,150,100,50,0,-50,-100,-150,-200,-250
750 FOR I% = 1 TO 11: READ A3$: LOCATE I% * 2 - 1, 1: PRINT A3$; : NEXT
I%
760 IF x% > = 640 THEN LINE (x%, 0)-(x%, 168), 0: x% = 30: LINE (x% - 1,
0)-(x% - 1, 168), 0
770 LINE (x% + 1, 0)-(x% + 1, 168), 0
780 LINE (x%, 0)-(x%, 168), 0
790 MD% = 1: D%(0) = 0: D%(1) = NCHAN% - 1
800 CALL DAS8(MD%, VARPTR(D%(0)), FLAG%)
810 MD% = 4
820 FOR Z% = 0 TO NCHAN% - 1
830 CALL DAS8(MD%, VARPTR(D%(0)), FLAG%)
840 IF FLAG < > 0 THEN PRINT #5, 'ERROR'
850 IF D%(0) > -1 THEN PRINT #5, D%(0) / 1000
860 IF VL = 0 THEN DIO%(Z%) = (D%(0) * 5 / 2047) ELSE DIO%(Z%) =
D%(0)
```

```
870 NEXT Z%
880 FOR Z% = 0 TO NCHAN% - 1
890 IF CH%(Z%) = 0 THEN GOTO 990
900 IF x% < 30 THEN x% = 30
910 Y% = DIO%(Z%)
920 IF YL%(Z%) = -32768 THEN GOTO 980
930 LINE (x% - 1, 84 + YL%(Z%) * 80 / 2047)-(x%, 84 + Y% * 80 / 2047)
940 XVALUE% = (x% - 1)
950 YVALUE% = (YL%(Z%) * 80 / 2047)
960 XVALUE1% = (x%)
970 YVALUE1% = (84 - Y% * 80 / 2047)
980 YL%(Z%) = Y%
990 NEXT Z%
1000 GOSUB 1190: IF Q + C% > T THEN GOTO 1030
1010 FOR I% = 1 TO 11: PSET (x%, I% * 16 - 12): NEXT I%
1020 Q = T
1030 x% = x% + 1
1040 U% = 200
1050 FOR I% = 1 TO U%
1060 A$ = INKEY$: IF A$ = "" GOTO 1170
1070 I% = U%
1080 IF ASC(A$) = 27 THEN LOCATE 1, 1: SCREEN 2: CLS : GOTO 1260
1090 IF A$ = "+" THEN U% = (U% / 2): IF U% = 1 THEN GOSUB 1220
1100 IF A$ = "-" AND U% < = 16000 THEN U% = (U% * 2): IF U% > 16000
THEN GOSUB 1220
1110 IF A$ = "-" AND U% > 16000 THEN GOSUB 1220
1120 IF U% < = 200 THEN C% = 1: LOCATE 23, 1: PRINT SPC(79); : LOCATE
23, 50: PRINT "GRID IN 1 SECOND INTERVALS";
1130 IF U% > 2000 THEN C% = 60: LOCATE 23, 1: PRINT SPC(79); : LOCATE
23, 50: PRINT "GRID IN 1 MINUTE INTERVALS"; : GOTO 1150
1140 IF U% > 200 THEN C% = 10: LOCATE 23, 1: PRINT SPC(79); : LOCATE
23, 50: PRINT "GRID IN 10 SECOND INTERVALS";
1150 IF A$ = "" THEN 1160 ELSE GOTO 1170
1160 IF INKEY$ = "" GOTO 1160
1170 NEXT I%
1180 GOTO 760
1190 T$ = TIME$
1200 T = 3600 * VAL(LEFT$(T$, 2)) + 60 * VAL(MID$(T$, 4, 2)) +
VAL(RIGHT$(T$, 2))
1210 RETURN
1220 IF U% = 1 THEN LOCATE 23, 1: PRINT "MAX SPEED";
1230 IF U% > 10000 THEN LOCATE 23, 1: PRINT "MIN SPEED";
1240 LOCATE 23, 1: PRINT "     ";
1250 RETURN
1270 END
```

BASIC PROGRAM FOR CALCULATING THE VOLUMETRIC WEAR LOSS
UNDER ABRASION WEAR.

```
10 REM PROGRAM FOR CALCULATING VOLUMETRIC WEAR LOSS
11 REM BY DAVID KENNEDY.
15 REM FOR A WORN AND IDEAL TOOL SHAPE.
16 REM CALCULATE WEAR FACTOR K
20 REM BY DAVID KENNEDY.
30 PRINT " WHAT MATERIAL IS UNDER TEST"
40 INPUT A$
50 LET P=3.14159
60 PRINT " HOW MANY CYCLES OF ABRASION"
70 INPUT CA
80 PRINT " WHAT IS THE NORMAL FORCE IN NEWTONS"
90 INPUT N
100 PRINT " WHAT IS THE SLIDING DISTANCE FOR ABRASIVE CONTACT
PER REVOLUTION IN METERS"
110 INPUT S
120 PRINT
130 PRINT " WHAT IS THE RADIUS OF THE STYLUS IN MILLIMETERS"
140 INPUT R
150 PRINT " WHAT IS THE WIDTH OF THE WEAR SCAR AT THE SURFACE
IN MILLIMETERS"
160 INPUT W
170 PRINT " WHAT IS THE WIDTH OF THE TIP OF THE STYLUS"
180 INPUT W1
185 PRINT
186 REM CALCULATE ADJACENT FOR WEAR SCAR SURFACE
190 LET X=SQR(R^2-(W/2)^2)
200 PRINT
205 REM CALCULATE ADJACENT FOR TIP OF WEAR TOOL
210 LET M=SQR(R^2-(W1/2)^2)
220 PRINT
230 REM CALCULATE CROSS SECTION OF WEAR SCAR FOR WORN OR
UNWORN TOOL
240 LET A= 0.5*R^2*(2*ATN(W/(2*X))-SIN((2*ATN(W/(2*X))))-
      2*ATN(W1/(2*M))+SIN((2*ATN(W1/(2*M)))))
250 PRINT "-----------------------------"
260 PRINT"  MATERIAL TESTED IS",A$
270 PRINT"  NUMBER OF WEAR CYCLES =",CA
280 PRINT"  CROSS SECTIONAL AREA OF WEAR SCAR =",A;"mm^2"
290 PRINT"  VOLUME OF MATERIAL REMOVED =", A*S*1000/2; "mm^3"
295 LET VOL = A*S*1000/2
300 PRINT"  WEAR FACTOR K=",            VOL/*(N*S*CA); "mm^3/NM"
310 PRINT" VOLUME LOSS PER CYCLE=",    VOL/CA;"mm^3"
320 PRINT" -----------------------------"
330 PRINT "VOLUME WEAR LOSS FOR AN IDEAL TOOL (NO WEAR)"
340 REM CALCULATE CROSS SECTION OF WEAR SCAR FOR AN IDEAL
TOOL
```

```
350 LET A1= 0.5*R^2*(2*ATN(W/(2*X))-SIN(2*ATN(W/(2*X))))
360 PRINT" MATERIAL TESTED IS ",A$
370 PRINT" NUMBER OF WEAR CYCLES =",CA
380 PRINT" CROSS SECTIONAL AREA OF WEAR SCAR =",A1;"mm^2"
390 PRINT" VOLUME OF MATERIAL REMOVED =" A1*S*1000/2; "mm^3"
395 LET VOL1 = A1*S*1000/2
400 PRINT" WEAR FACTOR K=",            VOL1/(N*S*CA); "mm^3/NM"
410 PRINT" VOLUME LOSS PER CYCLE=",    VOL1/CA;"mm^3
420 END
```

BASIC PROGRAMME FOR CALCULATING THE CRATER VOLUME PRODUCED IN SAMPLE.

```
10 REM PROGRAMME FOR CALCULATING THE CRATER VOLUME.
20 REM BY DAVID KENNEDY
25 LET P = 3.14159
30 PRINT " WHAT IS THE DEPTH OF THE CRATER"
40 INPUT HC
50 PRINT " WHAT IS THE NUMBER OF IMPACTS"
60 INPUT I
70 PRINT "WHAT IS THE CRATER DIAMETER AT THE SURFACE IN MILLIMETERS"
80 INPUT W
90 PRINT " WHAT IS THE RADIUS OF THE STYLUS"
100 INPUT R
110 PRINT " WHAT IS THE WIDTH OF THE TIP OF THE STYLUS"
120 INPUT W1
125 REM IF WIDTH AT TIP OF TOOL, W1 = 0, THEN VOL = VOLUME OF HEMISPHERICAL CRATER.
130 LET VOL = (P*HC/6)*(HC^2+3*(W1/2)^2+3*(W/2)^2)
140 PRINT "CRATER VOLUME =", VOL; "MM^3"
150 PRINT " AVERAGE CRATER VOLUME PER IMPACT=", VOL/I
160 PRINT
170 REM CURVATURE OF CRATER
171 LET R2= ((W)^2/4 +HC^2)/(2*HC)
172 PRINT "RADIUS OF CRATER=", R2
175 REM TABOR VOLUME CALCULATION FOR HEMISPHERICAL TIPPED TOOL
176 LET VR= (P*(T/2)^4)/(4*R2)
177 PRINT " CRATER VOLUME FROM TABOR EQUATION = ", VR
180 REM MEASURE THE COMBINED VOLUME WEAR FOR IMPACT AND ABRASION
190 REM VOLUME LOSS FOR COMBINED IMPACT ABRASION.
200 PRINT
210 PRINT " WHAT IS THE WEAR SCAR VOLUME"
220 INPUT WSV
230 PRINT " WHAT IS THE CRATER VOLUMES"
240 INPUT CV
250 PRINT "TOTAL VOLUME =",  WSV + CV
260 END
```

PAPERS PRESENTED WITH THIS RESEARCH

1. D.M. Kennedy & M.S.J. Hashmi, Characteristics of Tribological coatings applied to Tool Steels under dynamic abrasion test conditions. AMPT, August 1993, Dublin. Vol. 3, p2057-2068. Dublin City University Press.

2. D.M. Kennedy, M. Helali, & M.S.J. Hashmi, Dynamic Abrasion Wear resistance of coatings applied to engineering materials. Presented at ICMCTF, San Diego, 1994. Surface and coatings Technology, 68/69 (1994) 477-481.

3. D.M. Kennedy, & M.S.J. Hashmi, Methods of wear testing for advanced surface coatings and bulk materials. Presented at AMPT Conf., August 1995, Dublin. M.S.J. Hashmi(ed), AMPT95, Vol 1, 1995, 477-486. Published by Dublin City University Press.

4. D.M. Kennedy, & M.S.J. Hashmi, The influence of linear velocity on the wear behaviour of thermal sprayed coatings under dynamic abrasion test conditions. Presented at AMPT Conf., August 1995, Dublin. M.S.J. Hashmi(ed), AMPT95, Vol 1, 1995, 466-476. Published by Dublin City University Press.

REFERENCES

Chapter 1.

[1.1] T.S. Bell. Surface engineering, Its current future impact on tribology. J. Phys, D:Appl, Phys 25(1992) A297-A306.

[1.2] T.S. Eyre, Friction and Wear control in industry, Surface Engineering Conference, P.K. Datta & J.S. Gray (Editors), Newcastle Upon Tyne, March 1992.

[1.3] C. Spero, D.J. Hargreaves, R.K. Kirkcaldie, H.J. Flitt. Review of test methods for abrasive wear in ore grinding, Wear 146(1991) 389-408.

[1.4] J. Fohl, T. Weissenberg, J. Wiedemeyer. General Aspects for Tribological Applications of Hard Particle Coatings, Wear 1989, Volume 130,1 p 275-288.

[1.5] D. Dowson. Engineering at the interface., I.Mech.E Presidential address at Institution of Engineers of Ireland, May 1992.

[1.6] D. Klaffke. A. Skopp and I. Lenke. Triblogical Characterization of Coatings by Oscillating Sliding Testing, Bundesanstalt fur Metalforschung und-prufung (BAM) Laboratory 5.22 "Fretting, Cryotibology", 12200 Berlin, 1994.

[1.7] J.E. Kelley, J.J. Stiglich Jr, G.L. Sheldon. Methods of characterization of tribological properties of coatings, Surface modification Technologies 1988 p169-187.

[1.8] E. Bergmann, J. Vogel, R. Brink, R.Ballier. PVD Titanium Nitride Coating systems to Improve Tool Performance and reduce wear, Carbide and Tool Journal, Sept/Oct, 1986, pp 12-17.

[1.9] R.A. Higgins. Materials for the Engineering Technician, Published By Hodder and Stoughton 1980.

[1.10] C. Wick. Machining with PCBN Tools. Manufacturing Engineer journal, July 1988, p 73-78.

[1.11] Rocol Technical information sheet. MV-3 and MV-4 varnish coatings for the production of resin bonded molybdenum disulphide film, Rocol U.K.

[1.12] C. Subramanian, K.N. Strafford, T.P. Wilks and L.P. Ward, On the design of coating systems: Metallurgical and other considerations, In M.S.J. Hashmi(editor) Volume 2,pp1301-1313, AMPT 1993, Publishers Dublin City University Press.

[1.13] K.N. Strafford, C.Subramanian & T.P. Wilks, J. Mater. Processing Technol., 38(1993)431.

[1.14] A.Kassman, S.Jacobson, L.Erickson, P.Hedenqvist, M.Olsson. A new test method for the intrinsic abrasion resistance of thin coatings, Surface and coating technology, Vol 50, 1991, p75-84.

[1.15] R. Blickensderfer & J.H. Tylczak. Laboratory Tests of spalling, Breaking, and Abrasion of Wear-Resistant Alloys used in Mining and Mineral Processing, Department of the Interior, Bureau of Mines report of investigation 1985.

[1.16] A. Matthews & D.G. Teer, Evaluation of coating wear resistance for bulk metal forming, Thin Solid Films, 73(1980) 315-321.

[1.17] J.C. Knight & T.F. Page. Scratch induced subsurface deformation behaviour of thin ceramic coatings, Surface Engineering, 1990, Vol 6, No4, 263.

[1.18] P.C. Twigg., T. Page. Investigation of thick nitride coated systems for high load applications, Surface and Coatings Technology, 68/69 (1994) 453-458.

[1.19] O. Knotek, F. Loffler, A.Schrey, B. Bosserhoff. Behaviour of CVD and PVD Coatings Under Impact Load, Surface and Coating Technology, 68/69(1994) 489-493.

[1.20] K.J. Swick, G.W. Stachowiak, & A.W. Batchelor. Mechanism of wear of rotary percussive drilling bits and the effect of rock type on wear, Tribology International, 1992. Vol 25. No 1. p 83-88.

[1.21] S.R. Bradbury, M.Sarwar, D.B. Lewis. An assessment of enhancing the performance and wear characteristics of high speed steel circular saw blades through Ion implantation, ICMCTF 1994, San Diego.

[1.22] M. Sarwar, W. Ahmed, E. Ahmed. Improvements in the performance of cutting tools by the application of PVD and CVD hard coating technologies, ICMCTF 1994, San Diego.

[1.23] D.B. Lewis, S.R. Bradbury, M. Sarwar. The effects of substrate surface preparation on the performance and life of TiN coated high speed steel circular saw blades, ICMCTF 1994, San Diego.

[1.24] K. Lange(editor), Handbook of metal forming. Published by Mc Graw Hill, 1985, Chapter 27,pp 27.4.

[1.25] Classification and selection of tool steels, iron and steels. Metal Progress. June 1980 P-44.

[1.26] G. Viereggs, Zerspanung der Eisenwerkstoffe, Stahleisen, Dusseldorf, 2, Aufl., 1970.

[1.27] O. Knotek, F. Loffler, G. Kramer, Surf. Coat. Technol., 54-55 (1992) 241.

Chapter 2.

[2.1] M.I. Barlow, A.P. Roskilly, P.A. Logan, D.P. Monaghan. PC Based real time control of a closed field unbalanced magnetron sputter Ion plating system. ICMCTF 1994, San Diego.

[2.2] W. Konig, R.Fritsch & D.Kammermeier. Physically vapor deposited coatings on tools: performance and wear phenomena. Surface and coating technology, Vol 49, 1991 p 316- 324.

[2.3] M.S.J. Hashmi, Surface Engineering through thick and thin coatings, Dublin City University, Ireland, 1994.

[2.4] C. Wick. Coatings improve tool life, increase productivity. Manufacturing Engineer, December 1986, p-26.

[2.5] J. Fohl, T. Weissenberg, J. Wiedemeyer. General Aspects for Tribological Applications of Hard Particle Coatings. Wear 1989, Volume 130,1 p275-288.

[2.6] G. Burgin. Cutting Edge. Manufacturing Engineer, September 1989, p 27.

[2.7] A. Matthews and H. Sundquist. Titanium Nitride Coatings Boost Productivity. Materials Engineering. Jan 1983, P43-45.

[2.8] Sandvik Coromant. Coromants Basic Turning grades. The operator's metal cutting guide. Sandvik U.K.

[2.9] J.E. Sundgren & H.T.G. Hentzell, J. Vac Sci. Technology. A4(1986) 2259-2279.

[2.10] M.C. Vagle, Wear parts can be coated too. Modern Machine Shop. March 1990, p84-90.

[2.11] M. Andritschky and V. Teixeira, Residual stress in high temperature $ZrO_2(Y)$ coatings produced by magnetron sputtering, in MSJ Hashmi (editor) AMPT 1993, Vol 2, pp729-734, Published by Dublin City University press.

[2.12] X.Chu, S.A. Barnett, M.S. Wong, W.D. Sproul, Surface Coating Technology., 57 (1993) 13.

[2.13] G.J. Hammersley. Surface Prestressing by controlled shot peening to improve resistance to stress corrosion cracking. Surface Engineering Vol 2, (1992), 181-195. P.K. Datta & J.S. Gray (editors).

[2.14] Yu.V. Kolesnikov, V.A. Anan'evskii, and I.V. Govorov. Formation of coating resistance to contact impact loading by various Borochromizing methods. Fiziko-Khimicheskaya Mekhanika Materialov, No 1, pp. 101-104, January-February ,1989

[2.15] H. Valizadeh. Ion Implantation and its outstanding benefits in Engineering. Engineers Journal, April 1989, p20.

[2.16] G.A. Collins, R. Hutchings, J. Tendys & M. Samandi. Advance surface treatments by plasma ion implantation. Surface and Coatings Technology, 68/69(1994) 285-293.

[2.17] M.G. Hocking. Production of corrosion and wear resistant coating. Surface Engineerign Vol 2,(1992), P4-21. P.K. Datta & J.S. Gray (editors).

[2.18] P.J. Burnett & T.F.Page. The effects of ion-implantion on the surface mechanical properties of some engineering hard materials. Inst. Phys. Conf. Ser. No.75. 1984, Chapter 8. pp789-802.

[2.19] A.J. Perry, J.R. Treglio, D.G. Bhat, S.P. Boppana, T.Z. Kattamis, K.Schlichting, G. Dearnaley, & D.E. Geist. Effect of ion implantation on the residual stress, tribological and machining behavior of CVD and PVD TiN coated cemented carbide cutting tool inserts. Surface and coatings Technology, 68/69 (1994) 294-300.

[2.20] T.S. Eyre. Influence of ion implantation in extending tool life in polymer processing. Surface Engineering.(1992) P.K. Datta & J.S. Gray(Editors).

[2.21] Ion Implantation, Published by TECVAC Ltd, U.K.

[2.22] R.A. Higgins. Materials for the Engineering Technician. Published by Hodder and Stoughton 1980.

[2.23] A. Shibuya. Metal coating technologies. Transactions of the Iron and Steel Institute of Japan, 1985, Vol 25(8), p 796.

[2.24] D. Belforte & M. Levitt(eds). Industrial Laser Handbook. Penwell Books. Tulsa. OK, 1990.

[2.25] C.J.S. Guest. Plasma and Detonation gun coatings. Trans. IMF 1986, 64, 33 p33-38.

[2.26] A. Parker. Ceramic applications in reciprocating engines. Automotive Materials, Metals and Materials journal, January 1990, p25.

[2.27] M. Helali, M.S.J. Hashmi in M.S.J. Hashmi(ed.). Advances in Materials & Processing Technology, Vol. 2, Dublin, 1993, p.1315-1322.

[2.28] Ceramet Plasma Coatings Ltd, U.K.

[2.29] S.Grainger(Editor). Engineering Coatings, Design and Application, Abington publishing. 1989 p-189.

[2.30] G.S. Hunt. Developments in Arc, Laser and Friction Weld Surfacing processes. Arc Welding Department, British Welding Institute, Production Engineer, February 1989, p-42.

[2.31] C. F. Powell, J. H. Oxley, J.M. Blocher, Jr. Vapor deposition, p-3. The Electrochemical Society, U.K. Published by John Wiley & Sons, 1966.

[2.32] L.G. Carpenter. Vacuum Technology, Published by Bristol, A. Hilger(ed.), 1983, 2nd Edition.

[2.33] Vacuum Coating, LEYBOLD AG. U.K.

[2.34] L. Holland. Design and operating characteristics of low pressure plasma systems, Unit for Plasma materials processing, University of Sussex, U.K.

[2.35] G.D. Hughes. The design of production sputtering systems using high rate magnetron sources. Materials research Company Ltd, U.K. Vacuum 1978. Conference on Medium, high and Ultra high Vacuum technology, Vol 28, no 10/11.

[2.36] C. Subramanian, K.N. Stafford, T.P. Wilks, L.P. Ward, W. McMillan, Proc. Int. Conf on Metallurgical coatings and thin films(1993), San Diego.

[2.37] M. Berger, P. Stokley. PVD Protective coatings for wear. Surface Engineering, Vol 2, 1992, P 22-30. P.K. Datta & J.S. Gray (editors).

[2.38] R.F. Bunshah. Thin solid films, 80,255 1981.

[2.39] A. Matthews. PhD Thesis, University of Salford, 1980. Reference from D.S. Rickerby & A. Matthews. Ceramic Coatings by Physical Vapour Deposition. Review on Powder Metallurgy and Physical Ceramics. V4, n 3-4, 1991 p155-297.

[2.40] Engineering coatings-their applications and properties, p-2. National physical laboratory, Teddington, Middlesex, U.K.

[2.41] S.M. George. STEEL WORKS. Engineering and Fabrication, special products department, British steel strip products. Manufacturing Engineer. July/august 1989, p45-47.

[2.42] A. Heijered, M. Hellsing, H. Andren and H. Norden. The presence of cobalt at WC/WC Interfaces. Proceedings of the International Conference of Science of Hard Materials. Institute of Physics Conference series number 75. September 1984. P 303-310.

[2.43] Cobalt in Hard Metal. Cobalt News. Published by the Cobalt Development Institute. 94/4. October 1994. p6-8.

[2.44] H. Uetz. Abrasion and Erosion, Carl Hanser Verlag 1986.

[2.45] R. K. Schmid, A. R. Nicoll. Tailoring the wear resistance of hard metal spray coatings through microstructural modelling, Sulzer technical review, 1/1990.

[2.46] M.D. Ziaul Karim. Growth and characterization of BN thin films deposited by PACVD Ph.D. Thesis Feb 1993.

[2.47] C. Wick. Machining with PCBN Tools. Manufacturing Engineer journal, July 1988, p 73-78.

[2.48] S. Watanabe, S. Miyake, & M. Murakawa. Tribological properties of cubic, amorphous and hexagonal boron nitride films, Surface and Coating Technology, 49,(1991) 406-410.

[2.49] B. Goranchev, K.Schmidt, & K. Reichelt, Thin solid films, 149(1)(1987) L77-L80.

[2.50] R.F. Bunshah, C. Deshpandey, K.L. Chorpa & V.D. Vankar, U.S. patent application , August, 1985.

[2.51] R. Bliki, Composite cutting, Manufacturing Engineering, December, 1993.

[2.52] J.S. Chapin, Res & Dev., 25(1) (1974)37.

[2.53] D. Moskowitz, L.L. Terner, & M. Humenik Jr. Some Physical and metal-cutting properties of titanium carbonitride base materials. Proceedings of the International conference of Science of Hard Materials. Institute of Physics conference series number 75. September 1984. p. 605-617.

[2.54] D.S. Rickerby and A. Matthews. Ceramic coatings by Physical Vapour Deposition. Review on Powder Metallurgy and Physical Ceramics. V4, n 3-4, 1991 p155-297.

[2.55] J. Halling 16th Leeds-Lyon Symp. (1989)-Mechanics of Coating, Elsevier(1990)447.

[2.56] R.G. Duckworth. Thin Solid Films. 94(1981) 307.

[2.57] I.P. Hayward. Friction and wear properties of diamond and diamond coatings. Surface and Coatings Technology. 49(1991) 554-559.

[2.58] N. Kikuchi, T. Komatsu & Y. Yoshimura. Mater. Sci. Eng. A. 105/106 (1988) 525-534.

[2.59] S. Aisenberg & R. Chabot. J. Appl. Phys. 42(1971)2953.

[2.60] D.S. Kim, T.E. Fischer & B. Gallois. The effects of oxygen and humidity on friction and wear of diamond-like carbon films. Surface and Coatings Technology. 49(1991) 237-542.

[2.61] R. Memming, H.J. Tolle & P.E. Wierenga. Thin Solid Films, 143(1986) 31.

[2.62] D.P. Monaghan, K.C. Laing, P.A. Logan,P. Teer, & D.G. Teer. How to deposit DLC successfully. Material World, 1(1993) 347.

[2.63] L.Andersson. Thin Solid Films, 86(1981) 193.

[2.64] K. Donnelly, D.P. Dowling, E. Davitt, T.P. O'Brien and T.C. Kelly, Refractive index as an indication of plasma deposited diamond like carbon film durability. Proceedings of AMPT 1993. In MSJ Hashmi(editor). Published by Dublin City University Press.

Chapter 3.

[3.1] K. H. Zum Gahr. Microstructure and wear of materials. Elsevier. Tribology Series 10, 1987.

[3.2] K.G. Budinski. Friction in machine design. In Tribological Modeling for Mechanical Design. Ludema/Bayer(editors) July 1991, Vol 1105 p 89-126.

[3.3] K. Lange(editor), Handbook of metal forming. Published by Mc Graw Hill, 1985, . Chapter 6, pp 6.4-6.5

[3.4] Y. Berthier, L. Vincent and M. Godet, Velocity accommodation sites and modes in tribology. European journal of Mechanics. A/Solids, 11, No 1, 35-47, 1992.

[3.5] K. Kato, D.F. Diao, and M. Tsutsumi. The wear mechanism of ceramic coating film in repeated sliding wear. Wear of Materials ASME 1991.

[3.6] R. Chattopadhyay. Advances in wear protection methods and systems. Ninth International Conference on Industrial Tribology, India 1991, m115-123.

[3.7] J.M. Martin, Th. le Mogne. Interpretation of friction and wear of ceramics in terms of surface analysis. Surface and Coatings Technology, 49(1991) 427-434.

[3.8] B.J. Gill. Designing and Producing engineering surfaces. Union Carbide U.K. Ltd, Recent development in surface coating and modification processes, October 1985.

[3.9] P.K. Datta & J.S. Gray (Editors). Friction and Wear control in industry, T.S. Eyre, Surface Engineering Conference, Newcastle Upon Tyne, March 1992.

[3.10] T.S. Eyre. Influence of ion implantation in extending tool life in polymer processing. Surface Engineering, P.K. Datta & J.S. Gray(Editors), 1992.

[3.11] S.Grainger(Editor). Engineering Coatings, Design and Application, Abington publishing. 1989 p-189.

[3.12] R. Blickensderfer & J.H. Tylczak. Laboratory Tests of spalling, Breaking, and Abrasion of Wear-Resistant Alloys used in Mining and Mineral Processing. Department of the Interior, Bureau of Mines report of investigation 1985.

[3.13] J. Fohl, T. Weissenberg, J. Wiedemeyer. General Aspects for Tribological Applications of Hard Particle Coatings. Wear 1989, Volume 130,1 p 275-288.

[3.14] D. Klaffke. A. Skopp and I. Lenke. Triblogical Characterization of Coatings by Oscillating Sliding Testing, Bundesanstalt fur Materialforschung und-prufung. (BAM), Laboratory 5.22 "Fretting, Cryotibology", 12200 Berlin, 1994.

[3.15] I.L. Singer. A thermochemical model for analysing low wear rate materials. Surface and coatings technology, 49(1991) 474-481.

[3.16] L. Tellefsen. Handbook for Pelleting Technique, 1990, Jesma-Matador, Denmark.

[3.17] J. Larsen-Basse. Success and failure of simple models for abrasive wear. In Tribological Modeling for Mechanical Designers. Ludema/Bayer(editors) July 1991, Vol 1105 p51-76.

[3.18] D.R. Askeland, The Science and Engineering of Materials. Second S.I. Edition, Chapman and Hall. 1990, p 807.

[3.19] A. Mista and I.Finnie, A classification of three-body abrasive wear and design of a new tester. Wear, 60 (1980) 111-121.

[3.20] F. Borik and D.L. Sponseller. Gouging abrasion test for materials used in ore and rock crushing, Part 1, Description of the test. Journal of Materials 6(1971) 576-589.

[3.21] F.Borik and W.G. Scholz, Part 2- Effects of metallurgical variables on gouging wear. Journal of Materials 6(1971) 590-605.

[3.22] I.R. Sare, Repeated impact-abrasion of ore-crushing hammers, Wear 87(1983) 207-225.

245

[3.23] I.R. Sare and B.K. Arnold, Gouging abrasion of wear resistant alloy white cast irons, Wear 131(1989) 15-38.

[3.24] T. Sasada. Classification of metallic materials from a viewpoint of their antiwear behaviour. In Tribological Modeling for Mechanical Designers. Ludema/Bayer(editors) July 1991, Vol 1105 p143.

[3.25] V.N. Vinogradov, G.M. Sorokin and A. Yu. Albagachiev, Wear in the case of impact. Mashinostroenie, Moscow, 1982.

[3.26] G.M. Sorokin, Criteria of wear resistance of steel under conditions of abrasive impact, Mashinovedenie, no 3 pp-111-115, 1973.

[3.27] Yu. V. Kolesnikov, On the question of criteria of surface destruction of steels in the case of abrasive impact wear, Vestnik Mashinostroeniya. Vol 70, No 6. pp 16-19, 1990.

[3.28] D.S. Rickerby, P.J. Burnett. The wear and erosion resistance of hard PVD coatings. Surface and Coating Technology, 33(1987)191-211.

[3.29] D.V. Keller. Adhesion between Solid metals, Wear, 6, 353(1963).

[3.30] J.A. Nieminen, A.P. Sutton, J.B. Pethica, and K.Kaski, Mechanism of lubrication by a thin solid film on a metal surface. Mater. Sci. Eng. 1(1992) 83-90.

[3.31] M.S.J. Hashmi. Surface Engineering through thick and thin coatings. Dublin City University, Ireland, 1994

[3.32] R.J. Good. On the definition of adhesion. Journal of Adhesion. Volume 8,1,(1976).

[3.33] D.H. Buckley & R.L. Johnson. The influence of crystal structure and some properties of Hexagonal Metals on friction and adhesion. Wear, 11, 405, (1968).

[3.34] D.H. Buckley. Surface effects in adhesion, Friction, Wear and Lubrication. Elsevier, Amsterdam, (1981). In T.Bell, Surface Engineering, Its current and future impact on Tribology, J. Phys. D: Appl. Phys 25(1992) a297-a306.

[3.35] A.R. Lansdown & A.L. Price. Materials to resist wear, A guide to their selection and use. Pergamon Press, 1986, First Edition.

[3.36] S. Bahadur. The Structure of erosive wear models. In Tribological Modeling for Mechanical Designers. Ludema/Bayer(editors) July 1991, Vol 1105 p33-50.

[3.37] J.E. Field. & I.M. Hutchings. Materials at High Strain Rates. Elsevier Applied Science publishers Ltd. U.K. Chapter 7, 1987. p 243-293.

[3.38] R.A. Vaughan & A. Ball. The effects of hardness and toughness on the erosion of ceramic and ultrahard materials. Wear of Materials. ASME 1991 pp. 71-75.

[3.39] Metallurgical Failure Investigations of Components, Structures & Assemblies. Published by BHP Group Ltd, U.K. Dec, 1992.

[3.40] J.A. Sue, H.H. Troue. High temperature erosion behaviour of Titanium Nitride and Zirconium Nitride coatings. Surface and Coatings Technology, 49(1991) 31-39.

[3.41] F. Alonso, I. Fagoaga and P. Oregui. Erosion protection of carbon-epoxy composites by plasma-sprayed coatings. Surface and Coatings Technology, 49(1991) 482-488.

[3.42] M. Ignat, A. Armann, L. Moberg, F. Sibieude. Mechanical stability and adhesion of ceramic coatings deposited on steels. Surface and Coatings Technology, 49(1991) 514-518.

[3.43] S. Fouvry, P. Kapsa & L. Vincent. Fretting behaviour of hard coatings under high normal load. Surface and Coatings Technology, 68/69(1994) 494-499.

[3.44] I.V. Kragelsky. Some concepts and definitions which apply to friction and wear. Acad. Sci. USSR, Moscow, 12(1957).

[3.45] G.J. Hammersley. Surface Prestressing by controlled shot peening to improve resistance to stress corrosion cracking. Surface Engineering Vol 2, (1992), 181-195. P.K. Datta & J.S. Gray (editors).

[3.46] Ion Implantation, Company brochure, Published by TECVAC Ltd, Cambridge, U.K.

[3.47] W. B. Nowak. Thin metallic films for corrosion control. Surface and Coatings Technology, 49(1991) 71-77.

[3.48] K.N. Strafford, C. Subramanian & T.P. Wilks. Characteristics and Quality performance of advanced coatings. Surface Engineering, Volume 2, Engineering Applications p268- 271. 1992.

[3.49] J.D. Donaldson, S.J. Clark, Cobalt in superalloys, the monograph series, Published by The cobalt development institute, 1985, U.K. p 33-35.

[3.50] J. Munemasa, T.Kumakiri. Effect of the surface roughness of substrates on the corrosion properties of films coated by physical vapour deposition. Surface and Coatings Technology, 49(1991), 496-499.

[3.51] Engineering coatings, their applications and properties, p-2. Published by National physical laboratory, Teddington, Middlesex, U.K.

[3.52] D.S. Rickerby and A. Matthews. Ceramic coatings by Physical Vapour Deposition. Review on Powder Metallurgy and Physical Ceramics. V4, n 3-4, 1991 p155-297.

[3.53] P.J. Burnett, D.S. Rickerby. Assessment of coating hardness. Surface engineering. 1987 Vol 3, No 1, 69.

[3.54] W. Konig, R. Fritsch & D. Kammermeier. Physically vapor deposited coatings on tools: performance and wear phenomena. Surface and Coating Technology, Vol 49, 1991 p 316- 324.

[3.55] J.E. Sundgren & H.T.G. Hentzell, J. Vac Sci. Technology. A4(1986) 2259-2279.

[3.56] M.D. Ziaul Karim. Growth and characterization of BN thin films deposited by PACVD Ph.D. Thesis Feb 1993.

[3.57] C. Wick. Coatings improve tool life, increase productivity. Manufacturing Engineer, December 1986, p-26.

[3.58] C. Subramanian, K.N. Strafford, T.P. Wilks and L.P. Ward, On the design of coating systems: Metallurgical and other considerations. In M.S.J. Hashmi(editor). Volume 2, pp1301-1313, AMPT 1993, Publisher Dublin City University Press.

[3.59] D.S. Dugdale, M.S. Sarwar, Fatigue strength of bandsaws with hard coatings. In M.S.J. Hashmi(editor) Volume 2, pp 1301-1313, AMPT 1993, Publisher Dublin City University Press.

[3.60] A. Cudden & C.Allen, The wear of tungsten carbide-cobalt cemented carbides in a coal ash conditioner, Wear of materials, ASME 1991.

[3.61] A. Matthews & D.G. Teer, Evaluation of coating wear resistance for bulk metal forming. Thin Solid Films, 73(1980) 315-321.

[3.62] A. Kassman, S. Jacobson, L. Erickson, P. Hedenqvist, M. Olsson. A new test method for the intrinsic abrasion resistance of thin coatings. Surface and coating technology, Vol 50, 1991, p75-84.

[3.63] A.V. Byeli, A.A. Minevich, A.V. Stepanenko, L.G. Gick & O.V. Kholodilov. Wear resistance and structure of (Ti,Al)N coatings. J. Phys. D:Appl. Phys. 25 (1992) A292-A296.

[3.64] T.E. Hale, D.E. Graham. The Influence of coating thickness and composition upon metal-cutting performance. Publ by ASM, Metals park, Ohio, USA p175-191.

[3.65] D.T. Quinto, A.T. Santhanam & P.C. Jindal. Mechanical properties, Structure and performance of CVD and PVD Coated Carbide Tools. RM & HM June 1989. p95-101.

[3.66] D.T. Quinto, A.T. Santhanam & P.C. Jindal. Mechanical properties, Structure and performance of chemically Vapor-deposited and Physically Vapor-deposited Coated Carbide Tools. Materials Science and Engineering, A105/106(1988)443-452.

[3.67] O. Knotec, F. Loffler & G. Kramer. Arc-deposited Ti-ZrN coatings on cemented carbides for use in interrupted cutting. Surface and coating technology. 49(1991) 325-329.

[3.68] J. Monaghan & O. Quigley. The Machinability of Aerospace Alloys. Turning Inconel 718. Dept of Mechanical & Manufacturing Engineering, T.C.D., 1994, Dublin.

[3.69] A.V. Byeli, A.A. Minevicht, A.V. Stepanenko, L.A. Gick & O.V. Kholodilov. Wear resistance and structure of (Ti,Al)N coatings. J. Phys. D: Appl. Phys. 25(1992) A292-A296.

[3.70] D.P. Monaghan, K.C. Laing, P.A. Logan, P.Teer and D.G. Teer. How to deposit DLC successfully. Surface Engineering, June 1993, p347-349.

[3.71] D.P. Monaghan. High Technology coatings based on diamond like carbon and Molybdenum disulphide. Surface Engineering, 1992, Vol 8, No 4. p254-257.

[3.72] M. Sarwar, D. Gillibrand, & S.R, Bradbury. Forces, surface finish and friction characteristics in surface engineered single and multiple point cutting edges. Surface and coatings technology, 49(1991)443- 450.

[3.73] H. Ronkainen, I. Nieminen, K.Holmberg, A. Leyland, K.S. Fancey, A. Matthews, B. Matthes, E.Broszeit. Evaluation of some new titanium based ceramic coatings in tribological model wear and metal cutting tests. Material Science and Engineering. A140(1991)602-608.

[3.74] M. Murakawa and S. Takeuchi. Mechanical applications of thin and thick diamond films. Surface and Coatings Technology. 49(1991) 359-365.

[3.75] T.E. Norman. Climax Finds New Austenitic Alloy Ideal for Ultra-Abrasive Mine Mill Applications. Eng. and Min. J.,v.166, No. 4, 1965, pp.86-90.

[3.76] C. Spero, D.J. Hargreaves, R.K. Kirkcaldie & H.J. Flitt. Review of test methods for abrasive wear in ore grinding. Wear 146(1991) 389-408.

[3.77] C. F. Powell, J. H. Oxley, J.M. Blocher, Jr. Vapor deposition, p-3. The Electrochemical Society, Inc. Published by John Wiley & Sons, 1966.

[3.78] C. Weaver. J. Vac. Sci. Technol. 12,18(1975).

[3.79] S.S. Chiang, D.B. Marshall, & A.G. Evans. Surface and Interfaces in Ceramics and Ceramic-Metal Systems. Edited by J. Pask and A.G. Evans. (Plenum, New York, 1981), p.603.

[3.80] A.J. Perry, P. Laeng, & H.E. Hintermann. Proc. 8th Int. Conf. on Chemical Vapour Deposition, Electrochemical Society, Pennington. NJ 1981. p.475.

[3.81] H.J. Krokoszinski. Abrasion resistance of various thin film coatings on thick film resistor materials. Surface and Coatings Technology, 49(1991) 451-456.

[3.82] H.J. Krokoszinski. Proc. Int. Conf. on Diamond Films. Crans- Montana, September 17-19. in Surf.Coat. Technol. 47 (1991) 761.

[3.83] E.A. Almond, L.A. Lay & M.G. Gee. Comparison of sliding and abrasive wear mechanisms in ceramics and cemented carbides. Inst. Phys. Conf. Ser. No. 75: September 1984, Chapter 9. pp919-948.

[3.84] J.C. Knight, T.F. Page, & I.M. Hutchings. Surface Engineering. 1990, 6,(1),5563.

[3.85] A.J. Perry. Surface Engineering. 1986,2, 183.

[3.86] K. Bouslykhane, P. Moine, J.P. Villain & J. Grilhe. Mechanical properties and wear resistance of ion-beam assisted sputter-deposited NiTi(N) coatings. Surface and Coatings Technology, 49(1991) 457-461.

[3.87] Richard K. Schmid, Andrew R. Nicoll. Tailoring the wear resistance of hard metal spray coatings through microstructural modelling, Sulzer technical review, 1/1990.

[3.88] U. Makela and J.Valli, Tribolgia, Finnish Journal of Tribology, 4, (1985), 74.

[3.89] S. Watanabe, S. Miyake, & M. Murakawa. Tribological properties of cubic, amorphous and hexagonal boron nitride films., Surface and Coatings Technology, 49,(1991) 406-410.

[3.90] Ludema & Bayer(editors). Tribological Modeling for Mechanical Designers. ASTM special technical publication. July 1994. Vol 1105. p134.

[3.91] J. Kelley, J.J. Stiglich Jr, G.L. Sheldon. Methods of characterization of tribological properties of coatings. Surface modification Technologies 1988 p169-187.

[3.92] R. Blickensderfer, and J.H. Tylczar. A large scale Impact spalling Test. Wear, V. 84, No. 3, 1983, pp. 361 -373.

[3.93] D. Tabor, The hardness of Metals, Monographs on the Physics & Chemistry of materials. W. Jackson, H.Frohlich, N.F. Mott(eds), Oxford University Press, 1951, p-115.

[3.94] D.S. Clark, & D.A. Wood, The Tensile Impact properties of some metals and alloys, Transactions of American Society for Metals, 42(1950)45.

[3.95] V.O. Shestopal, and B. Chilcott. Impact Testing of Flexible Polyurethane Foams. Journal of Testing and Evaluation. May 1988, Vol. 16(N3)pp 312-318.

[3.96]   S.S. Brenner, H.A. Wriedt. & R.A. Oriani. Impact adhesion of Iron at elevated temperatures. Wear 68(1981) p169-190.

[3.97]   M. Fiset, G. Huard. J. Masounave. Correlation between a Laboratory impact-abrasion test and an in-situ marked-ball test. Tribology International. Oct 90. Vol 23. No 5. p 329-332.

[3.98]   A.E. Diniz, J.J. Liu & D.A. Dornfeld. Correlating tool life, tool wear and surface roughness by monitoring acoustic emission in finish turning. Wear 152(1992) 395-407.

[3.99]   Y. Kubo and M. Hashimoto. Mechanical properties of TiN films deposited by changed pressure r.f. sputtering. Surface and Coatings Technology. 49(1991) 342-347.

[3.100] J.H. Je, E. Gyarmati & A. Naoumidis. Thin Solid Films, 136(1986) 57.

[3.101] E. Erturk & H.J. Heuvel. Thin Solid Films. 153(1987)135.

[3.102] F.C. Chang, M.Levy, R.Huie, M.Kane, P.Buckley, T.Z. Kattamis, G.R. Lakshminarayan. Adhesion and corrosion behaviour of Al-Zn and TiN/Ti/TiN coatings on a DU-0.75wt% Ti Alloy. Surface and Coatings Technology, 49(1991) 87-96.

[3.103] ASTM G83-83 in 1985 Annual Book of ASTM Standards, Section 3, Volume 03.02-Erosion and wear; metal corrosion. Philadelphia, PA, 1985, pp 499-506.

[3.104] Y. Shimura, & Y. Mizutani. Wear of ceramics at high temperatures and its improvement by metallic coatings. Wear of Materials. ASME 1991. pp 405-410.

[3.105] C. Yang, & S. Bahadur. Friction and wear behaviour of alumina-based ceramics in dry and lubricated sliding against tool steel. Wear of Materials. ASME 1991. pp383-404.

[3.106] American Society for Testing and Materials. Standard Practise for ranking resistance of materials to sliding wear using Block on Ring wear test. ASTM G77-83 in 1985 Annual book of ASTM Standards, Section 3, Vol. 03.02- Erosion and Wear;Metal Corrosion. Philadelphia, PA,1985, pp.450-466.

[3.107] W. Cerri, R. Martinella, G.P. Mor, P. Bianchi, & D.D. Angelo. Laser deposition of carbide-reinforced coatings. Surface and Coatings Technology 49(1991) 40-50.

[3.108] P.A. Swanson. Comparison of Laboratory and Field Abrasion tests. Proc. Wear of Materials Conf. 1985. New York, ASME. PP 519-529.

[3.109] American Society for Testing and Materials. Standard test method for abrasive wear resistance of Cemented Carbides. ASTM611-76 in 1986 Annual Book of ASTM Standards, Section 2, Vol. 02.05. Metallic and inorganic coatings; Metal powder, Sintered P/M Structural parts. Philadelphia, PA,1986, pp 490-492.

[3.110] A.F. George and S.J. Radcliffe. Automated wear measurement on a computerised profilometer. Wear, Vol 83, No 2, Dec. 15th 1982, pp 327-377.

[3.111] K. Holmberg and A. Matthews, Coatings Tribology, A concept, critical aspects and further directions, Keynote address, ICMCTF 1994, San Diego.

Chapter 4.

[4.1] J. Fohl, T. Weissenberg, J. Wiedemeyer. General Aspects for Tribological applications of Hard Particle Coatings. Wear 1989, Volume 130,1 p 275-288.

[4.2] I. Efeoglu, K.C. Laing, D.P. Monaghan, D.G. Teer, R.D.Arnell. Correlation between hardness and wear rate for selection of Nitride and Alloy Nitride coatings. ICMCTF 1994, San Diego.

[4.3] ISO classification. Carbide application group.

[4.4] Kistler Piezo instrumentation. Quartz load washers.

[4.5] Keitley Metrabyte. Users guide for the DAS-8, DAS-8PGA & DAS8/AO data acquisition cards. July 1990.

[4.6] D. Kennedy, M.S.J. Hashmi in M.S.J. Hashmi(ed.). Advances in Materials & Processing Technology, Vol. 3, Dublin, 1993, p2057- 2069. Dublin City University Press.

[4.7] H. Dimigen & C.P. Klages. Microstructure and wear behaviour of metal-containing diamond-like coatings. Surface and Coatings Technology. 49. 1991 543-547.

[4.8] G. Lawes. Scanning Electron Microscopy and X-Ray Microanalysis. Analytical Chemistry by Open Learning Series. Wiley 1987.

[4.9] Goldstein, Newbury, Echlin, Joy, Romig, Lifshin. Scanning Electron Microscopy and X-RAy Microanalysis. 2nd edition, 1992, Plenum Press.

Chapter 5.

[5.1] J. Dobinson. Mathematics for Tehnology 1: Penguin Books. 1978.

[5.2] C. Spero, D.J. Hargreaves, R.K. Kirkcaldie, H.J. Flitt. Review of test methods for abrasive wear in ore grinding. Wear 146(1991) 389-408.

[5.3]. A.R. Lansdown & A.L. Price. Materials to resist wear, A guide to their selection and use. Pergamon Press, 1986, First edition.

[5.4] A. Kassman, S. Jacobson, L. Erickson, P. Hedenqvist, M. Olsson. A new test method for the intrinsic abrasion resistance of thin coatings. Surface and coating technology, Vol 50, 1991, p75-84.

[5.5] J.F. Archard. Contact and rubbing of flat surfaces. J.Appl. Phys. 24,981(1953).

[5.6] J. Larsen-Basse. Success and failure of simple models for abrasive wear. In Tribological Modeling for Mechanical Designers. Ludema/Bayer(editors) July 1991, Vol 1105 p51-76.

[5.7] D.S. Rickerby, P.J. Burnett. The wear and erosion resistance of hard PVD coatings. Surface and Coating Technology, 33(1987)191-211.

[5.8] D.R. Askeland. The Science and engineering of Materials. 2nd edition, Published by Chapman and Hall. 1990, p 809.

[5.9] J. Larsen-Basse. Success and failure of simple models for abrasive wear. In Tribological Modeling for Mechanical Designers. Ludema/Bayer(editors) July 1991, Vol 1105 p51-76.

[5.10] M.L. Boas. Mathematical Methods in The Physical Science. John Wiley and Son, 1983, Second edition, Chapter 13, pp 615.

[5.11] D. Tabor, Proc. R.Soc. London, Ser. A, 192(1948) 247-274.

[5.12] S.S. Brenner, H.A. Wriedt and R.A. Oriani. Impact adhesion of Iron at elevated temperatures. Wear, 68(1981) 169-190.

[5.13] D. Tabor, The hardness of Metals, Monographs on the Physics & Chemistry of materials. W. Jackson, H.Frohlich, N.F. Mott(eds) p-115. Oxford University Press, 1951.

[5.14] G. Sundararajan. The depth of plastic deformation beneath eroded surfaces-the influence of impact angle and velocity, particle shape and material properties. Wear of Materials, ASME 1991, p111-122.

[5.15] O. Richmond. U.S. Steel Corporation, Research Laboratory, Monroeville, PA 15146, in S.S. Brenner, H.A. Wriedt and R.A. Oriani. Impact adhesion of Iron at elevated temperatures. Wear, 68(1981) 169-190.

[5.16] K. Lange(editor), Handbook of metal forming. Mc Graw Hill, 1985, Chapter 17, pp 17.5.

[5.17] D.S. Rickerby and A. Matthews. Ceramic coatings by Physical Vapour Deposition. Review on Powder Metallurgy and Physical Ceramics. V4, n 3-4, 1991 p155-297.

[5.18] F.P. Beer, E. R. Johnston Jr. Vector Mechanics for Engineers. Second SI Metric Edition. McGraw-Hill Publishers 1990.

[5.19] H. Hertz. J. Reine Angew. Math.,92(1881) 156. in S.S. Brenner, H.A. Wriedt and R.A. Oriani. Wear, 68(1981) 169-190.

Chapter 6.

[6.1] Leitz Miniload Vickers Hardness Tester tables. Ernst Leitz Wetzlar GMBH.

[6.2] Metco Ltd. Materials Safety Data Sheet. Diamalloy 2003. Metco/50-315 UK, September 1993.

[6.3] Metco Ltd. Materials Safety Data Sheet. Diamalloy 2001. Metco/50-313 UK,October 1993.

Chapter 7.

[7.1] H.S. Avery, Wear of Materials (1977) pp 148-157 in R. K. Schmid, A. R. Nicoll. Tailoring the wear resistance of hard metal spray coatings through microstructural modelling, Sulzer technical review, 1/1990.

[7.2] K.J. Swick, G.W. Stachowiak, and A.W. Batchelor. Mechanisms of wear of rotary-percussive drilling bits and the effect of rock type on wear. Tribology International. Vol 25 No 1,1992 p83.

[7.3] O. Knotek, E. Lugscheider, F. Loffler, G. Kramer, H. Zimmermann., Abrasive wear resistance and cutting performance of complex PVD coatings, Surface and Coatings Technology, 68/69(1994) 489-493.